EXAMINATION OF PROSTATE CANCER STEM-LIKE CELL ASSOCIATED FACTORS FOR THEIR CONTRIBUTION TOWARDS THE DEVELOPMENT OF CASTRATION RESISTANT PROSTATE CANCER

By NICHOLAS WONG, B.Sc.

A Thesis Submitted to the School of Graduate Studies
in Partial Fulfilment of the Requirements for the Degree Doctor of Philosophy

McMaster University

DOCTOR OF PHILOSOPHY (Ph.D.) (2016) McMaster University
Department of Medical Sciences Hamilton, Ontario, Canada

TITLE: Examination of Prostate Cancer Stem-like Cell Associated Factors for their Contribution Towards the Development of Castration Resistant Prostate Cancer

AUTHOR: Nicholas Wong, B.Sc. (University of Waterloo)

SUPERVISOR: Dr. Damu Tang, Ph.D.

PAGES: xxvii, 279

ABSTRACT

Although early detection and treatment of prostate cancer (PC) shows some benefit, advanced PCs that progress despite androgen deprivation become castration resistant (CRPC). This stage becomes largely incurable as CRPCs are intimately associated with metastasis, the predominant cause of PC-related fatalities. Increasing evidence reveals the role of prostate cancer stem cells (PCSCs) in mediating PC progression. Taking advantage of our putative PCSC population derived from DU145 cells, we have examined a number of candidates for their contribution to PCSC-related PC progression and CRPC development.

PKM2 plays a major role in cancer cell metabolism by inducing a shift towards aerobic glycolysis (the Warburg effect) to convert metabolic intermediates into cellular building blocks. PKM2 has also been demonstrated in non-metabolic oncogenic functions. Here we reveal an association with higher Gleason PC tissues, and distinct post-translational modifications in our PCSCs. MUC1 is a well-known tumour associated antigen with widespread oncogenic effect. We demonstrate increased MUC1 expression in our PCSCs, upregulation following docetaxel treatment *in vivo*, and a unique MUC1 network gene signature which may be used to predict CRPC. FAM84B is a novel protein in cancer, and we demonstrate higher expression of FAM84B in our PCSCs and in two animal models of CRPC. Using gene expression databases, both MUC1 and FAM84B were revealed to associate with metastasis and CRPC. Lastly, CSCs are

widely regarded as being chemoresistant, and we have revealed elevated expression of a drug transporter ABCC2 in our PCSCs and in higher Gleason PC tissues. We also present preliminary evidence that ABCC2 may contribute to docetaxel resistance in DU145 sphere-derived subcutaneous xenografts.

Co-expression of these four factors in our putative DU145 PCSCs and their widespread impact on diverse mechanisms of cell proliferation and survival underscores the importance of PCSCs in promoting advanced prostate cancer.

ACKNOWLEDGEMENTS

I would first like to give a big thank you to my supervisor, Dr. Damu Tang, for advising me over the last six years. Although the long road of graduate school has been difficult at times, I could always go to you for encouragement and guidance. Your passion for science and endless positivity always inspired me to keep going, even when my results were less than ideal. You consistently pushed the limits of what I thought I could do, and for that I thank you. I know that as I end my journey here I come out a strong and well-rounded scientist, and that's all because of you.

I must also give gratitude to my committee members who made graduate school much more enjoyable; Dr. Peter Margetts and Dr. Laurie Doering. Peter, thank you for being a friendly face and encouraging my growth as a scientist. Laurie, thank you for all the advice and guidance along the way.

To the past and present members of the Tang lab, you all have made an impact on my life in your own ways, whether by giving advice or letting me take my mind off failed experiments. Brianne Hill, Yanyun Xie, Dr. Fengxiang Wei, and Dr. Lizhi He, your advice and tips when I was just starting out were invaluable and I'm grateful for that. Russell Shen, thank you for the presentation tips and de-stressing hot pot sessions. Nazihah Bakhtyar, we shared a lab bench for an entire year, and I could always count on you for random conversations and late night texts. We helped each other get through our Masters' and for that I

thank you. Dr. Judy Yan, your friendship and bubbly personality could always make the days (and nights) go faster. You taught me how to be a better researcher and I could always count on you for advice (both science-related and otherwise). I know you'll be an amazing mother and scientist. Dr. Jason De Melo, thank you for all the technical help along the way and for lending an ear to talk to. You will be an amazing professor and a great father. Xiaozeng Lin, I could always ask you to take over my experiments or use your endless supply of plasmids. I'm grateful for your help. Diane Ojo, thank you for all the scientific advice and help with experiments. You are one of the most driven and responsible people I have met and I know the future holds great things for you.

I would also like to thank my family. To my brother and sister-in-law, Sydney and Ann Wong, thank you for your support. Even though you're far away, I could always ask for your opinions or advice. To my parents, Doris and Shew Chiang Wong, words cannot articulate how much you've given me. You've faced many challenges and I'm grateful for you for raising me in conditions that cultivated my passion for science. I know I can always turn to you for guidance and to "grocery shop" at home every so often.

Last but definitely not least, my partner in life, Eric Quan. We've gone through so much together and whether I admit it or not, your drive for learning pushed me to pursue graduate school. You are the reason I've made it this far. From cooking and cleaning, to planning much needed vacations, to letting me vent my frustrations with research despite not having any context whatsoever, and putting in the effort to "edit" my reports, you've supported me in every way humanly possible. There aren't enough words to express how thankful I am for you.

PREFACE

This thesis is prepared in a "sandwich" thesis format as outlined in the "Guide for the Preparation of Master's and Doctoral Theses" available through McMaster University's School of Graduate Studies. The content within is composed of three individual manuscripts and a fourth set of unpublished work.

Chapter 1 begins by providing a general introduction and overall theme to the author's Ph.D. candidacy and ends with the goals and objectives of the research. Chapters 2 – 4 consist of independent studies organized into complete manuscripts, prefaced with details about author contributions and relation to this thesis. The manuscript in Chapter 2 was accepted and published in 2014, while Chapters 3 and 4 contain manuscripts which have been submitted and are under revision at the time this thesis was prepared. In Chapter 5, an additional set of unpublished work is organized and discussed as partial data to be included in a future manuscript. The Ph.D. candidate is/will be the first author of all work contained in this thesis. Lastly, Chapter 6 includes detailed discussions, future work, and clinical relevance of the author's research.

References cited within each manuscript are presented independently of one another and formatting styles are consistent with their respective journals. The remaining citations used throughout Chapters 1, 5, and 6 appear as a final Reference section following Chapter 6. Canadian spelling is used throughout the thesis; however American spelling is used in submitted manuscripts to comply

with journal standards (Chapters 2 – 4). License agreements for use of published work are included in the final Appendix section.

TABLE OF CONTENTS

LIST OF TABLES

LIST OF FIGURES

CHAPTER THREE

LIST OF ABBREVIATIONS

ABC	Avidin-Biotin Complex
ABCC2	ATP-Binding Cassette, Sub-Family C, Member 2
ADT	Androgen Deprivation Therapy
AKT/PKB	Protein Kinase B
ANOVA	Analysis of Variance
APC	Antigen Presenting Cell
AR	Androgen Receptor
ATCC	American Type Culture Collection
ATP	Adenosine Triphosphate
AUC	Area Under the Curve
BSA	Bovine Serum Albumin
cDNA	Complimentary Deoxyribonucleic Acid
CHAPS	3-[(3-Cholamidopropyl)Dimethylammonio]-1-Propanesulfonate
CNA	Copy Number Associations
CNV	Copy Number Variations
CRPC	Castration Resistant Prostate Cancer
CSC	Cancer Stem Cell
CTRL	Control
DC	Dendritic Cell
DFS	Disease Free Survival
DHT	Dihydrotestosterone
DMEM	Dulbecco's Modified Eagle Medium
DMSO	Dimethyl Sulfoxide
DNA	Deoxyribonucleic Acid
DTT	Dithiothreitol
ECL	Enhanced Chemiluminescence
EDTA	Ethylenediaminetetraacetic Acid
EGF	Epidermal Growth Factor
EGFR	Epidermal Growth Factor Receptor
EGTA	Ethyleneglycoltetraacetic Acid
EMT	Epithelial to Mesenchymal Transition
ERG	ETS-related Gene
EV	Empty Vector
FACS	Fluorescence Activated Cell Sorting
FAM84B	Family with Sequence Similarity 84, Member B
FBS	Fetal Bovine Serum
FDA	U.S. Food and Drug Administration
FDG-PET	Fluorodeoxyglucose-Position Emission Tomography
FFPE	Formalin Fixed Paraffin Embedded

GAPDH	Glyceraldehyde 3-Phosphate Dehydrogenase
GCN	Gene Copy Number
GEO	Gene Expression Omnibus
GS	Gleason Score
GTP	Guanosine Triphosphate
HER2	Human Epidermal Growth Factor Receptor 2
HGPIN	High Grade Prostatic Intra-epithelial Neoplasia
HIF-1α	Hypoxia Inducible Factor 1-alpha
Ig	Immunoglobulin
IgG	Immunoglobulin G
IHC	Immunohistochemistry
IPG	Immobilized pH Gradient
iPSC	Induced Pluripotent Stem Cell
KLF4	Kruppel-like Factor 4
LN	Lymph Node
mCRPC	Metastatic Castration Resistant Prostate Cancer
MEM	Minimum Essential Media
MET	Mesenchymal to Epithelial Transition
MMDFS	Median Months Disease Free Survival
mRNA	Messenger Ribonucleic Acid
mTOR	Mechanistic Target of Rapamycin
MUC1	Mucin1
NaCl	Sodium Chloride
NaF	Sodium Fluoride
NEPC	Neuroendocrine Prostate Cancer
NOD/SCID	Non-Obese Diabetic/Severe Combined Immunodeficiency
OCT4	Octamer-binding Transcription Factor 4
OS	Overall Survival
OXPHOS	Oxidative Phosphorylation
PAP	Prostatic Acid Phosphatase
PB-Cre4	Probasin-Cre Recombinase 4
PBS	Phosphate Buffered Saline
PC	Prostate Cancer
PCR	Polymerase Chain Reaction
PCSC	Prostate Cancer Stem Cell
PCSLC	Prostate Cancer Stem-like Cell
PESC	Prostate Epithelial Stem Cell
PI3K	Phosphoinositide 3-Kinase
PIN	Prostatic Intra-epithelial Neoplasia
PKM2	Pyruvate Kinase M2
PMSF	Phenylmethanesulfonyl Fluoride

POU5F1	POU Domain, Class 5, Transcription Factor 1
PSA	Prostate Specific Antigen
PTEN	Phosphatase and Tensin Homolog
RCC	Renal Cell Carcinoma
REB	Research Ethics Board
RNA	Ribonucleic Acid
ROC	Receiver Operating Characteristic
RPMI-1640	Roswell Park Memorial Institute 1640
RT-PCR	Reverse Transcription Polymerase Chain Reaction
SD	Standard Deviation
SDS-PAGE	Sodium Dodecyl Sulfate Polyacrylamide Gel Electrophoresis
SE	Standard Error
SF	Serum Free
SFM	Serum Free Media
shABCC2	Short Hairpin ATP-Binding Cassette, Sub-Family C, Member 2
shCTRL	Short Hairpin Control
SOX2	SRY (Sex Determining Region Y) Box 2
STAT3	Signal Transducer and Activator of Transcription 3
TAA	Tumour Associated Antigen
TCGA	The Cancer Genome Atlas
TMPRSS2	Transmembrane Protease, Serine 2
Tris-Cl	Tris-Chloride
TURP	Transurethral Resection of the Prostate
ZEB	Zinc Finger E-Box Binding Homeobox

DECLARATION OF ACADEMIC ACHIEVEMENT

This thesis is presented as a culmination of three manuscripts and one unpublished work. One manuscript has been published, and two are under revision at the time of writing. The manuscripts are as follows:

Nicholas Wong, Judy Yan, Diane Ojo, Jason De Melo, Jean-Claude Cutz, and Damu Tang. Changes in PKM2 Associate with Prostate Cancer Progression. *Cancer Investigation* **2014**, 32, pg 330-338. doi: 10.3109/07357907.2014.919306.

Nicholas Wong, Pierre Major, Anil Kapoor, Fengxiang Wei, Judy Yan, Tariq Aziz, Mingxing Zheng, Dulitha Jayasekera, Jean-Claude Cutz, Damu Tang. Amplification of MUC1 in prostate cancer metastasis and CRPC development. *Oncotarget* (submitted April 2016, in revision since May 2016).

Nicholas Wong, Yan Gu, Anil Kapoor, Xiaozeng Lin, Diane Ojo, Fengxiang Wei, Judy Yan, Jason De Melo, Pierre Major, Geoffrey Wood, Tariq Aziz, Jean-Claude Cutz, Michael Bonert, Arthur J. Patterson, Damu Tang. Upregulation of FAM84B during prostate cancer progression. *Oncotarget* (submitted May 2016, in revision since June 2016).

The fourth piece, an incomplete project, is entitled:

Contribution of ABCC2 to Docetaxel Chemoresistance in Castration Resistant Prostate Cancer

The author, Nicholas Wong, has also contributed to the following publications during the course of his Ph.D. candidacy:

Yanyun Xie, Yen Ting Shen, Anil Kapoor, Diane Ojo, Fengxiang Wei, Jason De Melo, Xiaozeng Lin, **Nicholas Wong**, Judy Yan, Lijian Tao, Pierre Major, and Damu Tang. CYB5D2 Displays Tumour Suppression Activities Towards Cervical Cancer. *BBA – Molecular Basis of Disease* **2016**, 1862, pg 556-565. doi: 10.1016/j.bbadis.2015.12.013.

Judy Yan, Diane Ojo, Anil Kapoor, Xiaozeng Lin, Jehonathan Pinthus, Tariq Aziz, Tarek Bismar, Fengxiang Wei, **Nicholas Wong**, Jason De Melo, Jean-Claude Cutz, Pierre Major, Geoffrey Wood, Hao Peng, and Damu Tang. Neural Cell Adhesion Protein CNTN1 Promotes the Metastatic Progression of Prostate Cancer. *Cancer Research* **2016**, 76, pg 1603-1614. doi: 10.1158/0008-5472.CAN-15-1898.

Yanyun Xie, Yen Ting Shen, Anil Kapoor, Diane Ojo, Fengxiang Wei, Jason De Melo, Xiaozeng Lin, **Nicholas Wong**, Judy Yan, Lijian Tao, Pierre Major, and Damu Tang. Dataset on the Effects of CYB5D2 on the Distribution of HeLa Cervical Cancer Cell Cycle. *Data in Brief* **2016**, 6, pg 811-816. doi: 10.1016/j.dib.2016.01.036.

Xiaozeng Lin, Diane Ojo, Fengxiang Wei, **Nicholas Wong**, Yan Gu, and Damu Tang. A Novel Aspect of Tumourigenesis – BMI1 Functions in Regulating DNA Damage Response. *Biomolecules* **2015**, 5, pg 3396-3415. doi: 10.3390/biom5043396.

Diane Ojo, Xiaozeng Lin, **Nicholas Wong**, Yan Gu, and Damu Tang. Prostate Cancer Stem-like Cells Contribute to the Development of Castration-Resistant Prostate Cancer. *Cancers* **2015**, 7, pg 2290-2308. doi: 10.3390/cancers7040890.

Diane Ojo, Anil Kapoor, Brianne Hill, Xiaozeng Lin, **Nicholas Wong**, Jehonathan Pinthus, and Damu Tang. RKIP is Commonly Downregulated in Clear Cell Renal Cell Carcinoma (ccRCC). *Cancer Cell & Microenvironment* **2015**, 5, e445. doi: 10.14800/ccm.445.

Elisa Giannoni, Maria Letizia Taddei, Andrea Morandi, Giuseppina Comito, Maura Calvani, Francesca Bianchini, Barbara Richichi, Giovanni Raugei, **Nicholas Wong**, Damu Tang, and Paola Chiarugi. Targeting Stromal-Induced Pyruvate Kinase M2 Nuclear Translocation Impairs OXPHOS and Prostate Cancer Metastatic Spread. *Oncotarget* **2015**, 6, pg 24061-24074. doi: 10.18632/oncotarget.4448.

Diane Ojo, Fengxiang Wei, Yun Liu, Enil Wang, Hongde Zhang, Xiaozeng Lin, **Nicholas Wong**, Anita Bane, and Damu Tang. Factors Promoting Tamoxifen in Breast Cancer Via Stimulating Breast Cancer Stem Cell Expansion. *Current Medicinal Chemistry* **2015**, 22, pg 2360-2374. doi: 10.2174/09298673226661504160957 44.

Fengxiang Wei, Diane Ojo, Xiaozeng Lin, **Nicholas Wong**, Lizhi He, Judy Yan, Sarah Xu, Pierre Major, and Damu Tang. BMI1 Attenuates Etoposide-Induced G2/M Checkpoints Via Reducing ATM Activation. *Oncogene* **2015**, 34, pg 3063-3075. doi: 10.1038/onc.2014.235.

Nicholas Wong, Diane Ojo, Judy Yan, and Damu Tang. PKM2 Contributes to Cancer Metabolism. *Cancer Letters* **2015**, 356, pg 184-191. doi: 10.1016/j.canlet.2014.01.031.

Nazihah Bakhtyar, **Nicholas Wong**, Anil Kapoor, Jean-Claude Cutz, Brianne Hill, Michelle Ghert, and Damu Tang. Clear Cell Renal Cell Carcinoma Induces Fibroblast-Mediated Production of Stromal Periostin. *European Journal of Cancer* **2013**, 49, pg 3537-3546. doi: 10.1016/j.ejca.2013.06.032.

Judy Yan, **Nicholas Wong**, Claudia Hung, Wendi Xin-Yi Chen, and Damu Tang. Contactin-1 Reduces E-Cadherin Expression Via Activating AKT in Lung Cancer. *PLoS ONE* **2013**, 8, e65463. doi: 10.1371/journal.pone.0065463.

Nicholas Wong, Jason De Melo, and Damu Tang. PKM2, a Central Point of Regulation in Cancer Metabolism. *International Journal of Cell Biology* **2013**. doi: 10.1155/2013/242513.

CHAPTER ONE

INTRODUCTION AND OVERALL OBJECTIVES

INTRODUCTION

1.1 - Prostate Cancer and Metastasis

The prostate is a walnut shaped gland surrounding the male urethra and is located just below the bladder. Found only in mammals, its primary function is to secrete enzymes, lipids, amines, and metal ions into seminal fluid which aid in sperm mobility and nutrition, protection from acidity and bacteria, and coagulation (Kumar & Majumder 1995). The prostate consists of three histologically distinct regions. The first is the peripheral zone (PZ) which covers approximately 70% of the prostate mass, and is the region from which most prostate carcinomas originate. The central zone (CZ) comprises 25%, and the transition zone encompasses the remaining 5% (Figure 1.1). To fulfill its role as a secretory organ the prostate is comprised of a ductal-acinar histology, which allows it to slowly accumulate and rapidly expel small volumes of fluid. This system is similar to that of larger secretory organs such as the pancreas (Abate-Shen 2000; McNeal 1988).

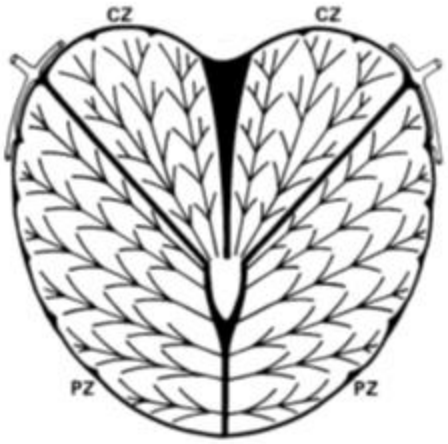

Figure 1.1. Histology and distinct regions of the normal prostate (adapted from McNeal 1988)

Comprising the prostatic epithelium are three major cell types which differ from each other on the basis of morphological characteristics, functional significance, and importance to carcinogenesis. They are organized into two separate compartments of the prostate gland; the basal layer and the luminal layer (Figure 1.2)(Miki 2010). The major prostate epithelial cell is the luminal cell, which is androgen-dependent and responsible for producing secretory proteins. Luminal cells have a low proliferative capacity, high rate of apoptosis, and are characterized by their expression of androgen receptor (AR), prostate specific antigen (PSA), cytokeratins 8 and 18 (CK8 and CK18), and the cell surface marker CD57. Forming a second layer in the prostate gland are basal cells, which are the second major cell type (Figure 1.2). Basal cells do not produce secretory proteins, but are marked by their expression of CK5, CK14, and CD44. They have

a high capacity for proliferation, low rate of apoptosis, and are androgen-independent. Neuroendocrine cells thought to provide peptide growth factors to the luminal cells make up the last type, and are androgen-independent cells dispersed throughout the basal layer (Abate-Shen 2000; Kasper 2008; Lam & Reiter 2006). Finally, the basal lamina encapsulates the entire glandular structure and separates it from the stroma and rest of the prostate.

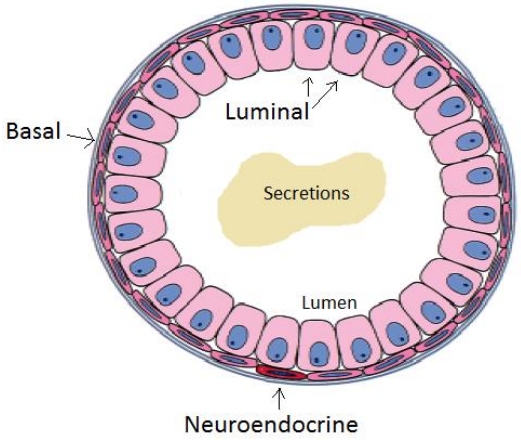

Figure 1.2. Cross section depicting the major cell types and layers of a normal prostate gland (adapted from Abate-Shen 2000)

Prostate cancer (PC) is the most often diagnosed cancer in men (Abate-Shen 2000), and according to the Canadian Cancer Society, approximately 24000 Canadian men were diagnosed and 4100 died from the disease in 2015. PC more often affects elderly men and is thus a larger concern in first-world countries. Three of the greatest risk factors for the development of PC are age, ethnic origin, and heredity, while exogenous factors such as food consumption and environmental exposure can also contribute. Early detection has been aided by the

testing of serum for increased levels of PSA (secreted by proliferating luminal cells) and digital rectal examination (Heidenreich et al. 2014), and treatment plans following diagnosis include active surveillance, local surgical excision, radiation, chemotherapy, and immunotherapy (Abate-Shen 2000; Gottesman et al. 2002). Progression of the disease and effectiveness of therapies can be tracked by testing for serum PSA levels or collecting prostate tissue biopsies with a small needle. Methods for early intervention and treatment have greatly reduced the number of fatalities caused by PC, but patients at advanced stages remain largely incurable (Abate-Shen 2000).

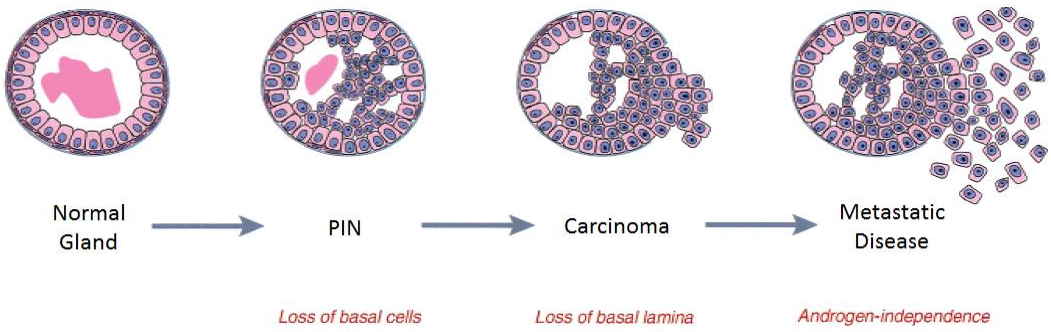

Figure 1.3. Prostate cancer progression from normal epithelium to metastatic disease (adapted from Abate-Shen 2000)

While mechanisms leading to PC initiation and progression remain incompletely understood, accumulative evidence reveals a major role of genomic instability. From this, abnormal processes such as telomere shortening, activation of driver oncogenes, loss-of-function mutations in tumour suppressor genes, and loss of heterozygosity can occur (Gonzalgo & Isaacs 2003). Whole genome

sequencing studies have revealed that, compared to other solid tumour types, PC demonstrates very few genomic mutations and instead is caused by deletions, translocations, and gene fusions. Important alterations involve deletion of the powerful tumour suppressor, phosphatase and tensin homolog (PTEN)(Di Cristofano & Pandolfi 2000), and amplification of AR (Kluth et al. 2015; Grasso et al. 2012). Aside from these, one of the most common occurrences in PC is fusion of the TMPRSS2 gene with members of the large ETS family responsible for transcriptional regulation. Fusions frequently occur with ERG, ETV1, ETV4, and ETV5. 40-70% of PC cases are positive for TMPRSS2-ERG fusion making it the most regularly altered member, likely because both genes are located at chromosomal locus 21q22 (Tomlins et al. 2008; Burdova et al. 2014). Studies have shown that although the TMPRSS2 gene codes for an untranslated mRNA, its androgen-responsive elements allow for overexpression of ERG via the gene fusion. Androgen mediated stimulation increases ERG expression in PC cells *in vitro* and castration of mice decreases its levels in xenografts. Knockdown of ERG inhibits invasion and reduces expression of genes associated with PC (Tomlins et al. 2005; Hendriksen et al. 2006; Mertz et al. 2007; Tomlins et al. 2008). Another genomic region that greatly impacts many cancer types including PC is cytoband 8q24. Classified as a gene desert because of a 1.2Mb long region absent of coding genes, flanking either end are the FAM84B and c-MYC (an important pluripotency factor discussed in Section 1.5) genes (Al Olama et al.

2009). Within the gene desert lies a pseudogene of OCT4 (a second important pluripotency factor discussed in Section 1.5), POU5F1P1/POU5F1B (Ghoussaini et al. 2008). Alterations in c-MYC have been well studied as contributing to PC tumourigenesis (Van Duin et al. 2005; Liu et al. 2008) and increased POU5F1P1 expression has also been observed (Kastler et al. 2010), indicating this genomic region is important in PC progression. Further studies determined that this gene desert contains regulatory elements and enhancers, and contributes to tumourigenesis by interacting with distant target genes (Meyer et al. 2011; Pomerantz et al. 2009; Du et al. 2015), emphasizing its impact on PC.

The accumulation of alterations in the prostate epithelia leads to loss of basal cells, the basal lamina, and ultimately metastasis. In the 1960s, a histology-based method of assessment was developed for prostate carcinoma by Dr. Donald F. Gleason and his colleagues. Now the most commonly used system for determining pathology of the disease, the Gleason grading system categorizes adenocarcinomas into five different grades based on histological patterns and glandular differentiation. The grading stages progress in order of severity from Grade 1 to Grade 5. When a histological section of prostate carcinoma is examined for diagnosis, a Gleason Score (GS) is given which provides grades for the two most common cell patterns. In doing this, a more definitive diagnosis can be made and an overall score adding the two grades together is provided. Therefore, GS ranges from 2-10 with 10 being the most severe (Humphrey 2004).

Gleason Grade 1 is identified by minimally differentiated glands which remain circular and individualized, appearing the most similar to healthy prostate. Throughout the stages up to Grade 5, the glands become more elongated and irregularly shaped, decrease in size, and begin forming chain-like structures. At the most detrimental stage, glands become extremely difficult to identify because of severe cell diffusion and decreased glandular size (Figure 1.4). At a more cellular level, prostate cancer progression is defined by the loss of basal lamina cells and proliferation/migration of luminal cells within the glands.

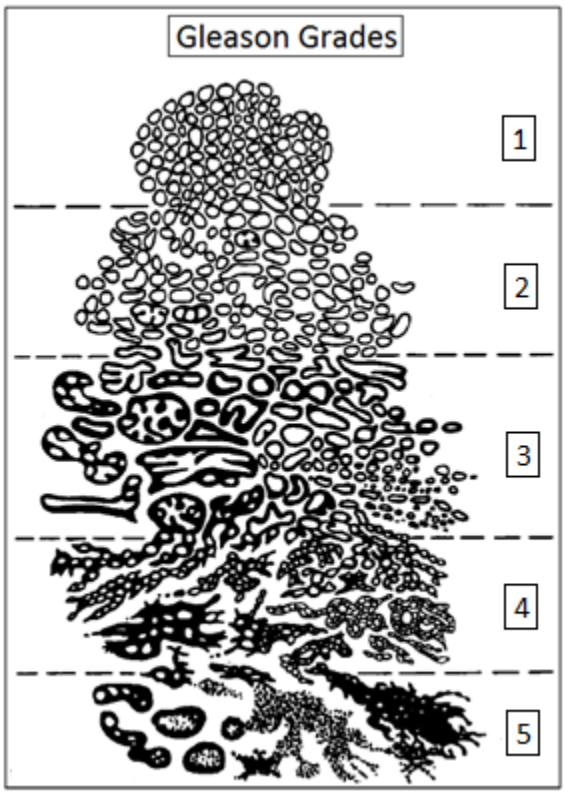

Figure 1.4. Representative drawings of the five different Gleason grades used to determine the pathology of prostate cancer tissues (adapted from Humphrey 2004)

The end result of failed therapies (discussed further in Section 1.2) is metastatic castration resistant prostate cancer (mCRPC), which is defined as a biochemically or clinically progressive metastatic disease despite the loss of serum testosterone levels (Collins et al. 2006), and is the cause of most prostate cancer related fatalities. At this stage, life expectancy is only between 1-4 years (West et al. 2014; Scher et al. 2008), and very few treatment options are available due to a lack of understanding of the cancer's progression (Watson et al. 2015). CRPCs may result from selection for androgen-independent cells already present in the heterogeneous tissue at the time of treatment, and/or an accumulation of genetic modifications and adaptive responses inferring survival to tumour initiating cells (Hadaschik & Gleave 2007). One major cause of castration resistance is the persistence of AR signalling despite attempts to abolish circulating androgen. Mechanisms include upregulation of AR expression, *in situ* steroid synthesis, point mutations in the DNA binding domain for continued activation of gene targets, constitutively active splice variants, and secondary pathways which can stimulate the AR pathway (Graham & Schweizer 2016).

The difficulty of treating PC is that the disease often progresses to metastasis, and out of all newly diagnosed cases roughly 20% are metastatic. The most common site for metastasis is bone, but other major sites include distant lymph nodes, the liver, and the thorax (Gandaglia et al. 2014). Initial hormonal therapies such as androgen deprivation therapy (ADT) cause considerable bone

loss (Shahinian et al. 2005; Diamond et al. 2004; Preston et al. 2002), so the impact of bone metastasis on the skeleton is tremendous. Migrated PC cells can also induce osteoblasts to increase bone formation and osteoclasts to upregulate bone absorption. Such compounding factors and excessive activity cause major symptoms including pain, bone fractures, spinal cord compression, suppression of bone marrow growth, and hypercalcemia, which are all key causes of morbidity (Bagi 2003). It was revealed that individuals with less than six bone metastases had a more favourable survival outcome than those with six or more (Soloway et al. 1988), highlighting the impact of bone metastasis on life expectancy.

1.2 – Therapeutic Approaches for Treating Prostate Cancer

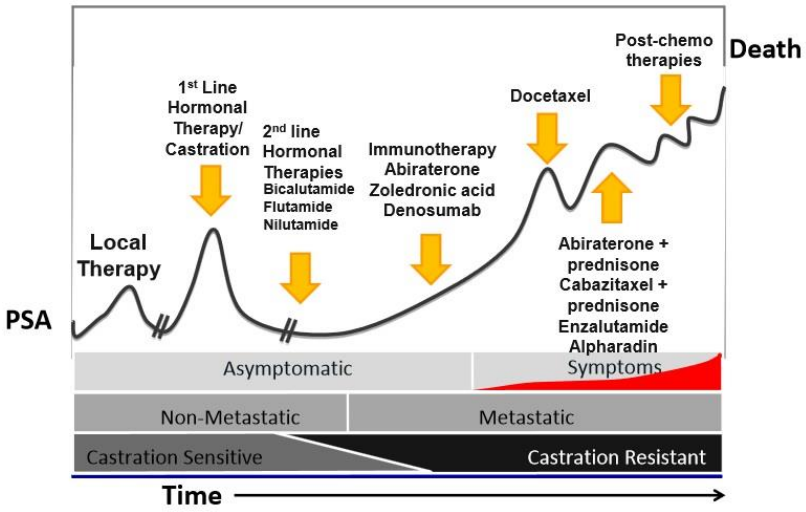

Figure 1.5. The course of prostate cancer therapies over time based on serum PSA concentrations (Acquired with permission from a presentation by Dr. Bobby Shayegan, 2014)

The progression of prostate cancer can be tracked by digital rectal examinations, tissue biopsies, and serum PSA concentrations (Figure 1.5). In the initial stages of development, the disease can be remedied through surgical excision of the tumour. More aggressive forms such as higher Gleason and metastatic cancer are treated using ADT, which acts to eliminate or block the function of testosterone in the body. Removal of testicular-derived androgens can be achieved through bilateral orchiectomy and/or administration of synthetic analogues of gonadotropin-releasing hormone or luteinizing hormone-releasing hormone. Adrenal glands also produce androgens which can be counteracted by additional anti-androgen synthetics (Eisenberger et al. 1998). The desired effect is apoptosis of androgen-dependent cancerous cells derived from normal androgen-dependent prostate epithelial cells (Abate-Shen 2000). Unfortunately this therapy is often short-term and leads to CRPC.

Normally when dihydrotestosterone (DHT) binds to AR in the cytoplasm, it induces a conformational change in the receptor which releases it from stabilizing chaperone proteins and allows for the formation of a homodimer and translocation to the nucleus. Here, AR activates transcription of target genes such as PSA, KLK2, NKX3A, TMPRSS2, TMEPA1, and SPAK involved in the growth, survival, and differentiation of PC cells (Tan et al. 2014; Nelson et al. 2002; Attar et al. 2009; Kahn et al. 2014). But in malignant cells, constant AR signalling leaves the expression of these genes unchecked. Consistent AR

signalling despite ADT is a key factor in the perpetuation of CRPC development. Therapeutic options used to help impede AR signalling include inhibitors of the androgen receptor, androgen biosynthesis blockers, and blockade of the AR signalling pathway. Antiandrogens such as bicalutamide, nilutamide, and flutamide act to block the receptor from binding testosterone. However these compounds provide modest benefits (Group 2000) and in the long term can actually act as agonists and stimulate AR signalling (Chen et al. 2004; Tran et al. 2009). A powerful androgen synthesis blocker, abiraterone, indirectly inhibits the production of testosterone from not only the testes and adrenal glands if the patient is pre-castration, but also from the cancerous tumour itself (Schweizer & Antonarakis 2012). Clinical trials examining the efficacy of abiraterone in mCRPC patients yielded positive and promising results by improving overall survival (Han et al. 2015). The first approved inhibitor of AR signalling, enzalutamide, functions using a novel mechanism of action. By blocking the binding of androgens to AR, impairing nuclear translocation, and inhibiting DNA binding, this compound revealed positive clinical responses in multiple studies involving mCRPC patients (Schalken & Fitzpatrick 2016).

An alternative modality for treating CRPC is immunotherapy, which takes advantage of the host's immune system and the concept that genetic and epigenetic changes in cancerous cells create new foreign antigens (Farkona et al. 2016). One major breakthrough for the treatment of mCRPC was development of

the sipuleucel-T vaccine. Peripheral blood mononuclear cells are purified from the patient's own blood and presented with a fusion protein of prostatic acid phosphatase (PAP) and granulocyte-macrophage colony stimulating factor (GM-CSF). This promotes differentiation into dendritic cells which when reintroduced back into the patient will generate PAP-derived immunogenic responses (Gulley et al. 2016). Sipuleucel-T is an example of an *ex vivo* vaccine where the patient's own immune cells are harvested, processed, and re-infused. On the other hand, *in vivo* vaccines act by injecting the patient with a cocktail of tumour associated antigens (TAAs) and targeting molecules to present the peptides to immune cells (Gerritsen 2012). TAAs are proteins expressed in both normal and cancer cells but are mutationally altered in the latter (de Paula Peres et al. 2015). The strategy of displaying these peptides to dendritic and other antigen presenting cells (APCs) can be applied to many different PC-related proteins including PAP, PSA, HLA-A2, and MUC1 (Gerritsen 2012; Major et al. 2012; McNeel 2007). Other forms of immunotherapy include the use of monoclonal antibodies targeted against antigens on the tumour cell surface, oncolytic viruses which specifically target and lyse cancer cells, and the use of immune checkpoint inhibitors (Farkona et al. 2016).

Following failure of ADT and immunotherapy strategies, the next line of defense against mCRPC is chemotherapy. One class of powerful anti-cancer drugs is the taxanes, derived from the bark of the yew tree but later on produced

synthetically. They are able to stably bind to tubulin in microtubules and prevent their depolymerisation, leading to a disruption in cytoskeletal dynamics, mitotic arrest, and eventual apoptosis (Baker et al. 2006; Abidi 2013). The first agent discovered was paclitaxel in 1967 (Wani et al. 1971) and approved for clinical use for multiple cancers in 1995 (Jordan & Wilson 2004). Clinical trials with mCRPC patients examining its use alone or in combination with other drugs demonstrated increases in overall survival and a decline in PSA levels (Solit et al. 2003; Smith et al. 2003; Trivedi et al. 2000). In 2004 the semisynthetic taxane docetaxel, a more active derivative of paclitaxel (Paller & Antonarakis 2011), was approved by the FDA. Several clinical trials involving men diagnosed with mCRPC revealed the efficacy of docetaxel treatment over paclitaxel in improving median survival and quality of life while reducing pain and serum PSA levels. Unfortunately, the survival benefit of docetaxel was found to only be 2 to 3 months (Petrylak et al. 2004; Tannock et al. 2004; Berthold et al. 2008). In addition, some tumours may either develop docetaxel resistance or be entirely insensitive to its effects (Paller & Antonarakis 2011). For these reasons, a second-generation taxane, cabazitaxel, was approved for clinical use in 2010. This agent similarly binds to microtubules and interrupts cellular dynamics, but although its mechanism of action is similar to paclitaxel and docetaxel, studies revealed an increased efficiency due to low substrate affinity to ATP-dependent drug efflux pumps, higher intratumoural accumulation, and targeting of its own distinct

molecular pathways (De Leeuw et al. 2015; de Morrée et al. 2016; Borst et al. 2000). Early experiments in 2000 established cabazitaxel's superior effectiveness in treating models of paclitaxel and docetaxel resistance (Bono et al. 2010). Clinical trials examining treatment with cabazitaxel revealed an improvement in overall survival by another 2 to 3 months for mCRPC patients who had become docetaxel-resistant (Bono et al. 2010; Mita et al. 2009). To this day, docetaxel and cabazitaxel remain the first and second lines of defense against mCRPC.

1.3 - Prostate Cancer Stem Cells

The severity of advanced PC owes to the extremely complex network of characteristics such as cell heterogeneity, adaptation to therapeutic treatment, and a variety of cellular events which all come together to both initiate and perpetuate the disease (Chang et al. 2014). One viewpoint to understand this heterogeneity is the stochastic model (Figure 1.6), which states that all cells of a tumour are biologically equivalent but can be influenced by intrinsic and extrinsic factors which alter their gene expression. Therefore, any cancer cell is capable of initiating tumour formation, and cannot be isolated based on unique traits. However, one of the growing cancer models widely referred to today is the cancer stem cell (CSC) or hierarchy model (Figure 1.6), which states that the disease can originate from or be re-populated by only a small percentage of cells with stem-like characteristics and differentiation potential. In this paradigm, tumour

initiating cells may be isolated based on their intrinsic traits for future *in vitro* study (Dick 2009).

By definition, a stem cell is able to differentiate into a heterogeneous group of cells, have the capacity for self-renewal, and maintain homeostatic control according to environmental signals (Dalerba et al. 2007). They are also known to exist in a quiescent state (Dean et al. 2005), growing slowly and only proliferating in times of tissue repair. It is also widely accepted that normal and cancer SCs possess anti-apoptotic and drug-resistant properties to ensure survival. In 1971 it was revealed that although mouse myelomas can arise from a single cell, the resulting tumour cells are not identical, providing evidence of tumour heterogeneity (Park et al. 1971). Additionally, serial transplantations of putative CSCs from mouse to mouse provided evidence of their self-renewal capacities. However, the question of whether CSCs are originally normal stem cells or if they are cancer cells with acquired stem-like traits remains to be determined (Regenbrecht et al. 2008).

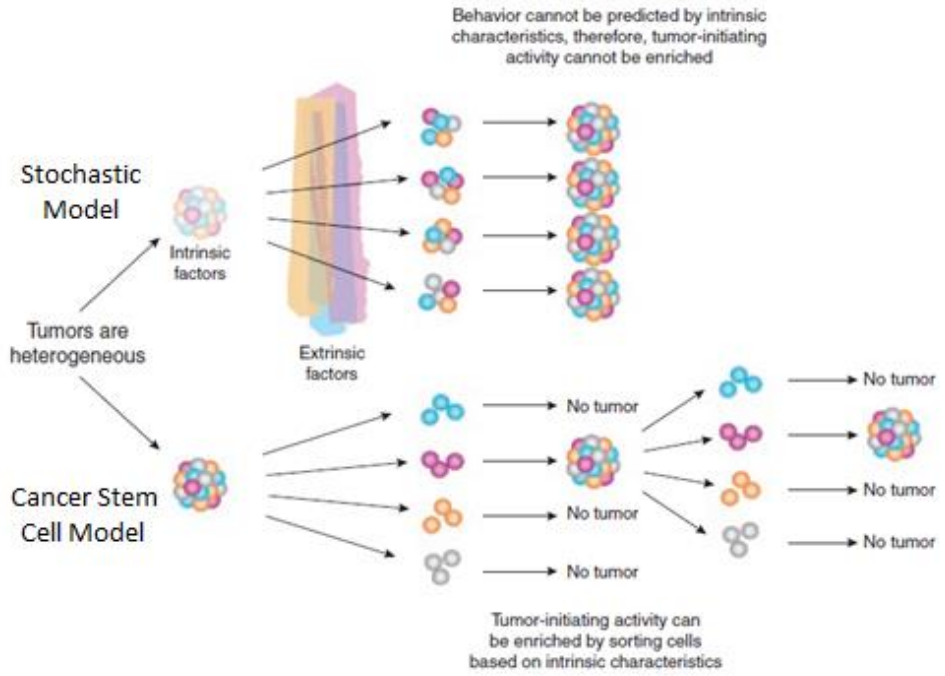

Figure 1.6. The two models of tumour heterogeneity (adapted from Dick 2009)

If tumours can truly be regenerated from a small population of slowly proliferating CSCs, then aggressive treatment strategies which rely on targeting actively dividing cells such as chemotherapy and radiotherapy would prove ineffective. For this reason it became apparent to develop stem cell specific approaches, and to do that, isolation methods became imperative. One such approach established in the 1990s is the exclusion of Hoechst 33342, a fluorescent dye commonly used for DNA staining in live cells. In staining murine bone marrow cells, researchers observed an unusual emission pattern which led them to discover a small subset of cells which expressed haematopoietic stem cell surface markers, greater stem cell activity, and higher *in vivo* tissue reconstitution

capacity. Further examination identified an ATP-dependent drug transporter protein as the cause of Hoechst dye efflux (Goodell et al. 1996). This led to the principle of Hoechst dye exclusion in identifying CSCs, deemed the side-population, in various cancers such as brain, breast, lung, intestine, liver, and ovarian (Szotek et al. 2006; Chiba et al. 2006; Komuro et al. 2007; Hirschmann-Jax et al. 2004; Kondo et al. 2004). The exclusion of dye governed by drug-transporter proteins implies the ability to evade anti-mitotic effects of cytotoxic drugs, which is one of the main causes of cancer relapse for many organ types.

Due to the proposed similarities between normal and cancer SCs, many have attempted to isolate CSCs using the same cell surface markers indicative of their counterparts from normal tissue. Once the expression of these markers is confirmed, the small population of cells can be isolated *in vitro* as a single cell suspension from the bulk tumour (Dalerba et al. 2007). The first CSCs to be identified originated from acute myeloid leukemia, and expressed markers similar to normal haematopoietic stem cells ($CD34^{+}CD38^{-}$). This population possessed high proliferative and self-renewal characteristics, and were able to generate leukemia in NOD/SCID mice (Bonnet & Dick 1997). Since then, researchers have been able to extend these strategies to identify CSCs from a variety of other organs including the brain, breast, colon, pancreas, and prostate (Li et al. 2007; Ricci-Vitiani et al. 2007; Al-Hajj et al. 2003; Singh et al. 2003). All of these stem-like cells displayed specific surface markers allowing for separation from the rest

of the heterogeneous population. Work *in vitro* demonstrated that these cells possessed self-renewal capacity and increased rates of proliferation. Studies *in vivo* in NOD/SCID mice further supported these findings, determining that fewer cells with these antigenic profiles were able to initiate tumours histologically indistinguishable from human samples while cells lacking the cell surface markers could not form tumours at all.

Once the CSC population is identified and isolated through Hoechst dye exclusion or cell surface marker status by fluorescence activated cell sorting (FACS), it can be propagated and studied *in vitro* under anchorage-independent conditions. Under serum free media (SFM) conditions CSCs can be enriched for and propagated as spheres in suspension (Li et al. 2007; Ricci-Vitiani et al. 2007; Al-Hajj et al. 2003; Singh et al. 2003), a concept that was first demonstrated for normal neural stem cells (Reynolds & Weiss 1992) and eventually extended to many cancer types such as brain, lung, ovarian, breast, prostate, and colon (Dubrovska et al. 2008; Dontu et al. 2003; Wei et al. 2007; Eramo et al. 2008; Zhang et al. 2008; Kondo et al. 2004; Ricci-Vitiani et al. 2007). One of the advantages to spheroid culture is its similarity to 3D tissues, allowing researchers to test treatment regimens on a multidimensional model. Anti-cancer strategies such as chemotherapy and radiotherapy act differently in single versus multi-layer cellular organizations, making sphere-based studies a powerful *in vitro* tool prior to animal studies (Hirschhaeuser et al. 2010).

In the normal prostate, a gland is separated into the basal and luminal layers. Luminal cells express AR and rely on androgens for growth while basal cells are largely negative for AR. Androgen depletion studies performed on murine models in the 1980s uncovered that following ADT, 90% of luminal cells underwent apoptosis causing involution of the gland, while the basal cells preferentially survived (Kyprianou & Isaacs 1988). If androgen was resupplied, secretory glandular structures could be restored. This cycle of cell death and regeneration could be repeated up to 30 times, suggesting the survival of a small population of prostatic epithelial stem cells (PESCs) in the basal layer capable of restoring tissue and function (Tsujimura et al. 2002). Throughout the years it has been shown that basal cells are mostly undifferentiated and retain a high proliferative potential while growing slowly under normal conditions, further supporting the existence of quiescent PESCs in the basal layer (Schalken & Van Leenders 2003). Using prostate basal cells as a starting point, cell surface markers that have been determined to identify PESCs include CD44, α2β1 integrin, and CD133 (Collins et al. 2001; Richardson et al. 2004; Vander Griend et al. 2008; Patrawala et al. 2007). CD133 was first used to identify haematopoietic and endothelial stem cells (Shmelkov et al. 2005), but was later extended to many tissue and cancer types. Studies examining the co-expression of markers demonstrated that this cell surface signature represents only about 1% of the population which agrees well with the stem cell model (Pellacani et al. 2011).

Cells with the $CD44^{+}\alpha2\beta1^{hi}CD133^{+}$ phenotype could be isolated from tumours with varying Gleason Grade and metastatic status, suggesting that such antigenic profiles may also identify prostate cancer stem cells (PCSCs). Characterization of these cells revealed a higher capacity for proliferation, self-renewal, differentiation, and invasion (Collins et al. 2005). Hoechst dye exclusion has also been used to isolate stem-like populations from multiple PC cell lines which demonstrated greater colony formation and tumourigenic potential (Chen et al. 2012). Enrichment of stem-like cells as non-adherent spheres in SFM conditions has also been done for several other PC cell lines with similar observations (Zhang et al. 2012).

1.4 - Cancer Metabolism and Prostate Cancer Stem Cells

Efficient breakdown and use of energy sources is imperative for cell survival and proliferation, and cancer cells are no different. In normal cells, glucose metabolism in the presence of oxygen is primarily governed by mitochondrial oxidative phosphorylation (OXPHOS). In the cytoplasm, glucose is metabolized via glycolysis through a series of intermediates into the final product pyruvate, which enters the mitochondria and is further oxidized for energy production. Oxygen, as the final electron acceptor, is necessary for this process. Alternatively in the absence of oxygen, cells undergo anaerobic glycolysis in which pyruvate is converted into lactate. OXPHOS generates 36 mol ATP/mol of

glucose, making it the more efficient of the two pathways (Figure 1.7, left)(Heiden et al. 2009).

Almost a century ago, Otto Warburg was the first to discover that cellular respiration in cancer cells was altered, revealing an accelerated process of glycolysis in conjunction with a decreased need for oxygen consumption (Higgins et al. 2009; Warburg et al. 1927; Warburg 1956). More specifically, increased levels of lactate were observed even in the presence of oxygen, indicating cancer cells were shuttling glucose through the glycolysis pathway despite 4 mol ATP/mol glucose produced (Figure 1.7, right)(Heiden et al. 2009). This was eventually termed aerobic glycolysis, or the Warburg effect (Warburg 1956; Warburg et al. 1927). Studies have shown that cancer cells upregulate aerobic glycolysis by altering pathways which enhance its activity, such as the PI3K/AKT/mTOR pathway, HIF-1α, and c-MYC (Porporato et al. 2011; Chaneton & Gottlieb 2012). All of these observations pointed towards a significant phenomenon occurring in tumourigenic cells. Further investigations established that the glycolytic intermediates could be utilized as cellular building blocks, acting as preliminary structures for conversion into nucleotides, amino acids, and lipids. With a pool of macromolecules standing by, cellular proliferation can continue on with fewer resource-limiting restrictions (Wong et al. 2013; Hsu & Sabatini 2008; Heiden et al. 2009).

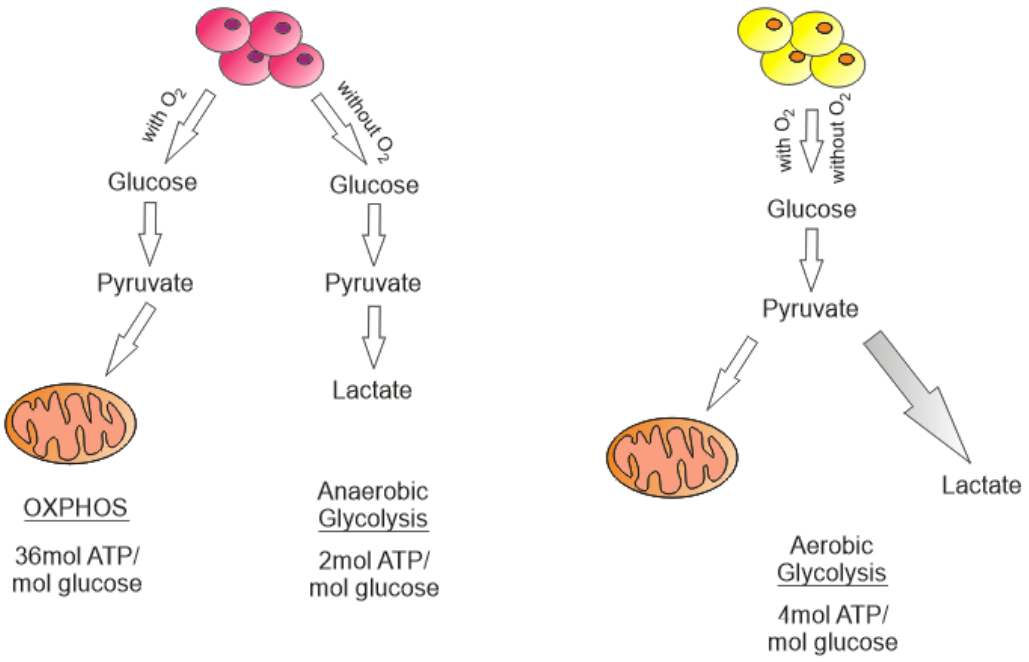

Figure 1.7. Schematics of the oxidative phosphorylation, anaerobic glycolysis, and aerobic glycolysis pathways

ADT significantly reduces blood flow to the prostate inducing a hypoxic environment which can alter growth and sensitivity to apoptotic signals (Ghafar et al. 2003). Hypoxia is the deprivation of oxygen supply, and can also arise within solid tumours when the speed of proliferation outpaces proper vascularization for oxygen delivery. Studies have shown that growth in hypoxic conditions leads to more aggressive and less responsive disease (Semenza 2000; Vaupel et al. 2001; Ghafar et al. 2003). In DU145 cells hypoxia induced higher expression of HIF-1α (Bourdeau-Heller & Oberley 2007), a transcription factor responsible for regulating anaerobic metabolism, proliferation, and metastasis (Carmeliet et al. 1998; Semenza 2007). Hypoxia is also important in maintaining the tumour

microenvironment for CSCs by influencing self-renewal and differentiation, in part by upregulating stemness factors (Li & Rich 2010). Additionally, epigenetic modifications can promote metabolic reprogramming and induction of CSCs which have been found to overexpress important metabolic proteins such as glycine decarboxylase and pyruvate kinase M2 (Luo & Semenza 2012; Zhang et al. 2013; Vincent & Van Seuningen 2012; Dominy et al. 2012). Taken together, ADT, hypoxia, and altered metabolic pathways may create a microenvironment ideal for CSC maintenance and progenitor proliferation.

1.5 - Prostate Cancer Stem Cells Allow for Chemoresistance and Metastasis

The CSC model (Figure 1.6) states that the heterogeneity of tumours is due to a small sub-population of tumour-initiating cells that retain stem-like characteristics. These CSCs are thought to remain in a quiescent state and able to produce more differentiated progenitor cells when needed to constitute the bulk tumour mass. Accumulating knowledge now points towards PCSCs as being a cause of PC relapse, chemoresistance, and metastasis (Clarke & Fuller 2006; Gupta et al. 2009), with many mechanisms being upregulated which contribute to their therapeutic resistance (McCubrey et al. 2010). Thus, specific targeting of these pathways in CSCs has become crucial to controlling CRPC. However, because of the limited choice of markers which differentiate CSCs from normal stem cells, this remains challenging.

A large effort has been made to establish the possible signalling pathways which provide mechanisms for chemoresistance in PCSCs. The PI3K/AKT/mTOR pathway has been associated with both tumourigenesis and therapeutic resistance in many cancers owing to its control over many cellular functions including cell survival, proliferation, metabolism, angiogenesis, differentiation, and migration (Bitting & Armstrong 2013). In PC specifically, its activation has been strongly correlated with disease progression (Taylor et al. 2010; Pourmand et al. 2007; Reid et al. 2010). Activity of the PI3K/AKT/mTOR pathway is governed by the potent tumour suppressor PTEN, which is a frequently mutated gene in human cancers (Di Cristofano & Pandolfi 2000), and in PC these alterations lead to higher Gleason Score, poorer prognosis, castration-resistant growth, and higher incidence of metastasis (Pourmand et al. 2007; Mulholland et al. 2011). It has been established that PTEN mutation results in CSC emergence, maintenance, and tumourigenic capacity (Yilmaz et al. 2006; Dubrovska et al. 2008), and $PTEN^-$ PC cells demonstrated greater resistance to doxorubicin and paclitaxel by induction of ABC transporter expression (Lee et al. 2004). PCSCs were also found to be more resistant to etoposide and docetaxel treatment (Yan & Tang 2014). Inhibition of the PI3K/AKT/mTOR pathway reduced sphere formation capacity and chemoresistance in a population of stem-like PC cells (Ni et al. 2014). Targeting of this pathway using a dual inhibitor sensitized CRPC cells to docetaxel both *in vitro* and *in vivo* (Yasumizu et al.

2014). Based on the considerable amount of data which exists on this topic, it is evident that the PI3K/AKT/mTOR pathway greatly contributes to PC progression and chemoresistance, which may be attributable to PCSCs.

The Wnt/β-Catenin signalling pathway controls cell fate, proliferation, and migration, enhances AR transcriptional activity, and has been implicated in chemoresistance and CSC biology. Stimulation of Wnt/β-Catenin along with AR expression strongly correlated with the aggression and metastasis of PC cases (Truica et al. 2000; Jung et al. 2013). Activation of this pathway was found to promote PC progression in an animal model (Yu et al. 2011), and downregulation reduced stem-like characteristics in PC cells, tissues, and *in vivo* models (Hsieh et al. 2013). Wnt/β-Catenin signalling also contributes to the self-renewal of normal and cancer SCs from multiple organ types including prostate. In PC cell lines, activation of the pathway caused upregulation of sphere size and self-renewal, while inhibition decreased both sphere formation and sphere size (Bisson & Prowse 2009). In brain and liver cancer cell lines chemoresistance to 5-fluorouracil and docetaxel was mediated by the Wnt/β-Catenin pathway (Flahaut et al. 2009; Noda et al. 2009), and upstream signalling may also co-activate ABC transporters as suggested in ovarian cancer cells (Chau et al. 2012).

The Hedgehog and Notch signalling pathways have important roles in tumour progression, metastasis, and the self-renewal of CSCs. Increased expression of these proteins was found in CRPC cells and patient-derived

circulating and tumour CRPC samples, as well as in a sub-population of PCSCs exhibiting docetaxel resistance (Zhu et al. 2013; Shaw & Prowse 2008; Domingo-Domenech et al. 2012). Inhibition of either pathway leads to reduced cell growth, apoptosis, and resensitization to taxane therapy both *in vitro* and *in vivo*. Additionally, inhibition of Hedgehog signalling abolished the PCSC population in mCRPC cells while overexpression increased it (Singh et al. 2012; Wang et al. 2011; Ye et al. 2012; Chang et al. 2011). Taken together, there are a number of different molecular signalling pathways prominent in PC that can impact PCSC biology, induction of chemoresistance, and development towards mCRPC. To make matters more complicated, compounding and overlapping mechanisms between the pathways also exist, underscoring the importance of targeting these signals for clinical success.

There are two possibilities to address the origin of CSCs. Either a pre-existing normal stem cell is transformed into a CSC as a result of mutation, or differentiated tumourigenic cells acquire stem-like characteristics such as self-renewal and therapeutic resistance. Although many biological models describe a unidirectional modality of stem cell to differentiated progeny, more recent studies have demonstrated the reverse where terminally differentiated normal epithelial cells are able to de-differentiate back into stem-like cells. The same was true for tumourigenic cells which could convert back into CSC-like cells (Chaffer et al. 2011). Termed epithelial to mesenchymal transition (EMT), this process is

characterized by the conversion of an epithelial cell into a mesenchymal cell (Giannelli et al. 2016) and normally occurs during embryogenesis and adult tissue repair (Okada et al. 1997). This event is marked by downregulation of epithelial traits such as cell-to-cell and cell-to-extracellular matrix adhesion, and a corresponding increase in mesenchymal traits like greater migration, invasion, and anti-apoptotic characteristics (Kalluri & Weinberg 2009). Coincidentally, these attributes are precisely what is necessary for cancer cells to undergo metastasis to distant sites (Dunning et al. 2011).

The landmark discovery that ectopic expression of just four transcription factors could reprogram differentiated epithelial cells into induced pluripotent stem cells (iPSCs) had an enormous impact on the field of stem cell biology (Takahashi & Yamanaka 2006). Further studies revealed that iPSCs can form progeny of any cell type as evidenced by the formation of teratomas in mice (Park et al. 2008). Since then, transduction of the four transcription factors (SOX2, OCT4, c-MYC, and KLF4) has successfully reprogrammed primary prostate stromal fibroblasts into prostatic iPSCs which could differentiate into luminal-like cells expressing AR and PSA (Moad et al. 2013). These observations supported the possibility that PC cells could also undergo EMT through activation of the four pluripotency factors. In support of this, OCT4 expression and activation of its target genes was found to be increased in a docetaxel resistant line which also displayed greater tumourigenicity *in vivo* (Linn et al. 2010). Furthermore, the

upregulation of SOX2 and OCT4 in PC stem-like populations has been reported by multiple groups, as well as greater transcript levels in PC tissues compared to normal prostate (Bae et al. 2010; Gu et al. 2007; Rybak & Tang 2013). From this it could be inferred that PCSCs initiate metastasis by upregulating pluripotency factors to allow for greater plasticity and EMT. Studies have shown isolated stem populations as being AR^- (Patrawala et al. 2006; Collins et al. 2005), and the cell surface marker CD166 which is high in CRPC cases corresponded with increased sphere formation *in vitro* (Jiao et al. 2012). Together these reveal a connection between PCSCs and CRPC which may provide explanation for the increased incidence of metastases at this stage.

1.6 - Overall Objectives

In recent years, our laboratory's own research has demonstrated the isolation and characterization of a PC cell line with sphere-propagating capabilities and stem-like properties. The DU145 cell line was derived from a human prostatic carcinoma that had metastasized to the brain and was found to be androgen-independent (Mickey et al. 2007). This cell line is thus a good model for mCRPC, and is ideal to address the questions of androgen-independent metastasis. When seeded in serum free media (SFM), 1.25% of DU145 monolayer cells are capable of forming DU145 spheres (or prostate cancer stem-like cells, PCSLCs) which grow in suspension. 26% of these sphere cells are then able to

initiate the formation of secondary spheres, which creates a line that can be passaged over 30 times without significant loss of their stem-like features (Rybak et al. 2011). Cell surface marker characterization of these PCSLCs indicated the expression of basal and luminal prostate epithelial cytokeratins as well as CSC markers such as CD44, CD24, and α2β1 integrin. Experimentation *in vitro* demonstrated the stem-ness of these PCSLCs. When seeded back into serum conditions, the spheres are able to differentiate back into the heterogeneous population of monolayer cells (validated by a reduction in stem cell surface marker expression), and can then be re-isolated back into spheres under serum free conditions. This aspect of our PCSLCs indicates a high capacity for plasticity. DU145 PCSLCs also displayed an enhanced tumourigenic capacity in NOD/SCID mice. 100-fold fewer cells were required to form tumours of the same volume compared to DU145 monolayer cells (Rybak et al. 2011). All of these findings have substantiated our belief that our DU145 PCSLCs represent a possible PCSC line.

Investigating the differences between our DU145 monolayer and DU145 PCSLC lines may help to uncover the genes and mechanisms which allow for CSC maintenance and survival. Characteristics associated with advanced PC such as proliferation potential, cell plasticity, greater tumourigenicity and invasion, and increased chemoresistance can be inspected more closely in our DU145 PCSLCs. In examining these two cell populations our lab has conducted Affymetrix

microarray analysis, and in doing so created a list of the top twenty upregulated and downregulated genes in our PCSLCs compared to the parental cells.

The overall intent of the author's research was to characterize as many candidates as possible and evaluate whether these genes are relevant in PC progression and clinical application. As such, this thesis is organized into 6 major chapters where four different candidate proteins are assessed for their contribution to PCSC biology and the stages of PC development. Chapter 2 discusses PKM2, the rate limiting enzyme of glycolysis which controls the metabolic fate of pyruvate. This work focuses on the differences of PKM2 in CSCs and its relation to PC progression. In Chapter 3 we investigate the glycoprotein MUC1 which apart from epithelial cell protection plays an important part in oncogene activation in PC. Here we examine its expression in PCSCs and its association with the various stages of PC. Chapter 4 attempts to shed light on FAM84B, which to date has had very little attention in the field of PC research. Its close chromosomal proximity and co-expression with pluripotency factors makes it an intriguing candidate in our PCSLCs and in advanced stages of cancer. Chapter 5 examines the possible contribution of an ATP-dependent drug transporter ABCC2 to docetaxel chemoresistance in PC. Lastly, Chapter 6 will discuss the overall significance of these candidates in CSC biology and clinical relevance for PC therapy.

CHAPTER TWO

CHANGES IN PKM2 ASSOCIATE WITH PROSTATE CANCER PROGRESSION

Nicholas Wong,[1,2,3] Judy Yan,[1,2,3] Diane Ojo,[1,2,3] Jason De Melo,[1,2,3] Jean-Claude Cutz,[4] and Damu Tang[1,2,3,#]

[1]Division of Nephrology, Department of Medicine, McMaster University; [2]Father Sean O'Sullivan Research Institute, [3]the Hamilton Center for Kidney Research, St. Joseph's Hospital; [4]Department of Pathology and Molecular Medicine, McMaster University, Hamilton, Ontario, Canada

Cancer Investigation **2014**, 32, pg 330-338. doi: 10.3109/07357907.2014.919306.

Author Contributions

Dr. D. Tang and N. Wong designed the experiments. N. Wong carried out the experiments, organized data, and analyzed the results. Dr. J. Yan helped design experiments. D. Ojo performed the 2-D gel electrophoresis. Dr. J. De Melo searched for and identified applicable primary prostate tissues to include in the study. Dr. J.C. Cutz verified and confirmed all prostate cancer tissues. Dr. D. Tang and N. Wong prepared and edited the manuscript.

Relationship to Ph.D. research

The work here reveals that PCSLCs may be metabolically different from PC progenitor cells *in vitro* and/or *in vivo* on the basis of PKM2 expression, the rate limiting enzyme of aerobic glycolysis. This research demonstrated an association between PKM2 and advanced PC based on primary tissues and by utilizing PCSLCs as a disease model. Unique post-translational modifications were also identified in this population. Upregulation of aerobic glycolysis and protein-protein interactions with PKM2 in PCSCs may lead to altered cellular proliferation and/or more aggressive disease.

Preface

Increases in PKM2 expression were found to associate with more advanced stages of PC (Gleason score 8-10) and DU145 PCSLC-derived subcutaneous xenograft tumours. Although comparable levels of PKM2 protein were detected in the DU145 parental and PCSLC lines, unique post-translational modifications were observed in the latter. These findings suggest alternative mechanisms of action and/or protein interactions in PCSCs that may allow for aggressive development of PC. As PCSCs typically grow slower than more differentiated cells, the possibility of alternative non-metabolic PKM2 mechanisms is highly plausible.

Changes in PKM2 associate with Prostate Cancer Progression

Nicholas Wong,[1,2,3] Judy Yan,[1,2,3] Diane Ojo,[1,2,3] Jason De Melo,[1,2,3] Jean-Claude Cutz,[4] and Damu Tang [1,2,3, #]

[1]Division of Nephrology, Department of Medicine, McMaster University; [2]Father Sean O'Sullivan Research Institute, [3]the Hamilton Center for Kidney Research, St. Joseph's Hospital; [4]Department of Pathology and Molecular Medicine, McMaster University, Hamilton, Ontario, Canada

#Correspondence:
Damu Tang
T3310, St. Joseph's Hospital
50 Charlton Ave East
Hamilton, Ontario, Canada
L8N 4A6
Tel: (905) 522-1155, ext. 35168
Fax: (905) 521-6181
E-mail: damut@mcmaster.ca

Running title: PKM2 in prostate cancer

Key words: PKM2, Prostate cancer, and Cancer Metabolism

ABSTRACT

Pyruvate kinase M2 (PKM2) is essential for aerobic glycolysis, the dominant metabolic pathway utilized by cancer cells. To determine the association of PKM2 with prostate cancer (PC), we examined 29 primary PC and 3 lymph node metastatic tumors; elevation of PKM2 was observed in Gleason 8--10 tumors compared to Gleason 6-7 carcinomas. High PKM2 was detected by immunohistochemistry in more aggressive xenograft tumors derived from PC stem-like cells (PCSCs), compared to those produced from non-PCSCs. While PCSCs and non-PCSCs expressed comparable levels of PKM2, distinct post-translational modifications were observed. Collectively, upregulation and specific modification to PKM2 associate with PC progression.

INTRODUCTION

Cancer cells commonly elevate glucose uptake and increase lactate production concurrent with a reduction of oxidative phosphorylation in the presence of abundant oxygen, a phenomenon called aerobic glycolysis or the Warburg effect (1, 2). The increase in aerobic glycolysis together with its dynamic process enables glycolytic intermediates to be redirected for the biosynthesis of cellular building blocks (nucleotides, amino acids, and lipids) while also producing ATP. Therefore, aerobic glycolysis meets the demands of proliferating cells for both macromolecular synthesis and energy production (3, 4). The M2 isoform of pyruvate kinase (PKM2) is an essential component in executing aerobic glycolysis in cancer cells, owing to its low level of pyruvate kinase activity, especially the dimeric form of PKM2, which controls glycolytic flux to direct intermediate metabolites towards the biosynthesis of cellular building blocks (5).

A large body of evidence demonstrates that cancers predominantly express PKM2 (6). Immunohistochemical (IHC) analysis revealed the common expression of PKM2 in colon cancer (7), renal cell carcinoma (RCC) (8) and lung cancer (9). PKM2 is a potential marker for RCC (10, 11) and testicular cancer (12), and high levels of serum PKM2 were observed in patients with colon cancer (13), breast cancer (14), urological tumors (15), lung carcinoma, cervical cancer, and gastrointestinal tumors (16). Mass spectrometry has confirmed increases in

PKM2 levels, and its predominant presence in RCC, bladder carcinoma, hepatocellular carcinoma, colorectal cancer, lung carcinoma, and follicular thyroid adenoma (17). High levels of PKM2 indicate poor prognosis for patients with signet ring cell gastric cancer (18), and a unique pattern of four expressed genes, including PKM2, has predictive value on outcomes for mesothelioma patients undergoing surgery (19). Tumorigenic events commonly enhance glycolysis via regulating PKM2. The PI3K-AKT-mTOR pathway upregulates PKM2 (20, 21), while PTEN (which inhibits this pathway) suppresses PKM2 expression (5, 22, 23). Collectively, accumulating evidence reveals an important role of PKM2 in promoting tumorigenesis via directing aerobic glycolysis.

This is in contrast to most normal differentiated cells of the body, in which cells maximize the production of ATP by metabolizing glucose through the oxidative phosphorylation pathway in mitochondria (5). However, the prostate is an exception. The prostate epithelium is unique in its ability to secrete high amounts of citrate into the prostatic fluid (up to 180 mM) (24) which is used as a source of ATP for sperm (25, 26). The secretion of citrate by prostate epithelial cells is executed through a truncated Krebs cycle and results in lower ATP production, a process that shares similarities to aerobic glycolysis reported in cancer cells. Due to the heterogeneous co-existence of normal and cancerous cells in the prostate, there is an overlap of glucose utilization between the two populations especially during early stages of prostate cancer. Because of this

overlap, ^{18}F-FDG PET has very limited application as an imaging tool for diagnosing and staging prostate cancer (27).

However, this unique property of prostate epithelial cells does not exclude the possibility that prostate cancer cells dominantly use aerobic glycolysis to meet their proliferative needs. Prostate cancer (PC) is the most common cancer affecting men and the second leading cause of cancer-related deaths in males in the developed world (28, 29). The disease progresses from intraepithelial neoplasia or de novo, locally invasive carcinoma to metastatic cancer that advances to castration refractory prostate cancers (CRPCs). CRPCs contribute virtually to all PC associated deaths (30, 31), and the disease's aggressiveness and resistance to therapy can be associated with prostate cancer stem cells among other factors. We have made an initial attempt to examine the changes in PKM2 protein expression levels during PC progression using patient tissues obtained through prostatectomy, as well as PC stem-like cells (PCSCs) and non-PCSCs. In general, elevation of PKM2 expression determined by immunohistochemistry staining is associated with more advanced stages of PC, and in comparison to non-PCSCs, post-translational modifications to PKM2 were observed in PCSC-derived xenograft tumors.

MATERIALS AND METHODS

Collecting primary prostate cancer tissues

Prostate tissues were collected from patients who underwent radical prostatectomy at St. Joseph's Hospital in Hamilton, Ontario, Canada following patient consent and approval from the local Ethics Board.

Immunohistochemistry (IHC)

IHC was performed on 29 paraffin embedded and serially cut prostate cancer or lymph node tissues obtained from St. Joseph's Hospital, Hamilton, Ontario, Canada. Slides were deparaffinized in xylene, cleared in ethanol series, and heat-treated for 20 minutes in sodium citrate buffer (pH = 6.0) in a food steamer. Tissues were blocked for 1 hour in PBS containing 1% BSA and 10% normal goat serum (Vector Laboratories). Primary antibody specific for PKM2 (Santa Cruz catalog number sc-365684, used at 0.8μg/ml) was incubated with the sections overnight at 4°C. Secondary antibody only was used as the negative control. Biotinylated goat anti-mouse IgG and Vector ABC reagent (Vector Laboratories) were subsequently incubated according to the manufacturer's instructions. Washes were performed with PBS. Chromogenic reaction was carried out with diaminobenzidine (Vector Laboratories). Semi-quantitative assessment was performed by three individuals in a blinded fashion; the staining

intensity was measured using a scale of 0 to 3 (0 - negative or background staining, 1 – weak staining, 2 – modest staining, and 3 – strong staining); the percentage of cells positive for the intensity was determined; and quantification of staining was obtained by multiplying intensity by the respective percentage.

Tissue culture and generation of PCSCs (DU145 spheres)

DU145 cells were purchased from ATCC and cultured in MEM supplemented with 10% FBS and 1% Penicillin/Streptomycin (Invitrogen). DU145 prostate cancer stem-like cells (PCSCs or spheres) were isolated and propagated as we have previously published (32). Briefly, DU145 monolayer cells were individualized by using phenol red-free TrypLE Express solution (Life Technologies) and 40 μm cell strainers (BD Biosciences), and subsequently resuspended at a cell concentration of 5000 cells/ml in serum-free (SF) media (DMEM/F12 at a 3:1 mixture) (Life Technologies) containing 0.4% bovine serum albumin (BSA) (Bioshop Canada Inc.) and 0.2× B27 lacking Vitamin A (Life Technologies) in T75 flasks. Typical DU145 spheres were formed in 10 to 12 days.

Xenograft tumor formation

DU145 monolayer (non-PCSCs) and sphere (PCSCs) cells were resuspended in MEM/Matrigel mixture (1:1 volume), followed by implantation of 0.1 ml subcutaneously (s.c.) into the flanks of 8 week-old male NOD/SCID mice (The Jackson Laboratory). 10^6 DU145 monolayer cells and 10^4 DU145 sphere cells were injected, based on our previous reports that DU145 spheres display a 100-fold higher capacity to form xenograft tumors (32). Mice were inspected for tumor appearance, by observation and palpation, and tumor growth was measured weekly using a caliper. Mice were sacrificed when tumor volumes reached ≥ 1000 mm^3. All animal work was carried out according to experimental protocols approved by the McMaster University Animal Research Ethics Board.

Western blot analysis

Cell lysates were prepared in a buffer containing 20 mM Tris (pH 7.4), 150mM NaCl, 1mM EDTA, 1mM EGTA, 1% Triton X-100, 25mM sodium pyrophosphate, 1mM NaF, 1 mM β-glycerophosphate, 0.1mM sodium orthovanadate, 1mM PMSF, 2μg/ml leupeptin and 10μg/ml aprotinin. 50μg of total cell lysate was separated on SDS-PAGE gel and transferred onto Immobilon-P membranes (Millipore). Membranes were blocked with 5% skim milk and then incubated with the indicated antibodies at 4^oC overnight. Signals were detected

using an ECL Western Blotting Kit (Amersham). Primary antibodies and concentrations used were: anti-PKM2 (Santa Cruz, 1:1000) and anti-Actin (Santa Cruz, 1:1000).

Two-dimensional gel separation of proteins was carried out as detailed in other publications (33, 34). Samples were solubilized in rehydration buffer (7M urea, 2M thiourea, 4% CHAPS, 0.2% biolytes, and 1% DTT) and subjected to rehydration with IPG strips (7cm, pH 310, BioRad) for 16 hours (50V at 20^{O}C). IEF was carried out using Protean IEF system (BioRad) at 20^{O}C with the following conditions; Step 1: 250V for 1 hour; Step 2: 500V for 1 hour; Step 3: 4000V for 2 hours; Step 4: 4000V for 20000 Vhrs. IPG strips were equilibrated in a buffer containing 6M urea, 2% SDS, 0.375M Tris-Cl, 20% glycerol and 130mM DTT for 10 minutes followed by equilibration in a subsequent buffer containing 6M urea, 2% SDS, 0.375M Tris-Cl, 20% glycerol and 135mM iodoacetamide for 10 minutes.

Statistical analysis

Statistical analysis was performed using student t-test, with $p < 0.05$ being considered statistically significant.

RESULTS

Elevation of PKM2 following prostate cancer progression

Elevation of PKM2 levels occurs in multiple cancers including colon cancer (7), renal cell carcinoma (8) and lung cancer (9). To examine PKM2 protein expression in prostate cancer, we collected 29 primary prostate cancer tissues consisting of 14 Gleason 6-7 carcinomas, 15 Gleason 8-10 tumors, and 3 lymph node metastasis tissues (Table 2.1). Slides were prepared and analyzed for PKM2 expression using IHC. While a low level of PKM2 was detected in prostatic glands, high levels of PKM2 expression were observed in PIN and carcinomas (Figure 2.1A). In prostate glands, PKM2 signals were largely restricted to the basal cells. In PIN lesions, we frequently detected high levels of PKM2 in the basal cells and lower levels of PKM2 in the luminal cells (Figure 2.1A), consistent with the concept that abnormalities in basal epithelial cells of the prostate play an initiation role in human prostate tumorigenesis (35). While variations in the intensity of PKM2 staining occurred in carcinomas of different severities, a general trend of elevated PKM2 staining from Gleason grade 3 (or Gleason score 3+4) carcinomas to Gleason grades 4 (or Gleason score 4+4) and 5, and metastatic prostate cancers was observed (Figure 2.1A). This trend can also be seen in Table 2.2, where an increasing number of $PKM2^{+}$ cells associates with higher Gleason score. Because of our relatively small sample size, we have divided prostate cancers into early stage tumors (Gleason scores 6-7) and

advanced stage carcinomas (Gleason scores 8-10) for statistical analysis, which demonstrated a significant increase of PKM2 in advanced prostate carcinomas compared to early stage prostate tumors (Figure 2.1B).

Increase in PKM2 detected by IHC in advanced xenograft prostate tumors

We have previously demonstrated that xenograft tumors derived from DU145 spheres (PCSCs) displayed more characteristics associated with advanced prostate cancer compared to xenograft tumors generated from DU145 monolayers (non-PCSCs) (32), and are able to form tumors of equal size with 100-fold fewer cells (Figure 2.2). Specifically, xenograft tumors derived from DU145 spheres were composed of 85.7±1.6% $CD44^+$ cells, versus 54.2±2.5% $CD44^+$ cells ($p < 0.05$) observed in tumors derived from monolayers (32). The $CD44^+$ DU145 cells are more tumorigenic compared to DU145 $CD44^-$ cells (36). To take advantage of this knowledge, we produced xenograft tumors from DU145 monolayer and sphere cells as a representation of PC progression to examine PKM2 protein expression *in vivo*. Following IHC staining, we found that PKM2 protein was readily detected in xenograft tumors produced by both cells (Figure 2.3). In comparison to DU145 monolayer cell-derived xenograft tumors, DU145 sphere cell-produced xenograft tumors exhibited in general a more intensive PKM2 staining (Figure 2.3B). However, as DU145 sphere cell-produced xenograft tumors reached the end point (tumor volume ≥ 1000 mm3) slower than DU145

monolayer cell-derived xenograft tumors (Figure 2.2), we could not exclude the possibility that the low levels of PKM2 detected by IHC staining in xenograft tumors produced by DU145 monolayer cells was due to less time for tumor growth in NOD/SCID mice. On the other hand, similar sizes of DU145 monolayer cell and DU145 sphere cell-produced xenograft tumors were used for the IHC staining. Collectively, these observations support the concept that an increase in PKM2 expression associates with more advanced prostate cancer and its progression.

Prostate cancer stem-like cells express PKM2 with unique post-translational modifications

To further investigate PKM2 expression in DU145 monolayer and DU145 sphere cells, we determined PKM2 levels in these cells by western blot. Although a marginal increase in PKM2 was observed in passages 10 and 23 DU145 sphere cells compared to DU145 monolayer cells, the differences were not statistically significant (Figure 2.4A). Similar results were also obtained in xenograft tumors produced by DU145 sphere and monolayer cells. In comparison to DU145 monolayer cell-derived xenograft tumors, the sphere cell-produced xenograft tumors displayed a slight increase in PKM2; the differences, however, were not statistically significant (Figure 2.4B). These results are not consistent with the observed elevation of PKM2 detected by IHC in DU145 sphere cell-produced

xenograft tumors (Figure 2.3). It is thus possible the higher levels of PKM2 observed by IHC staining in sphere cell-derived xenograft tumors may be attributable to differential PKM2 modifications in xenograft tumors generated by monolayer and sphere cells.

This possibility is in accordance with PKM2 being subjected to a variety of post-translational modifications which impact its ability to regulate aerobic glycolysis (37-39). To investigate this possibility, we have examined the potential modifications of PKM2 in DU145 monolayer and sphere cells by two-dimensional gel-based western blot. In comparison to PKM2 in DU145 monolayer cells, PKM2 in sphere cells displayed a different pI distribution (Figure 2.5A). The major differences are the cluster of PKM2 within pI 8-9 for monolayer cells, and a more widely distributed pattern with a clear spot at pI 6 for PKM2 derived from DU145 sphere cells (Figure 2.5A). To further investigate unique post-translational modifications of PKM2, we also examined the potential modifications of PKM2 in the xenograft tumors generated. Similar to DU145 monolayer cells, PKM2 from monolayer cell-produced xenograft tumors was largely present between pI 8-9 with no apparent spotting at pI 6 observed (Figure 2.5B). In comparison, PKM2 from sphere cell-derived xenograft tumors displayed a wide pI distribution with a clear presence of protein at pI 6 (Figure 2.5B). While different pI distributions were observed between cells in culture and xenograft tumors derived from them (Figure 2.5), the major differences in pI distribution

were preserved, suggesting that the unique post translational modifications to PKM2 in DU145 sphere cells play a role in prostate cancer progression.

DISCUSSION

While it has been recently reported that PKM2 is not required for the maintenance and growth of tumors (41), a large body of evidence clearly demonstrates a critical role of PKM2 in tumorigenesis and progression (5). However, we have no knowledge of whether PKM2 contributes to prostate cancer. Our investigation here that elevation of the PKM2 protein detected by IHC in general associates with more advanced prostate cancers compensates for this lack of data, and is consistent with the demonstrated oncogenic role of PKM2. Prostate cancers with Gleason scores 6 and 7 are regarded as early stages, and those with Gleason scores 8-10 are considered advanced prostate carcinomas. In line with this knowledge, Gleason 8-10 prostate cancer tissues were found to express generally higher levels of PKM2 compared to those of Gleason 6-7. This is supported with our understanding that more advanced prostate cancers are associated with increased cell proliferation. It is thus plausible that elevated proliferation status may demand higher levels of aerobic glycolysis and increased PKM2 expression may contribute to this process. This concept is in accordance with the observed elevation of AKT activation following increasing severity during prostate cancer progression (42). While our study using a limited number

of lymph node metastasis cases indicates that metastatic prostate tumors do not express lower levels of PKM2 in comparison to local Gleason 8-10 prostate cancers, investigations utilizing additional metastatic cases, including bone metastasis, will be required to draw a firm conclusion regarding PKM2 expression in metastatic prostate cancer. Additionally, more cases of prostate cancer with individual Gleason grades of 3, 4, and 5 will be needed to dissect a correlation of PKM2 expression with prostate cancer severity. Nonetheless, our research provides initial evidence that PKM2 expression correlates with prostate cancer progression. Additional evidence to support that greater PKM2 expression associates with prostate tumorigenesis is our observation of more intense IHC staining in DU145 sphere cell-derived xenograft tumors compared to monolayer cell-derived xenograft tumors (Figure 2.3).

Whether the observed elevation of PKM2 in advanced PC can be attributable to transcription upregulation is unclear. Analysis of PKM2 expression using Oncomine^{TM} in prostate adenocarcinomas produced an inconsistent message, showing both up and downregulation in prostate cancer compared to normal tissue (Table 2.3). This inconsistency may be attributed to the highly heterogeneous nature of prostate cancer, and predominantly early stages of prostate cancers analyzed (early stages are well differentiated and proliferate slowly). These observations do not exclude the possibility of increased PKM2 transcription in advanced prostate cancers (Gleason scores $\geq$ 8, and metastatic

disease).

PKM2 expression may also be associated with prostate cancer initiation. It is widely regarded that the basal epithelial cells of the prostate gland harbour prostate stem cells (35), and that abnormalities in these cells contribute to the initiation of prostate cancer. In supporting this notion, we observed abundant PKM2 expression in the basal epithelial cells in PIN lesions, but low levels of PKM2 detected in the basal cells of normal prostate glands (Figure 2.1A). It cannot be excluded whether the low levels of PKM2 in prostate glands adjacent to PIN (Figure 2.1A, left panel) are a result of early oncogenic signals, but the expression is consistent with its reported presence in most of normal tissues (43,44). It is intriguing that although the luminal epithelial cells are the source of citrate secretion and associated with a truncated Krebs cycle, PKM2 is largely expressed in the basal layer of epithelial cells (Figure 2.1A, left panel). Collectively, these observations support the notion that basal epithelial cells are likely the origin of human prostate cancer.

It has become increasingly clear that cancer stem cells (CSCs) play a critical role in tumorigenesis, especially in tumor progression and metastasis (45). While aerobic glycolysis meets the demand of biosynthesis for non-stem proliferating cells, the degree of aerobic glycolysis in CSCs of the tumor might differ, as both populations have different proliferation rates (45, 46). This possibility is supported by a report demonstrating that glioma CSCs may not use

aerobic glycolysis to the same degree as differentiated cancer cells (47); an intriguing idea which may also apply here regarding the unique post-translational modifications we have observed in prostate cancer stem-like cells. This knowledge is important, as prostate cancer stem cells are critical players in prostate cancer progression and castration-resistant prostate cancers (CRPCs) (48). As the development of new therapies for treating CRPC patients is an urgent task (49), advancing our understanding of how PKM2 associates with PCSC--mediated CRPC pathogenesis may lead to the development of novel therapies.

While we could not conclusively demonstrate elevated levels of the PKM2 protein in DU145 sphere cell-derived xenograft tumors in comparison to monolayer cell-derived xenograft tumors (Figure 2.4), it is apparent that PKM2 in DU145 sphere cells is subjected to different modifications (Figure 2.5). Although reports indicate various post-translational modifications to PKM2 including phosphorylation, acetylation, and oxidation (37, 39, 50-53), PKM2 regulation specifically within the prostate remains unclear. One possibility is the switch from tetrameric PKM2 to dimeric PKM2, which has been shown to require specific modifications. This would allow for aerobic glycolysis and accumulation of glycolytic intermediates for synthesis of cellular building blocks. As nuclear PKM2 regulates gene expression (58-60), it is possible that nuclear PKM2 is important to prostate tumorigenesis. This possibility was supported by the observed nuclear presence of PKM2 in the xenograft tumors (Figure 2.3). It

would be an intriguing research avenue to identify these unique PKM2 modifications within the pI range of 6-8 (Figure 2.5) observed in DU145 sphere-derived xenografts, if they are in fact the changes required for the switch to dimeric PKM2, and whether this serves any functional purpose within only prostate cancer stem cells during disease progression.

ACKNOWLEDGEMENTS

This work was supported in part by Prostate Cancer Canada to D. Tang, by Division of Nephrology, Department of Medicine, McMaster University, and by St. Joseph's Healthcare in Hamilton, Ontario, Canada through financial support to the Hamilton Centre for Kidney Research (HCKR). We would also like to acknowledge Sanpreet Sihota, Rammdeep Saini, and Adam Sivitilli for their help with IHC staining and quantification.

DECLARATION OF INTERESTS

The authors declare no conflict of interest.

REFERENCES

1. Warburg, O.; Wind, F.; Negelein, E. The metabolism of tumors in the body. J Gen Physiol **1927**, *8*, 519-530.
2. Warburg, O. On the origin of cancer cells. Science **1956**, *123*, 309-314.
3. Hsu, P.P.; Sabatini D.M. Cancer cell metabolism: Warburg and beyond. Cell **2008**, *134*, 703707.
4. Vander Heiden, M.G.; Cantley, L.C.; Thompson, C.B. Understanding the Warburg effect: the metabolic requirements of cell proliferation. Science **2009**, *324*, 1029-1033.
5. Wong, N.; De Melo, J.; Tang, D. PKM2, a central point of regulation in cancer metabolism. Int J Cell Biol **2013**, 2013: 242-513.
6. Yamada, K.; Noguchi, T. Nutrient and hormonal regulation of pyruvate kinase gene expression. Biochem J **1999**, 337, 111.
7. Christofk, H.R.; Vander Heiden, M.G.; Harris, M.H.; Ramanathan, A.; Gerszten, R.E.; Wei, R.; Fleming, M.D.; Schreiber, S.L.; Cantley, L.C. The M2 splice isoform of pyruvate kinase is important for cancer metabolism and tumor growth. Nature **2008**, *452*, 230-233.
8. Brinck, U.; Eigenbrodt, E.; Oehmke, M.; Mazurek, S.; Fischer, G. Land. M2 - pyruvate kinase expression in renal cell carcinomas and their metastases. Virchows Archiv **1994**, *424*, 177-185.
9. Schneider, J.; Neu, K.; Grimm, H.; Velcovsky, H.G.; Weisse, G.; Eigenbrodt, E. Tumor M2pyruvate kinase in lung cancer patients: immunohistochemical detection and disease monitoring. Anticancer Res **2002**, *22*, 311-318.
10. Wechsel, H.W.; Petri, E.; Bichler, K.H.; Feil, G. Marker for renal cell carcinoma (RCC): the dimeric form of pyruvate kinase type M2 (Tu M2PK). Anticancer Res **1999**, *19*, 2583-2590.
11. Oremek, G.M.; Teigelkamp, S.; Kramer, W.; Eigenbrodt, E.; Usadel, K.H. The pyruvate kinase isoenzyme tumor M2 (Tu M2PK) as a tumor marker for renal carcinoma. Anticancer Res **1999**, *19*, 2599-2601.
12. Pottek, T.; Müller, M.; Blum, T.; Hartmann, M. TuM2PK in the blood of testicular and cubital veins in men with testicular cancer. Anticancer Res **2000**, *20*, 5029-5033.
13. Eigenbrodt, E.; Basenau, D.; Holthusen, S.; Mazurek, S.; Fischer, G. Quantification of tumor type M2 pyruvate kinase (Tu M2PK) in human carcinomas. Anticancer Res **1997**, *17*, 3153-3156.

14. Lüftner, D.; Mesterharm, J.; Akrivakis, C.; Geppert, R.; Petrides, P.E.; Wernecke, K.D.; Possinger, K. Tumor type M2 pyruvate kinase expression in advanced breast cancer. Anticancer Res **2000**, *20*, 5077-5082.

15. Roigas, J.; Schulze, G.; Raytarowski, S.; Jung, K.; Schnorr, D.; Loening, S.A. Tumor M2 pyruvate kinase in plasma of patients with urological tumors. Tumour Biol **2001**, *22*, 282-285.

16. Mazurek, S.; Boschek, C.B.; Hugo, F.; Eigenbrodt, E. Pyruvate kinase type M2 and its role in tumor growth and spreading. Semin Cancer Biol **2005**, *15*, 300-308.

17. Bluemlein, K.; Grüning, N.M.; Feichtinger, R.G.; Lehrach, H.; Kofler, B.; Ralser, M. No evidence for a shift in pyruvate kinase PKM1 to PKM2 expression during tumorigenesis. Oncotarget **2011**, *2*, 393-400.

18. Lim, J.Y.; Yoon, S.O.; Seol, S.Y.; Hong, S.W.; Kim, J.W.; Choi, S.H.; Cho, J.Y. Overexpression of the M2 isoform of pyruvate kinase is an adverse prognostic factor for signet ring cell gastric cancer. World J Gastroenterol **2012**, *18*, 4037-4043.

19. Gordon, G.J.; Dong, L.; Yeap, B.Y.; Richards, W.G.; Glickman, J.N.; Edenfield, H.; Mani, M.; Colquitt, R.; Maulik, G.; Van Oss, B.; Sugarbaker, D.J.; Bueno, R. Four gene expression ratio test for survival in patients undergoing surgery for mesothelioma. J Natl Cancer Inst **2009**, *101*, 678-686.

20. Sun, Q.; Chen, X.; Ma, J.; Peng, H.; Wang, F.; Zha, X.; Wang, Y.; Jing, Y.; Yang, H.; Chen, R.; Chang, L.; Zhang, Y.; Goto, J.; Ondo, H.; Chen, T.; Wang, M.R.; Lu, Y.; You, H.; Kwiatkowski, D.; Zhang, H. Mammalian target of rapamycin upregulation of pyruvate kinase isoenzyme type M2 is critical for aerobic glycolysis and tumor growth. Proc Natl Acad Sci USA **2011**, *108*, 4129-4134.

21. Chen, M.; Zhang, J.; Manley, J.L. Turning on a fuel switch of cancer: hnRNP proteins regulate alternative splicing of pyruvate kinase mRNA. Cancer Res **2012**, *70*, 8977-8980.

22. GarciaCao, I.; Song, M.S.; Hobbs, R.M.; Laurent, G.; Giorgi, C.; de Boer, V.C.; Anastasiou, D.; Ito, K.; Sasaki, A.T.; Rameh, L.; Carracedo, A.; Vander Heiden, M.G.; Cantley, L.C.; Pinton, P.; Haigis, M.C.; Pandolfi, P.P. Systemic elevation of PTEN induces a tumor suppressive metabolic state. Cell **2012**, *149*, 49-62.

23. Nemazanyy, I.; Espeillac, C.; Pende, M.; Panasyuk, G. Role of PI3K, mTOR, and Akt2 signalling in hepatic tumorigenesis via the control of PKM2 expression. Biochem Soc Trans **2013**, *41*, 917-922.

24. Kavanagh, J. P. Isocitric and citric acid in human prostatic and seminal fluid: implications for prostatic metabolism and secretion. Prostate **1994**, *24*, 139–142.

25. Medrano, A.; Fernandez-Novell, J. M.; Ramio, L.; Alvarez, J.; Goldberg, E.; Montserrat River M.; Guinovart J.J.; Rigau T.; Rodriguez-Gil J.E. Utilization of citrate and lactate through a lactate dehydrogenase and ATP-regulated pathway in boar spermatozoa. Mol Reprod Dev **2006**, *73*, 369–378.

26. Mycielska M.E.; Patel A.; Rizaner N.; Mazurek M.P.; Keun H.; Patel A.; Ganapathy V.; Djamgoz M.B. Citrate transport and metabolism in mammalian cells: prostate epithelial cells and prostate cancer. Bioessays **2009**, *31*, 10-20.

27. Jadvar H. Molecular imaging of prostate cancer with PET. J Nucl Med **2013**, *54*,1685-1688.

28. Jemal, A.; Siegel, R.; Ward, E.; Murray, T.; Xu, J.; Thun, M.J. Cancer statistics. CA Cancer J Clin **2007**, *57*, 43-66.

29. Williams, H.; Powell, I.J. Epidemiology, pathology, and genetics of prostate cancer among African Americans compared with other ethnicities. Methods Mol Biol **2009**, *472*, 439-453.

30. Ross, J.S. The androgen receptor in prostate cancer: therapy target in search of an integrated diagnostic test. Adv Anat Pathol **2007**, *14*, 353-357.

31. Moon, C.; Park, J.C.; Chae, Y.K.; Yun, J.H.; Kim, S. Current status of experimental therapeutics for prostate cancer. Cancer Lett **2008**, *266*, 116--134.

32. Rybak, A.P.; He, L.; Kapoor, A.; Cutz, J.C.; Tang, D. Characterization of sphere-propagating cells with stem-like properties from DU145 prostate cancer cells. Biochim Biophys Acta**2011**, *1813*, 683-694.

33. O'Farrell, P.H. High resolution two-dimensional electrophoresis of proteins. J Biol Chem **1975**, *250*, 4007-4021.

34. Gorg, A.; Drews, O.; Luck, C.; Weiland, F.; Weiss, W. 2DE with IPGs. Electrophoresis **2009**, *30*, S122-S132.

35. Zellweger, T.; Stürm, S.; Rey, S.; Zlobec, I.; Gsponer, J.R.; Rentsch, C.A.; Terracciano, L.M.; Bachmann, A.; Bubendorf, L.; Ruiz, C. Estrogen receptor β expression and androgen receptor phosphorylation correlate with a poor clinical outcome in hormone naive prostate cancer and are elevated in castration resistant disease. Endocr Relat Cancer **2013,** *20*, 403-413.

36. Patrawala, L.; Calhoun, T.; SchneiderBroussard, R.; Li, H.; Bhatia, S.; Tang, J.G.; Reilly, J.G.; Chandra, D.; Zhou, J.; Claypool, K.; Coghlan, L.; Tang,

D.G. Highly purified $CD44^+$ prostate cancer cells from xenograft human tumors are enriched in tumorigenic and metastatic progenitor cells. Oncogene **2006**, *25*, 1696-1708.

37. Lv, L.; Li, D.; Zhao, D.; Lin, R.; Chu, Y.; Zhang, H.; Zha, Z.; Liu, Y.; Li, Z.; Xu, Y.; Wang, G.; Huang, Y.; Xiong, Y.; Guan, K.L.; Lei, Q.Y. Acetylation targets the M2 isoform of pyruvate kinase for degradation through chaperone - mediated autophagy and promotes tumor growth. Mol Cell **2011**, *42*, 719-730.
38. Anastasiou, D.; Poulogiannis, G.; Asara, J.M.; Boxer, M.B.; Jiang, J.K.; Shen, M.; Bellinger, G.; Sasaki, A.T.; Locasale, J.W.; Auld, D.S.; Thomas, C.J.; Vander Heiden M.G.; Cantley, L.C. Inhibition of pyruvate kinase M2 by reactive oxygen species contributes to cellular antioxidant responses. Science **2011**, *334*, 1278-1283.
39. Tamada, M.; Suematsu, M.; Saya, H. Pyruvate kinase M2: multiple faces for conferring benefits on cancer cells. Clin Cancer Res **2012**, *18*, 5554-5561.
40. Tamada, M.; Nagano, O.; Tateyama, S.; Ohmura, M.; Yae, T.; Ishimoto, T.; Sugihara, E.; Onishi, N.; Yamamoto, T.; Yanagawa, H.; Suematsu, M.; Saya, H. Modulation of glucose metabolism by CD44 contributes to antioxidant status and drug resistance in cancer cells. Cancer Res **2012**, *72*, 1438-1448.
41. CortésCros, M.; Hemmerlin, C.; Ferretti, S.; Zhang, J.; Gounarides, J.S.; Yin, H.; Muller, A.; Haberkorn, A.; Chene, P.; Sellers, W.R.; Hofmann, F. M2 isoform of pyruvate kinase is dispensable for tumor maintenance and growth. Proc Natl Acad Sci USA **2013**, *110*, 489-494.
42. Hammarsten, P.; Cipriano, M.; Josefsson, A.; Stattin, P.; Egevad, L.; Granfors, T.; Fowler, C.J. Phospho-Akt immunoreactivity in prostate cancer: relationship to disease severity and outcome, Ki67 and phosphorylated EGFR expression. PLoS One **2012**, *7*, e47994.
43. Bluemlein K.; Grüning N.M.; Feichtinger R.G.; Lehrach H.; Kofler B.; Ralser M. No evidence for a shift in pyruvate kinase PKM1 to PKM2 expression during tumorigenesis. Oncotarget **2011**, *2*, 393-400.
44. Wong N.; Ojo D.; Yan J.; Tang D. PKM2 contributes to cancer metabolism. Cancer Lett. **2014**, Advance online publication. PMID: 24508027.
45. Baccelli, I.; Trumpp, A. The evolving concept of cancer and metastasis stem cells. J Cell Biol **2012**, *198*, 281-293.
46. Visvader, J.E.; Lindeman, G.J. Cancer stem cells in solid tumours: accumulating evidence and unresolved questions. Nat Rev Cancer **2008**, *8*, 755-768.

47. Vlashi, E.; Lagadec, C.; Vergnes, L.; Matsutani, T.; Masui, K.; Poulou, M.; Popescu, R.; Della Donna, L.; Evers, P.; Dekmezian, C.; Reue, K.; Christofk, H.; Mischel, P.S.; Pajonk, F. Metabolic state of glioma stem cells and nontumorigenic cells. Proc Natl Acad Sci USA **2011**, *108*, 16062-16067.

48. Qin, J.; Liu, X.; Laffin, B.; Chen, X.; Choy, G.; Jeter, C.R.; CalhounDavis, T.; Li, H.; Palapattu, G.S.; Pang, S.; Lin, K.; Huang, J.; Ivanov, I.; Li, W.; Suraneni, M.V.; Tang, D.G. The PSA (/lo) prostate cancer cell population harbors self-renewing long-term tumor-propagating cells that resist castration. Cell Stem Cell **2012,** *10*, 556-569.

49. Moul, J.W.; Dawson, N. Quality of life associated with treatment of castration-resistant prostate cancer: a review of the literature. Cancer Invest **2012,** *30*, 112.

50. Hitosugi T.; Kang S.; Vander Heiden M.G.; Chung T.; Elf S.; Lythgoe K.; Dong S.; Lonial S.; Wang X.; Chen G.Z.; Khuri F.R.; Gilliland D.G.; Cantley L.C.; Kaufman J.; Chen J. Tyrosine phosphorylation inhibits PKM2 to promote the Warburg effect and tumor growth. Sci Signal **2009**, *97*, ra73.

51. Yu Z.; Zhao X.; Huang L.; Zhang T.; Yang F.; Xie L.; Song S.; Miao P.; Zhao L.; Sun X.; Liu J.; Huang G. Proviral insertion in murine lymphomas 2 (PIM2) oncogene phosphorylates pyruvate kinase (PKM2) and promotes glycolysis in cancer cells. J Biol Chem **2013**, *288*, 35406-35416.

52. Lv L.; Xu Y.; Zhao D.; Li F.; Wang W.; Sasaki N.; Jiang Y.; Zhou X.; Li T.; Guan K.; Lei Q.; Xiong Y. Mitogenic and oncogenic stimulation of K433 acetylation promotes PKM2 protein kinase activity and nuclear localization. Mol Cell **2013**, *52*, 340-352.

53. Yang W.; Zheng Y.; Xia Y. Ji H.; Chen X.; Guo F.; Lyssiotis C.A.; Aldape K.; Cantley L.C.; Lu Z. ERK1/2-dependent phosphorylation and nuclear translocation of PKM2 promotes the Warburg effect. Nat Cell Biol **2012**, *14*, 1295-1304.

54. Taylor B.S.; Schultz N.; Hieronymus H.; Gopalan A.; Xiao Y.; Carver B.S.; Arora V.K.; Kaushik P.; Cerami E.; Reva B.; Antipin Y.; Mitsiades N.; Landers T.; Dolgalev I.; Major J.E.; Wilson M.; Socci N.D.; Lash A.E.; Heguy A.; Eastham J.A.; Scher H.I.; Reuter V.E.; Scardino P.T.; Sander C.; Sawyers C.L.; Gerald W.L. Integrative genomic profiling of human prostate cancer. Cancer Cell **2010**, *18*, 11-22.

55. LaTulippe E.; Satagopan J.; Smith A.; Scher H.; Scardino P.; Reuter V.; Gerald W.L. Comprehensive gene expression analysis of prostate cancer reveals distinct transcriptional programs associated with metastatic disease. Cancer Res **2002**, *62*, 4499-4506.

56. Yu Y.P.; Landsittel D.; Jing L.; Nelson J.; Ren B.; Liu L.; McDonald C.; Thomas R.; Dhir R.; Finkelstein S.; Michalopoulos G.; Becich M.; Luo J.H. Gene expression alterations in prostate cancer predicting tumor aggression and preceding development of malignancy. J Clin Oncol **2004**, *22*, 2790-2799.

57. Wallace T.A.; Prueitt R.L.; Yi M.; Howe T.M.; Gillespie J.W.; Yfantis H.G.; Stephens R.M.; Caporaso N.E.; Loffredo C.A.; Ambs S.; Tumor immunobiological differences in prostate cancer between African-American and European-American men. Cancer Res **2008**, *68*, 927-936.

58. Gao X.; Wang H.; JYang J.J.; Liu X.; Z.R. Liu Z.R.; Pyruvate kinase M2 regulates gene transcription by acting as a protein kinase, Mol Cell **2012,** *45,* 598-609.

59. Yang W.; Xia Y.; Ji H., Zheng Y.; Liang J.; Huang W.; Gao X.; Aldape K.; Lu Z.; Nuclear PKM2 regulates β-catenin transactivation upon EGFR activation, Nature **2011,** *480*, 118-122.

60. Yang W.; Xia Y.; Hawke D.; Li X.; Liang J.; Xing D.; Aldape K.; Hunter T.; Yung W.K.; Lu Z.; PKM2 phosphorylates histone H3 and promotes gene transcription and tumorigenesis, Cell **2012,** *150,* 685-96.

TABLES

Table 2.1. Pathological Information and PKM2 Staining Score in Prostatic Adenocarcinoma Patients

Patient	Age	Pathology[1,2]	Gleason Grade	Metastasis	Average Score
1	69	PA	5	No	90.0
2	76	PA	6	No	143.33
3	53	PA	6	No	160.0
4	58	PA	6	No	83.33
5	55	PA	6	No	200.0
6	57	PA	6	No	53.33
7	48	PA	6	No	86.67
8	58	PA	6	No	30.0
9	64	PA	6	No	200.0
10	52	PA	6	No	56.67
11	70	PA	7	No	66.67
12	74	PA	7	No	100.0
13	63	PA	7	No	76.67
14	62	PA	7	No	93.33
15	50	PA	7	No	113.33
16	50	PA	7	No	60.0
17	74	PA	7	No	63.33
18	76	PA	7	No	73.33
19	58	PA	8	Yes[*]	160.0
20	56	PA	8	Yes[+]	140.0
21	68	PA	8	No	76.67
22	79	PA	8	No	186.67
23	55	PA	9	No	50.0
24	71	PA	9	No	53.33
25	82	PA	9	No	110.0
26	75	PA	9	No	116.67
27	49	PA	9	No	146.67
28	64	PA	9	No	220.0
29	72	PA	9	No	80.0
30	65	PA	9	Yes[#]	176.67
31	60	PA	9	No	53.33
32	80	PA	9	No	70.0
33	77	PA	9	No	43.33
34	86	PA	10	No	146.67
35	68	PA	10	No	50.0

36	75	PA	10	No	250.0
19*	58	LN	Metastasis	N/A	270.0
20+	56	LN	Metastasis	N/A	126.67
30#	65	LN	Metastasis	N/A	83.33

1 – Prostatic Adenocarcinoma, 2 – Lymph Node, *+# Matched Patient Tissues

Table 2.2. Number of $PKM2^+$ Cells Counted Per Area for IHC Staining

Gleason Score	Mean $PKM2^+$ Cells Per $150000\mu m^2$	p-value[a]
6	139 ± 74	
7	227 ± 42	
8	347 ± 106	$p<0.0001$
9	259 ± 94	
10	760 ± 177	

a: Statistical analysis was performed by One-way ANOVA

Table 2.3. Microarray Datasets Conducting Differential Analysis Between Normal Prostate and Malignant Tissue, Separated into Early Stage (Gleason 6-7) and Late Stage (Gleason 8-10) Prostate Cancer*

Researcher	Unknown Gleason	Early Stage (Gleason 6-7)	Late Stage (Gleason 8-10)	Fold Change	p-value	Reference
Taylor	29	115	15	-1.280	6.68×10^{-7}	54
LaTulippe	12	16	7	-1.199	0.011	55
Yu	48	42	19	-1.131	0.013	56
Wallace	20	65	3	1.310	0.026	57

*Oncomine™ (Compendia Bioscience, Ann Arbor, MI) was used for analysis and visualization.

FIGURES

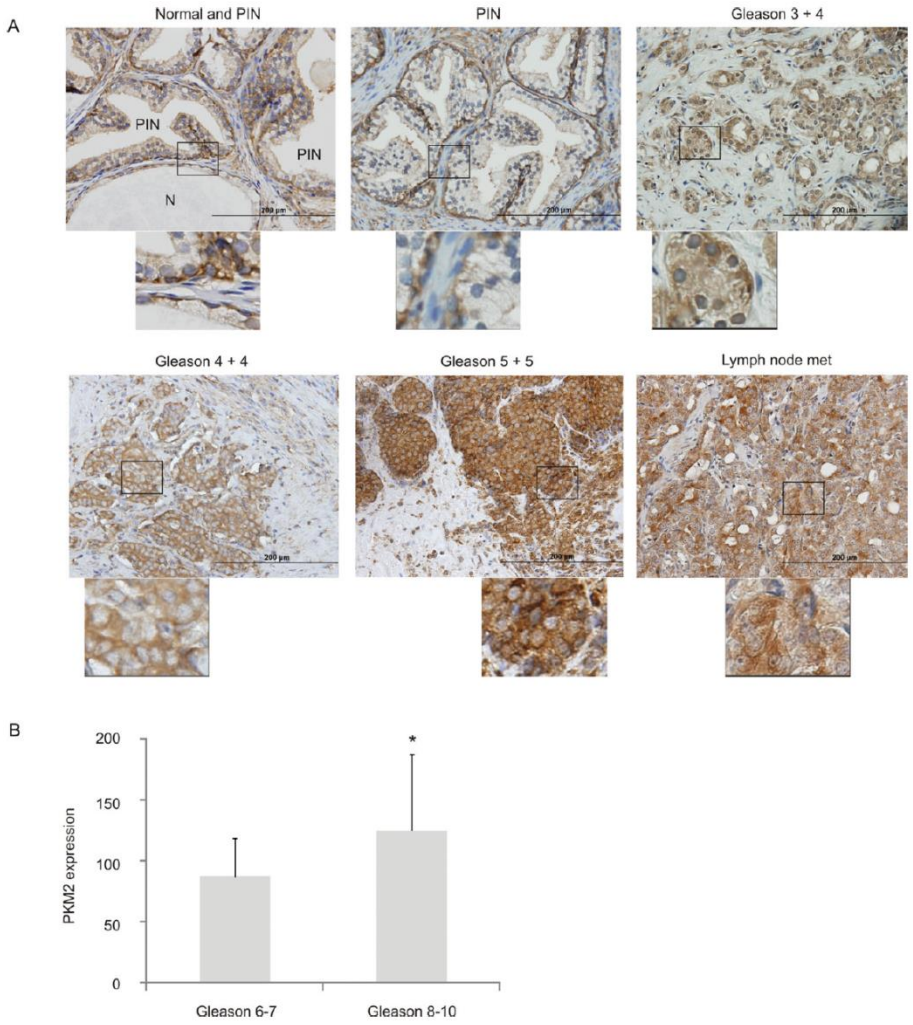

Figure 2.1. Increase of PKM2 protein expression following prostate cancer progression. (**A)** Prostatic gland, PIN, and prostate carcinomas with the indicated Gleason grades were IHC stained with anti-PKM2 antibody. Representative images for each Gleason score are included. Scale bars represent 200μm. The marked areas are enlarged 3-fold and placed underneath the individual panels. In the top left panel, "N" indicates normal prostate glands. **(B)** The IHC staining was quantified by three individuals based on the intensity and percentage of cells stained (see Materials and Methods for details). The average scores ± SDs (standard deviations) for the Gleason 6-7 and Gleason 8-10 tumors are graphed. *$p < 0.05$.

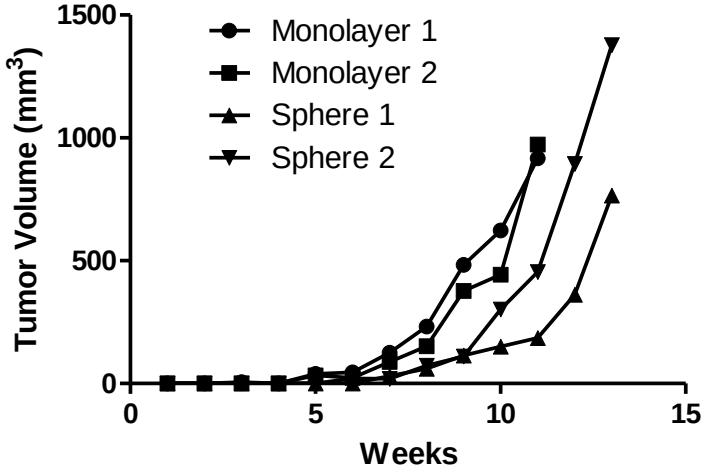

Figure 2.2. Volumes and growth curve of xenograft tumors produced using DU145 monolayer and sphere cells. Cells were implanted into NOD/SCID mice according to our published conditions (32). Tumors were followed until their volumes reached $\geq$ 1000 mm^3.

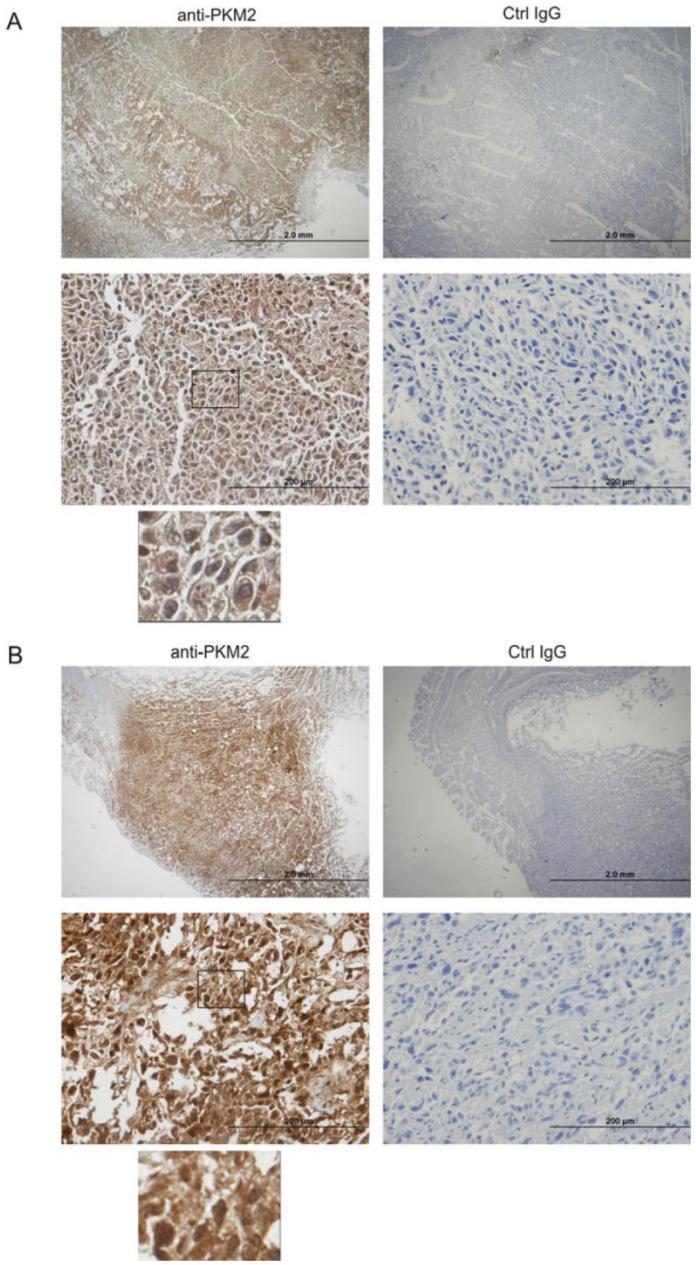

Figure 2.3. PKM2 protein expression in xenograft tumors derived from DU145 monolayer or sphere cells. Xenograft tumors were produced using DU145 monolayer cells (**A**) and sphere cells (**B**) implanted into NOD/SCID mice. Images in the top and bottom panels are different magnifications from the same xenograft tumors. Scale bars at the top and bottom panes represent 2mm and 200µm, respectively. The marked areas are enlarged 3-fold and placed underneath the individual panels.

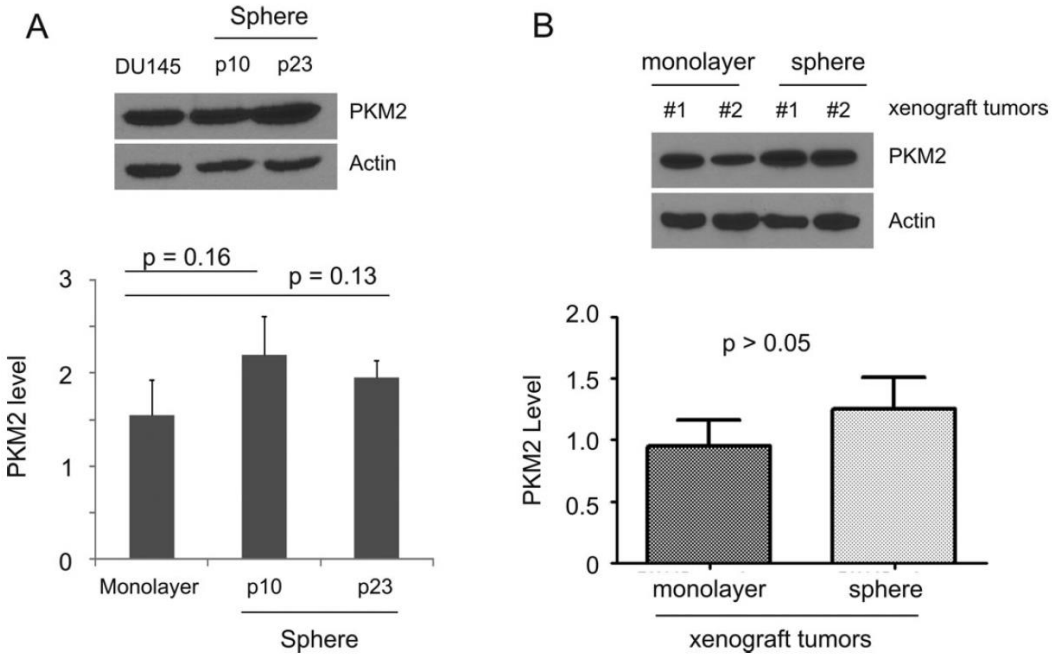

Figure 2.4. Comparable levels of PKM2 protein in xenograft tumors derived from DU145 monolayer and sphere cells. **(A)** PKM2 protein in cultured DU145 monolayer and sphere cells with passage 10-11 and 23 or 27 (P10, P23) were analyzed by Western blot three times. Typical results from a single repeat are shown (top panel). PKM2 levels were normalized to actin and averages ± SDs are graphed (bottom panel). **(B)** PKM2 protein in two xenograft tumors derived from either DU145 monolayer or sphere cells was determined by Western blot three times. Typical results from a single repeat are shown (top panel). PKM2 levels were normalized to actin and averages ± SDs are graphed (bottom panel).

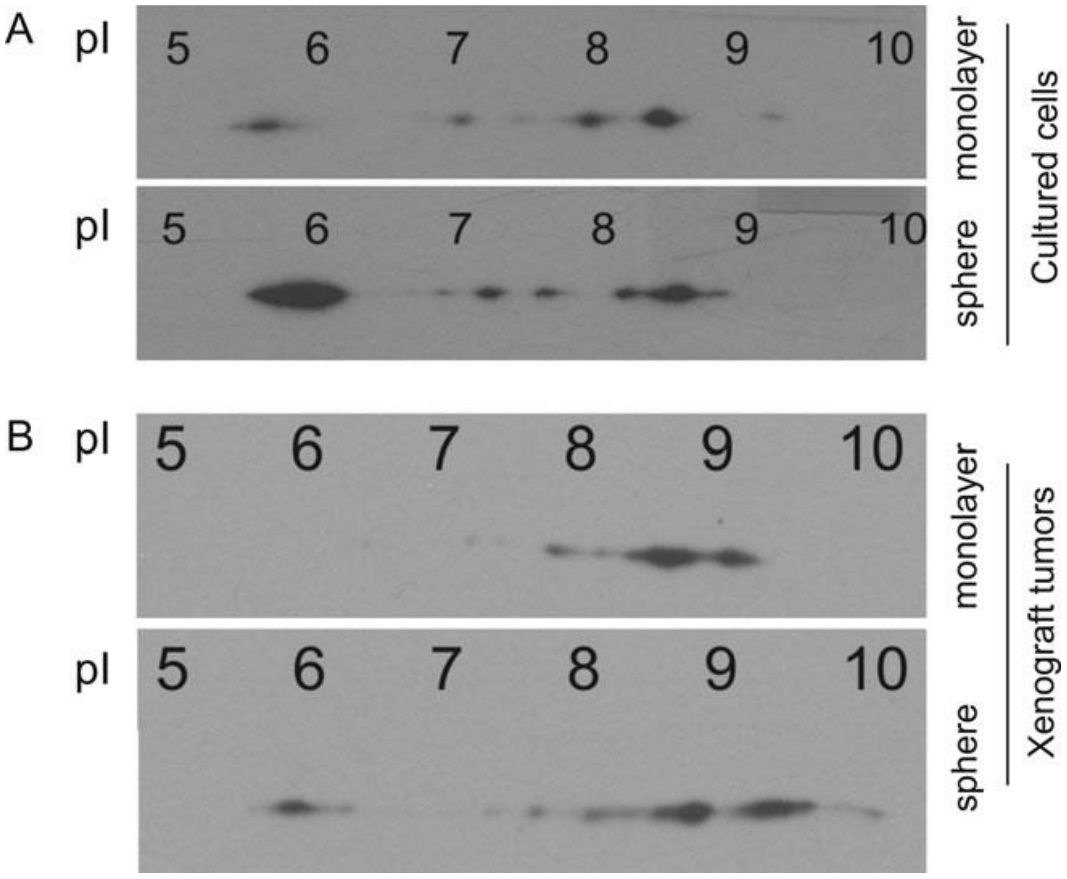

Figure 2.5. PKM2 is differentially modified in xenograft tumors derived from DU145 monolayer and sphere cells. Two-dimensional gel analysis was performed using strips with a pH range of 3-10, followed by Western blot analysis. The pH range (pI) is indicated. Results were from cultured DU145 monolayer and sphere cells **(A)**, and from xenograft tumors generated from these two cell lines **(B)**. Two-dimensional analysis was performed on two xenograft tumors derived from each; typical images from each type of tumor are shown.

CHAPTER THREE

AMPLIFICATION OF MUC1 IN PROSTATE CANCER METASTASIS AND CRPC DEVELOPMENT

Nicholas Wong,[1,2,3] Pierre Major,[4] Anil Kapoor,[2,5] Fengxiang Wei,[1,2,3,6] Judy Yan,[1,2,3] Tariq Aziz,[7] Mingxing Zheng,[8,9] Dulitha Jayasekera,[1,2,3] Jean-Claude Cutz,[7] and Damu Tang [1,2,3, #]

[1]Division of Nephrology, Department of Medicine, McMaster University; [2]Father Sean O'Sullivan Research Institute, [3]the Hamilton Center for Kidney Research, St. Joseph's Hospital; [4]Division of Medical Oncology, Department of Oncology, McMaster University, [5]Department of Surgery, McMaster University, Hamilton, Ontario, Canada; [6]the Genetics Laboratory, Longgang District Maternity and Child Healthcare Hospital, Longgang District, Shenzhen, Guangdong, P.R. China; [7]Department of Pathology and Molecular Medicine, McMaster University, Hamilton, Ontario, Canada; [8]Department of Respiratory Medicine, Shenzhen 2nd People's Hospital and [9]the First Affiliated Hospital of Shenzhen University Medical School, Shenzhen, Guangdong 518035, China

Submitted to *Oncotarget* in **April 2016**. Under revision since **May 2016**.

Author Contributions

Dr. D. Tang and N. Wong designed the experiments. N. Wong carried out the experiments, organized data, and analyzed the results. Dr. P. Major conducted the phase I/II clinical trial using a Tn-MUC1 peptide-based cell vaccine and provided the anti-MUC1-N antibody. Dr. A. Kapoor and Dr. J.C. Cutz verified and confirmed all prostate cancer tissues. Dr. F. Wei provided funding for this research. Dr. J. Yan first identified MUC1 in our PCSLCs and performed the initial RT-PCR confirmations. Dr. T. Aziz kindly provided the prostate cancer bone metastasis tissues. M. Zheng assisted with data analysis. D. Jayasekera performed and analyzed the IHC data on primary prostate cancer tissues and xenografts. Dr. D. Tang and N. Wong prepared and edited the manuscript.

Relationship to Ph.D. research

This work reveals an association between PCSLCs and advanced PC on the basis of MUC1, a glycoprotein typically involved in epithelial cell protection but also demonstrated to have nuclear function. Nuclear MUC1 has been implicated in a wide array of cellular processes known to promote cell proliferation and EMT. Increased expression in our PCSLCs correlates with chemoresistance and metastatic features, and through computational analysis of PC gene expression datasets we have revealed a high association of MUC1 with metastasis and CRPC.

Preface

Affymetrix microarray analysis identified a 3.78 fold increase of MUC1 transcript levels in our DU145 PCSLCs versus parental DU145s. This upregulation was confirmed through qRT-PCR and Western blotting, and also observed in xenograft tumours derived from each cell line. Additionally, treatment of these tumours with the cytotoxic agent docetaxel heightened MUC1 expression further, creating an association with docetaxel-resistant CRPC cases.

Further computational analysis with multiple gene expression databases revealed greater MUC1 transcript levels and GCNs in metastatic samples compared to localized PC cases. These GCNs also correlated more with CRPCs than metastatic PCs, and with its 25-gene network associates more highly with neuroendocrine prostate cancers (NEPCs), a more aggressive type of PC. As a whole, the MUC1 gene network may be a more effective gene signature than the commonly used AR-network at predicting CRPC.

Amplification of MUC1 in prostate cancer metastasis and CRPC development

Nicholas Wong,[1,2,3] Pierre Major,[4] Anil Kapoor,[2,5] Fengxiang Wei,[1,2,3,6] Judy Yan,[1,2,3] Tariq Aziz,[7] Mingxing Zheng,[8,9] Dulitha Jayasekera,[1,2,3] Jean-Claude Cutz,[7] and Damu Tang [1,2,3, #]

[1]Division of Nephrology, Department of Medicine, McMaster University; [2]Father Sean O'Sullivan Research Institute, [3]the Hamilton Center for Kidney Research, St. Joseph's Hospital; [4]Division of Medical Oncology, Department of Oncology, McMaster University, [5]Department of Surgery, McMaster University, Hamilton, Ontario, Canada; [6]the Genetics Laboratory, Longgang District Maternity and Child Healthcare Hospital, Longgang District, Shenzhen, Guangdong, P.R. China; [7]Department of Pathology and Molecular Medicine, McMaster University, Hamilton, Ontario, Canada; [8]Department of Respiratory Medicine, Shenzhen 2nd People's Hospital and [9]the First Affiliated Hospital of Shenzhen University Medical School, Shenzhen, Guangdong 518035, China

#Correspondence:
Damu Tang
T3310, St. Joseph's Hospital
50 Charlton Ave East
Hamilton, Ontario, Canada
L8N 4A6
Tel: (905) 522-1155, ext. 35168
Fax: (905) 521-6181
E-mail: damut@mcmaster.ca

Conflict of interest: All authors declare no conflict of interest

Key words: MUC1, prostate cancer, prostate cancer stem cells, metastasis, castration resistant prostate cancer

Number of figures: 10

Number of tables: 3

ABSTRACT

We report here MUC1 upregulation in prostate cancer stem-like cells (PCSLCs). In comparison to DU145 non-PCSLCs, DU145 PCSLCs expressed a higher level of MUC1 and produced similar xenograft tumors resistant to docetaxel treatment. Remarkably, docetaxel robustly enhanced MUC1 expression in xenografts. While immunohistochemistry staining of 34 primary PCs revealed variability in MUC1, Nanostring technology demonstrated elevated MUC1 mRNA levels in 4 of 7 PCs compared to their normal matched tissues. We subsequently obtained MUC1 mRNA data from several large datasets within Oncomine™, and observed an increase in MUC1 mRNA in 82 metastases versus 280 primary PCs. This increase is supported by MUC1 expression in bone metastases. Furthermore, an elevation in MUC1 gene copy number (GCN) in 37 metastases over 181 primary tumors was also shown using these datasets. Additional detailed analyses of genomic datasets within cBioPortal revealed increases in MUC1 GCN in 2% (6/333) of primary PCs, 6% (9/150) of metastatic PCs, and 33% (27/82) of castration resistant PCs (CRPCs); in comparison, the respective increase in androgen receptor (AR) GCN was 1%, 63%, and 56%, revealing a specific increase in MUC1 GCN in CRPC. Furthermore, a 25-gene MUC1 network was amplified in 52% of CRPCs compared to 69% of CRPCs displaying GCN increases in an AR co-regulator group. While genomic alterations in the MUC1 network largely overlap with those in the AR group, 18

CRPCs (in which 66.7% were neuroendocrine PC) showed genomic alterations only in the MUC1 network. Moreover, genomic alterations in the MUC network correlated with PC relapse.

INTRODUCTION

Prostate cancer (PC) is the most prevalent male-specific cancer in the developed world [1]. PC progresses from high grade prostatic intra-epithelial neoplasia (HGPIN), to local carcinoma, to metastatic disease with bone as the preferential site [2]. Localized tumors can be effectively managed through a variety of approaches, including watchful waiting, surgical removal, and radiation. In contrast, options for patients with metastatic PC remain limited. Androgen deprivation therapy (ADT), a strategy that was pioneered by Charles Huggins in the 1940s [3, 4], remains the standard of care in these patients. However, the treatment is only palliative, as resistant tumors in the form of castration resistant PC (CRPC) inevitably arise. Until recently, these patients were commonly treated with docetaxel-based chemotherapy. Cumulative research efforts have revealed the dependency of androgen receptor (AR) signalling despite androgen deprivation for a large proportion of CRPCs [5, 6], which led to the recent development of abiraterone and enzalutamide for treatment [7, 8]. Additionally, the cell-based vaccine sipuleucel-T has recently become available [9, 10], a therapy that depends on tumor associated antigens (TAAs).

Mucin 1 (MUC1) is the most well-characterized TAA [11]. The glycoprotein is a transmembrane member of the mucin family, and is broadly expressed on the apical surface of most epithelial tissues, including the pancreas, breast, lung, and gastrointestinal tract [11, 12]. MUC1 is a heterodimer consisting

of a large N-terminal fragment (MUC1-N) that is anchored to the cell membrane on the extracellular side by binding to the transmembrane C-terminal MUC1 subunit (MUC1-C). Mature MUC1 is formed from auto-cleavage of a pre-peptide [13-15]. MUC1-N contains a variable number of conserved tandem repeats of 20 amino acids, which are highly glycosylated by *O*-linked glycans. The MUC1 protein is expressed on the apical surface of epithelium and plays a protective role for the mucosal epithelial surface [16]. However, it is aberrantly expressed in numerous malignancies with respect to loss of polarity in cancer cells, overexpressed in over 70% of cancers, and differentially glycosylated [11, 17]. The cancer-associated MUC1 with aberrant glycosylation is highly immunogenic [18-20]. These properties have made the MUC1 TAA a major focus in developing antigen-specific immunotherapies for multiple tumor types [12].

Our recent phase I/II clinical trial using a Tn-MUC1 peptide-based cell vaccine (dendritic cells/DC) revealed that this approach was able to delay the doubling of prostate specific antigen (PSA) levels in CRPC patients, demonstrating utility in developing MUC1-based DC vaccines in treating this population [21]. However there are contradictory findings in the literature, depending on which antibody is used, regarding the detection of MUC1 overexpression in PC progression. Increases in the MUC1 protein and aberrant MUC1 glycosylation were reported in PC [22-24]. However, using a different antibody (anti-MUC1-N, HMFG2), increased MUC1 expression in PC

progression could not be demonstrated [25]. To investigate the association of MUC1 expression with PC tumorigenesis, we have attempted to track MUC1 though PC progression. In our immunohistochemical examination of MUC1 expression, we were also unable to show a MUC1 increase in PCs with Gleason scores (GS) ≥8 in comparison to those with GS6-7. We reasoned that the differences among individual investigations might be attributable to the antibodies used, recognizing MUC1-N which can be shed off from the cell surface [17]. With this in mind, we used an alternative approach and have examined increases in MUC1 mRNA and gene copy number (GCN) following PC progression. Our findings clearly demonstrate elevated MUC1 mRNA levels in metastatic PCs and amplification of the MUC1 gene in CRPCs.

RESULTS

Association of MUC1 with prostate cancer stem-like cells (PCSLCs) and PC progression

There is accumulating evidence demonstrating an association of MUC1 upregulation with cancer progression [26], including PC [27]. It is also clear that cancer consists of heterogeneous cell populations [28-30], in which cancer stem cells (CSCs) are critical for cancer progression [31-33]. In accordance with this concept, MUC1 has previously been reported to associate with and contribute to the development of breast cancer stem cells [34, 35]. Similarly, prostate cancer stem cells (PCSCs) are essential for PC progression [36], suggesting a relationship between MUC1 and PCSCs. By taking advantage of our recently established PCSLCs (sphere cells) derived from DU145 monolayer cells [37], we have demonstrated a significant upregulation of MUC1 in DU145 sphere cells at both mRNA and protein levels (Figure 3.1A, B). Prolonged film exposure also depicts low MUC1 protein expression in DU145 monolayer, PC3, and LNCaP cells (data not shown). Furthermore, an increase in MUC1 was also demonstrated in xenograft tumors generated from DU145 sphere cells compared to those produced by DU145 monolayer cells (Figure 3.1C). Taken together, the above observations reveal an association of MUC1 with PCSLCs.

We have previously demonstrated that DU145 sphere cells possess a 100-fold higher capability of tumorigenesis [37] and are more resistant to a genotoxic reagent-induced cytotoxicity [38] in comparison to DU145 monolayer cells, further suggesting an association of MUC1 upregulation with chemoresistance in PC. To examine this possibility, we produced xenograft tumors from DU145 monolayer and sphere cells. Docetaxel treatment for 2 weeks significantly reduced tumor volume for monolayer cell-derived xenografts but not for sphere cell-derived xenografts (Figure 3.2A). Upon analysis, the latter expressed elevated levels of MUC1 in comparison (Figure 3.2B, mock treatment). Intriguingly, docetaxel treatment increased MUC1 expression in xenograft tumors produced by both cell types. Sphere cell-derived xenografts displayed a robust elevation of MUC1 in response to docetaxel when compared to monolayer cell-derived tumors (Figure 3.2B). These observations are in line with a recent report demonstrating that docetaxel treatment increased MUC1 expression in LNCaP cell-derived xenograft tumors [39]. Collectively, our study supports an association of MUC1 upregulation with PC progression.

MUC1 increases in metastatic PCs

To further study the above association, we have examined MUC1 protein expression in 34 primary PCs consisting of 13 low grade (GS6-7) and 21 high grade PCs (GS8-10) (Table 3.1). By using an anti-MUC1-N antibody (BD), MUC1 presence was clearly detected in PC tumors (Figure 3.3A), but with variable levels (Table 3.1). MUC1 expression was not greater in high grade PCs than low grade PCs (Figure 3.3B) as we had expected. Since tumor cells can shed off MUC1-N [17], detection of MUC1 by immunohistochemistry (IHC) against this antigen may not truly reveal the status of MUC1 expression. As most anti-MUC1 antibodies used in IHC recognize MUC1-N, we went on to investigate MUC1 mRNA in 7 pairs of PC and benign prostate tissues using state-of-the-art Nanostring technology. The PC tissues contained 60-80% carcinoma tissue. This was validated by demonstrating PTEN downregulation and ERG upregulation (indicative of TMPRSS2-ERG fusion) in 5/7 of the PC tissues (Table 3.2). In comparison to their respective benign prostate tissues, MUC1 mRNA was elevated in 4 PC cases (Table 3.2), supporting the notion of MUC1 upregulation in PC.

To thoroughly investigate the relationship of MUC1 mRNA levels and PC progression, we downloaded MUC1 mRNA data from four datasets in the Oncomine^{TM} database (Compendia Bioscience, Ann Arbor, MI); the Grasso,

Lapointe, Taylor, and Tomlins datasets [27, 40-42]. In the analysis of MUC1 mRNA in 221 PCs (60+131+30) and 92 normal prostate tissues (40+29+23), MUC1 mRNA was actually reduced in primary PCs (Figure 3.4C, D, and E). However, an increase in MUC1 mRNA was observed in metastatic PCs compared to primary tumors in the Grasso (Figure 3.4A) and Tomlins datasets (Figure 3.4E). This difference is particularly clear between primary and distant metastasis (Figure 3.4D, right panel). Additionally, this elevation differentiated metastases from organ-confined tumors according to ROC curves (Figure 3.4B and F). Collectively, these analyses suggest a general increase in MUC1 mRNA following PC metastatic progression.

The above concept is supported by increases in MUC1 gene copy number (GCN) in metastatic PCs compared to primary tumors (Figure 3.5A). Once again, this increase is able to separate metastases from primary PC via an area under curve (AUC) value of 0.75 (Figure 3.5B). Lastly, among 124 PC tumors and 61 benign prostate tissues analyzed in the TCGA dataset, a significant increase in MUC1 GCN could only be demonstrated in GS9 PCs compared to benign prostate tissues (Figure 3.5C). Taken together, these results support MUC1 upregulation as being a late event during PC progression and in metastatic cases.

Finally, we also made an effort to examine MUC1 protein in PC bone metastasis. In four bone metastases examined, MUC1 was detected

heterogeneously among patients, among different tumor masses within the same tissue, and among different cancer cells within the same tumor mass (Figure 3.6, Supplementary Figure 3.1). We could not detect MUC1 expression in patient #2 (Figure 3.6, Supplementary Figure 3.1), which might be attributable to a relative low level of tumor load (Supplementary Figure 3.1). For the other three patients, while the number of cells expressing MUC1 varied, its presence was readily detected in positive cells (Figure 3.6). This pattern of heterogeneous expression is consistent with MUC1's association with our prostate cancer stem-like cells. Although it is impossible to compare MUC1 protein expression in our limited number of bone metastases to local PCs, bone metastases clearly express MUC1 (Figure 3.6).

Specific amplification of the MUC1 gene in CRPC

Advances in next-generation (second-generation) sequencing (NGS) technologies have made whole genome sequencing a reality. There are currently 10 datasets of genome sequencing studies deposited into the cBioPortal database [43, 44], and these resources cover primary, metastatic, and castration resistant PC (cBioPortal/ http://www.cbioportal.org/index.do). By taking advantage of this rich source of PC genomic data, we have systemically analyzed alterations in MUC1 GCN. Among 333 prostate adenocarcinomas [45], 150 metastatic PCs

[46], and 107 CRPCs [47], MUC1 gene is amplified in 1.8%, 6%, and 30% of the patient cohorts, respectively (Table 3.3), demonstrating a unique amplification of the MUC1 gene in CRPCs.

To further study the relationship between MUC1 gene amplification and CRPC, we noticed a MUC1 gene network consisting of the seed node MUC1 and 24 linker nodes, which were generated using the cBioPortal system (see Supplementary Figure 3.2 for details). The network contains two major components (see Discussion for a second major group): notably, a group of tyrosine kinases including EGFR and non-receptor tyrosine kinases (ABL1, ERBB2-4, LCK, LYN, SRC1, and ZAP70) (Supplementary Figure 3.2). These proteins have been demonstrated to have functional connections with MUC1-C [16, 17] and contribute to PC and CRPC development (Supplementary Table 3.1). After investigating whether this network is connected with PC progression, our analyses revealed that genomic alteration (amplification or deep deletion) of these genes occurred in 26% of primary PCs, 25% of metastatic PCs, and 52% of CRPCs (Figure 3.7).

Genomic alteration in the MUC1 network is more specific to CRPC than genomic changes in androgen receptor (AR) groups

Persistent AR signalling by alterations in AR, a pioneer factor FOXA1, and three steroid receptor coactivators (NCOA1/SRC-1, NCOA2/SRC-2, and NCOA3/SRC-3) is known to contribute to CRPC progression [5, 48]. Amplification of *NCOA2*, which activates AR signalling [5, 41], occurs in 24.3% of metastatic PCs. Although evidence supports that AR transcriptional activity is repressed by nuclear receptor corepressor 1 (NCOR1), NCOR2, and PLZF/ZBTB16 [49-51], genomic alterations in AR, FOXA1, and these corepressors were reported in a large CRPC cohort [47]. We thus analyzed genomic alterations (GNs) in AR and its coactivators (FOXA1 and NCOA1-3) or AR coregulators (FOXA1, NCOR1, NCOR2, and ZBTB16). GNs in the AR gene predominantly occurred in the form of amplification, in 56% of CRPCs (Figure 3.8A). Consistent with the MUC1 gene network's concurrent GCN increases in individual CRPCs (Figure 3.7), co-amplification of AR and its coregulators (Figure 3.8A) or coactivators (Supplementary Figure 3.3) was also observed. In primary PC, metastatic PC, and CRPC populations, the AR gene was altered in 1%, 63%, and 56% of tumors, respectively (Figure 3.8). In these cohorts, the MUC1 gene was amplified in 2%, 6%, and 33%, respectively (Figure 3.7). Genomic alterations occurred in 16%, 73%, and 69% in the above cohorts for the AR coregulator group respectively, (Figure 3.8) as well as 14%, 73%, and 71%

for the AR coactivator group (Supplementary Figure 3.3). Corresponding changes in the MUC1 network were 26%, 25%, and 52% (Figure 3.7). Collectively, these analyses support the concept that genomic alterations in MUC1 and the MUC1 network are more specific to CRPC progression compared to AR and the AR groups.

Genomic alterations in the MUC1 network bi-associate with CRPC adenocarcinoma and neuroendocrine PC (NEPC)

We subsequently performed an analysis to compare genomic alterations in the MUC1 network to those in the AR gene. Genomic alterations (amplification, deep deletion, and mutations) in the MUC1 network display both concordant and independent signatures with the AR gene (Figure 3.9A). A large proportion of changes detected in the MUC1 network overlap with those observed in the AR gene (Figure 3.9A). In CRPC however, a minor proportion of genomic alterations to the MUC1 network occurs independently of changes in the AR gene (Figure 3.9A, see those CRPCs lined with two dot lines). In the latter group, the JUP gene displays no changes (Figure 3.9A). The most interesting feature in this group is the enrichment of NEPC cases, which compose 66.7% (12/18) of the CRPC cases (Figure 3.9A), suggesting that this gene signature (AR and JUP genes are genomic alteration free, while there are a number of genomic changes in the MUC1 network) shows greater specificity towards this type of CRPC.

While in the primary PC cohort independency was observed between genomic alterations of the MUC1 network and AR gene (Supplementary Figure 3.4), both concordance and independency could be identified in the metastatic PC cohort (Figure 3.9B). Since all metastatic PCs will progress to CRPC as either adenocarcinoma or NEPC, it will be interesting to examine whether metastases with genomic alterations only in the MUC1 network will progress into NEPCs.

Genomic alterations in the MUC1 network associate with a reduction in disease free survival (DFS)

CRPC is a major form of PC progression; the association of genomic alterations in the MUC1 network with CRPC strongly suggests a correlation of these changes with PC recurrence (DFS) and/or overall survival (OS). To test this possibility, we first performed a time-to-event analysis using a Kaplan-Meier curve to determine whether elevation of MUC1 mRNA associates with rapid kinetics of PC metastatic progression. By using the data available from the Grasso dataset within Oncomine^{TM} (Compendia Bioscience, Ann Arbor, MI), we could not observe a correlation (Supplementary Figure 3.5).

We subsequently examined a potential association of genomic alterations in the MUC1 network with DFS and OS. Among the 10 datasets related to genomic alteration in PC from cBioPortal [43, 44], one contained follow-up data

for PC relapse of 84 patients [41] and another had follow-up information for PC-related mortality of 49 cases [40]. Consistent with a small number of cases with MUC1 genomic alterations in a large primary PC and metastasis population (Figure 3.7), MUC1 genomic alterations were also infrequently detected in these small cohorts [40, 41] (Supplementary Figure 3.6). To perform a meaningful Kaplan-Meier analysis, we thus used cases with and without alterations in the MUC1 network, and we are able to show that the genomic alterations significantly associated with a reduction in DFS (Figure 3.10A) but not OS (Figure 3.10B). Similar observations were also obtained for the AR coregulator group (Figure 3.10C, D); the detailed genomic alterations for this group are included in Supplementary Figure 3.7. Surprisingly, genomic changes in the AR coactivator group do not correlate with either DFS or OS (Supplementary Figure 3.8). Collectively, genomic alterations in the MUC1 network or the AR coregulator group facilitate PC recurrence, but not patient survival following metastatic events. Nonetheless, by comparing the reduction curve and median months disease free survival (MMDFS) associated with genomic alterations in the MUC1 network to those in the AR coregulator group, the former is likely to have a greater impact on promoting PC recurrence.

DICUSSION

MUC1 is the most attractive TAA, a status that is attributable not only to its dramatic alterations in cancer but also to the prevalence of these changes across multiple tumor types [11, 12, 17]. Furthermore, the MUC1-C subunit promotes the actions of multiple critical oncogenic pathways, including those of EGFR, ERBB, non-receptor tyrosine kinases, β-catenin, NF-κB, PKM2, and others [16, 17, 52]. However, although there is evidence supporting an association of MUC1 amplification with PC tumorigenesis, this relationship seems variable depending on the antibodies used. As such, the relationship between MUC1 expression and PC progression has not been thoroughly investigated or established.

By employing comprehensive experimental systems and analyses involving *in vitro* and *in vivo* studies, as well as examining the changes in MUC1 protein, mRNA, and genomic DNA, our research reveals several novel observations: MUC1 upregulation associates with PCSLCs, MUC1 levels are increased in the late phases of PC progression (metastasis and CRPC development), there is specific copy number amplification of the MUC1 gene and its associated gene network in CRPC, genomic alterations in the MUC1 network together with non-alteration of the AR gene could be potentially utilized as an NEPC signature, and the correlation of genomic alterations in the MUC1 network with PC relapse.

For the association with PC recurrence, it appears that not all MUC1 network associated genes display genomic alterations in the primary PC cohort (Supplementary Figure 3.6, left panel). As expected, removal of these unchanged genes does not affect the network's association with DFS based on this cohort (data not shown). While this may suggest that the remaining 12 genes (ABL1, APC, CTNNB1, EGFR, ERBB2, ERBB3, ERBB4, GALNT1, GALNT2, GRB2, LYN, and SOS1) are a signature of PC relapse, it should be taken with caution as this cohort is rather small. Future research will need to address this issue.

Our observed upregulation of MUC1 in PCSLCs suggests a mechanism underlying MUC1 overexpression in PC. It is becoming clearer that the plasticity of cancer stem cells is critical in cancer evolution in response to endogenous and exogenous selective pressures (such as therapies). This plasticity likely contributes to the acquisition of new properties that drive cancer metastasis and development of therapeutic resistance. In this regard, PCSC-associated plasticity may contribute to MUC1 upregulation. In support of this possibility, we have recently reported a new PC metastatic factor contactin 1 (CNTN1) that was also derived from PCSLCs [53]. In a similar manner, PCSC-derived MUC1 may be specifically important for metastatic progression, considering genomic amplification in the MUC1 gene is an infrequent event in metastatic PCs (Figure 3.7).

In CRPC however, genomic amplification is likely a major mechanism underlying MUC1 upregulation (Figure 3.7). While the different mechanisms for increasing MUC1 levels in PC metastasis over CRPC development could be revealed in the future, it is likely that androgen deprivation is a contributing factor to MUC1 gene amplification in CRPC. This concept is supported by the importance of persistent AR signalling in CRPC development [5] and in promoting genomic stability [54-56]. Additionally, this concept is also in line with the observed concordance between AR gene amplification and MUC1 GCN increases in CRPC (Figure 3.9A). However, the genomic amplifications which occur in MUC1 and its gene network are not merely a side effect of AR signalling-caused genomic instability, which can be reflected by the independent genomic alterations between the MUC1 network (Figure 3.7) and the AR groups (Figure 3.8, Supplementary Figure 3.3).

The MUC1 network contains 9 tyrosine kinases (ALB1, EGFR, ERBB2, ERBB2, ERBB4, LCK, LYN, SRC1, and ZAP70), GRB2, and SOS1 (Supplementary Table 3.1); both GRB2, and SOS1 facilitate tyrosine kinase signalling [57]. Thus, proteins contributing to tyrosine kinase function compose 45.8% (11/24) of the network's linker nodes (Supplementary Figure 3.2). Tyrosine kinase activity is well known to promote cancer progression, which is likely a major attribute to the specific association of the MUC1 network and CRPC. The second major group of proteins in the MUC1 network are enzymes

(GALNT1, GALNT2, GALNT10, GALNT12, GALNT15, OSGEP, and SIGLEC1) that contribute to MUC1 glycosylation (Supplementary Table 3.1). The involvement of these proteins in tumorigenesis has not been well studied. Nonetheless, their co-amplification with MUC1 in CRPC suggests a contribution to at least the generation of MUC1 as a CRPC-associated antigen. The MUC1 network also possesses APC1, JUP, and PRKCD genes that display tumor suppression functions (Supplementary Table 3.1), which are also co-amplified (Supplementary Table 3.1). The function of their amplification remains unclear. It may be a result from the prevalence of genomic amplification over deletion in the CRPC cohort [47]. However, it will be a challenge to reconcile their amplification in CRPC with their deep deletion in primary tumors (Figure 3.7). The same situation also applies to GALNT2 (Figure 3.7). It is a provocative thought that the primary PCs with these deletions are unlikely to progress to CRPC. An equally provocative possibility is that their amplification contributes to CRPC development in some way. These uncertainties may be solved in the future. Nonetheless, our analysis supports an intriguing connection of the MUC1 network with CRPC.

Similar ambiguities are also observed in the AR groups. While co-amplification of the AR gene with its coactivators is in line with the importance of persistent AR signalling in CRPC development [5], co-amplification of AR with its repressors (NCOR1, NCOR2, and ZBTB16) may play a different role in the

process. Both NCOR1 and NCOR2 reduce agonist and antagonist-elicited AR activity [58], indicating a complex role of these factors in modulating AR function. Intriguingly, addition of NCOR1, NCOR2, and ZBTB16 to AR and FOXA1 empowers an association with PC recurrence (Figure 3.10C); in fact AR plus NCOR1, NCOR2, and ZBTB16 is almost sufficient to predict a reduction in DFS (Supplementary Figure 3.9). Intriguingly, the AR coactivator group does not possess this ability (Supplementary Figure 3.8), suggesting that co-amplification of AR with its repressors impacts CRPC development.

Considering the well-established associations of genomic alterations in the AR and its co-activator genes with CRPC [5, 41, 47, 48, 59], it is remarkable that respective aberrations in the MUC1 network are likely more specific in identifying CRPC. While this needs to be further examined, it is also rather intriguing that genomic alterations in the MUC1 network and AR largely overlap (Figure 3.9A), indicating a positive regulation between AR and MUC1. However, current evidence supports the opposite possibility of mutual inhibition [60, 61]; this negative feedback may contribute to the MUC1 network's unique genomic changes in NEPCs (Figure 3.9A), suggesting MUC1’s contribution to the generation of NEPC during ADT.

In our investigation we have uncovered a specific upregulation of MUC1 in CRPC, which is not only novel but also implies a role of MUC1 in CRPC

development. In accordance with the essential contribution of PCSCs in CRPC progression [36], the increase of MUC1 levels in our PCSLCs (Figure 3.1) provides additional support to this statement. This development would suggest an addition of a MUC1-based immunotherapy during ADT. This combination is particularly appealing in view of our recent phase I/II clinical trial using dendritic cell-based MUC1 vaccination in treating patients with CRPC. Furthermore, a recent publication reported a significant survival advantage to combining docetaxel and ADT, compared to ADT alone, in treating patients with metastatic PC [62]. Based on MUC1's association with PCSLCs and upregulation of MUC1 expression following docetaxel treatment reported here, it could be expected that combinational therapy involving docetaxel, ADT, and MUC1-based immunotherapy may provide an additional survival benefit over that of just docetaxel+ADT. MUC1 has already been explored for cancer immunotherapy strategies based on cancer-associated alterations in MUC1-N. However, a recent development identifying GO-203 that specifically targets MUC1-C [63] instead is an attractive addition to MUC1-based therapies for CRPC.

MATERIALS AND METHODS

Cell culture and generation of DU145 spheres (PCSLCs)

LNCaP, PC3, and DU145 cells were purchased from American Type Culture Collection (ATCC), and cultured in RPMI-1640 (LNCaP), F12 (PC3) and MEM (DU145) media supplemented with 10% FBS (Sigma Aldrich) and 1% Penicillin-Streptomycin (Thermo Fisher Scientific). DU145 spheres were generated and cultured according to our published conditions [37]. Briefly, DU145 monolayer cells (non-PCSLCs) were individualized and seeded at a density of 5,000 cells/mL in serum-free (SF) media (3:1 DMEM/F12 mixture) (Thermo Fisher Scientific) containing 0.4% bovine serum albumin (BSA) (Bioshop Canada Inc.) supplemented with 0.2x concentration of B27 minus Vitamin A (Thermo Fisher Scientific) and 10ng/ml EGF (Sigma Aldrich), in T75 flasks. Typical spheres were formed in 10 to 12 days.

Collecting primary prostate cancer

Prostate biopsies and radical prostatectomy tissues were obtained at St. Joseph's Hospital in Hamilton, Ontario, Canada under approval from the local Research Ethics Board (REB# 11-3472) and with patient consent.

Nanostring technology

Patient tissues were obtained as above. Formalin fixed paraffin embedded (FFPE) PC tissues containing 60-80% carcinoma were collected as 10μm curls, and RNA was isolated using the High Pure FFPET RNA Isolation Kit (Roche) following the manufacturer's instructions. Purified RNA was then sent to the McMaster Farncombe Institute (Hamilton, Ontario, Canada) for analysis via the nCounter Nanostring Technologies platform. Matched benign prostate tissue was used as control. Gene expression of TMPRSS2-ERG fusion and PTEN were used as positive controls to confirm specific examination of PC tissue. A low, medium, and high expressing housekeeping gene were used as normalization controls (ABCF1, TUBB, GAPDH), by taking the total input RNA and dividing by their geometric mean.

Xenograft tumor formation and docetaxel treatment

DU145 monolayer (non-PCSLCs) and sphere (PCSLCs) cells were resuspended in 0.1 ml MEM/Matrigel mixture (BD) (1:1 volume), followed by subcutaneous implantation into the flanks of 8 week-old male NOD/SCID mice (The Jackson Laboratory). 10^6 DU145 monolayer cells and 10^4 DU145 sphere cells were implanted, based on our previous report that DU145 spheres display a 100-fold higher capacity to form xenografts [37]. Tumors were assessed through

observation and palpation, and tumor growth was measured weekly using calipers. Tumor volume was determined using the formula $V = L \times W^2 \times 0.52$. Once tumors reached a volume of at least $100mm^3$, mice were treated with either DMSO control or docetaxel (Santa Cruz) at 10mg/kg once a week for three weeks by intraperitoneal injection. After a week of recovery, treatment was repeated until tumors reached a volume $\geq 1000\ mm^3$, at which point animals were sacrificed. All animal work was carried out according to experimental protocols approved by the McMaster University Animal Research Ethics Board.

Western blot analysis

Cells were lysed in a buffer containing 20mM Tris (pH 7.4), 150mM NaCl, 1mM EDTA, 1mM EGTA, 1% Triton X-100, 25mM sodium pyrophosphate, 1mM NaF, 1mM β-glycerophosphate, 0.1mM sodium orthovanadate, 1mM PMSF, 2μg/ml leupeptin and 10μg/ml aprotinin. 50μg of whole cell lysate was separated on SDS-PAGE gel, and transferred onto Hybond ECL nitrocellulose membranes (Amersham), followed by blocking with 5% skim milk at room temperature for one hour. Primary antibodies were incubated overnight at 4^oC with agitation, and secondary antibodies incubated for one hour at room temperature. Signals were then developed (ECL Western Blotting Kit, Amersham). Primary antibodies: anti-MUC1 1:50 (BD) and anti-Actin 1:1000 (Santa Cruz).

Quantitative real-time PCR analysis of MUC1 expression

Total RNA was isolated from DU145 monolayer and DU145 sphere cells with TRIZOL, and reverse transcription was carried out using Superscript III (Thermo Fisher Scientific) according to the manufacturer's instructions. Quantitative real-time PCR was performed using the ABI 7500 Fast Real-Time PCR System (Applied Biosystems) using SYBR-green (Thermo Fisher Scientific). All samples were run in triplicate. MUC1 (Forward): 5'-TGCCGCCGAAAGAACTACG-3', MUC1 (Reverse): 5'-TGGGGTACTCGCTCATAGGAT-3'. β-Actin (Forward): 5'-ACCGAGCGCGGCTACAG-3', β-Actin (Reverse): 5'-CTTAATGTCACGCACGATTTCC -3'.

Immunohistochemistry (IHC)

IHC was performed on 34 paraffin embedded and serially cut prostate cancer tissues obtained from St. Joseph's Hospital, Hamilton, Ontario, Canada. Slides were deparaffinized in xylene and cleared in an ethanol series. Antigen retrieval was performed in a food steamer for 20 minutes using sodium citrate buffer (pH = 6.0). Tissues were blocked for 1 hour in PBS containing 1% BSA and 10% normal goat serum (Vector Laboratories). MUC1 antibody (1:200, BD) was incubated overnight at 4°C. Secondary antibody biotinylated goat anti-mouse

IgG and Vector ABC reagent (Vector Laboratories) were incubated according to the manufacturer's instructions. Secondary antibody only was used as negative control. Washes were performed with PBS. Chromogenic reaction was carried out with diaminobenzidine (Vector Laboratories), and slides were counterstained with haemotoxylin (Sigma Aldrich). Image analysis was performed using ImageScope software (Leica Microsystems Inc.). Staining intensity values derived from ImageScope were converted to an HScore using the formula [HScore = (% Positive) x (intensity) + 1]. The HScore was normalized through background subtraction and averaged amongst ≤ 5 images per tissue sample.

Gene expression studies

The specific methods of how each study obtained gene expression, gene alteration, and copy number variation data for deposit into Oncomine™, cBioPortal, or Gene Expression Omnibus (GEO), can be found in their respective publications. In general, DNA and RNA were purified from frozen or FFPE tissues and analyzed via comparative genomic hybridization platforms, whole exome sequencing, paired-end sequencing, and cDNA microarrays. For examination of raw data, many groups aligned to the hg19 build of the human reference genome.

Oncomine™ and GEO data was downloaded and analyzed using GraphPad Prism 5.0 software. Information from cBioPortal was examined using the online tools provided.

Statistical analysis

Statistical analysis was performed using student t-test, with $p < 0.05$ being considered statistically significant.

ACKNOWLEDGEMENTS

This work was supported in part by a GAP funding from McMaster University and St. Joseph's Hospital in Hamilton, an award from Teresa Cascioli Charitable Foundation Research Award in Women's Health to D.T., as well as by grants from the National Natural Science Foundation of China (Grant No. 81201568), the Natural Science Foundation of Guangdong Province (Grant No. 2014A030313749), the National Natural Science Foundation of Heilongjiang Province (Grant No. C2015033), and the Shenzhen Program of Innovation and Entrepreneurship for Overseas Elites (Grant No. KQCX20120814150420241) to F.W. The results shown here are in part based upon data generated by the TCGA Research Network (http://cancergenome.nih.gov/) and by Oncomine™ (https://www.oncomine.org/).

CONFLICT OF INTEREST

All authors declare no conflict of interest

REFERENCES

1. Ferlay J, Soerjomataram I, Dikshit R, Eser S, Mathers C, Rebelo M, Parkin DM, Forman D and Bray F. Cancer incidence and mortality worldwide: sources, methods and major patterns in GLOBOCAN 2012. Int J Cancer. 2015; 136(5):E359-386.
2. Heidenreich A, Bastian PJ, Bellmunt J, Bolla M, Joniau S, van der Kwast T, Mason M, Matveev V, Wiegel T, Zattoni F and Mottet N. EAU guidelines on prostate cancer. Part II: Treatment of advanced, relapsing, and castration-resistant prostate cancer. Eur Urol. 2014; 65(2):467-479.
3. Rosenberg J and Small EJ. Prostate cancer update. Curr Opin Oncol. 2003; 15:217-221.
4. Ross JS. The androgen receptor in prostate cancer: therapy target in search of an integrated diagnostic test. Adv Anat Pathol. 2007; 14:353-357.
5. Mitsiades N. A road map to comprehensive androgen receptor axis targeting for castration-resistant prostate cancer. Cancer research. 2013; 73(15):4599-4605.
6. Mateo J, Smith A, Ong M and de Bono JS. Novel drugs targeting the androgen receptor pathway in prostate cancer. Cancer Metastasis Rev. 2014; 33(2-3):567-579.
7. de Bono JS, Logothetis CJ, Molina A, Fizazi K, North S, Chu L, Chi KN, Jones RJ, Goodman OB, Jr., Saad F, Staffurth JN, Mainwaring P, Harland S, Flaig TW, Hutson TE, Cheng T, et al. Abiraterone and increased survival in metastatic prostate cancer. N Engl J Med. 2011; 364(21):1995-2005.
8. Scher HI, Fizazi K, Saad F, Taplin ME, Sternberg CN, Miller K, de Wit R, Mulders P, Chi KN, Shore ND, Armstrong AJ, Flaig TW, Flechon A, Mainwaring P, Fleming M, Hainsworth JD, et al. Increased survival with enzalutamide in prostate cancer after chemotherapy. N Engl J Med. 2012; 367(13):1187-1197.
9. Chaturvedi S and Garcia JA. Novel agents in the management of castration resistant prostate cancer. Journal of carcinogenesis. 2014; 13:5.
10. Drake CG. Prostate cancer as a model for tumour immunotherapy. Nat Rev Immunol. 2010; 10(8):580-593.
11. de Paula Peres L, da Luz FA, Dos Anjos Pultz B, Brigido PC, de Araujo RA, Goulart LR and Silva MJ. Peptide vaccines in breast cancer: The immunological basis for clinical response. Biotechnol Adv. 2015; 33(8):1868-1877.

12. Wurz GT, Kao CJ, Wolf M and DeGregorio MW. Tecemotide: an antigen-specific cancer immunotherapy. Hum Vaccin Immunother. 2014; 10(11):3383-3393.

13. Ligtenberg MJ, Kruijshaar L, Buijs F, van Meijer M, Litvinov SV and Hilkens J. Cell-associated episialin is a complex containing two proteins derived from a common precursor. The Journal of biological chemistry. 1992; 267(9):6171-6177.

14. Levitin F, Stern O, Weiss M, Gil-Henn C, Ziv R, Prokocimer Z, Smorodinsky NI, Rubinstein DB and Wreschner DH. The MUC1 SEA module is a self-cleaving domain. The Journal of biological chemistry. 2005; 280(39):33374-33386.

15. Macao B, Johansson DG, Hansson GC and Hard T. Autoproteolysis coupled to protein folding in the SEA domain of the membrane-bound MUC1 mucin. Nat Struct Mol Biol. 2006; 13(1):71-76.

16. Singh PK and Hollingsworth MA. Cell surface-associated mucins in signal transduction. Trends in cell biology. 2006; 16(9):467-476.

17. Kufe DW. Mucins in cancer: function, prognosis and therapy. Nature reviews Cancer. 2009; 9(12):874-885.

18. Gendler S, Taylor-Papadimitriou J, Duhig T, Rothbard J and Burchell J. A highly immunogenic region of a human polymorphic epithelial mucin expressed by carcinomas is made up of tandem repeats. The Journal of biological chemistry. 1988; 263(26):12820-12823.

19. Hanisch FG, Schwientek T, Von Bergwelt-Baildon MS, Schultze JL and Finn O. O-Linked glycans control glycoprotein processing by antigen-presenting cells: a biochemical approach to the molecular aspects of MUC1 processing by dendritic cells. Eur J Immunol. 2003; 33(12):3242-3254.

20. Hiltbold EM, Alter MD, Ciborowski P and Finn OJ. Presentation of MUC1 tumor antigen by class I MHC and CTL function correlate with the glycosylation state of the protein taken Up by dendritic cells. Cell Immunol. 1999; 194(2):143-149.

21. Major P, Lacombe L, Fradet Y, Foley R, Scheid E, Bergeron A, Mukherjee S, Finn OJ, Gariepy J, Sekaly RP, Hotte S and Chou S. (2012). A phase I/II clinical trial of a MUC1-glycopeptide dendritic cell vaccine in castrate resistant non-metastatic prostate cancer patients Cancer research, pp. Abstract nr A16. .

22. Cozzi PJ, Wang J, Delprado W, Perkins AC, Allen BJ, Russell PJ and Li Y. MUC1, MUC2, MUC4, MUC5AC and MUC6 expression in the progression of prostate cancer. Clinical & experimental metastasis. 2005; 22(7):565-573.

23. Rabiau N, Dechelotte P, Guy L, Satih S, Bosviel R, Fontana L, Kemeny JL, Boiteux JP, Bignon YJ and Bernard-Gallon D. Immunohistochemical staining of mucin 1 in prostate tissues. In Vivo. 2009; 23(2):203-207.

24. Arai T, Fujita K, Fujime M and Irimura T. Expression of sialylated MUC1 in prostate cancer: relationship to clinical stage and prognosis. Int J Urol. 2005; 12(7):654-661.

25. Singh AP, Chauhan SC, Bafna S, Johansson SL, Smith LM, Moniaux N, Lin MF and Batra SK. Aberrant expression of transmembrane mucins, MUC1 and MUC4, in human prostate carcinomas. Prostate. 2006; 66(4):421-429.

26. Nath S and Mukherjee P. MUC1: a multifaceted oncoprotein with a key role in cancer progression. Trends in molecular medicine. 2014; 20(6):332-342.

27. Lapointe J, Li C, Higgins JP, van de Rijn M, Bair E, Montgomery K, Ferrari M, Egevad L, Rayford W, Bergerheim U, Ekman P, DeMarzo AM, Tibshirani R, Botstein D, Brown PO, Brooks JD, et al. Gene expression profiling identifies clinically relevant subtypes of prostate cancer. Proceedings of the National Academy of Sciences of the United States of America. 2004; 101(3):811-816.

28. Fidler IJ and Hart IR. Biological diversity in metastatic neoplasms: origins and implications. Science. 1982; 217(4564):998-1003.

29. Heppner GH and Miller BE. Tumor heterogeneity: biological implications and therapeutic consequences. Cancer Metastasis Rev. 1983; 2(1):5-23.

30. Nowell PC. Mechanisms of tumor progression. Cancer research. 1986; 46(5):2203-2207.

31. Bonnet D and Dick JE. Human acute myeloid leukemia is organized as a hierarchy that originates from a primitive hematopoietic cell. Nature medicine. 1997; 3(7):730-737.

32. Greaves M. Cancer stem cells as 'units of selection'. Evolutionary applications. 2013; 6(1):102-108.

33. Visvader JE and Lindeman GJ. Cancer stem cells in solid tumours: accumulating evidence and unresolved questions. Nature reviews Cancer. 2008; 8(10):755-768.

34. Leth-Larsen R, Terp MG, Christensen AG, Elias D, Kuhlwein T, Jensen ON, Petersen OW and Ditzel HJ. Functional heterogeneity within the CD44 high

human breast cancer stem cell-like compartment reveals a gene signature predictive of distant metastasis. Mol Med. 2012; 18:1109-1121.

35. Alam M, Rajabi H, Ahmad R, Jin C and Kufe D. Targeting the MUC1-C oncoprotein inhibits self-renewal capacity of breast cancer cells. Oncotarget. 2014; 5(9):2622-2634.
36. Ojo D, Lin X, Wong N, Gu Y and Tang D. Prostate Cancer Stem-like Cells Contribute to the Development of Castration-Resistant Prostate Cancer. Cancers (Basel). 2015; 7(4):2290-2308.
37. Rybak AP, He L, Kapoor A, Cutz JC and Tang D. Characterization of sphere-propagating cells with stem-like properties from DU145 prostate cancer cells. Biochimica et biophysica acta. 2011; 1813(5):683-694.
38. Yan J and Tang D. Prostate cancer stem-like cells proliferate slowly and resist etoposide-induced cytotoxicity via enhancing DNA damage response. Experimental cell research. 2014; 328(1):132-142.
39. Hodge JW, Garnett CT, Farsaci B, Palena C, Tsang KY, Ferrone S and Gameiro SR. Chemotherapy-induced immunogenic modulation of tumor cells enhances killing by cytotoxic T lymphocytes and is distinct from immunogenic cell death. Int J Cancer. 2013; 133(3):624-636.
40. Grasso CS, Wu YM, Robinson DR, Cao X, Dhanasekaran SM, Khan AP, Quist MJ, Jing X, Lonigro RJ, Brenner JC, Asangani IA, Ateeq B, Chun SY, Siddiqui J, Sam L, Anstett M, et al. The mutational landscape of lethal castration-resistant prostate cancer. Nature. 2012; 487(7406):239-243.
41. Taylor BS, Schultz N, Hieronymus H, Gopalan A, Xiao Y, Carver BS, Arora VK, Kaushik P, Cerami E, Reva B, Antipin Y, Mitsiades N, Landers T, Dolgalev I, Major JE, Wilson M, et al. Integrative genomic profiling of human prostate cancer. Cancer cell. 2010; 18(1):11-22.
42. Tomlins SA, Mehra R, Rhodes DR, Cao X, Wang L, Dhanasekaran SM, Kalyana-Sundaram S, Wei JT, Rubin MA, Pienta KJ, Shah RB and Chinnaiyan AM. Integrative molecular concept modeling of prostate cancer progression. Nature genetics. 2007; 39(1):41-51.
43. Cerami E, Gao J, Dogrusoz U, Gross BE, Sumer SO, Aksoy BA, Jacobsen A, Byrne CJ, Heuer ML, Larsson E, Antipin Y, Reva B, Goldberg AP, Sander C and Schultz N. The cBio cancer genomics portal: an open platform for exploring multidimensional cancer genomics data. Cancer discovery. 2012; 2(5):401-404.
44. Gao J, Aksoy BA, Dogrusoz U, Dresdner G, Gross B, Sumer SO, Sun Y, Jacobsen A, Sinha R, Larsson E, Cerami E, Sander C and Schultz N.

Integrative analysis of complex cancer genomics and clinical profiles using the cBioPortal. Sci Signal. 2013; 6(269):pl1.

45. Cancer Genome Atlas Research N. The Molecular Taxonomy of Primary Prostate Cancer. Cell. 2015; 163(4):1011-1025.
46. Robinson D, Van Allen EM, Wu YM, Schultz N, Lonigro RJ, Mosquera JM, Montgomery B, Taplin ME, Pritchard CC, Attard G, Beltran H, Abida W, Bradley RK, Vinson J, Cao X, Vats P, et al. Integrative clinical genomics of advanced prostate cancer. Cell. 2015; 161(5):1215-1228.
47. Beltran H, Prandi D, Mosquera JM, Benelli M, Puca L, Cyrta J, Marotz C, Giannopoulou E, Chakravarthi BV, Varambally S, Tomlins SA, Nanus DM, Tagawa ST, Van Allen EM, Elemento O, Sboner A, et al. Divergent clonal evolution of castration-resistant neuroendocrine prostate cancer. Nature medicine. 2016; 22(3):298-305.
48. Augello MA, Hickey TE and Knudsen KE. FOXA1: master of steroid receptor function in cancer. The EMBO journal. 2011; 30(19):3885-3894.
49. Lopez SM, Agoulnik AI, Zhang M, Peterson LE, Suarez E, Gandarillas GA, Frolov A, Li R, Rajapakshe K, Coarfa C, Ittmann M, Weigel N and Agoulnik IU. Nuclear Receptor Corepressor 1 expression and output declines with prostate cancer progression. Clinical cancer research : an official journal of the American Association for Cancer Research. 2016.
50. Kikugawa T, Kinugasa Y, Shiraishi K, Nanba D, Nakashiro K, Tanji N, Yokoyama M and Higashiyama S. PLZF regulates Pbx1 transcription and Pbx1-HoxC8 complex leads to androgen-independent prostate cancer proliferation. Prostate. 2006; 66(10):1092-1099.
51. Buchanan G, Need EF, Barrett JM, Bianco-Miotto T, Thompson VC, Butler LM, Marshall VR, Tilley WD and Coetzee GA. Corepressor effect on androgen receptor activity varies with the length of the CAG encoded polyglutamine repeat and is dependent on receptor/corepressor ratio in prostate cancer cells. Molecular and cellular endocrinology. 2011; 342(1-2):20-31.
52. Wong N, Ojo D, Yan J and Tang D. PKM2 contributes to cancer metabolism. Cancer letters. 2015; 356(2 Pt A):184-191.
53. Yan J, Ojo D, Kapoor A, Lin X, Pinthus JH, Aziz T, Bismar TA, Wei F, Wong N, De Melo J, Cutz JC, Major P, Wood G, Peng H and Tang D. Neural Cell Adhesion Protein CNTN1 Promotes the Metastatic Progression of Prostate Cancer. Cancer research. 2016; 76(6):1603-1614.

54. Haffner MC, Aryee MJ, Toubaji A, Esopi DM, Albadine R, Gurel B, Isaacs WB, Bova GS, Liu W, Xu J, Meeker AK, Netto G, De Marzo AM, Nelson WG and Yegnasubramanian S. Androgen-induced TOP2B-mediated double-strand breaks and prostate cancer gene rearrangements. Nature genetics. 2010; 42(8):668-675.

55. Nyquist MD and Dehm SM. Interplay between genomic alterations and androgen receptor signaling during prostate cancer development and progression. Horm Cancer. 2013; 4(2):61-69.

56. Berger MF, Lawrence MS, Demichelis F, Drier Y, Cibulskis K, Sivachenko AY, Sboner A, Esgueva R, Pflueger D, Sougnez C, Onofrio R, Carter SL, Park K, Habegger L, Ambrogio L, Fennell T, et al. The genomic complexity of primary human prostate cancer. Nature. 2011; 470(7333):214-220.

57. Ichaso N and Dilworth SM. Cell transformation by the middle T-antigen of polyoma virus. Oncogene. 2001; 20(54):7908-7916.

58. Agoulnik IU, Krause WC, Bingman WE, 3rd, Rahman HT, Amrikachi M, Ayala GE and Weigel NL. Repressors of androgen and progesterone receptor action. The Journal of biological chemistry. 2003; 278(33):31136-31148.

59. Wang Q, Li W, Zhang Y, Yuan X, Xu K, Yu J, Chen Z, Beroukhim R, Wang H, Lupien M, Wu T, Regan MM, Meyer CA, Carroll JS, Manrai AK, Janne OA, et al. Androgen receptor regulates a distinct transcription program in androgen-independent prostate cancer. Cell. 2009; 138(2):245-256.

60. Rajabi H, Ahmad R, Jin C, Joshi MD, Guha M, Alam M, Kharbanda S and Kufe D. MUC1-C oncoprotein confers androgen-independent growth of human prostate cancer cells. Prostate. 2012; 72(15):1659-1668.

61. Rajabi H, Joshi MD, Jin C, Ahmad R and Kufe D. Androgen receptor regulates expression of the MUC1-C oncoprotein in human prostate cancer cells. Prostate. 2011; 71(12):1299-1308.

62. Sweeney CJ, Chen YH, Carducci M, Liu G, Jarrard DF, Eisenberger M, Wong YN, Hahn N, Kohli M, Cooney MM, Dreicer R, Vogelzang NJ, Picus J, Shevrin D, Hussain M, Garcia JA, et al. Chemohormonal Therapy in Metastatic Hormone-Sensitive Prostate Cancer. N Engl J Med. 2015; 373(8):737-746.

63. Raina D, Agarwal P, Lee J, Bharti A, McKnight CJ, Sharma P, Kharbanda S and Kufe D. Characterization of the MUC1-C Cytoplasmic Domain as a Cancer Target. PloS one. 2015; 10(8):e0135156.

TABLES

Table 3.1. Patient information and MUC1 Score

Patient #	Age[a]	Gleason	Metastasis	PSA (μg/L)[b]	Average Score[c]
1	76	3+3	No	12	51.79 ± 19.76
2	55	3+3	No	5.13	44.14 ± 16.54
3	53	3+3	No	7.3	22.55 ± 12.72
4	52	3+3	No	Unknown	39.77 ± 18.04
5	58	3+3	No	18	130.63 ± 98.65
6	59	3+3	No	6	8.20 ± 6.48
7	50	3+4	No	Unknown	37.03 ± 5.04
8	-	3+4	No	Unknown	113.14 ± 32.31
9	70	3+4	No	Unknown	43.76 ± 15.42
10	78	3+4	No	Unknown	24.32 ± 15.95
11	70	3+4	No	7.7	3.64 ± 4.08
12	50	4+3	No	714	34.01 ± 18.05
13	74	4+3	No	14	84.61 ± 38.31
14	79	4+4	No	39	16.81 ± 4.97
15	56	4+4	Yes[d]	Unknown	18.76 ± 24.62
16	58	4+4	Yes[d]	Unknown	57.89 ± 26.93
17	60	4+4	No	Unknown	12.19 ± 10.54
18	75	4+5	No	74	13.35 ± 3.45
19	82	4+5	No	28	6.19 ± 5.83
20	72	4+5	No	Unknown	38.36 ± 7.09
21	55	4+5	No	22	11.41 ± 2.93
22	49	4+5	No	61	11.61 ± 8.4
23	64	4+5	No	Unknown	4.24 ± 4.7
24	71	4+5	No	29	4.22 ± 5.14
25	65	4+5	No	Unknown	10.06 ± 6.15
26	81	4+5	No	> 900	7.99 ± 14.96
27	89	5+4	No	Unknown	69.16 ± 29.67
28	77	5+4	No	Unknown	43.00 ± 18.93
29	65	5+4	Yes[d]	Unknown	1.73 ± 0.73
30	80	5+4	No	Unknown	57.85 ± 22.02
31	74	5+5	No	Unknown	62.09 ± 26.33
32	68	5+5	No	Unknown	34.78 ± 47.69
33	91	5+5	No	Unknown	0.58 ± 0.96
34	98	5+5	No	Unknown	112.84 ± 14.86

a: age at diagnosis, b: PSA at diagnosis, c: average score of stain intensity ± SD, d: patient also demonstrates metastasis to lymph node

Table 3.2. Nanostring Analysis of Gene Expression in Primary Prostate Cancer Tissues

Genes	P1[a]	P2[a]	P3[a]	P4[a]	P5[a]	P6[a]	P7[a]
MUC1	+2	+2.4	N[c]	+3.1	N	+1.4	N
TMPRSS2-ERG[b]	+16.2	+30.2	N	N	+17	+25.3	+27.3
PTEN[b]	-1.4	-1.4	N	N	-1.4	-1.3	-2.6

a: patients 1-3 (GS6), patients 4-6 (GS7, 4+3 for P4,5, and 3+4 for P6), and P7 (GS4+4).
b: TMPRSS2-ERG and PTEN were used as positive controls for upregulated and downregulated genes in PC. downregulated or upregulated genes
c: no downregulation or upregulation
Student's t-test was used to determine the p-values for changes in MUC1 ($p=0.044$), PTEN ($p=0.051$), and ERG ($p=0.004$)

Table 3.3. MUC1 Gene Copy Amplification in Prostate Cancer[a]

PC Type	Cases[b]	Amp Cases[c]	%	References
CRPC	77	27	35	1
Metastatic PC	150	9	6	2
Local PC	333	6	1.8	3

a: data was obtained from cBioPortal
b: total number of PC cases
c: the number of cases with the MUC1 gene copy number amplification

FIGURES

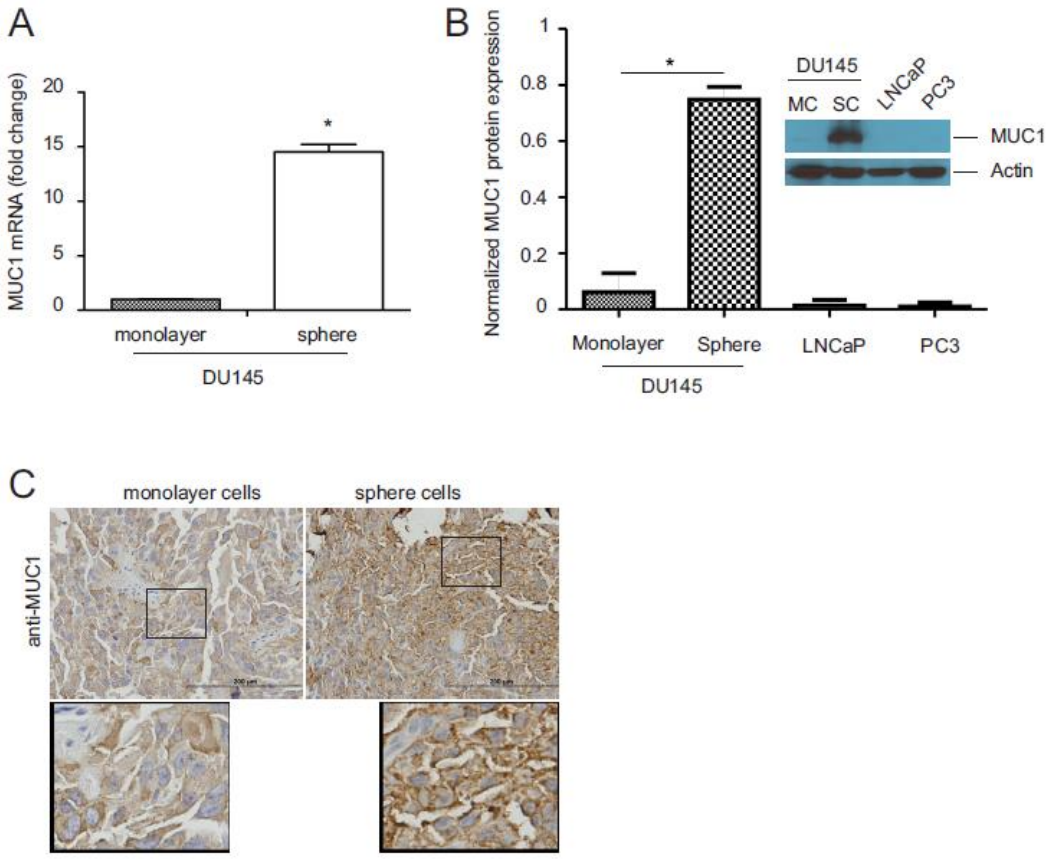

Figure 3.1. Upregulation of MUC1 in prostate cancer stem-like cells (PCSLCs). (A) Real-time PCR analysis of MUC1 mRNA in DU145 monolayer and DU145 sphere cells (PCSLCs). β-actin was used as an internal control. Experiments were repeated three times. MUC1 mRNA abundance in DU145 sphere cells is graphed as a fold change to monolayer cells; Mean ± SE (standard error of the mean) are graphed. *$p<0.05$ by a 2-tailed Student's *t*-test. **(B)** MUC1 protein expression in DU145 monolayer cells (MC) and sphere cells (SC), LNCaP, and PC3 cells was determined by Western blot. Experiments were repeated three times; typical images from a single repeat are shown (inset). MUC1 protein levels were normalized to the respective actin; mean±SE are graphed. *$p<0.05$ by a 2-tailed Student's *t*-test in comparison to DU145 monolayer cells. (**C**) MUC1 expression in xenograft tumors produced by DU145 monolayer or sphere cells was determined by immunohistochemistry (IHC). The indicated areas are enlarged three fold and placed underneath the original panel.

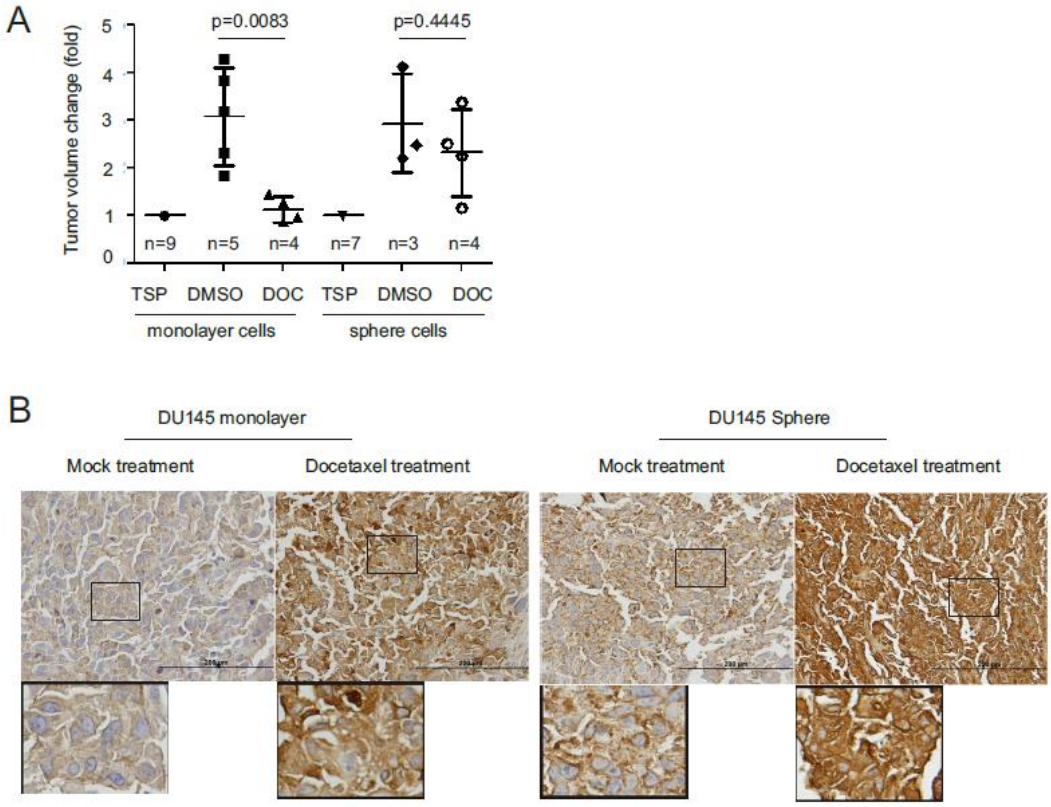

Figure 3.2. Docetaxel upregulates MUC1 expression in xenograft tumors. (A) DU145 monolayer (10^6) or sphere (10^4) cells were subcutaneously implanted into 9 and 7 NOD/SCID mice, respectively. When tumors reached 100mm^3 (treatment starting point/TSP), mice were randomly assigned to receive DMSO or docetaxel (see Materials and Methods for details). Tumor volumes are expressed as fold change two weeks after the TSP. Statistical analyses were performed using Student's *t*-test. **(B)** IHC staining for MUC1 in xenograft tumors generated from DU145 monolayer and sphere cells. Typical images are shown. The indicated regions are enlarged three fold and placed underneath the original panel.

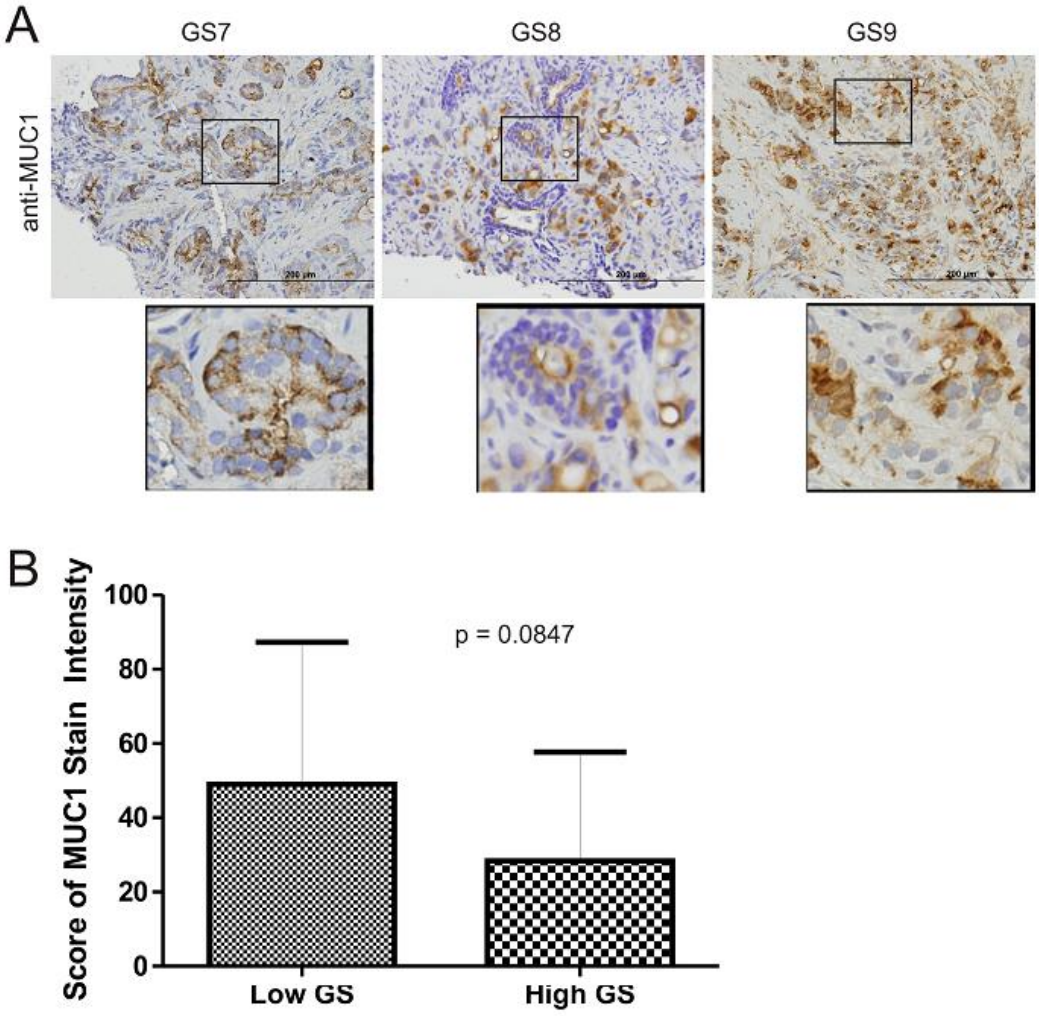

Figure 3.3. Detection of MUC1 in primary prostate cancers. (A) IHC staining for MUC1 in 34 primary PC tissues (Table 1). Typical images for Gleason score (GS) 7, 8, and 9 tumors are shown. Scale bars represent 200μm. (**B**) IHC staining was quantified through ImageScope software (see Materials and Methods for details). Average HScores ± SDs are included in Table 1. The average scores ± SDs for low Gleason score (GS6-7) and high Gleason score (GS8-10) tissues are graphed. Statistical analyses were performed using Student's *t*-test.

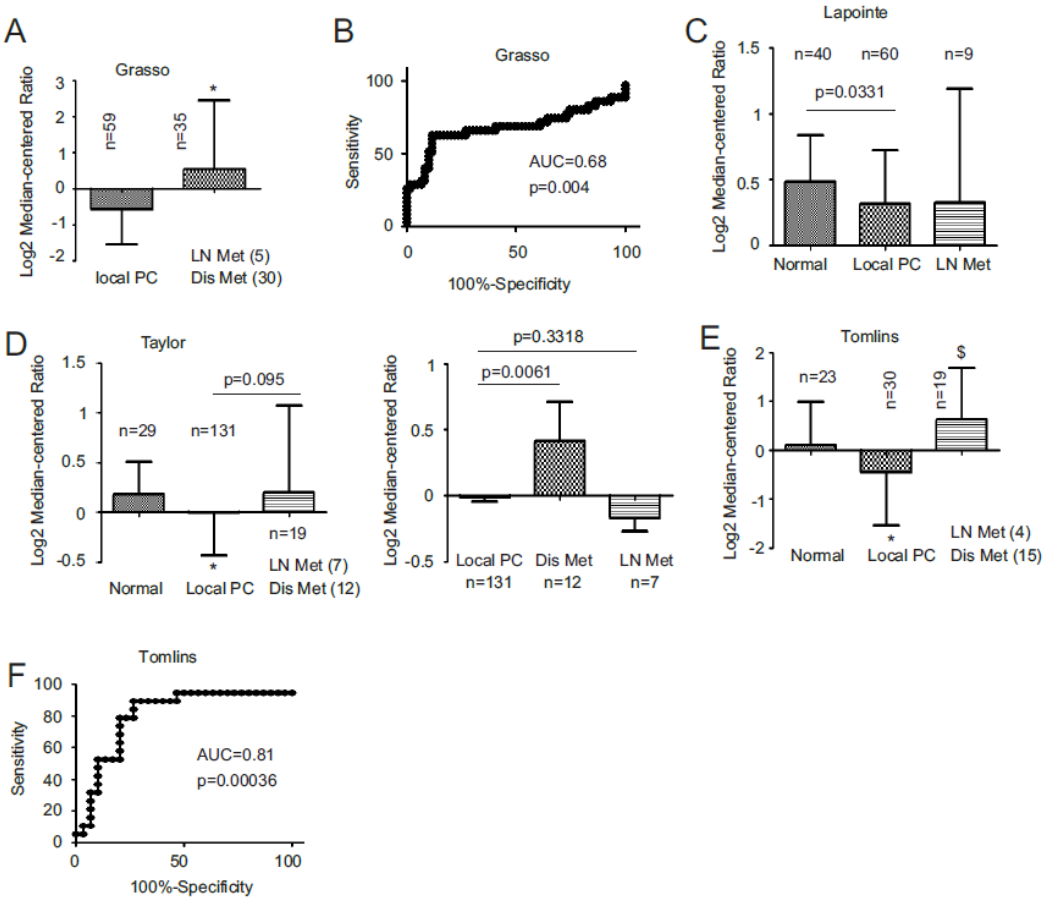

Figure 3.4. Upregulation of MUC1 mRNA in metastatic PC. Data was downloaded from the Grasso (**A, B**), Lapointe (**C**), Taylor (**D**), and Tomlins (**E, F**) datasets from the Oncomine™ database (Compendia Bioscience, Ann Arbor, MI), and analyzed for changes in MUC1 mRNA. Mean±SD are graphed (A, C, D, E). (**B, F**) A receiver-operating characteristic (ROC) curve of local versus metastatic PC was derived from the data taken from the Grasso (**B**) and Tomlins datasets (**D**). AUC: area under the curve. LN Met (4): lymph node metastasis (n=4); Dis Met (12): distant metastasis (n=12).

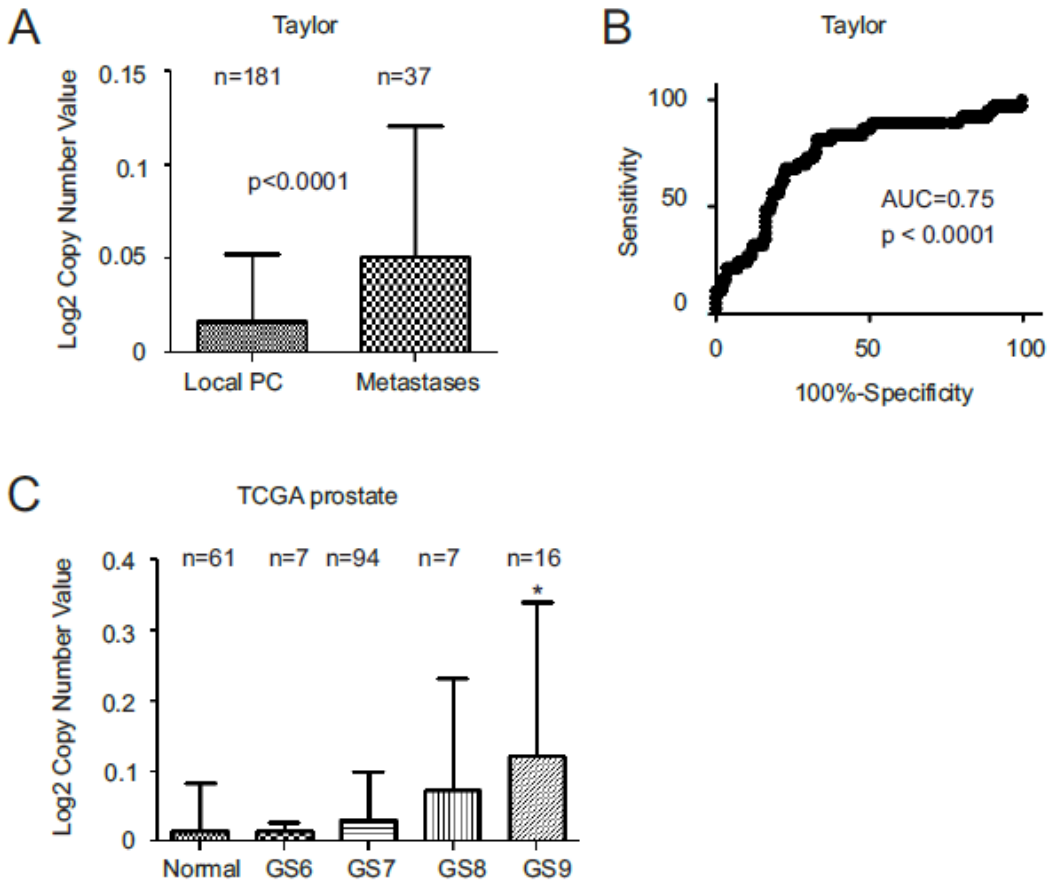

Figure 3.5. Increases in MUC1 gene copy number in advanced and metastatic PC. Data related to MUC1 gene copy number was downloaded from the Taylor (**A, B**) and TCGA (**C**) (generated by the TCGA Research network, http://cancergenome.nih.gov/) datasets from Oncomine™ (Compendia Bioscience, Ann Arbor, MI); Mean ± SD (A and C) and a ROC curve of primary versus metastatic PC were calculated and graphed. Statistical analyses were performed using Student's *t*-test. AUC: area under the curve.

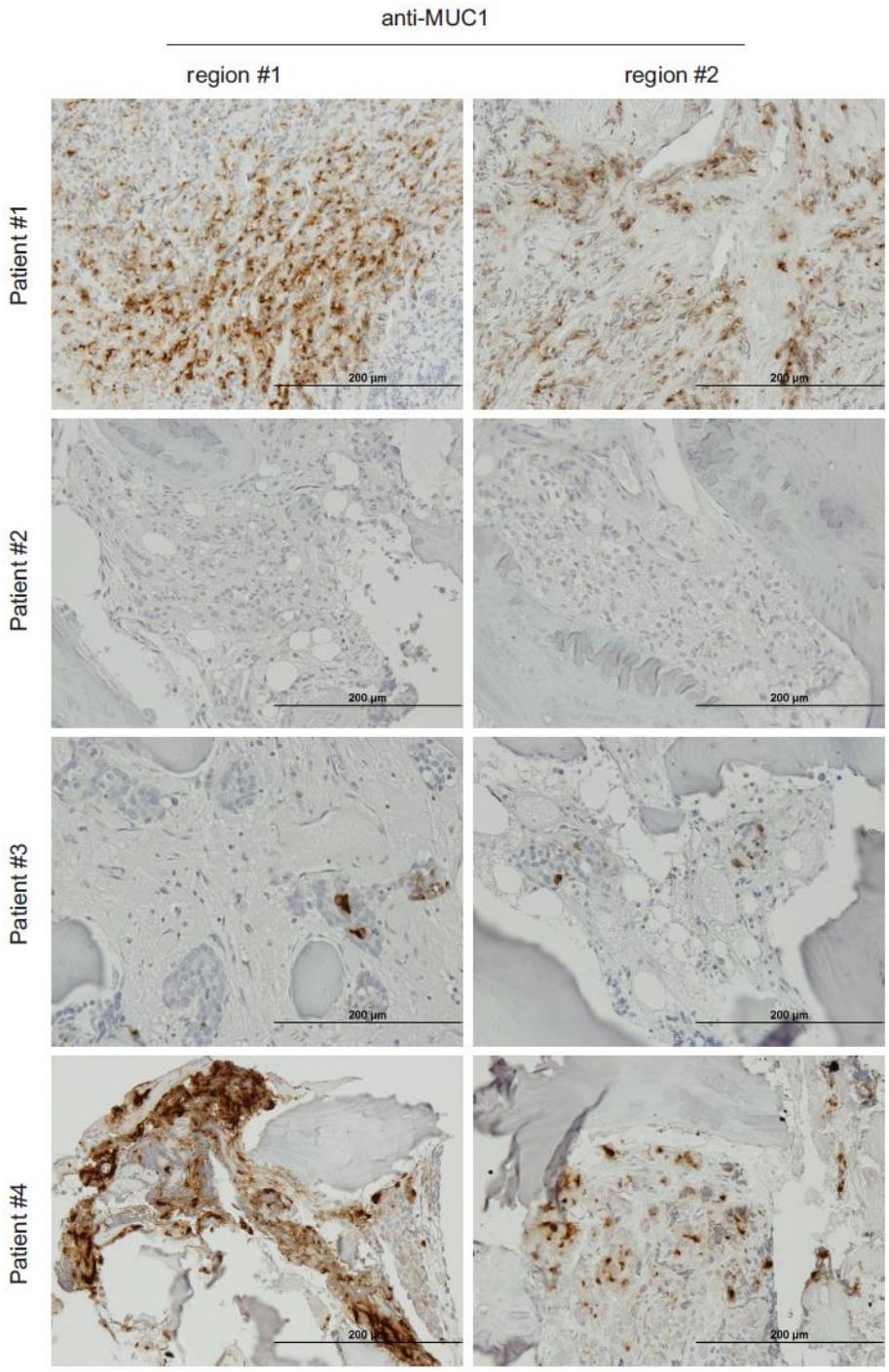

Figure 3.6. Expression of MUC1 in PC bone metastases. IHC staining of four PC bone metastases. Two typical regions from each patient are shown. The overall staining (low magnification) is presented in Supplementary Figure 3.1.

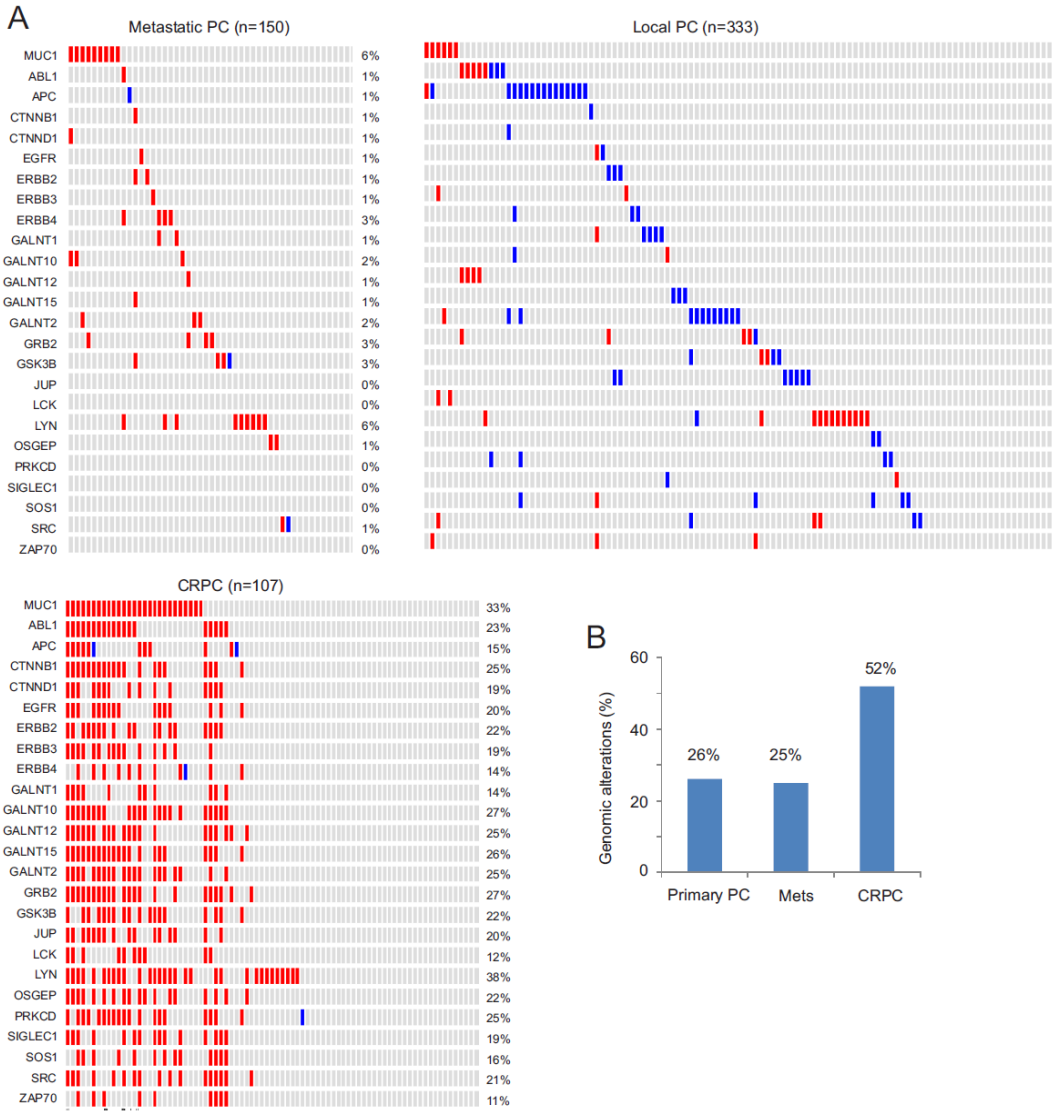

Figure 3.7. Genomic alterations of genes in the MUC1 network. The MUC1 network (see Supplementary Figure 3.2 and Supplementary Table 3.1 for details) was analyzed for genomic alterations using the 3 largest and representative prostate cancer datasets within the cBioPortal database [43,44]. These datasets were deposited from studies as a result of their publications [45-47], and cover 333 primary PCs [45], 150 metastatic PCs [46], and 107 CRPCs derived from 77 patients [47]. **(A)** Analyses were performed using the tools provided by cBioPortal [43,44]. For the primary and metastatic population, only a proportion of cohorts containing the tumors with the relevant genomic alterations are included. Each column represents an individual tumor; red and blue slots are for

gene amplification and deep deletion, respectively. Gene names and their rates of alteration are shown on the left and right of individual rows, respectively. **(B)** Summary of genomic alterations in the MUC1 network in the primary, metastatic and castration resistant PC cohort.

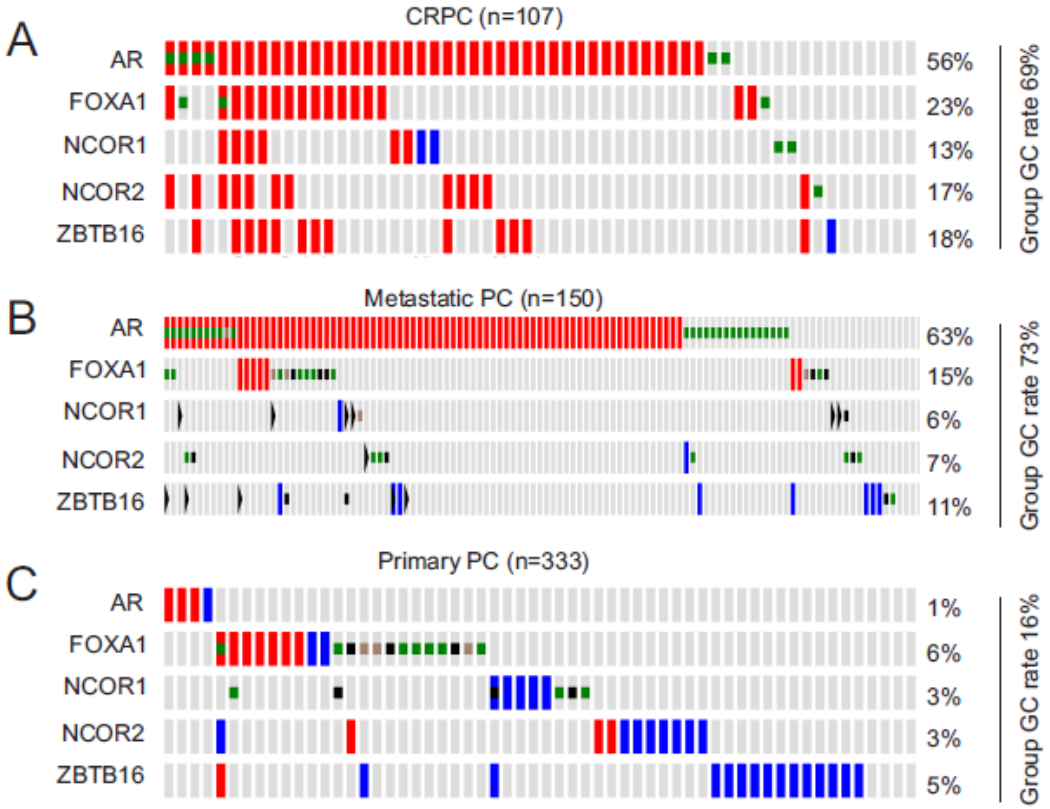

Figure 3.8. Genomic changes in the AR gene and its coregulators. Genomic alterations in the AR gene, FOXA1, NCOR1, NCOR2, and ZBTB1 were analyzed in the primary, metastatic, and castration resistant PC cohort within the cBioPortal database [43, 44]. The group rates of genomic change (GC) are provided. Red and blue slots are for amplification and deep deletion, respectively; green, brown, and black squares indicate missense, inframe, and truncating mutations, respectively.

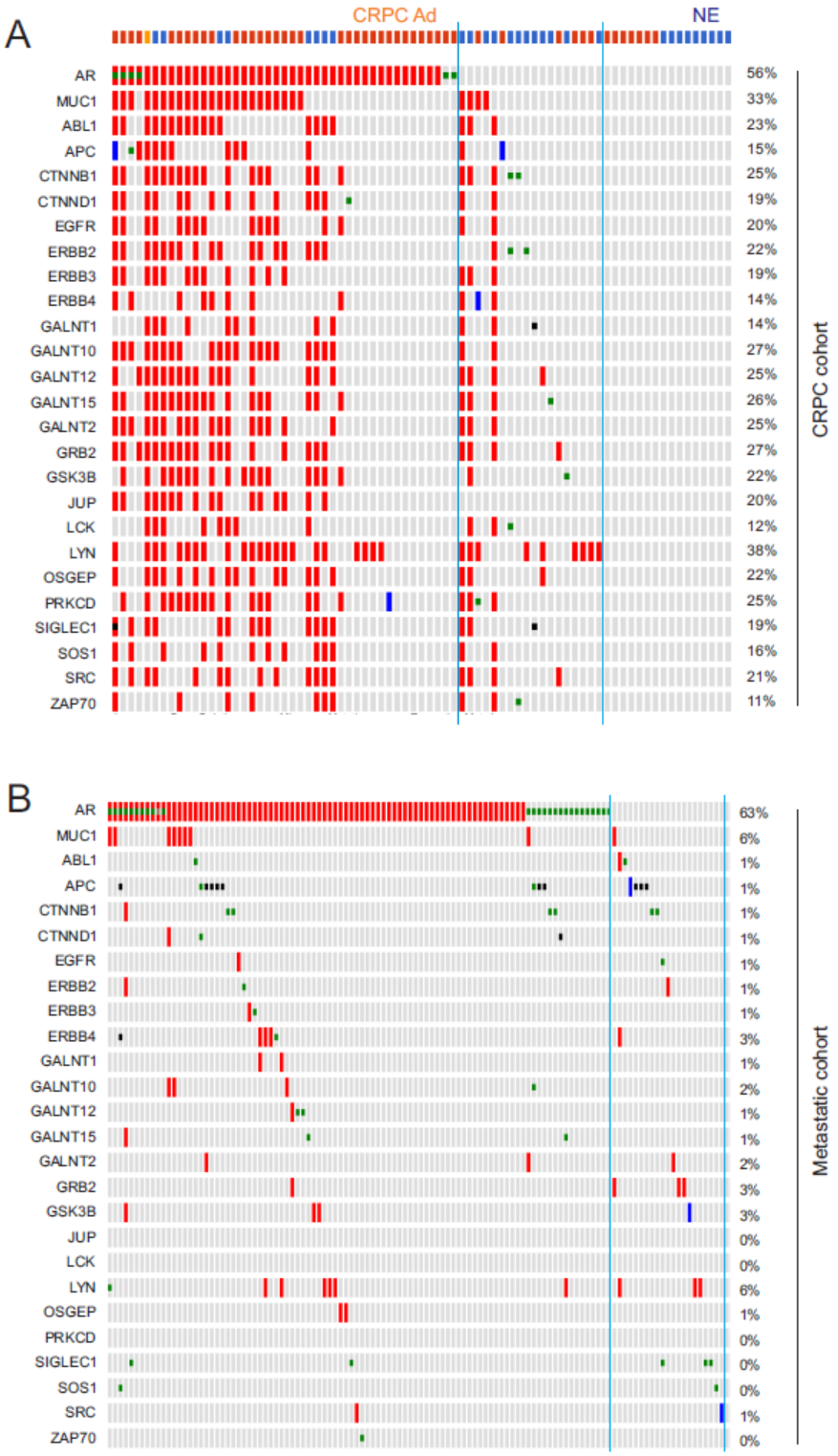
A
CRPC Ad
NE
AR 56%
MUC1 33%
ABL1 23%
APC 15%
CTNNB1 25%
CTNND1 19%
EGFR 20%
ERBB2 22%
ERBB3 19%
ERBB4 14%
GALNT1 14%
GALNT10 27%
GALNT12 25%
GALNT15 26%
GALNT2 25%
GRB2 27%
GSK3B 22%
JUP 20%
LCK 12%
LYN 38%
OSGEP 22%
PRKCD 25%
SIGLEC1 19%
SOS1 16%
SRC 21%
ZAP70 11%
CRPC cohort
B
AR 63%
MUC1 6%
ABL1 1%
APC 1%
CTNNB1 1%
CTNND1 1%
EGFR 1%
ERBB2 1%
ERBB3 1%
ERBB4 3%
GALNT1 1%
GALNT10 2%
GALNT12 1%
GALNT15 1%
GALNT2 2%
GRB2 3%
GSK3B 3%
JUP 0%
LCK 0%
LYN 6%
OSGEP 1%
PRKCD 0%
SIGLEC1 0%
SOS1 0%
SRC 1%
ZAP70 0%
Metastatic cohort

Figure 3.9. Concurrent and independent genomic alterations between the AR gene and the MUC1 gene network. Gene amplification (red slot), deep deletion (blue slot), missense mutation (green square), inframe mutation (brown square), and truncating mutation (black square) in the AR gene and those genes in the MUC1 network were taken from the CRPC and metastatic PC dataset within cBioPortal [43, 44]. **(A)** The top row demonstrates pathologies for individual CRPC: red for CRPC adenocarcinoma (CRPC Ad); blue for neuroendocrine PC (NE); and orange for CRPC adenocarcinoma mixed with NEPC. CRPC cases bordered by the two blue lines have genomic changes only in the MUC1 network. **(B)** Genomic alterations in the AR gene and the MUC1 network in a metastatic PC cohort.

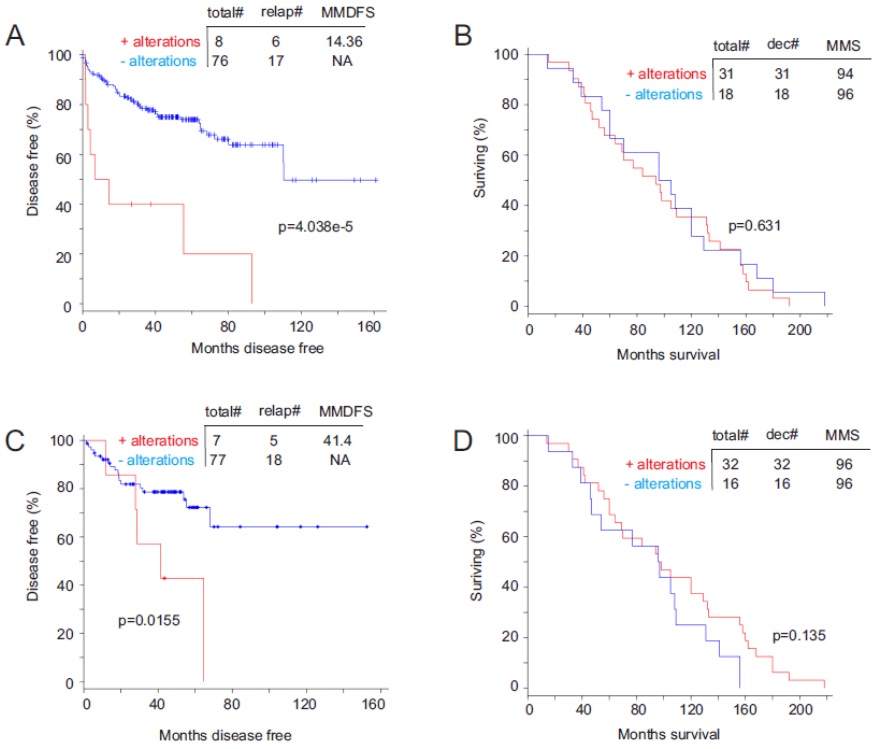

Figure 3.10. Genomic alterations in the MUC1 network associate with a reduction in disease free survival (DFS). A dataset of primary PC [41] (**A, C**) and a dataset of metastatic PC [40] (**B, D**) within the cBioPortal database [43, 44] were used to assess the impact of the MUC1 network on DFS (**A**) and OS (**B**) as well as the effects of the AR network on DFS (**C**) and OS (**D**). Statistical analysis was performed using Logrank Test. Total#: total number of cases; relap#: number of relapsed cases; dec#: number of deceased cases; MMDFS: median months disease free survival; MMS: median months survival; NA: not available.

SUPPLEMENTARY TABLES

Supplementary Table 3.1. The MUC1 Network and its Roles in PC Progression

Gene	*Amp*	*Role in PC and CRPC*	*Ref*
ABL1	20.2%	Abelson tyrosine-protein kinase 1. Promotes the progression of prostate cancer through activation of proliferation, invasion, tumorigenesis and metastasis. Increased expression observed in prostate cancer tissues.	1,2
APC	8.8%	Adenomatous polyposis coli. Functions as a scaffold that targets β-catenin for phosphorylation and subsequent proteasomal degradation. In the presence of WNT ligands or APC mutation, β-catenin is no longer degraded and can accumulate in both the cytosol and nucleus where it activates target genes. Allelic deletion of APCs locus in many human cancers suggests it as a tumour suppressor. In PC cases β-catenin is found in the nucleus, suggesting the pathway is frequently de-regulated. This observation corresponds with a decrease in APC mRNA expression.	3,4
CTNNB1	19.3%	Catenin beta 1. Involved in cadherin-mediated cell adhesion and is under regulation of the Wnt signalling pathway. It localizes to the nuclei in many CRPC tissues and may be involved with advanced PC pathogenesis.	5
CTNND1	14.9%	Catenin delta 1. Increased expression is correlated with higher PC Gleason score. Overexpression in PC cell lines reduced cell-cell adhesion (E-cadherin) which is seen in PC progression.	6
EGFR	14.9%	Epidermal growth factor receptor. Increased expression in PC, and is associated with high Gleason and advanced disease (CRPC). When activated, downstream signalling such as AKT and MAPK pathways leads to enhanced proliferation,	7

		migration and survival.	
ERBB2	18.4%	Erb-B2 receptor tyrosine kinase 2. Overexpression of ERBB2 in androgen independent cells DU145 and PC3 increased metastatic potential in *in vitro* assays. This effect was not seen in androgen dependent LNCaP or Myc-CaP (murine) cells, suggesting a collaboration with androgen signalling.	8
ERBB3	14.9%	Erb-B2 receptor tyrosine kinase 3. Co-expressed with the AKT, MAPK, and JAK/STAT pathways. Contributes to progression of castration-resistant prostate cancer. While typically expressed in cytoplasm, increased nuclear localization was observed in higher Gleason score and CRPC tissues.	9,10
ERBB4	8.8%	Erb-B2 receptor tyrosine kinase 4. Approximately 30% of prostate cancer patients present with ERBB4 overexpression. High levels in PC cell lines correlated with greater proliferation rates.	11,12
GALNT1	12.3%	Polypeptide N-acetylgalactosaminyltransferase 1. Catalyzes the initial reaction in O-linked oligosaccharide biosynthesis, the transfer of an N-acetyl-D-galactosamine residue to a serine or threonine residue on the protein receptor. Has a broad spectrum of substrates for peptides such as EA2, Muc5AC, Muc1a, Muc1b and Muc7.	Uniprot[*,26]
GALNT2	21.9%	Polypeptide N-acetylgalactosaminyltransferase 2. Catalyzes the initial reaction in O-linked oligosaccharide biosynthesis, the transfer of an N-acetyl-D-galactosamine residue to a serine or threonine residue on the protein receptor. Has a broad spectrum of substrates for peptides such as EA2, Muc5AC, Muc1a, Muc1b. Probably involved in O-linked glycosylation of the immunoglobulin A1	Uniprot

		(IgA1) hinge region.	
GALNT10	20.2%	Polypeptide N-acetylgalactosaminyltransferase 10. Catalyzes the initial reaction in O-linked oligosaccharide biosynthesis, the transfer of an N-acetyl-D-galactosamine residue to a serine or threonine residue on the protein receptor. Has activity toward Muc5Ac and EA2 peptide substrates.	Uniprot
GALNT12	20.2%	Polypeptide N-acetylgalactosaminyltransferase 12. Catalyzes the initial reaction in O-linked oligosaccharide biosynthesis, the transfer of an N-acetyl-D-galactosamine residue to a serine or threonine residue on the protein receptor. Has activity toward non-glycosylated peptides such as Muc5AC, Muc1a and EA2, and no detectable activity with Muc2 and Muc7. Displays enzymatic activity toward the Gal-NAc-Muc5AC glycopeptide, but no detectable activity to mono-GalNAc-glycosylated Muc1a, Muc2, Muc7 and EA2. May play an important role in the initial step of mucin-type oligosaccharide biosynthesis in digestive organs.	Uniprot
GALNT15	20.2%	Polypeptide N-acetylgalactosaminyltransferase 15. Catalyzes the initial reaction in O-linked oligosaccharide biosynthesis, the transfer of an N-acetyl-D-galactosamine residue to a serine or threonine residue on the protein receptor. Although it displays a much weaker activity toward all substrates tested compared to GALNT2, it is able to transfer up to seven GalNAc residues to the Muc5AC peptide, suggesting that it can fill vicinal Thr/Ser residues in cooperation with other GALNT proteins. Prefers Muc1a as substrate.	Uniprot
GRB2	21.1%	Growth factor receptor bound protein 2.	13

		Indirectly targets androgen receptor through the MAPK pathway, promoting cell proliferation and survival.	
GSK3β	16.7%	Glycogen synthase kinase 3 beta. While GSK-3 is upregulated in many cancers, GSK-3β was found to correlate more with higher Gleason score (GSK-3α correlated more with lower Gleason). GSK-3β promoted AR transcriptional activity and AKT activation in 22Rv1 cells.	14
JUP	16.7%	Junction plakoglobin. An important component of desmosomes and adherence junctions. Studies demonstrate a key role in controlling epithelial cell motility, with low levels leading to higher metastatic potential. In PC cell lines, JUP was found to interact with SOX4 by promoting its nuclear export. In this way, SOX4s transcriptional role in differentiation, proliferation, and cancer progression may be inhibited, suggesting JUP as a tumour suppressor.	15,16
LCK	8.8%	Lymphocyte cell-specific protein-tyrosine kinase. Aberrantly expressed in prostate cancer tissues with preferential expression in metastatic lesions. May contribute to neoplastic transformation.	17
LYN	31.6%	Lck/Yes-related novel protein tyrosine kinase. Expressed in PC cell lines, normal prostate epithelia and the majority of PC tissues, it is involved in cell proliferation and anti-apoptosis. Upregulated expression in CRPC. Overexpression increased AR transcriptional activity both *in vitro* and *in vivo*.	18,19
OSGEP	17.5%	O-sialoglycoprotein endopeptidase. Component of the EKC/KEOPS complex that is required for the formation of a threonylcarbamoyl group on adenosine at position 37 (t_6A37) in tRNAs that read codons beginning with adenine. The complex is probably involved in the transfer	Uniprot

		of the threonylcarbamoyl moiety of threonylcarbamoyl-AMP (TC-AMP) to the N6 group of A37. OSGEP likely plays a direct catalytic role in this reaction, but requires other protein(s) of the complex to fulfill this activity.	
PRKCD	19.3%	Protein kinase C delta. Involved in apoptosis in response to anti-cancer agents, its expression is decreased in PC cells. Overexpression in LNCaP cells reduced cell number by acting as a mediator for phorbol esters.	20,21
SIGLEC1	16.7%	Sialic acid binding Ig like lectin 1. Acts as an endocytic receptor mediating clathrin dependent endocytosis. Macrophage-restricted adhesion molecule that mediates sialic-acid dependent binding to lymphocytes, including granulocytes, monocytes, natural killer cells, B-cells and CD8 T-cells. Preferentially binds to alpha-2,3-linked sialic acid (By similarity). Binds to SPN/CD43 on T-cells (By similarity). May play a role in haemopoiesis.	Uniprot
SOS1	12.3%	Son of sevenless homolog 1. Found to be overexpressed in primary PC cells derived from African American men, who have an increased risk of developing PC. Expression correlated with Gleason score. Knockdown in PC3 and DU145 cells decreased proliferation, migration, and invasion.	22
SRC1	20.2%	SRC proto-oncogene. Involved in androgen-independent growth, and plays an important role in normal and dysregulated bone functioning (bone metastasis). In local androgen-dependent tumours, expression correlates with more advanced disease.	23,24
ZAP70	7.9%	Zeta chain of T cell receptor associated protein kinase 70kDa. Overexpressed in PC cell lines and tissues, and promotes migration and invasion.	25

* Protein description taken from The UniProt Consortium (http://www.uniprot.org/)

SUPPLEMENTARY REFERENCES

1. Ganguly SS, Plattner R. Activation of abl family kinases in solid tumors. Genes Cancer. 2012; 3(5-6): 414-425.
2. Arora S, Saini S, Fukuhara S, Majid S, Shahryari V, Yamamura S, Chiyomaru T, Deng G, Tanaka Y, Dahiya R. MicroRNA-4723 inhibits prostate cancer growth through inactivation of the Abelson family of nonreceptor protein tyrosine kinases. PLoS One. 2013; 8(11): e78023.
3. Bjerke GA, Pietrzak K, Melhuish TA, Frierson HF, Paschal BM, Wotton D. Prostate cancer induced by loss of Apc is restrained by TGFβ signaling. PLoS One. 2014; 9(3): e92800.
4. Gao X, Zacharek A, Grignon D, Liu H, Sakr W, Porter A, Chen Y, Honn K. High-frequency of loss of expression and allelic deletion of the apc and mcc genes in human prostate-cancer. International Journal of Oncology. 1995; 6(1): 111-117.
5. Wan X, Liu J, Lu JF, Tzelepi V, Yang J, Starbuck MW, Diao L, Wang J, Efstathiou E, Vazquez ES, Troncoso P, Maity SN, Navone NM. Activation of β-catenin signaling in androgen receptor-negative prostate cancer cells. Clinical Cancer Research. 2012; 18(3): 726-736.
6. Lu Q, Dobbs LJ, Gregory CW, Lanford GW, Revelo MP, Shappell S, Chen YH. Increased expression of delta-catenin/neural plakophilin-related armadillo protein is associated with the down-regulation and redistribution of E-cadherin and p120ctn in human prostate cancer. Human Pathology. 2005; 36(10): 1037-1048.
7. de Muga S, Hernández S, Agell L, Salido M, Juanpere N, Lorenzo M, Lorente JA, Serrano S, Lloreta J. Molecular alterations of EGFR and PTEN in prostate cancer: association with high-grade and advanced-stage carcinomas. Modern Pathology. 2010; 23(5): 703-712.
8. Tome-Garcia J, Li D, Ghazaryan S, Shu L, Wu L. ERBB2 increases metastatic potentials specifically in androgen-insensitive prostate cancer cells. PLoS One. 2014; 9(6): e99525.
9. Lee Y, Ma J, Lyu H, Huang J, Kim A, Liu B. Role of erbB3 receptors in cancer therapeutic resistance. Acta Biochimica et Biophysica Sinica (Shanghai). 2014; 46(3): 190-198.

10. Koumakpayi IH, Diallo JS, Le Page C, Lessard L, Gleave M, Bégin LR, Mes-Masson AM, Saad F. Expression and nuclear localization of ErbB3 in prostate cancer. Clinical Cancer Research. 2006; 12(9): 2730-2737.
11. Vexler A, Lidawi G, Loew V, Barnea I, Karaush V, Lev-Ari S, Shtabsky A, Ben-Yosef R. Anti-ERBb4 targeted therapy combined with radiation therapy in prostate cancer. Results of in vitro and in vivo studies. Cancer Biology and Therapy. 2008; 7(7): 1090-1094.
12. Ben-Yosef R, Sarid D, Vexler A, Lidawi G, Inbar M, Marmor S, Starr A, Yaal Hahoshen N. Nuclear and cytoplasmic expression of ErbB-4 in prostate cancer. The International Journal of Biological Markers. 2007; 22(3): 181-185.
13. Samaan S, Lichner Z, Ding Q, Saleh C, Samuel J, Streutker C, Yousef GM. Kallikreins are involved in an miRNA network that contributes to prostate cancer progression. The Journal of Biological Chemistry. 2014; 395(9): 991-1001.
14. Darrington RS, Campa VM, Walker MM, Bengoa-Vergniory N, Gorrono-Etxebarria I, Uysal-Onganer P, Kawano Y, Waxman J, Kypta RM. Distinct expression and activity of GSK-3α and GSK-3β in prostate cancer. International Journal of Cancer. 2012; 131(6): E872-E883.
15. Lu L, Zeng H, Gu X, Ma W. Circulating tumor cell clusters-associated gene plakoglobin and breast cancer survival. Breast Cancer Research and Treatment. 2015; 151(3): 491-500.
16. Lai YH, Cheng J, Cheng D, Feasel ME, Beste KD, Peng J, Nusrat A, Moreno CS. SOX4 interacts with plakoglobin in a Wnt3a-dependent manner in prostate cancer cells. BMC Cell Biology. 2011; 12: 50.
17. Naito M, Komohara Y, Ishihara Y, Noguchi M, Yamashita Y, Shirakusa T, Yamada A, Itoh K, Harada M. Identification of Lck-derived peptides applicable to anti-cancer vaccine for patients with human leukocyte antigen-A3 supertype alleles. British Journal of Cancer. 2007; 97(12): 1648-1654.
18. Goldenburg-Furmanov M, Stein I, Pikarsky E, Rubin H, Kasem S, Wygoda M, Weinstein I, Reuveni H, Ben-Sasson SA. Lyn is a target gene for prostate cancer: sequence-based inhibition induces regression of human tumor xenografts. Cancer Research. 2004; 64(3): 1058-1066.
19. Zardan A, Nip KM, Thaper D, Toren P, Vahid S, Beraldi E, Fazli L, Lamoureux F, Gust KM, Cox ME, Bishop JL, Zoubeidi A. Lyn tyrosine

kinase regulates androgen receptor expression and activity in castrate-resistant prostate cancer. Oncogenesis. 2014; 3: e115.

20. Sumitomo M, Ohba M, Asakuma J, Asano T, Kuroki T, Asano T, Hayakawa M. Protein kinase C delta amplifies ceramide formation via mitochondrial signaling in prostate cancer cells. The Journal of Clinical Investigation. 2002; 109(6): 827-836.
21. Fujii T, Garcia-Bermejo ML, Bernabó JL, Caamaño J, Ohba M, Kuroki T, Li L, Yuspa SH, Kazanietz MG. Involvement of protein kinase C delta (PKCdelta) in phorbol ester-induced apoptosis in LNCaP prostate cancer cells. Lack of proteolytic cleavage of PKCdelta. The Journal of Biological Chemistry. 2000; 275(11); 7574-7582.
22. Timofeeva OA, Zhang X, Ressom HW, Varghese RS, Kallakury BV, Wang K, Ji Y, Cheema A, Jung M, Brown ML, Rhim JS, Dritschilo A. Enhanced expression of SOS1 is detected in prostate cancer epithelial cells from African-American men. International Journal of Oncology. 2009; 35(4): 751-760.
23. Fizazi K. The role of Src in prostate cancer. Annals of Oncology. 2007; 18(11): 1765-1773.
24. Agoulnik IU, Vaid A, Bingman WE 3rd, Erdeme H, Frolov A, Smith CL, Ayala G, Ittmann MM, Weigel NL. Role of SRC-1 in the promotion of prostate cancer cell growth and tumor progression. Cancer Research. 2005; 65(17): 7959-7967.
25. Fu D, Liu B, Zang LE, Jiang H. MiR-631/ZAP70: A novel axis in the migration and invasion of prostate cancer cells. Biochemical and Biophysical Research Communications. 2016; 469(3): 345-351.
26. The UniProt Consortium. UniProt: a hub for protein information. Nucleic Acids Research. 2015; 43: D204-D212.

SUPPLEMENTARY FIGURES

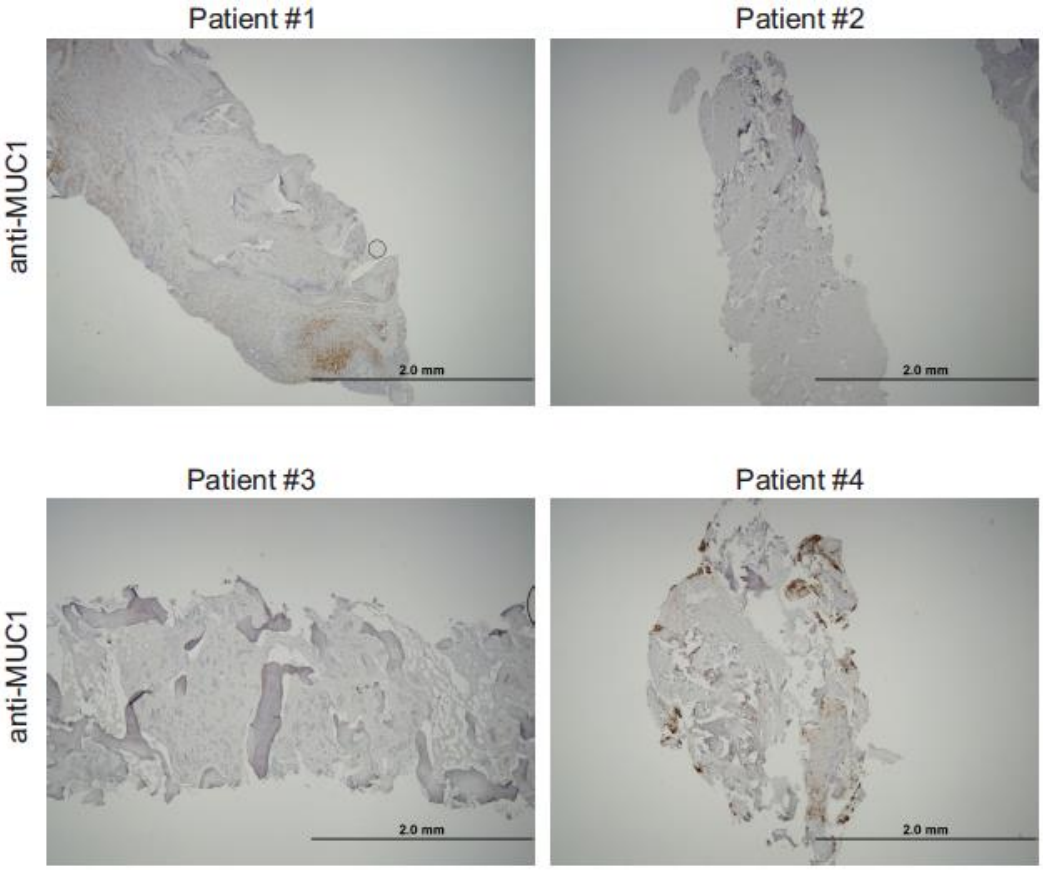

Supplementary Figure 3.1. **The overall IHC staining for MUC1 in four PC bone metastases**. Scale bar represents 2mm.

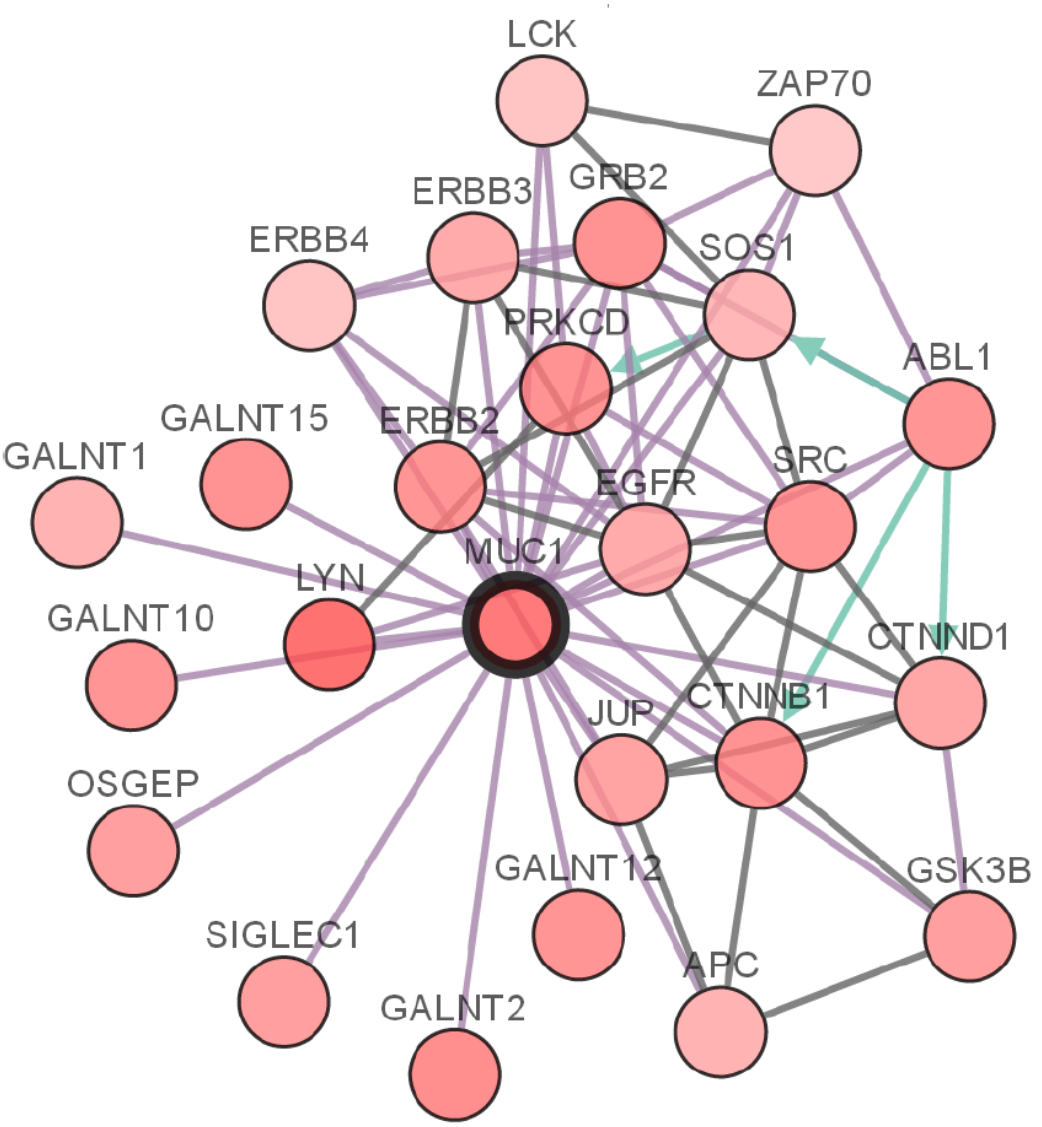

Supplementary Figure 3.2. The MUC1 gene network. The network was generated using MUC1 as the seed node; the linker nodes were identified using the pathway data and interaction data from HPRD, Reactome, NCI-Nature Pathway Interaction Database, and the MSKCC Cancer Cell Map. The pathway was constructed by the system provided by cBioPortal (http://www.cbioportal.org/) (also see Supplementary Table 3.1).

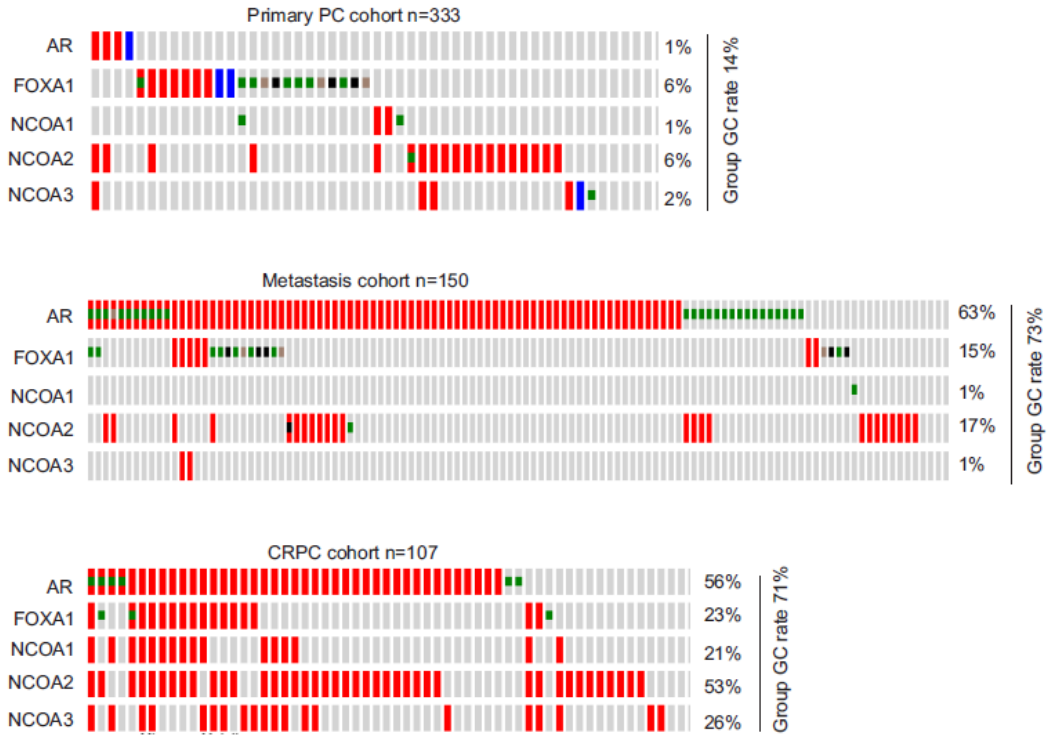

Supplementary Figure 3.3. Genomic alterations of genes in the AR coactivator group. The AR, FOXA1, NCOA1, NCOA2, and NCOA3 genetic alterations in the indicated datasets were analyzed. These datasets were deposited from their respective publications [45-47] into cBioPortal. For each dataset, only the proportions of tumors containing the indicated genomic changes are included. Each column represents an individual tumor. Gene names and their rates of alteration are shown on the left and right of individual rows, respectively. The group rates of genomic changes (GC) are also provided. Red and blue slots represent gene amplification and deep deletion, respectively; green, brown, and black squares represent missense, inframe, and truncating mutations, respectively.

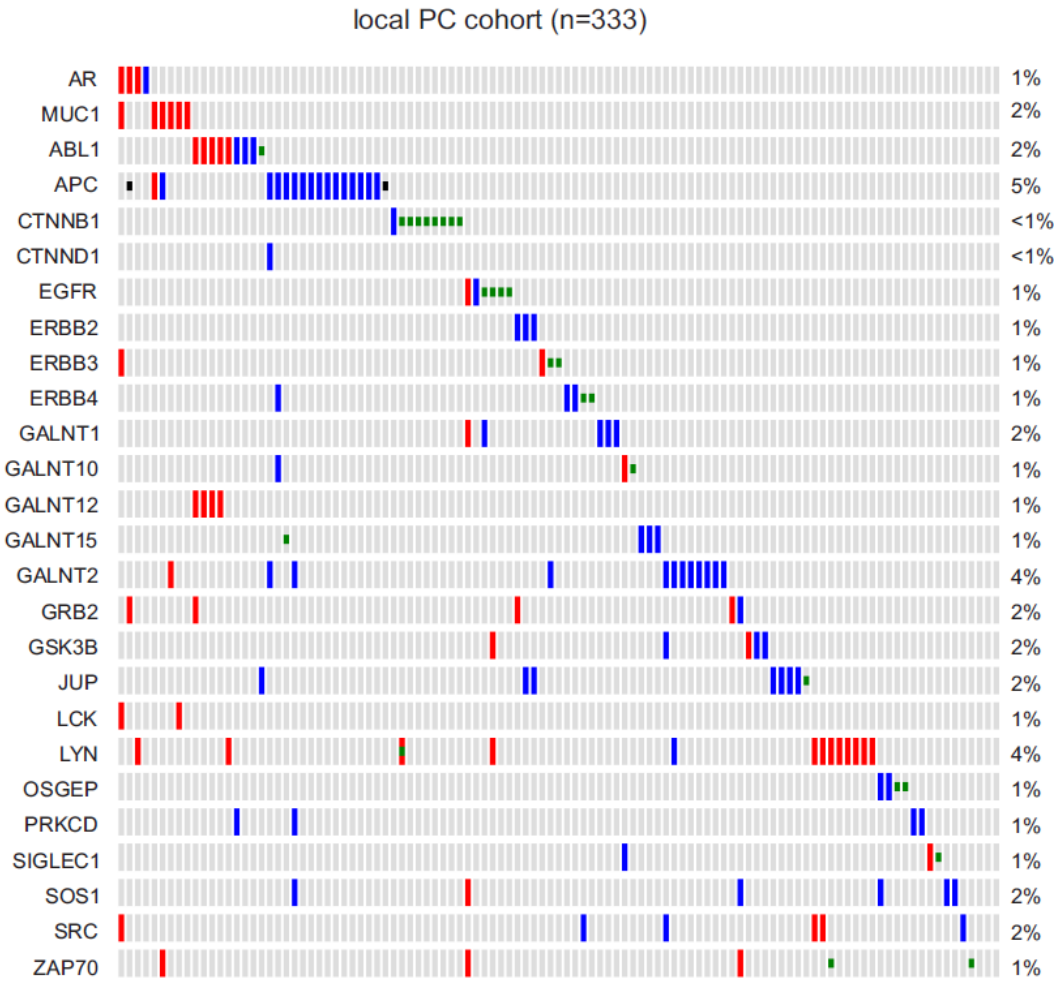

Supplementary Figure 3.4. Independent occurrence of genomic alterations in the AR gene and the MUC1 network. Gene amplification (red slot), deep deletion (blue slot), missense mutation (green square), and truncating mutation (black square) in the AR gene and the MUC1 network genes were downloaded from the largest cohort of primary PC within cBioPortal. Genomic alterations in the AR gene and the MUC1 network in the cohort are shown.

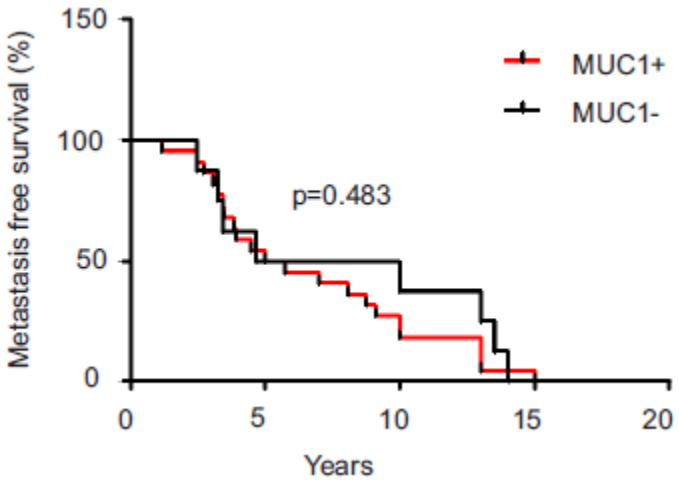

Supplementary Figure 3.5. High levels of MUC1 mRNA does not enhance PC metastasis. Data was taken from the Grasso dataset within Oncomine^{TM} and analyzed for metastasis free survival according to MUC1^{+} (with MUC1 mRNA upregulation) and MUC1^{-} tumors. Statistical analysis was performed using Logrank Test.

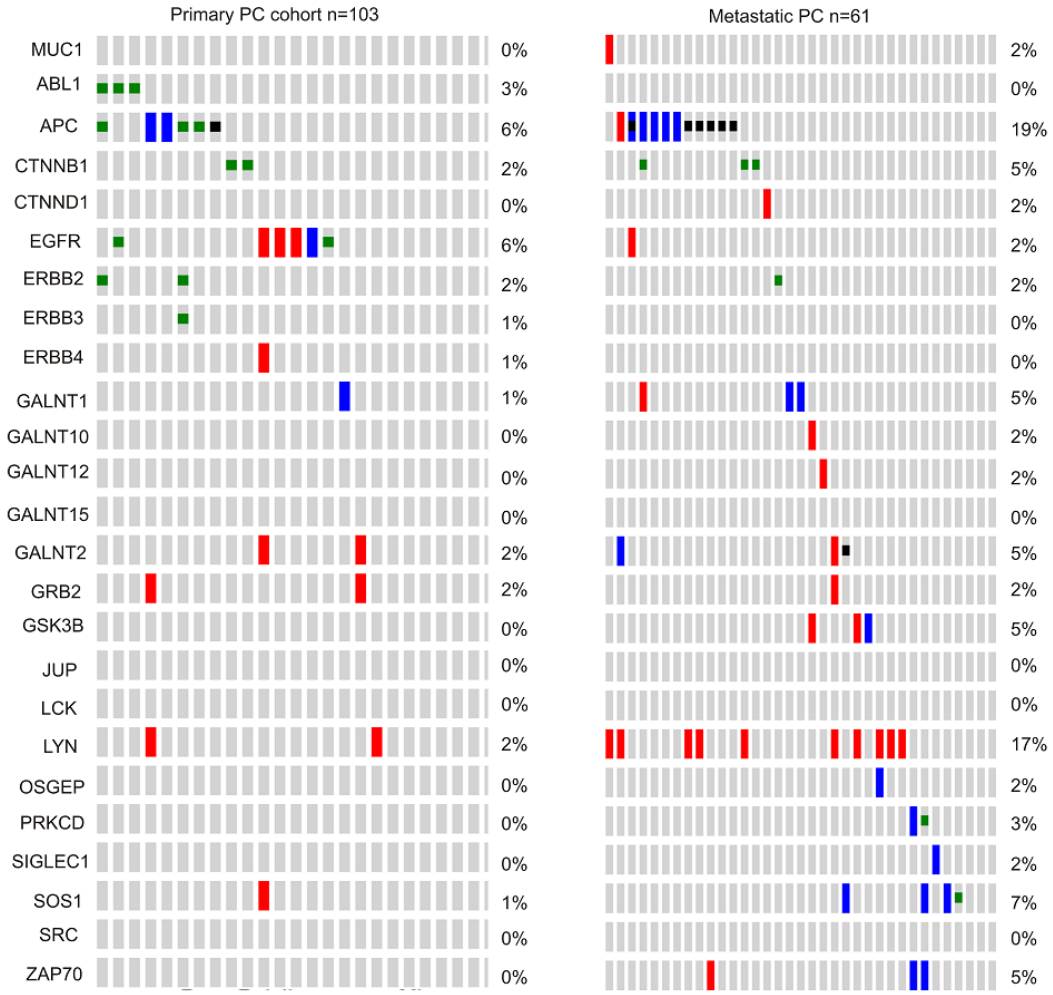

Supplementary Figure 3.6. Genomic alterations of the MUC1 network in the indicated patient cohorts. Genomic data of a primary PC [41] and metastatic PC cohort [40] within cBioPortal was used for the analyses. For each dataset, only the proportions of tumors containing the indicated genomic changes are included. Each column represents an individual tumor. Gene names and their rates of alteration are shown on the left and right of individual rows, respectively. Red and blue slots represent gene amplification and deep deletion, respectively; green and black squares represent missense and truncating mutations, respectively.

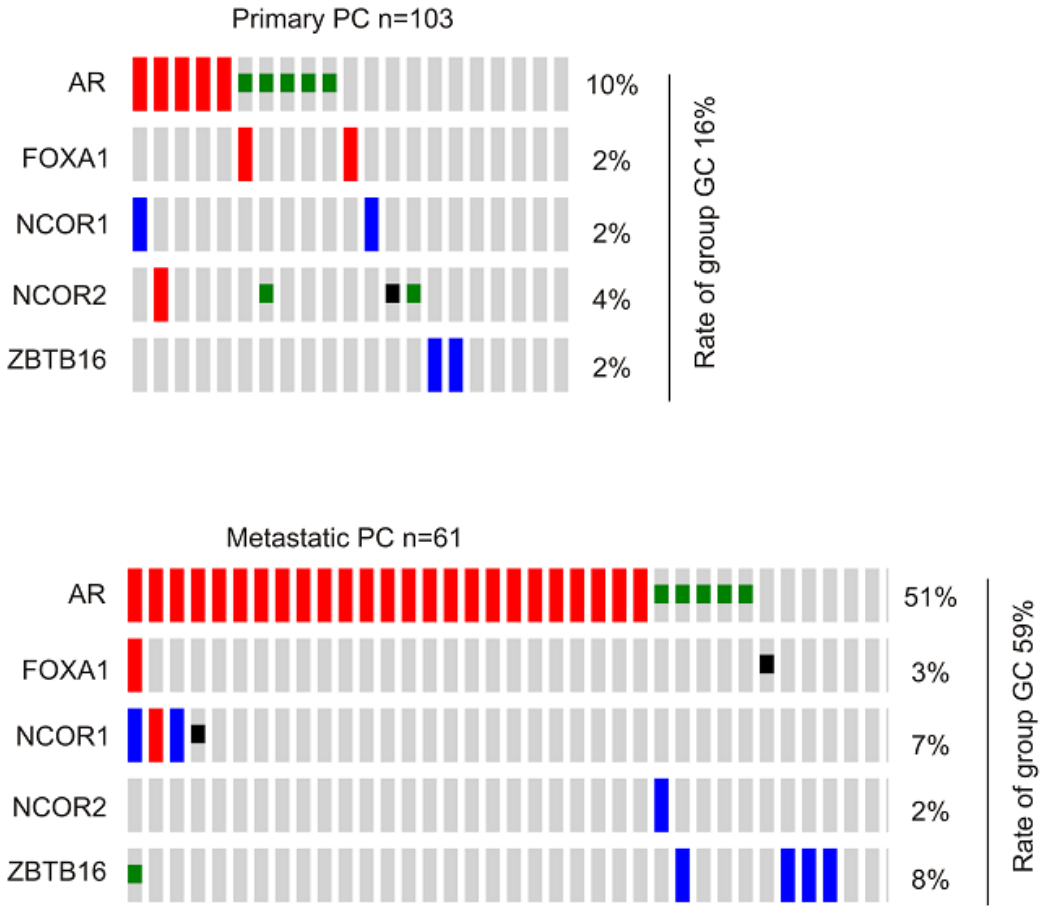

Supplementary Figure 3.7. Genomic changes in the AR coregulator group. Genomic data of a primary PC [41] **(A)** and metastatic PC cohort [40] **(B)** within cBioPortal was used for the analyses. Gene names and their rates of alteration are shown on the left and right of individual rows, respectively. The group rates of genomic changes (GC) are also provided. Red and blue slots represent gene amplification and deep deletion, respectively; green and black squares represent missense and truncating mutations, respectively.

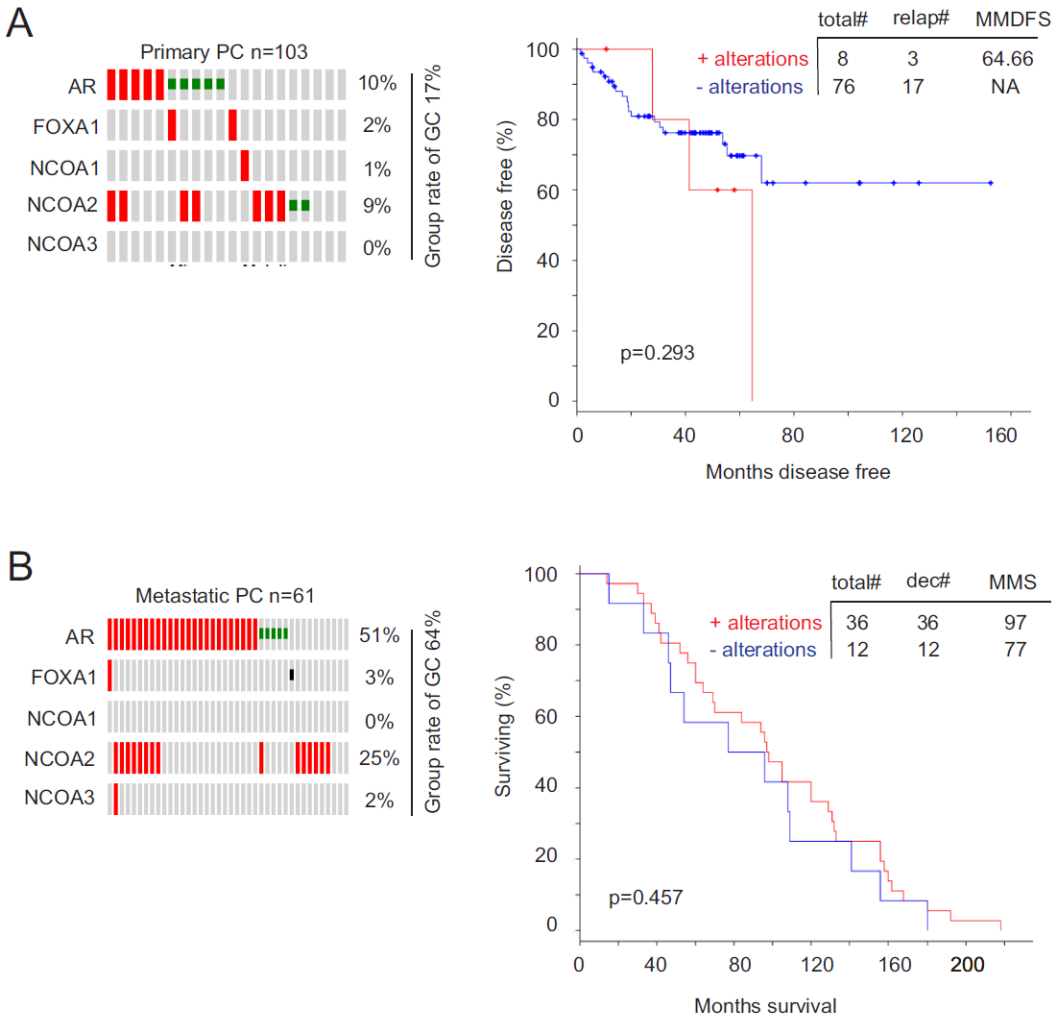

Supplementary Figure 3.8. Genomic alterations in the AR coactivator group do not correlate with DFS and OS. A primary PC dataset [41] and metastatic PC dataset [40] within the cBioPortal were used to assess the impact on DFS **(A)** and OS (**B**). Statistical analysis was performed using Logrank Test. Total#: total number of cases; relap#: number of relapsed cases; dec#: number of deceased cases; MMDFS: median months disease free survival; MMS: median months survival; NA: not available. The respective genomic changes are indicated in the left panels. For each dataset, only the proportions of tumors containing the indicated genomic changes are included; the total number of cases (n) is also included. The group rates of genomic changes (GC) are also provided. Red slot: genomic amplification; green square: missense mutation; black square: truncating mutation.

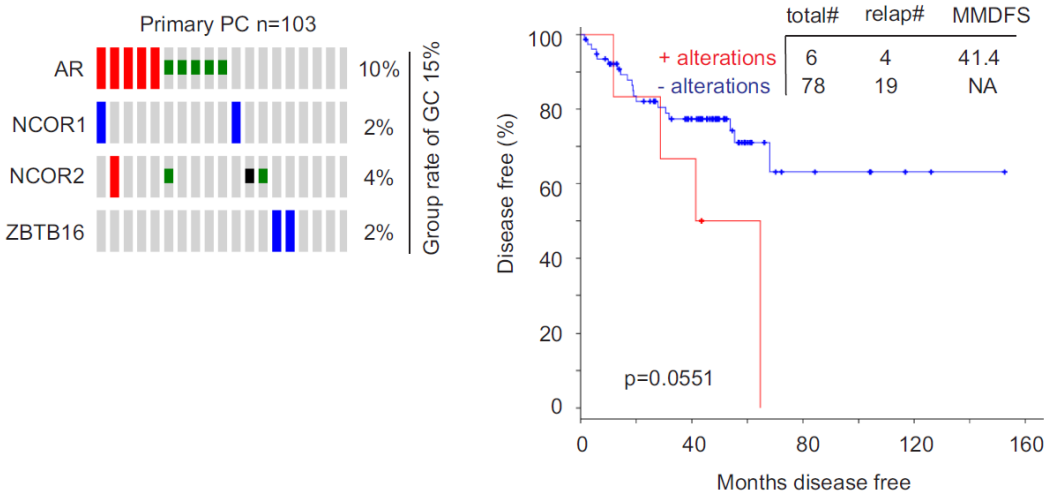

Supplementary Figure 3.9. Genomic changes in AR, NCOR1, NCOR2, and ZBTB16 are likely associated with a reduction in DFS. A dataset of primary PC cohort [41] within cBioPortal was used to analyze for genetic alterations in these genes (left panel) and for a potential association of these changes with DFS (right panel). Only the proportions of tumors in the cohort containing the indicated genomic changes are included and the total number of cases (n) is indicated (left panel). The group rate of genomic changes (GC) is also shown. Red and blue slots represent gene amplification and deep deletion, respectively; green and black squares represent missense and truncating mutations, respectively. Total#: total number of cases; relap#: number of relapsed cases; and MMDFS: median months disease free survival.

CHAPTER FOUR

UPREGULATION OF FAM84B DURING PROSTATE CANCER PROGRESSION

Nicholas Wong,[1,2,3] Yan Gu,[1,2,3] Anil Kapoor,[2,4] Xiaozeng Lin,[1,2,3] Diane Ojo,[1,2,3] Fengxiang Wei,[1,2,3,5] Judy Yan,[1,2,3] Jason de Melo,[1,2,3] Pierre Major,[6] Geoffrey Wood,[7] Tariq Aziz,[8] Jean-Claude Cutz,[8] Michael Bonert,[8] Arthur J. Patterson,[1,2,3] and Damu Tang [1,2,3, #]

[1]Division of Nephrology, Department of Medicine, McMaster University; [2]Father Sean O'Sullivan Research Institute, [3]the Hamilton Center for Kidney Research, St. Joseph's Hospital; [4]Department of Surgery, McMaster University, Hamilton, Ontario, Canada; [5]the Genetics Laboratory, Longgang District Maternity and Child Healthcare Hospital, Longgang District, Shenzhen, Guangdong, P.R. China; [6]Division of Medical Oncology, Department of Oncology, McMaster University; [7]Department of Veterinary Pathology, University of Guelph, Guelph, Ontario, Canada; [8]Department of Pathology and Molecular Medicine, McMaster University, Hamilton, Ontario, Canada

Submitted to *Oncotarget* in **May 2016**. Under revision since **June 2016**.

Author Contributions

Dr. D. Tang and N. Wong designed the experiments. N. Wong carried out the experiments, organized data, and analyzed the results. Y. Gu performed the LNCaP xenograft experiments. Dr. A. Kapoor, Dr. J.C. Cutz, and Dr. M. Bonert verified and confirmed all prostate cancer tissues. X. Lin assisted with data analysis. D. Ojo and A.J. Patterson assisted with the Oncomine™ analyses. Dr. F. Wei provided funding for this research. Dr. J. Yan first identified FAM84B in our PCSLCs. Dr. J. De Melo searched for and identified applicable primary prostate tissues to include in the study. Dr. P. Major and Dr. G. Wood assisted with experimental design and analysis. Dr. T. Aziz kindly provided the prostate cancer bone metastasis tissues. Dr. D. Tang and N. Wong prepared and edited the manuscript.

Relationship to Ph.D. research

This work investigates the increased expression of FAM84B in our PCSLCs which may be co-upregulated along with pluripotency factors during stem cell maintenance. It has also been shown to be involved with cell proliferation, migration, and invasion. We report here that FAM84B associates with both CRPC and metastasis which are widely accepted to be initiated by CSCs, a source of aggressive disease.

Preface

Through Affymetrix microarray analysis our lab has initially identified a 2.2 fold increase of FAM84B expression in our DU145 PCSLCs versus the parental DU145s. This was confirmed by qRT-PCR and Western blotting. In this manuscript we demonstrate higher transcript levels and/or greater protein expression in PC versus normal adjacent tissues, bone metastases cases, and two different animal models of CRPC. The first model being subcutaneous LNCaP xenografts grown in androgen depleted (surgical castration) conditions, and the second being the transgenic prostate-specific Pten knockout model also under a castration environment. Further computational analyses revealed increases in FAM84B mRNA and gene copy number in PC compared to normal tissues, and in CRPC compared to PC cases.

Although not mentioned in the manuscript, the transgenic Pten knockout line utilizing the Cre-Lox system required over one year to establish and represents a large investment of the author's time. Further discussed in Supplementary Figure 4.7, breeding to obtain prostate-specific Pten knockout mice involved two starting strains and three separate crosses to obtain animals of the desired genotype before initiating any experiments. Development of the strain was originally conducted by Wang and colleagues (Wang et al. 2003) and appropriated for our research. These animals may be used to identify additional CRPC-related factors in the future.

Upregulation of FAM84B during prostate cancer progression

Nicholas Wong,[1,2,3] Yan Gu,[1,2,3] Anil Kapoor,[2,4] Xiaozeng Lin,[1,2,3] Diane Ojo,[1,2,3] Fengxiang Wei,[1,2,3,5] Judy Yan,[1,2,3] Jason de Melo,[1,2,3] Pierre Major,[6] Geoffrey Wood,[7] Tariq Aziz,[8] Jean-Claude Cutz,[8] Michael Bonert,[8] Arthur J. Patterson,[1,2,3] and Damu Tang [1,2,3, #]

[1]Division of Nephrology, Department of Medicine, McMaster University; [2]Father Sean O'Sullivan Research Institute, [3]the Hamilton Center for Kidney Research, St. Joseph's Hospital; [4]Department of Surgery, McMaster University, Hamilton, Ontario, Canada; [5]the Genetics Laboratory, Longgang District Maternity and Child Healthcare Hospital, Longgang District, Shenzhen, Guangdong, P.R. China; [6]Division of Medical Oncology, Department of Oncology, McMaster University; [7]Department of Veterinary Pathology, University of Guelph, Guelph, Ontario, Canada; [8]Department of Pathology and Molecular Medicine, McMaster University, Hamilton, Ontario, Canada

#Correspondence:
Damu Tang
T3310, St. Joseph's Hospital
50 Charlton Ave East
Hamilton, Ontario, Canada
L8N 4A6
Tel: (905) 522-1155, ext. 35168
Fax: (905) 521-6181
E-mail: damut@mcmaster.ca

Conflict of interest: All authors declare no conflict of interest

Key words: FAM84B, prostate cancer, prostate cancer stem cells, metastasis, castration resistant prostate cancer

Number of figures: 11

Number of tables: 3

ABSTRACT

Although the *FAM84B* gene lies within chromosome 8q24, a locus frequently altered in prostate cancer (PC), its alteration during prostate tumorigenesis has not been well studied. We report here FAM84B upregulation in DU145 cell-derived prostate cancer stem-like cells (PCSLCs) and DU145 cell-produced lung metastases compared to subcutaneous xenograft tumors. FAM84B protein was detected in bone metastases and primary PCs. Nanostring examination of 7 pairs of tumor adjacent normal and PC tissues revealed elevations in FAM84B mRNA levels in all carcinomas. Furthermore, through analysis of FAM84B expression using large datasets within the Gene Expression Omnibus and Oncomine^{TM} database, we demonstrate significant increases in FAM84B mRNA in 343 primary PCs versus 181 normal tissues, and elevations in the FAM84B gene copy number (GCN) in 171 primary PCs versus 61 normal tissues. While FAM84B was not detected at higher levels via immunohistochemistry in high grade (Gleason score/GS 8-10) tumors compared to GS6-7 PCs, analyses of FAM84B mRNA and GCN using datasets within the cBioPortal database demonstrated FAM84B upregulation in 12% (67/549) of primary PCs and 18% (73/412) of metastatic castration resistant PCs (mCRPCs), and GCN increases in 4.8% (26/546) of primary PCs and 26% (121/467) of mCRPCs, revealing an association of the aforementioned changes with CRPC development. Of note, an increase in FAM84B expression was observed in

xenograft CRPCs produced by LNCaP cells. Furthermore, FAM84B upregulation and GCN increases correlate with decreases in disease free survival and overall survival. Collectively, we demonstrate a novel association of FAM84B with PC tumorigenesis and CRPC progression.

INTRODUCTION

Prostate cancer (PC) is the most frequently diagnosed cancer type in men in the developed world [1]. The disease likely originates from high grade prostatic intra-epithelial neoplasia (HGPIN) and progresses to metastatic PC with bone as the most common site [2]. Organ-confined tumors can be managed through multiple means, such as active surveillance, surgery, or radiation. Patients with advanced and metastatic disease can be treated with androgen deprivation therapy (ADT), a strategy pioneered by Charles Huggins in the 1940s [3, 4] and remains the current standard of care. The treatment however, is not curative, as resistant tumors, known as castration resistant PCs (CRPCs), inevitably develop. While CRPC development is likely mediated by multiple mechanisms, the best understood property of this progression is its dependency of androgen receptor (AR) signalling. Despite low serum testosterone levels following castration (<50ng/ml), persistent AR signalling continues, making it a critical contributing factor in CRPC development [5-7]. However, it appears that AR-independent mechanisms are also involved in CRPC acquisition, such as AR-negative neuroendocrine PC (NEPC) [8], an aggressive type of CRPC. ADT [9, 10] and inhibition of AR signalling through both abiraterone and enzalutamide [11, 12] induce NEPCs. Nevertheless, our understanding of mechanisms underlying PC progression (metastasis and CRPC development) remains incomplete.

The chromosomal locus 8q24 is one of the most frequently amplified and altered regions in a variety of cancer types, including ovarian [13], colorectal [14-17], breast [18-22], prostate [23-28], and others. The 8q24.21 locus specifically is attractive, partly because it is the location of the most commonly amplified gene in cancer, MYC. As expected, the 8q24.21 region is amplified in PCs [29, 30]. Variations in the locus associate with an increased risk of PC development [15, 24-26, 31, 32]. The 8q24.21 locus contains a 1.2Mb gene desert bounded by FAM84B and MYC at the centromeric and telomeric end, respectively [15, 21, 24, 25, 27]. A pseudogene of POU5F1, POU5F1P1/POU5F1B, lies within this gene desert [33] and elevations of POU5F1P1 at both the mRNA and protein levels were observed in PCs [34]. While alterations in MYC is well demonstrated during PC tumorigenesis [29, 35], changes in this locus for FAM84B in PCs remain unclear.

We demonstrate for the first time that the FAM84B gene is amplified and expression is upregulated during prostate tumorigenesis, and follows PC progression. FAM84B upregulation was observed in DU145 cell-derived prostate cancer stem like cells (PCSLCs) in comparison to non-PCSLCs and in prostate carcinoma compared to normal prostate tissues. The upregulation and FAM84B gene amplifications are particularly clear in CRPCs.

RESULTS

Increased levels of FAM84B in PCSLCs

MYC resides in 8q24.21 and is one of four genes that were initially identified to program fibroblast cells into induced pluripotent stem cells (iPSCs) [36]. Considering *MYC* and *FAM84B* are located at either end of the 8q24.21 gene desert (Supplementary Figure 4.1), a potential association of FAM84B with PCSLCs was examined. We have recently established PCSLCs grown as spheres in suspension from DU145 monolayer cells [37]. To examine FAM84B expression in spheres cells versus monolayer cells, we analyzed their gene expression profiles by conducting three separate Affymetrix microarrays. A significant increase in FAM84B mRNA in spheres was observed (Figure 4.1A), while no changes in both MYC and POU5F1P1 were detected, suggesting that the upregulation of FAM84B was specific. This elevation was confirmed by real time PCR and Western blot (Figure 4.1B, C). In comparison to DU145 cells, PC3 and LNCaP cells express higher levels of FAM84B at both the protein and mRNA levels (Figure 4.1D). To further examine PCSLC-associated FAM84B upregulation, we analyzed its expression in xenograft tumors produced by either DU145 monolayer or sphere cells. Despite a significantly higher level of FAM84B expression in sphere cells *in vitro* (Figure 4.1A. B), there were no clear differences in FAM84B expression between the two types of xenograft tumors (Figure 4.1E, Supplementary Figure 4.2). These observations suggest that the

mechanisms underlying FAM84B upregulation in DU145 PCSLCs are attributable to epigenetic changes instead of gene amplification, which may contribute to only FAM84B's increased expression among the three genes (*FAM84B*, *POU5F1P1*, and *MYC*) in the 8q24.21 gene desert (Supplementary Figure 4.1).

FAM84B upregulation associates with PC tumorigenesis

We have previously shown that DU145 sphere cells (PCSLCs) display a 100-fold higher tumorigenic ability [37]. While we did not detect elevated FAM84B expression in sphere cell-derived xenograft tumors (see Discussion for details) (Figure 4.1E, Supplementary Figure 4.2), it remains possible that FAM84B upregulation associates with PC tumorigenesis and/or progression. To investigate this scenario, we produced subcutaneous (s.c.) xenograft tumors and lung metastasis (via tail vein injection) using DU145 monolayer cells [38]. FAM84B expression was heterogeneously detected in both tumor types (Supplementary Figure 4.3A); FAM84B is largely a cytosolic protein (Figure 4.2A, enlarged images). However, FAM84B is clearly expressed at an elevated level in lung metastasis (Figure 4.2A, B; Supplementary Figure 4.3A). Interestingly, the staining showed higher levels of expression in the tumor edges adjacent to normal mouse lung tissue (Supplementary Figure 4.3A), suggesting a role of FAM84B in facilitating PC metastasis. This concept is supported by our

demonstration of FAM84B expression in 2 out of 4 human PC bone metastases (Figure 4.2C, Supplementary Figure 4.3B). Collectively, these observations support an association of FAM84B upregulation with PC progression.

To further investigate this association, we determined FAM84B mRNA levels in 7 pairs of PC and benign prostate tissues using Nanostring technology. The PC tissues contained 60-80% cancer tissue. This collection of samples revealed PTEN reductions and ERG increases (indicative of TMPRSS2-ERG fusion) in 5/7 of the PC cases (Table 4.1), which validated these tissues for analysis of PC-associated gene expression. Impressively, an elevation of FAM84B mRNA was detected in all carcinomas compared to the matched non-tumor prostate tissues (Table 4.1; p=0.002 by a 2-tailed Student's *t*-test), supporting FAM84B upregulation in PCs.

To further examine this concept, we analyzed gene expression data available from three major databases; Gene Expression Omnibus (GEO) (http://www.ncbi.nlm.nih.gov/geo/) [39], Oncomine^{TM} (Compendia Bioscience, Ann Arbor, MI), and cBioPortal [40, 41] (http://www.cbioportal.org/index.do). We downloaded FAM84B mRNA expression data from GSD2546 (dataset2546) (http://www.ncbi.nlm.nih.gov/sites/GDSbrowser) in GEO [42, 43] (Supplementary Figure 4.4). The dataset contained 17 normal prostate, 59 tumor adjacent normal prostate tissues (n=76), 66 primary PCs, and 25 metastases

(lymph node, liver, kidney, and others) (Supplementary Figure 4.4). A significant increase in FAM84B mRNA can be demonstrated following PC progression from normal prostate tissues to carcinoma and to metastasis (Figure 4.3A). Elevated FAM84B mRNA in primary PCs over normal prostate tissues was also observed using the FAM84B mRNA data taken from the Taylor, Grasso, Lapointe, and Vanaja datasets [44] (Figure 4.3B-E) within the Oncomine^{TM} database [45-47]. While metastatic PCs expressed higher levels of FAM84B than the normal prostate tissues (Figure 4.3B-D), a significant increase in metastases over primary tumors can only be demonstrated in the Taylor dataset (Figure 4.3B). Together the five datasets contain 181 normal prostates and 343 primary PCs (Figure 4.3A-E), and validate the association of FAM84B upregulation with prostate tumorigenesis. This concept is further supported by their respective receiver-operating characteristic (ROC) curves that separate normal prostates from primary PCs via an area under curve (AUC) value ranging from 0.69 to 0.9 (Figure 4.3F-H). Nonetheless, the concept of whether FAM84B upregulation correlates with PC progression to metastatic disease warrants further investigations.

Higher levels of FAM84B in primary PCs may be in part attributable to increases in gene copy number (GCN). In an analysis of FAM84B GCN data downloaded from the TCGA dataset within Oncomine^{TM}, FAM84B GCN is significantly increased in 171 primary PCs compared to 61 normal prostate tissues

(Figure 4.4A). The differences separate the two groups with an AUC value of 0.86 ($p<0.0001$) (Figure 4.4B).

FAM84B expression does not correlate with primary PC progression

Primary PCs can be divided into and analyzed as low grade (Gleason score 6-7/GS6-7) and high grade (GS8-10) tumors [48]. FAM84B mRNA data obtained from the Taylor dataset [45] supports the analysis. FAM84B mRNA levels in both low and high grade PCs are significantly higher than in normal prostates (Figure 4.5A). Although the number of cases with high grade PCs was limited, high grade PCs does not seem to display higher levels of FAM84B than low grade PCs (Figure 4.5A). We further examined FAM84B protein expression via immunohistochemistry in our limited patient cohort consisting of 4 low and 18 high grade prostate carcinomas (Supplementary Table 4.1). The FAM84B protein was clearly detected in low and high grade PCs (Figure 4.5B). However, we could not demonstrate higher levels of FAM84B expression in high grade PCs (Figure 4.5C). While FAM84B is largely a cytosolic protein in PC cells (Figure 4.5B), nuclear staining was also observed in high grade cases (Supplementary Figure 4.5).

FAM84B upregulation correlates with CRPC development

A critical form of PC progression is the development of CRPC. To examine whether FAM84B upregulation associates with this, we determined FAM84B expression *in vitro* and *in vivo* under androgen deprivation conditions. Androgen free media for 24 hours robustly reduced prostate specific antigen (PSA) expression in LNCaP cells, as expected (Supplementary Figure 4.6A), however, FAM84B mRNA levels were only slightly reduced (Supplementary Figure 4.6B). This suggests that FAM84B transcription is not directly controlled by AR signaling.

To further investigate FAM84B expression in the process of CRPC development, we generated xenograft tumors using LNCaP cells in intact and castrated NOD/SCID mice (Figure 4.6A). Castration delayed tumor growth, which was followed by the generation of castration resistant tumors as indicated by changes in PSA levels following castration (Figure 4.6A). In comparison to xenograft tumors in intact mice, castration resistant tumors demonstrated increases in FAM84B mRNA expression (Figure 4.6B).

We also examined FAM84B expression in PCs generated in prostate-specific PTEN$^{-/-}$ mice with and without castration. Prostate specific *PTEN*$^{-/-}$ mice were castrated at 23 weeks and euthanized after 13 weeks, and presented with CRPC (Supplementary Figure 4.7A, B). In comparison to hormone naive tumors,

prostate tumors produced in castrated *PTEN*$^{-/-}$ mice exhibited an elevated level of FAM84B protein expression (Figure 4.6C). Interestingly, FAM84B is heterogeneously expressed and the positive cells can be clearly detected as cell clusters particularly in castrated mice (Figure 4.6C; Supplementary Figure 4.7C), suggesting that FAM84B-positive cells may contribute to the clonal expansion of CRPC cells. Additionally, they were located at the edges of tumor adjacent to normal prostate tissue (Supplementary Figure 4.7C, image #3). Taken together, the above observations support a correlation between FAM84B upregulation and CRPC development.

To continue examining this correlation, we downloaded FAM84B mRNA information from cBioPortal datasets and performed analyses using tools provided on the website [40, 41]. There are currently 5 datasets containing mRNA data in cBioPortal, which cover primary prostate tumors and metastatic castration resistant prostate cancers (mCRPCs) (cBioPortal/ http://www.cbioportal.org/index.do) [45, 49-52]. In two datasets with 549 primary PCs, increases in FAM84B mRNA were detected in 12% (11-13%) of PCs (Table 4.2); in comparison, FAM84B upregulation occurred in 18% (9-27%) of mCRPCs in three datasets consisting of 412 mCRPCs (Table 4.2). The differences in the distribution of tumors with FAM84B upregulation in primary PCs and mCRPCs are statistically significant ($p<0.025$, Table 4.2). Collectively, our comprehensive analyses (xenograft tumors, PCs generated in prostate specific PTEN$^{-/-}$ mice, and

primary PCs) strongly support the notion that FAM84B upregulation correlates with CRPC development.

FAM84B gene amplification correlates with CRPC development

We subsequently analyzed FAM84B gene amplification and its association with CRPC. The Taylor dataset within Oncomine^{TM} contains GCN data for 181 primary PCs and 37 metastatic prostate tumors [45]. FAM84B GCN is significantly increased in metastatic PCs compared to primary tumors (Figure 4.7A, left panel). The metastatic PCs consist of mCRPC and lymph node (LN) metastases [45]; the significant increases in FAM84B GCN observed in the metastatic PC population were attributed to mCRPCs (Figure 4.7B, left panel). Additionally, the respective ROC curves differentiate primary PCs from mCRPCs (distant metastases) with increased accuracy (AUC=0.82; Figure 4.7B, right panel) compared to all metastases including LNs (AUC=0.75; Figure 4.7A, right panel).

The association of FAM84B gene amplification was also demonstrated using seven large datasets within the cBioPortal database [45, 46, 50-54] (Table 4.3). While the FAM84B gene was amplified in 4.8% (0.9-7%) of 546 primary PCs, an average rate of 26% (13-44%) was found in 467 mCRPCs (Table 4.3, $p<0.0001$).

Persistent AR signalling though alterations in AR is known to contribute to CRPC progression [5], suggesting a relationship between genomic changes of the FAM84B and AR genes. In support of this possibility, we obtained evidence for a co-occurrence of AR genomic changes and increased FAM84B GCNs; co-occurrence of the two covers a large proportion of the mCRPCs with FAM84B gene amplification in individual datasets (Figure 4.8A, Supplementary Figure 4.8A) [46, 50-52]. The co-occurrence also includes AR and FAM84B mRNA upregulation (Figure 4.8B, Supplementary Figure 4.8B), suggesting a role of AR signalling in FAM84B's genomic alterations and upregulation.

These changes in FAM84B also take place independently of AR signalling (Figure 4.8, Supplementary Figure 4.8). Intriguingly, in those mCRPCs, 58% (7/12) are the neuroendocrine type (NEPC) (Figure 4.8A); with FAM84B mRNA upregulation included, the NEPC enrichment reaches 80% (8/10) (Figure 4.8B), suggesting that CRPCs with changes occurring only in FAM84B are likely NEPCs. In the other three datasets, it would be interesting to examine how many NEPC cases are among the 25 mCRPCs with changes detected only in FAM84B (Supplementary Figure 4.8).

FAM84B genomic changes and mRNA upregulation associate with a reduction in disease free survival (DFS)

CRPC is a major stage of PC evolution. Our observed correlation of FAM84B changes (genomic alterations and mRNA upregulation) with CRPC development indicates a relationship with PC recurrence (DFS). Of note, by extracting and analyzing genomic and mRNA data from 194 prostate tumors with copy number alterations (CNA) from the "MSKCC, Cancer Cell 2010" dataset [45] within cBioPortal, we were able to show that FAM84B gene amplification alone and with its mRNA upregulation (Supplementary Figure 4.9A) associate with decreases in DFS (Figure 4.9A). As expected, similar changes in the AR gene (Supplementary Figure 4.9B) resulted in a rapid PC recurrence (Figure 4.9B). Although the combination of changes in AR and FAM84B decreases the power of AR-associated changes in predicting PC recurrence (comparing the respective curves and p values in panel B and C, Figure 4.9), the combination covers more recurrent tumors; 7 for AR versus 9 for AR+FAM84B (left panels of Figure 4.9B, C) and 15 for AR vs 21 for AR+FAM84B (right panels of Figure 4.9B, C). These analyses thus support the notion that genomic changes and mRNA upregulation in FAM84B contribute to AR-associated reduction in DFS, a concept that is in line with the aforementioned changes in FAM84B occurring concurrently and independently of the respective changes in AR in this patient cohort (Supplementary Figure 4.9C).

To further investigate FAM84B gene amplification-associated reductions in DFS, we analyzed a cohort of 492 patients in the TCGA dataset within the cBioPortal database (http://www.cbioportal.org/) in which the PCs have been examined for copy number variations (CNVs) [49]. FAM84B CNVs (largely amplification) were detected in 8% (37/492) of PCs, while AR CNVs occurred in 1% of prostate tumors (Supplementary Figure 4.10A). In this patient cohort, FAM84B CNVs correlate with a trend of DFS decreases (Figure 4.10A) and the combination of FAM84B and AR CNVs increased the prediction power (comparing the p values in Figure 10A to that in Supplementary Figure 4.10C). However, the differences do not reach the $p<0.05$ level of significance (Supplementary Figure 4.10C).

FAM84B has not been thoroughly studied in the current literature, which results in our lack of knowledge about the proteins or factors that affect FAM84B function. Nonetheless, the cBioPortal database indicates an interactive network between FAM84B and CTNNA1 (α-catenin 1) (Supplementary Figure 4.11A). In a mCRPC cohort of 107 tumors obtained from 77 patients [52], the CTNNA1 gene was amplified in 21% (16/77) of patients and 15% (16/107) of mCRPCs (Supplementary Figure 4.11B). Importantly, CTNNA1 gene amplification displays co-occurrence and independence with FAM84B gene amplification (Supplementary Figure 4.11B). The co-occurrence is also observed with AR and becomes more apparent when mRNA upregulations are included in the

comparisons (Supplementary Figure 4.11C). These observations together with the different chromosomal locations for FAM84B (8q24.21) and CTNNA1 (5q31.2) collectively support a network relationship between the two proteins. Of note, we noticed that although CTNNA1 genomic alterations were detected in 1% of the TCGA cohort of 492 patients (Supplementary Figure 4.10A), genomic alterations in the network are likely associated with DFS reductions (Figure 4.10B). Furthermore, the combination of AR genomic changes with those of the network associates with a decline in DFS (Figure 4.10C). Taken together, evidence supports an association of FAM84B genomic alterations with decreases in DFS in PC patients.

FAM84B genomic alterations correlate with a reduction in overall survival (OS)

We examined a potential association of FAM84B genomic alterations with OS. Among the 11 datasets related to genomic alteration in PC from cBioPortal [40, 41], two have follow-up data for OS, one for mCRPC patients [46] and another for primary PCs (n=492) with CNVs determined (TCGA, http://www.cbioportal.org/) [49]. Genomic changes in AR, FAM84B, and CTNNA1 individually or in any combination have no relationship with OS in mCRPC patients (data not shown). In the primary PC patient cohort, the 8% of genomic alterations in the FAM84B gene significantly associate with a reduction

in OS (Figure 4.11A). Although the number of cases associated with PC-caused fatality is small (n=6), a third (3/9) of these deaths occurred in patients with prostate tumors in which the FAM84B gene has been altered (Figure 4.11A). Combination with either CTNNA1 or AR does not enhance the association (Figure 4.11B, C). In fact, all fatalities in patients with PC harboring either AR or CTNNA1 genomic alterations were observed in patients with tumors containing FAM84B genomic alterations. Taken together, evidence suggests that genomic alterations in the FAM84B gene correlate with poor prognosis in patients with primary prostate tumors.

DICUSSION

The chromosome locus 8q24 is one of the most frequently modified loci in cancer and these alterations are associated with the development of PC and other cancer types [27, 33]. The tumorigenic functions conferred by the 8q24 regions can be attributable to the changes in a gene desert at 8q24.21 that is flanked by FAM84B and MYC [27, 28, 33, 55, 56]. While it has been puzzling as to why the non-coding region is frequently targeted during tumorigenesis, a recent development revealed the gene desert as being a regulatory hub in causing genomic alterations in other chromosome loci, including CD96 at 3q13, during prostate tumorigenesis via physical interaction [57]. While this research sheds light on the functional consequences of those alterations in the gene desert,

genomic changes of MYC have been well demonstrated in promoting tumorigenesis. However, the association of FAM84B, another major component of the gene desert at the 8q24.21 locus, (Supplementary Figure 4.1) with tumorigenesis remains unclear.

This research is the first attempt to thoroughly investigate the correlation of FAM84B with PC tumorigenesis and progression. By using comprehensive experimental systems involving tissue culture, xenograft tumors, and transgenic mice, by examining the alterations in the FAM84B gene and mRNA levels, as well as by analyzing multiple large datasets, this investigation reports several novel observations: FAM84B upregulation occurs in PCSLCs, FAM84B expression is elevated in primary PCs compared to normal prostate tissues, and there is a significant increase in FAM84B mRNA and gene amplification in CRPC development.

The significant upregulation of FAM84B in primary prostate tumors over normal prostate tissues suggests a contribution of FAM84B in PC initiation. However, the mechanisms underlying these changes in FAM84B are likely complex. Nonetheless, our observed FAM84B upregulation in DU145 cell-derived PCSLCs suggests PCSLC-associated plasticity as being a contributor to FAM84B upregulation during PC initiation. This is a possibility that is well in line with the concept of how PCSLCs are also referred to as prostate cancer

initiating cells. The contribution of PCSLCs to FAM84B upregulation is also supported by the heterogeneous expression of FAM84B protein in xenograft tumors (Figures 4.1E, 4.2A) and CRPCs produced in $PTEN^{-/-}$ mice (Figure 4.6C). PCSC-mediated FAM84B upregulation during PC tumorigenesis is also in accordance with an elevation of FAM84B mRNA during CRPC development. It is now well-regarded that the plasticity of cancer stem cells drives therapeutic resistance in response to therapies. This plasticity likely contributes to the acquisition of new properties underlying CRPC development. Thus, PCSC-derived plasticity is likely a contributing factor to FAM84B upregulation.

The functional impact of FAM84B on tumorigenesis in general and prostate oncogenesis in particular remains to be explored. Nonetheless, evidence suggests an important role of FAM84B in PC progression. We noticed a high level of FAM84B protein in the edge regions of DU145 cell-derived lung metastasis (Supplementary Figure 4.3A), indicating a possible role of FAM84B in mediating PC cell invasion. This concept is supported by recent observations in which knockdown of FAM84B reduced esophageal squamous cell carcinoma cell invasion *in vitro* and from forming xenograft tumors *in vivo* [58, 59]. Whether FAM84B performs a similar function in PC tumorigenesis, particularly in PC metastasis, will be examined in the future.

A possible role of FAM84B in PC progression lies in its potential contributions to CRPC. This possibility is supported by the specific FAM84B upregulation mentioned here (Table 4.2); this increase occurred uniquely in CRPC and was observed in several independent and large cohorts (Table 4.2). Furthermore, in a xenograft model for CRPC and a transgenic CRPC mouse model, CRPCs exhibited elevated levels of FAM84B compared to hormone naïve tumors (Figure 4.6). It is thus tempting to propose a role of FAM84B in promoting CRPC development. This hypothesis is supported by a robust elevation in the rate of FAM84B gene amplification from an average 4.8% among 546 primary prostate tumors to 26% in 467 mCRPCs (Table 4.3).

While detailed mechanisms leading to FAM84B gene amplification specifically in CRPC remain to be investigated, it is likely that the gene desert, which is bounded by FAM84B at the centromeric side, plays a role. The genomic regulatory elements within the 8q24.21 gene desert were reported to physically associate with FAM84B in a region from 266-440kb away from the 3' end of the FAM84B gene in multiple PC cell lines [57]. It is also likely that AR signaling during androgen deprivation also contributes to FAM84B gene amplification. This is in accordance with the importance of persistent AR signalling in CRPC development [5] and in causing genomic instability [60, 62]. Furthermore, this possibility is supported by the observed concordance between AR gene amplification and that of FAM84B (Figure 4.8).

MATERIALS AND METHODS

Cell culture and generation of DU145 spheres (PCSLCs)

LNCaP, PC3, and DU145 cells were purchased from American Type Culture Collection (ATCC), and cultured in RPMI-1640 (LNCaP), F12 (PC3) and MEM (DU145) media supplemented with 10% FBS (Sigma Aldrich) and 1% Penicillin-Streptomycin (Thermo Fisher Scientific). DU145 spheres were generated and cultured according to our published conditions [37]. Briefly, DU145 monolayer cells (non-PCSLCs) were individualized and seeded at a density of 5,000 cells/mL in serum-free (SF) media (3:1 DMEM/F12 mixture) (Thermo Fisher Scientific) containing 0.4% bovine serum albumin (BSA) (Bioshop Canada Inc.) supplemented with 0.2x concentration of B27 minus Vitamin A (Thermo Fisher Scientific) and 10ng/ml EGF (Sigma Aldrich), in T75 flasks. Typical spheres were formed in 10 to 12 days.

Collecting primary prostate cancer

Prostate biopsies and radical prostatectomy tissues were obtained at St. Joseph's Hospital in Hamilton, Ontario, Canada under approval from the local Research Ethics Board (REB# 11-3472) and with patient consent.

Nanostring technology

Patient tissues were obtained as above. Formalin fixed paraffin embedded (FFPE) PC tissues containing 60-80% carcinoma were collected as 10μm curls, and RNA was isolated using the High Pure FFPET RNA Isolation Kit (Roche) following the manufacturer's instructions. Purified RNA was then sent to the McMaster Farncombe Institute (Hamilton, Ontario, Canada) for analysis via the nCounter Nanostring Technologies platform. Matched benign prostate tissue was used as control. Gene expression of TMPRSS2-ERG fusion and PTEN were used as positive controls to confirm specific examination of PC tissue. A low, medium, and high expressing housekeeping gene were used as normalization controls (ABCF1, TUBB, GAPDH), by taking the total input RNA and dividing by their geometric mean.

Xenograft tumor formation

DU145 monolayer (10^6), DU145 sphere (10^4), or LNCaP cells ($5x10^6$) were resuspended in 0.1 ml culture media/Matrigel mixture (BD) (1:1 volume), followed by subcutaneous implantation into the flanks of 8 week-old male NOD/SCID mice (The Jackson Laboratory). Tumors were assessed through observation and palpation, and tumor growth was measured weekly using calipers. Tumor volume was determined using the formula $V = L \times W^2 \times 0.52$.

Animals were sacrificed once tumors reached a volume ≥ 1000 mm^3. For the generation of lung metastasis, 10^6 DU145 cells were resuspended into 0.3mL of PBS and injected through the tail vein of NOD/SCID mice. Lungs were harvested at 16 weeks post injection. All animal work was carried out according to experimental protocols approved by the McMaster University Animal Research Ethics Board.

Generation of castration resistant prostate cancer *in vivo*

LNCaP cells ($5x10^6$) were s.c. implanted into NOD/SCID mice. Tumor growth was monitored by measuring serum PSA levels (PSA kit, Abcam) and physically with calipers as described above. When tumor volume approached 100-200mm^3, mice were surgically castrated. Serum PSA was measured prior to and following castration. CRPC was defined when serum PSA rose while tumors continue to grow. Animals were sacrificed once tumors reached a volume ≥ 1000 mm^3.

$PTEN^{loxp/loxp}$ mice (C;129S4-*Pten*^{tm1Hwu}/J) were obtained from The Jackson Laboratory, and PB-Cre4 mice (B6.Cg-Tg(Pbsn-cre)4Prb) were obtained from the NCI Mouse Repository. Prostate specific $PTEN^{-/-}$ mice were produced by crossing the two strains. Surgical castration was performed when $PTEN^{-/-}$ mice were at 23 weeks old for 13 weeks before sacrificing.

Western blot analysis

Cells were lysed in a buffer containing 20mM Tris (pH 7.4), 150mM NaCl, 1mM EDTA, 1mM EGTA, 1% Triton X-100, 25mM sodium pyrophosphate, 1mM NaF, 1mM β-glycerophosphate, 0.1mM sodium orthovanadate, 1mM PMSF, 2μg/ml leupeptin and 10μg/ml aprotinin. 50μg of whole cell lysate was separated on SDS-PAGE gel, and transferred onto Hybond ECL nitrocellulose membranes (Amersham), followed by blocking with 5% skim milk at room temperature for one hour. Primary antibodies were incubated overnight at 4^{o}C with agitation, and secondary antibodies incubated for one hour at room temperature. Signals were then developed (ECL Western Blotting Kit, Amersham). Primary antibodies: anti-FAM84B 1:1000 (Proteintech) and anti-Actin 1:1000 (Santa Cruz).

Quantitative real-time PCR analysis of FAM84B expression

Total RNA was isolated from prostate cancer cell lines and xenograft tissues with Isol-RNA Lysis Reagent (5 PRIME), and reverse transcription was carried out using Superscript III (Thermo Fisher Scientific) according to the manufacturer's instructions. Quantitative real-time PCR was performed using the ABI 7500 Fast Real-Time PCR System (Applied Biosystems) using SYBR-green (Thermo Fisher Scientific). All samples were run in triplicate. FAM84B

(Forward): 5'-GACCCACCTAAGTTACAAGGAAG-3', FAM84B (Reverse): 5'-GTAGAACACGGAGCATTCCAC-3'. β-Actin (Forward): 5'-TGAAGGTGACAGCAGTCGGT-3', and β-Actin (Reverse): 5'-TAGAGAGAAGTGGGGTGGCT-3'.

Immunohistochemistry (IHC)

IHC was performed on 22 paraffin embedded and serially cut prostate cancer tissues obtained from St. Joseph's Hospital, Hamilton, Ontario, Canada, and on the various human xenograft tissues and $PTEN^{-/-}$ prostates. Slides were deparaffinized in xylene and cleared in an ethanol series. Antigen retrieval was performed in a food steamer for 20 minutes using sodium citrate buffer (pH = 6.0). Tissues were blocked for 1 hour in PBS containing 1% BSA and 10% normal goat serum (Vector Laboratories). FAM84B antibody (1:350, Proteintech) was incubated overnight at 4°C. Secondary antibody biotinylated goat anti-rabbit IgG and Vector ABC reagent (Vector Laboratories) were incubated according to the manufacturer's instructions. Secondary antibody only was used as negative control. Washes were performed with PBS. Chromogenic reaction was carried out with diaminobenzidine (Vector Laboratories), and slides were counterstained with haemotoxylin (Sigma Aldrich). Image analysis was performed using ImageScope software (Leica Microsystems Inc.). Staining intensity values derived from ImageScope were converted to an HScore using the formula [HScore = (%

Positive) x (intensity) + 1]. The HScore was normalized through background subtraction and averaged amongst > 5 images per tissue sample.

Gene expression studies

The specific methods of how each study obtained gene expression, gene alteration, and copy number variation data for deposit into Oncomine™, cBioPortal, or Gene Expression Omnibus (GEO), can be found in their respective publications. In general, DNA and RNA were purified from frozen or FFPE tissues and analyzed via comparative genomic hybridization platforms, whole exome sequencing, paired-end sequencing, and cDNA microarrays. For examination of raw data, many groups aligned to the hg19 build of the human reference genome.

Oncomine™ and GEO data was downloaded and analyzed using GraphPad Prism 5.0 software. Information from cBioPortal was examined using the online tools provided.

Statistical analysis

Statistical analysis was performed using Student's *t*-test, with $p < 0.05$ being considered statistically significant.

ACKNOWLEDGEMENTS

This work was supported in part by a GAP funding from McMaster University and St. Joseph's Hospital in Hamilton, a Teresa Cascioli Charitable Foundation Research Award in Women's Health to D.T., as well as by grants from the National Natural Science Foundation of China (Grant No. 81201568), the Natural Science Foundation of Guangdong Province (Grant No. 2014A030313749), the National Natural Science Foundation of Heilongjiang Province (Grant No. C2015033), and the Shenzhen Program of Innovation and Entrepreneurship for Overseas Elites (Grant No. KQCX20120814150420241) to F.W. Mouse strain B6.Cg-Tg(Pbsn-cre)4Prb obtained from the NCI Mouse Repository was kindly donated by Dr. Pradip Roy-Burman from the University of South Carolina. The results shown here are in part based upon data generated by Gene Expression Omnibus (http://www.ncbi.nlm.nih.gov/geo/), the TCGA Research Network (http://cancergenome.nih.gov/), and by Oncomine™ (https://www.oncomine.org/).

CONFLICT OF INTEREST

All authors declare no conflict of interest

REFERENCES

1. Ferlay J, Soerjomataram I, Dikshit R, Eser S, Mathers C, Rebelo M, Parkin DM, Forman D and Bray F. Cancer incidence and mortality worldwide: sources, methods and major patterns in GLOBOCAN 2012. Int J Cancer. 2015; 136(5):E359-386.
2. Heidenreich A, Bastian PJ, Bellmunt J, Bolla M, Joniau S, van der Kwast T, Mason M, Matveev V, Wiegel T, Zattoni F and Mottet N. EAU guidelines on prostate cancer. Part II: Treatment of advanced, relapsing, and castration-resistant prostate cancer. Eur Urol. 2014; 65(2):467-479.
3. Rosenberg J and Small EJ. Prostate cancer update. Curr Opin Oncol. 2003; 15:217-221.
4. Ross JS. The androgen receptor in prostate cancer: therapy target in search of an integrated diagnostic test. Adv Anat Pathol. 2007; 14:353-357.
5. Mitsiades N. A road map to comprehensive androgen receptor axis targeting for castration-resistant prostate cancer. Cancer research. 2013; 73(15):4599-4605.
6. Mateo J, Smith A, Ong M and de Bono JS. Novel drugs targeting the androgen receptor pathway in prostate cancer. Cancer Metastasis Rev. 2014; 33(2-3):567-579.
7. Ojo D, Lin X, Wong N, Gu Y and Tang D. Prostate Cancer Stem-like Cells Contribute to the Development of Castration-Resistant Prostate Cancer. Cancers (Basel). 2015; 7(4):2290-2308.
8. Pienta KJ, Walia G, Simons JW and Soule HR. Beyond the androgen receptor: new approaches to treating metastatic prostate cancer. Report of the 2013 Prouts Neck Prostate Cancer Meeting. Prostate. 2014; 74(3):314-320.
9. Palapattu GS, Wu C, Silvers CR, Martin HB, Williams K, Salamone L, Bushnell T, Huang LS, Yang Q and Huang J. Selective expression of CD44, a putative prostate cancer stem cell marker, in neuroendocrine tumor cells of human prostate cancer. Prostate. 2009; 69(7):787-798.
10. Bitting RL, Schaeffer D, Somarelli JA, Garcia-Blanco MA and Armstrong AJ. The role of epithelial plasticity in prostate cancer dissemination and treatment resistance. Cancer Metastasis Rev. 2014; 33(2-3):441-468.
11. Burgio SL, Conteduca V, Menna C, Carretta E, Rossi L, Bianchi E, Kopf B, Fabbri F, Amadori D and De Giorgi U. Chromogranin A predicts outcome in prostate cancer patients treated with abiraterone. Endocr Relat Cancer. 2014; 21(3):487-493.

12. Conteduca V, Burgio SL, Menna C, Carretta E, Rossi L, Bianchi E, Masini C, Amadori D and De Giorgi U. Chromogranin A is a potential prognostic marker in prostate cancer patients treated with enzalutamide. Prostate. 2014; 74(16):1691-1696.

13. Braem MG, Schouten LJ, Peeters PH, van den Brandt PA and Onland-Moret NC. Genetic susceptibility to sporadic ovarian cancer: a systematic review. Biochimica et biophysica acta. 2011; 1816(2):132-146.

14. Haerian MS, Baum L and Haerian BS. Association of 8q24.21 loci with the risk of colorectal cancer: a systematic review and meta-analysis. J Gastroenterol Hepatol. 2011; 26(10):1475-1484.

15. Haiman CA, Le Marchand L, Yamamato J, Stram DO, Sheng X, Kolonel LN, Wu AH, Reich D and Henderson BE. A common genetic risk factor for colorectal and prostate cancer. Nature genetics. 2007; 39(8):954-956.

16. Broderick P, Carvajal-Carmona L, Pittman AM, Webb E, Howarth K, Rowan A, Lubbe S, Spain S, Sullivan K, Fielding S, Jaeger E, Vijayakrishnan J, Kemp Z, Gorman M, Chandler I, Papaemmanuil E, et al. A genome-wide association study shows that common alleles of SMAD7 influence colorectal cancer risk. Nature genetics. 2007; 39(11):1315-1317.

17. Tomlinson I, Webb E, Carvajal-Carmona L, Broderick P, Kemp Z, Spain S, Penegar S, Chandler I, Gorman M, Wood W, Barclay E, Lubbe S, Martin L, Sellick G, Jaeger E, Hubner R, et al. A genome-wide association scan of tag SNPs identifies a susceptibility variant for colorectal cancer at 8q24.21. Nature genetics. 2007; 39(8):984-988.

18. Hindorff LA, Gillanders EM and Manolio TA. Genetic architecture of cancer and other complex diseases: lessons learned and future directions. Carcinogenesis. 2011; 32(7):945-954.

19. Vargas AC, Lakhani SR and Simpson PT. Pleomorphic lobular carcinoma of the breast: molecular pathology and clinical impact. Future Oncol. 2009; 5(2):233-243.

20. Garcia-Closas M and Chanock S. Genetic susceptibility loci for breast cancer by estrogen receptor status. Clinical cancer research : an official journal of the American Association for Cancer Research. 2008; 14(24):8000-8009.

21. Easton DF, Pooley KA, Dunning AM, Pharoah PD, Thompson D, Ballinger DG, Struewing JP, Morrison J, Field H, Luben R, Wareham N, Ahmed S, Healey CS, Bowman R, collaborators S, Meyer KB, et al. Genome-wide association study identifies novel breast cancer susceptibility loci. Nature. 2007; 447(7148):1087-1093.

22. Schumacher FR, Feigelson HS, Cox DG, Haiman CA, Albanes D, Buring J, Calle EE, Chanock SJ, Colditz GA, Diver WR, Dunning AM, Freedman ML, Gaziano JM, Giovannucci E, Hankinson SE, Hayes RB, et al. A common 8q24 variant in prostate and breast cancer from a large nested case-control study. Cancer research. 2007; 67(7):2951-2956.

23. Nakagawa H, Akamatsu S, Takata R, Takahashi A, Kubo M and Nakamura Y. Prostate cancer genomics, biology, and risk assessment through genome-wide association studies. Cancer Sci. 2012; 103(4):607-613.

24. Amundadottir LT, Sulem P, Gudmundsson J, Helgason A, Baker A, Agnarsson BA, Sigurdsson A, Benediktsdottir KR, Cazier JB, Sainz J, Jakobsdottir M, Kostic J, Magnusdottir DN, Ghosh S, Agnarsson K, Birgisdottir B, et al. A common variant associated with prostate cancer in European and African populations. Nature genetics. 2006; 38(6):652-658.

25. Freedman ML, Haiman CA, Patterson N, McDonald GJ, Tandon A, Waliszewska A, Penney K, Steen RG, Ardlie K, John EM, Oakley-Girvan I, Whittemore AS, Cooney KA, Ingles SA, Altshuler D, Henderson BE, et al. Admixture mapping identifies 8q24 as a prostate cancer risk locus in African-American men. Proceedings of the National Academy of Sciences of the United States of America. 2006; 103(38):14068-14073.

26. Gudmundsson J, Sulem P, Manolescu A, Amundadottir LT, Gudbjartsson D, Helgason A, Rafnar T, Bergthorsson JT, Agnarsson BA, Baker A, Sigurdsson A, Benediktsdottir KR, Jakobsdottir M, Xu J, Blondal T, Kostic J, et al. Genome-wide association study identifies a second prostate cancer susceptibility variant at 8q24. Nature genetics. 2007; 39(5):631-637.

27. Haiman CA, Patterson N, Freedman ML, Myers SR, Pike MC, Waliszewska A, Neubauer J, Tandon A, Schirmer C, McDonald GJ, Greenway SC, Stram DO, Le Marchand L, Kolonel LN, Frasco M, Wong D, et al. Multiple regions within 8q24 independently affect risk for prostate cancer. Nature genetics. 2007; 39(5):638-644.

28. Yeager M, Orr N, Hayes RB, Jacobs KB, Kraft P, Wacholder S, Minichiello MJ, Fearnhead P, Yu K, Chatterjee N, Wang Z, Welch R, Staats BJ, Calle EE, Feigelson HS, Thun MJ, et al. Genome-wide association study of prostate cancer identifies a second risk locus at 8q24. Nature genetics. 2007; 39(5):645-649.

29. Liu W, Xie CC, Zhu Y, Li T, Sun J, Cheng Y, Ewing CM, Dalrymple S, Turner AR, Sun J, Isaacs JT, Chang BL, Zheng SL, Isaacs WB and Xu J. Homozygous deletions and recurrent amplifications implicate new genes involved in prostate cancer. Neoplasia. 2008; 10(8):897-907.

30. Gudmundsson J, Sulem P, Gudbjartsson DF, Blondal T, Gylfason A, Agnarsson BA, Benediktsdottir KR, Magnusdottir DN, Orlygsdottir G, Jakobsdottir M, Stacey SN, Sigurdsson A, Wahlfors T, Tammela T, Breyer JP, McReynolds KM, et al. Genome-wide association and replication studies identify four variants associated with prostate cancer susceptibility. Nature genetics. 2009; 41(10):1122-1126.

31. Chung CC, Hsing AW, Edward Y, Biritwum R, Tettey Y, Adjei A, Cook MB, De Marzo A, Netto G, Tay E, Boland JF, Yeager M and Chanock SJ. A comprehensive resequence-analysis of 250 kb region of 8q24.21 in men of African ancestry. Prostate. 2014; 74(6):579-589.

32. Bensen JT, Xu Z, McKeigue PM, Smith GJ, Fontham ET, Mohler JL and Taylor JA. Admixture mapping of prostate cancer in African Americans participating in the North Carolina-Louisiana Prostate Cancer Project (PCaP). Prostate. 2014; 74(1):1-9.

33. Ghoussaini M, Song H, Koessler T, Al Olama AA, Kote-Jarai Z, Driver KE, Pooley KA, Ramus SJ, Kjaer SK, Hogdall E, DiCioccio RA, Whittemore AS, Gayther SA, Giles GG, Guy M, Edwards SM, et al. Multiple loci with different cancer specificities within the 8q24 gene desert. J Natl Cancer Inst. 2008; 100(13):962-966.

34. Kastler S, Honold L, Luedeke M, Kuefer R, Moller P, Hoegel J, Vogel W, Maier C and Assum G. POU5F1P1, a putative cancer susceptibility gene, is overexpressed in prostatic carcinoma. Prostate. 2010; 70(6):666-674.

35. van Duin M, van Marion R, Vissers K, Watson JE, van Weerden WM, Schroder FH, Hop WC, van der Kwast TH, Collins C and van Dekken H. High-resolution array comparative genomic hybridization of chromosome arm 8q: evaluation of genetic progression markers for prostate cancer. Genes Chromosomes Cancer. 2005; 44(4):438-449.

36. Wernig M, Meissner A, Foreman R, Brambrink T, Ku M, Hochedlinger K, Bernstein BE and Jaenisch R. In vitro reprogramming of fibroblasts into a pluripotent ES-cell-like state. Nature. 2007; 448(7151):318-324.

37. Rybak AP, He L, Kapoor A, Cutz JC and Tang D. Characterization of sphere-propagating cells with stem-like properties from DU145 prostate cancer cells. Biochimica et biophysica acta. 2011; 1813(5):683-694.

38. Yan J, Ojo D, Kapoor A, Lin X, Pinthus JH, Aziz T, Bismar TA, Wei F, Wong N, De Melo J, Cutz JC, Major P, Wood G, Peng H and Tang D. Neural Cell Adhesion Protein CNTN1 Promotes the Metastatic Progression of Prostate Cancer. Cancer research. 2016; 76(6):1603-1614.

39. Edgar R, Domrachev M and Lash AE. Gene Expression Omnibus: NCBI gene expression and hybridization array data repository. Nucleic acids research. 2002; 30(1):207-210.

40. Cerami E, Gao J, Dogrusoz U, Gross BE, Sumer SO, Aksoy BA, Jacobsen A, Byrne CJ, Heuer ML, Larsson E, Antipin Y, Reva B, Goldberg AP, Sander C and Schultz N. The cBio cancer genomics portal: an open platform for exploring multidimensional cancer genomics data. Cancer discovery. 2012; 2(5):401-404.

41. Gao J, Aksoy BA, Dogrusoz U, Dresdner G, Gross B, Sumer SO, Sun Y, Jacobsen A, Sinha R, Larsson E, Cerami E, Sander C and Schultz N. Integrative analysis of complex cancer genomics and clinical profiles using the cBioPortal. Sci Signal. 2013; 6(269):pl1.

42. Chandran UR, Ma C, Dhir R, Bisceglia M, Lyons-Weiler M, Liang W, Michalopoulos G, Becich M and Monzon FA. Gene expression profiles of prostate cancer reveal involvement of multiple molecular pathways in the metastatic process. BMC Cancer. 2007; 7:64.

43. Yu YP, Landsittel D, Jing L, Nelson J, Ren B, Liu L, McDonald C, Thomas R, Dhir R, Finkelstein S, Michalopoulos G, Becich M and Luo JH. Gene expression alterations in prostate cancer predicting tumor aggression and preceding development of malignancy. J Clin Oncol. 2004; 22(14):2790-2799.

44. Vanaja DK, Cheville JC, Iturria SJ and Young CY. Transcriptional silencing of zinc finger protein 185 identified by expression profiling is associated with prostate cancer progression. Cancer research. 2003; 63(14):3877-3882.

45. Taylor BS, Schultz N, Hieronymus H, Gopalan A, Xiao Y, Carver BS, Arora VK, Kaushik P, Cerami E, Reva B, Antipin Y, Mitsiades N, Landers T, Dolgalev I, Major JE, Wilson M, et al. Integrative genomic profiling of human prostate cancer. Cancer cell. 2010; 18(1):11-22.

46. Grasso CS, Wu YM, Robinson DR, Cao X, Dhanasekaran SM, Khan AP, Quist MJ, Jing X, Lonigro RJ, Brenner JC, Asangani IA, Ateeq B, Chun SY, Siddiqui J, Sam L, Anstett M, et al. The mutational landscape of lethal castration-resistant prostate cancer. Nature. 2012; 487(7406):239-243.

47. Lapointe J, Li C, Higgins JP, van de Rijn M, Bair E, Montgomery K, Ferrari M, Egevad L, Rayford W, Bergerheim U, Ekman P, DeMarzo AM, Tibshirani R, Botstein D, Brown PO, Brooks JD, et al. Gene expression profiling identifies clinically relevant subtypes of prostate cancer. Proceedings of the National Academy of Sciences of the United States of America. 2004; 101(3):811-816.

48. Yan J, De Melo J, Cutz JC, Aziz T and Tang D. Aldehyde dehydrogenase 3A1 associates with prostate tumorigenesis. British journal of cancer. 2014; 110(10):2593-2603.

49. Cancer Genome Atlas Research N. The Molecular Taxonomy of Primary Prostate Cancer. Cell. 2015; 163(4):1011-1025.

50. Kumar A, Coleman I, Morrissey C, Zhang X, True LD, Gulati R, Etzioni R, Bolouri H, Montgomery B, White T, Lucas JM, Brown LG, Dumpit RF, DeSarkar N, Higano C, Yu EY, et al. Substantial interindividual and limited intraindividual genomic diversity among tumors from men with metastatic prostate cancer. Nature medicine. 2016; 22(4):369-378.

51. Robinson D, Van Allen EM, Wu YM, Schultz N, Lonigro RJ, Mosquera JM, Montgomery B, Taplin ME, Pritchard CC, Attard G, Beltran H, Abida W, Bradley RK, Vinson J, Cao X, Vats P, et al. Integrative clinical genomics of advanced prostate cancer. Cell. 2015; 161(5):1215-1228.

52. Beltran H, Prandi D, Mosquera JM, Benelli M, Puca L, Cyrta J, Marotz C, Giannopoulou E, Chakravarthi BV, Varambally S, Tomlins SA, Nanus DM, Tagawa ST, Van Allen EM, Elemento O, Sboner A, et al. Divergent clonal evolution of castration-resistant neuroendocrine prostate cancer. Nature medicine. 2016; 22(3):298-305.

53. Barbieri CE, Baca SC, Lawrence MS, Demichelis F, Blattner M, Theurillat JP, White TA, Stojanov P, Van Allen E, Stransky N, Nickerson E, Chae SS, Boysen G, Auclair D, Onofrio RC, Park K, et al. Exome sequencing identifies recurrent SPOP, FOXA1 and MED12 mutations in prostate cancer. Nature genetics. 2012; 44(6):685-689.

54. Hieronymus H, Schultz N, Gopalan A, Carver BS, Chang MT, Xiao Y, Heguy A, Huberman K, Bernstein M, Assel M, Murali R, Vickers A, Scardino PT, Sander C, Reuter V, Taylor BS, et al. Copy number alteration burden predicts prostate cancer relapse. Proceedings of the National Academy of Sciences of the United States of America. 2014; 111(30):11139-11144.

55. Al Olama AA, Kote-Jarai Z, Giles GG, Guy M, Morrison J, Severi G, Leongamornlert DA, Tymrakiewicz M, Jhavar S, Saunders E, Hopper JL, Southey MC, Muir KR, English DR, Dearnaley DP, Ardern-Jones AT, et al. Multiple loci on 8q24 associated with prostate cancer susceptibility. Nature genetics. 2009; 41(10):1058-1060.

56. Gudmundsson J, Sulem P, Gudbjartsson DF, Masson G, Agnarsson BA, Benediktsdottir KR, Sigurdsson A, Magnusson OT, Gudjonsson SA, Magnusdottir DN, Johannsdottir H, Helgadottir HT, Stacey SN, Jonasdottir A, Olafsdottir SB, Thorleifsson G, et al. A study based on whole-genome

sequencing yields a rare variant at 8q24 associated with prostate cancer. Nature genetics. 2012; 44(12):1326-1329.

57. Du M, Yuan T, Schilter KF, Dittmar RL, Mackinnon A, Huang X, Tschannen M, Worthey E, Jacob H, Xia S, Gao J, Tillmans L, Lu Y, Liu P, Thibodeau SN and Wang L. Prostate cancer risk locus at 8q24 as a regulatory hub by physical interactions with multiple genomic loci across the genome. Hum Mol Genet. 2015; 24(1):154-166.

58. Cheng C, Cui H, Zhang L, Jia Z, Song B, Wang F, Li Y, Liu J, Kong P, Shi R, Bi Y, Yang B, Wang J, Zhao Z, Zhang Y, Hu X, et al. Genomic analyses reveal FAM84B and the NOTCH pathway are associated with the progression of esophageal squamous cell carcinoma. GigaScience. 2016; 5:1.

59. Hsu FM, Cheng JC, Chang YL, Lee JM, Koong AC and Chuang EY. Circulating mRNA Profiling in Esophageal Squamous Cell Carcinoma Identifies FAM84B As A Biomarker In Predicting Pathological Response to Neoadjuvant Chemoradiation. Sci Rep. 2015; 5:10291.

60. Haffner MC, Aryee MJ, Toubaji A, Esopi DM, Albadine R, Gurel B, Isaacs WB, Bova GS, Liu W, Xu J, Meeker AK, Netto G, De Marzo AM, Nelson WG and Yegnasubramanian S. Androgen-induced TOP2B-mediated double-strand breaks and prostate cancer gene rearrangements. Nature genetics. 2010; 42(8):668-675.

61. Nyquist MD and Dehm SM. Interplay between genomic alterations and androgen receptor signaling during prostate cancer development and progression. Horm Cancer. 2013; 4(2):61-69.

62. Berger MF, Lawrence MS, Demichelis F, Drier Y, Cibulskis K, Sivachenko AY, Sboner A, Esgueva R, Pflueger D, Sougnez C, Onofrio R, Carter SL, Park K, Habegger L, Ambrogio L, Fennell T, et al. The genomic complexity of primary human prostate cancer. Nature. 2011; 470(7333):214-220.

TABLES

Table 4.1. Nanostring analysis of gene expression in primary prostate cancer tissues

Genes	P1[a]	P2[a]	P3[a]	P4[a]	P5[a]	P6[a]	P7[a]
FAM84B	+1.3	+3	1.2	+2.6	+1.6	+2.7	+2.1
TMPRSS2-ERG[b]	+16.2	+30.2	N[c]	N	+17	+25.3	+27.3
PTEN[b]	-1.4	-1.4	N	N	-1.4	-1.3	-2.6

a: patients 1-3 (GS6), patients 4-6 (GS7, 4+3 for P4,5, and 3+4 for P6), and P7 (GS4+4).
b: TMPRSS2-ERG and PTEN were used as positive controls for upregulated and downregulated genes in PC. downregulated or upregulated genes
c: no downregulation or upregulation

Table 4.2[a]. Upregulation of FAM84B mRNA following PC progression

Dataset	PC Type	Cases[b]	Upregulation[c] (%)	Ref
CGARN	Primary PC	333	11% (38/333)	Cell 163, 1011-25, 2015
Taylor et al	Primary PC	216	13% (29/216)	Cancer Cell 18, 11-22, 2010
Total		**549**	**12% (67/549)**	
Kumar et al	mCRPC[d]	176	9% (16/176)	Nat Med 22, 369-28, 2016
Robinson et al	mCRPC	118	22% (26/118)	Cell 161, 1215-28, 2015
Beltran et al	mCRPC	114	27% (31/114)	Nat Med 22, 298-305, 2016
Total		**412**	**18% (73/412)***	

a: data was downloaded from cBioPortal
b: number of cases
c: upregulation was defined by zscore ≥ 2;
d: metastatic castration resistant prostate cancer;
*$p<0.025$ in comparison to the average rate of FAM84B upregulation by Fisher's Exact Test.

Table 4.3[a]. FAM84B gene amplification in CRPCs

Dataset	PC Type	Cases[b]	Upregulation[c] (%)	Ref
Barbieri et al	Primary PC	109	0.9% (1/109)	Nat Genet 44, 685-9, 2012
Hieronymus et al	Primary PC	104	2% (2/104)	PNAS 111, 11139-44, 2014
Taylor et al	Primary PC	333	7% (23/333)	Cancer Cell 18, 11-22, 2010
Total		**546**	**4.8% (26/546)**	
Kumar et al	mCRPC[c]	149	30% (44/149)	Nat Med 22, 369-28, 2016
Robinson et al	mCRPC	150	13% (20/150)	Cell 161, 1215-28, 2015
Grasso et al	mCRPC	61	16% (10/61)	Nature 487, 239-43, 2012
Beltran et al	mCRPC	107	44% (47/107)	Nat Med 22, 298-305, 16
Total		**467**	**26% (121/467)***	

a: data was downloaded from cBioPortal
b: number of cases
c: metastatic castration resistant prostate cancer
*: $p<0.0001$ in comparison to the average rate of FAM84B gene amplification by Fisher's Exact Test.

FIGURES

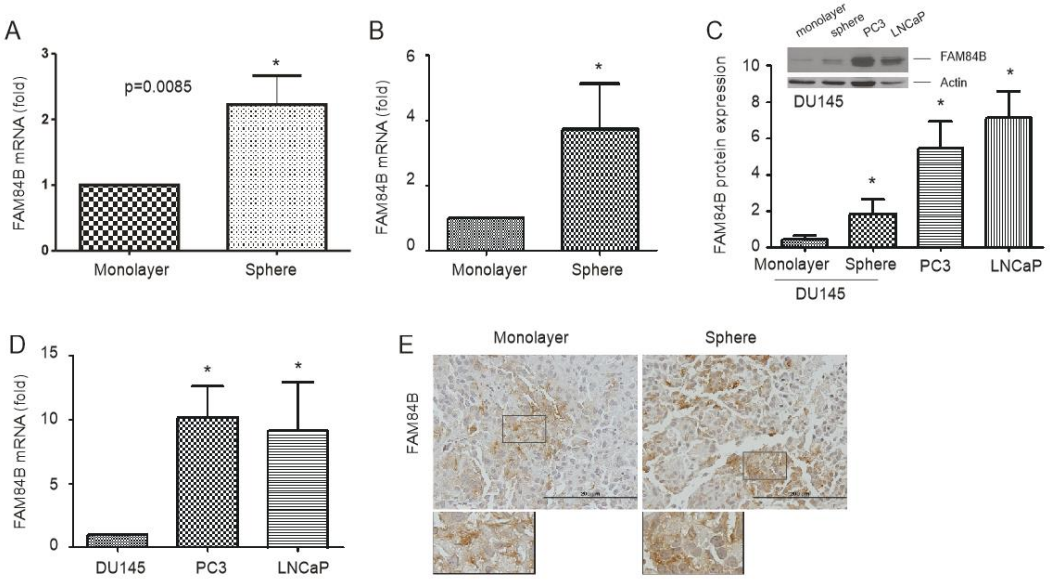

Figure 4.1. Upregulation of FAM84B in prostate cancer stem-like cells (PCSLCs). (A) Affymetrix profiling of gene expression in DU145 monolayer and sphere cells. The profiling was carried out three times with duplicates for each repeat. FAM84B mRNA is expressed as fold change compared to monolayer cells. Mean ± SD (standard derivation) are graphed. Statistical analysis was performed using 2-tailed Student's *t*-test. (**B, D**) Real-time PCR analysis of FAM84B mRNA in DU145 monolayer, DU145 sphere cells (PCSLCs), and the indicated PC lines. β-actin was used as an internal control. Experiments were repeated three times. FAM84B mRNA abundance is graphed as a fold change to DU145 monolayer cells; mean ± SD are graphed. *$p<0.05$ by a 2-tailed Student's *t*-test. **(C)** Western blot examination of FAM84B protein expression in DU145 monolayer and sphere, PC3, and LNCaP cells. Experiments were repeated three times; typical images from a single repeat are shown (inset). FAM84B protein levels were normalized to actin; mean ± SD are graphed. *$p<0.05$ by a 2-tailed Student's *t*-test in comparison to DU145 monolayer cells. (**E**) FAM84B protein expression in xenograft tumors produced by either DU145 monolayer or sphere cells. The overall patterns of FAM84B expression at low magnification are presented in Supplementary Figure 4.2.

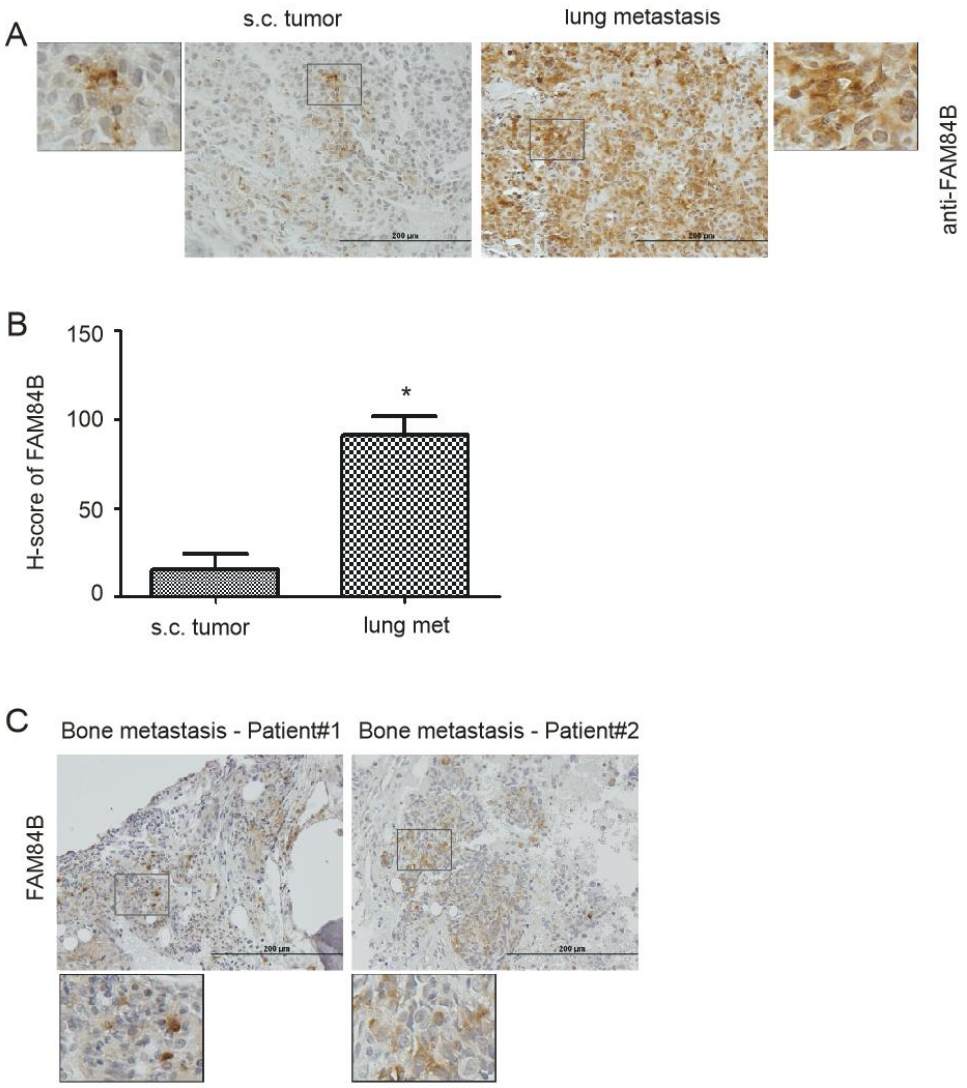

Figure 4.2. Upregulation of FAM84B in metastatic PC. DU145 subcutaneous (s.c.) xenograft tumors and lung metastasis were produced in NOD/SCID mice (5 mice per group). **(A)** Typical IHC staining for FAM84B in s.c. tumors and lung metastasis (see Supplementary Figure 4.3 for overall staining). The indicated regions are enlarged three fold and placed on the side of the original panel. (**B**) IHC staining was quantified through ImageScope software. Average HScores ± SDs are graphed. *$p<0.05$ by a 2-tailed Student's *t*-test. (**C**) IHC staining for FAM84B was performed on four human bone metastases; two tumors with positive staining are shown here (see Supplementary Figure 4.3 for additional images). Indicated regions are enlarged 2.5 fold and placed beneath the original panel.

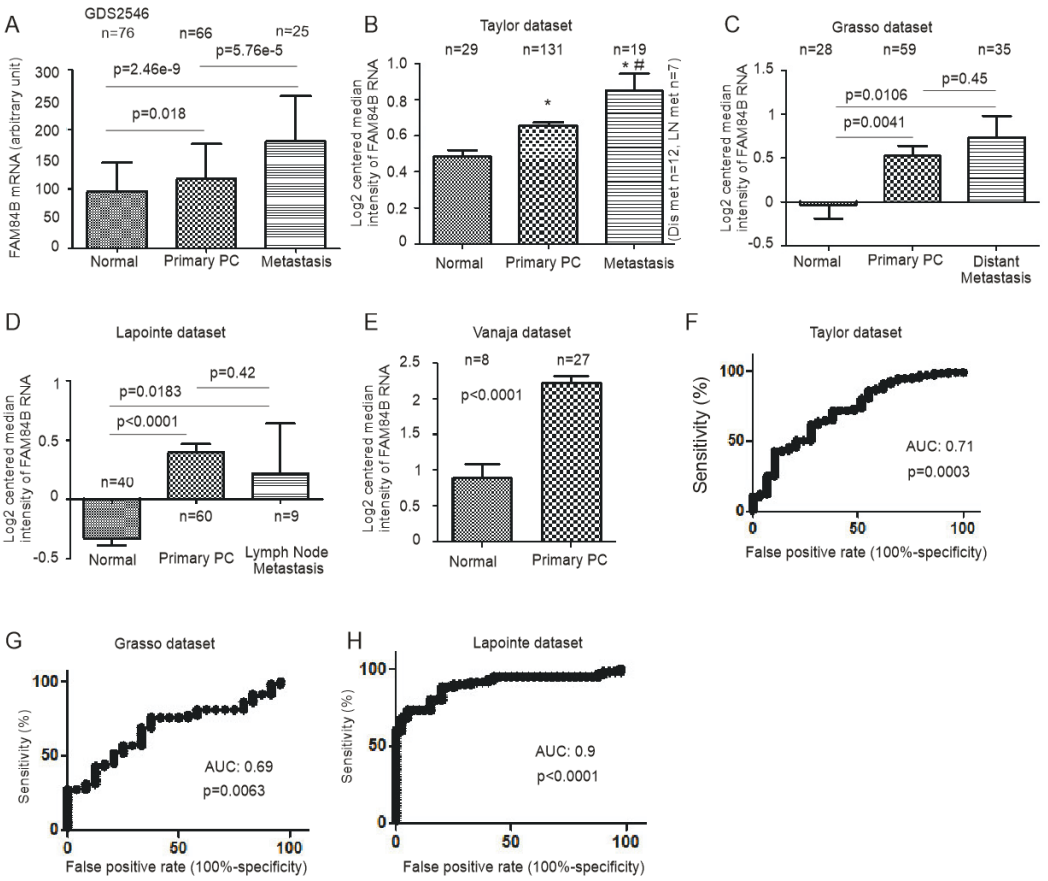

Figure 4.3. FAM84B upregulation associates with PC tumorigenesis. Data was downloaded from GDS2546 (Gene Expression Omnibus) (**A**), and Oncomine™ (Compendia Bioscience, Ann Arbor, MI) datasets Taylor (**B**), Grasso (**C**), Lapointe (**D**), and Vanaja (**E**) for analysis of changes in FAM84B mRNA. Mean ± SD are graphed. *p<0.05 by a 2-tailed Student's *t*-test in comparison to Normal; #p<0.05 in comparison to primary PC (2-tailed Student's *t*-test). (**F-H**) A receiver-operating characteristic (ROC) curve of primary prostate tumors versus metastatic PCs was derived from the indicated datasets. AUC: area under the curve.

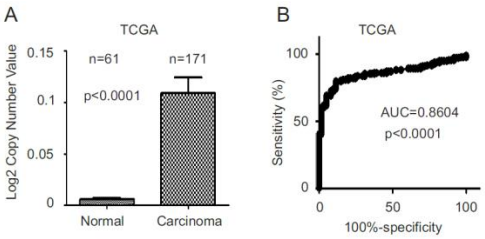

Figure 4.4. FAM84B gene amplification in prostate tumors. FAM84B gene copy variation data was downloaded from the TCGA dataset within the Oncomine™ database. (**A**) Mean ± SD are graphed. Statistical analysis was performed using 2-tailed Student *t*-test. (**B**) A ROC curve of primary PC versus normal prostate tissues was calculated.

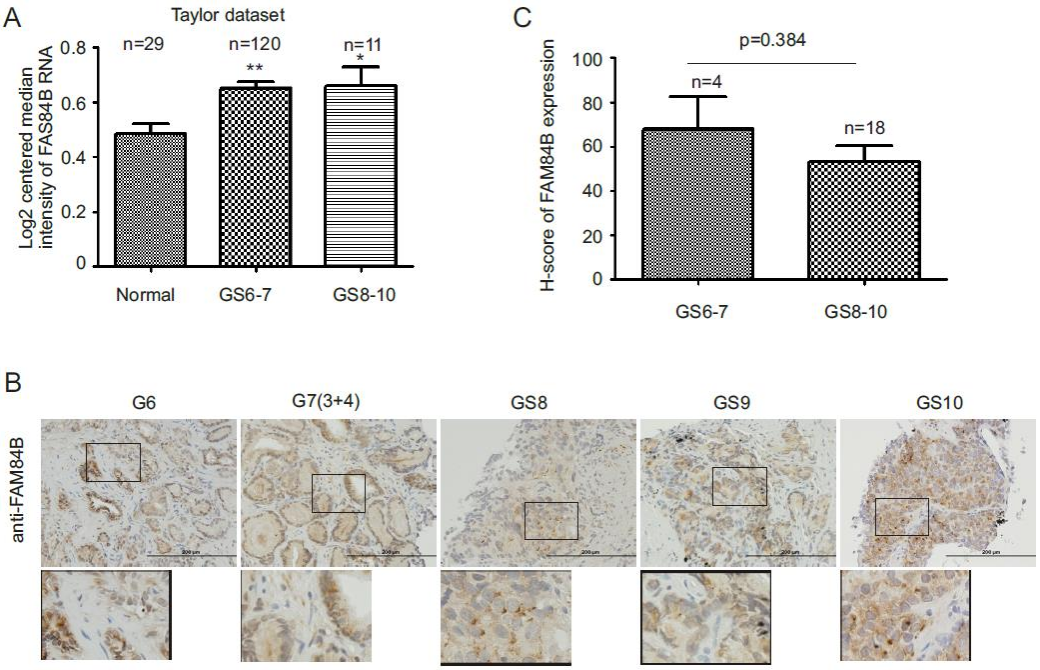

Figure 4.5. FAM84B upregulation does not associate with Gleason score (GS) advancement. (A) FAM84B mRNA expression data was taken from the Taylor dataset in the Oncomine™ database, and was analyzed as low Gleason score (GS6-7) or high Gleason score (GS8-10) PCs. *p<0.05 and **p<0.01 in comparison to normal prostate tissues (2-tailed Student's *t*-test). (**B**) IHC staining for FAM84B in 22 primary PC tissues (Supplementary Table 4.1). Typical images for tumors with the indicated GS are shown. Scale bars represent 200μm (see Supplementary Figure 4.5 for additional images). (**C**) IHC staining was quantified through ImageScope software. Average HScores ± SDs are graphed (for detailed scores, see Supplementary Table 4.1). Statistical analyses were performed using Student's *t*-test.

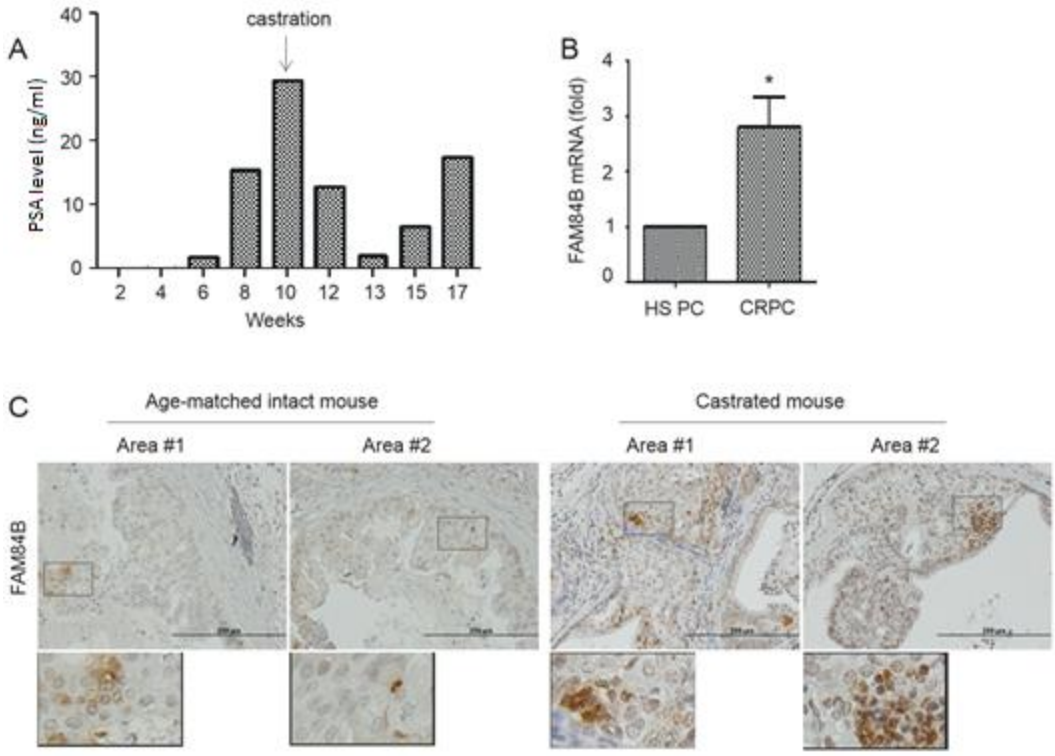

Figure 4.6. Alterations of FAM84B expression in animal models of castration resistant PC. (**A**) PSA levels in NOD/SCID mice bearing LNCaP cell-derived xenograft tumors prior to and after castration. (**B**) Real time PCR analysis of FAM84B mRNA in hormone naive and castration resistant PC (LNCaP xenograft tumors). *p<0.05 by a 2-tailed Student's *t*-test in comparison to hormone naive xenograft tumors. HS PC: hormone sensitive prostate cancer. (**C**) IHC staining of FAM84B in prostate tumors produced in intact and castrated $PTEN^{-/-}$ mice (see Supplementary Figure 4.7 for the production of prostate specific $PTEN^{-/-}$ mice). Indicated regions are enlarged 2.5 fold and placed beneath the original panel.

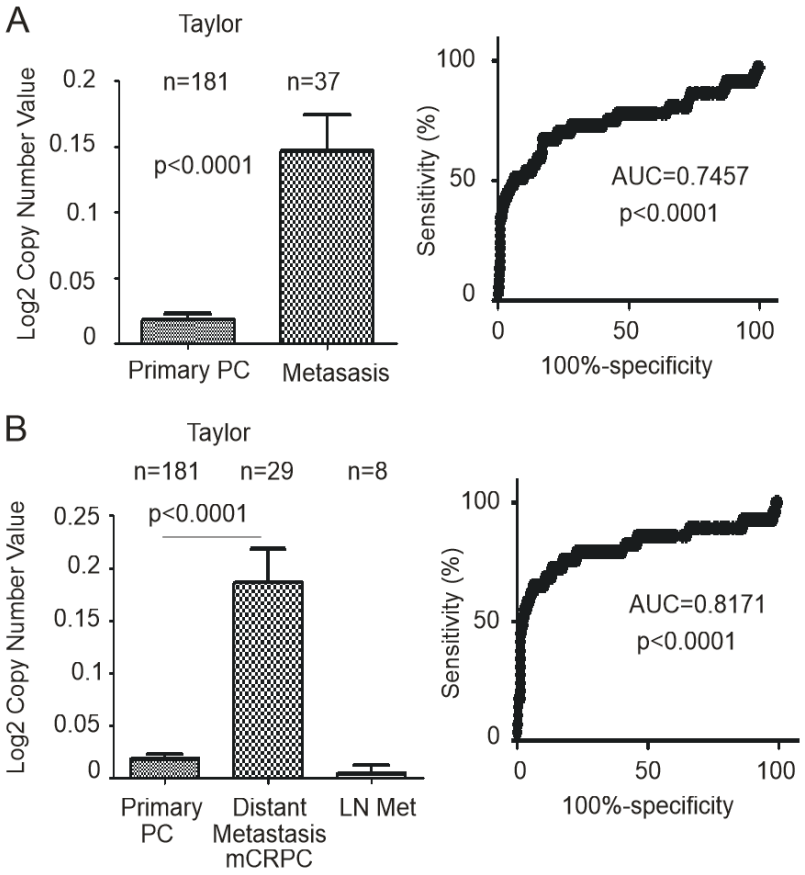

Figure 4.7. FAM84B is increased in metastatic castration resistant prostate cancer (mCRPC). Data related to FAM84B gene copy number was downloaded from the Taylor dataset within Oncomine™ (Compendia Bioscience, Ann Arbor, MI). (**A**) Mean ± SD (left panel) and a ROC curve (right panel) of primary versus metastatic PC were calculated and graphed. Statistical analyses were performed using Student's *t*-test. (**B**) The same data was analyzed by separating out distant metastasis (Dis met)/mCRPC from lymph node metastases (LN met). An ROC curve for this arrangement is also shown.

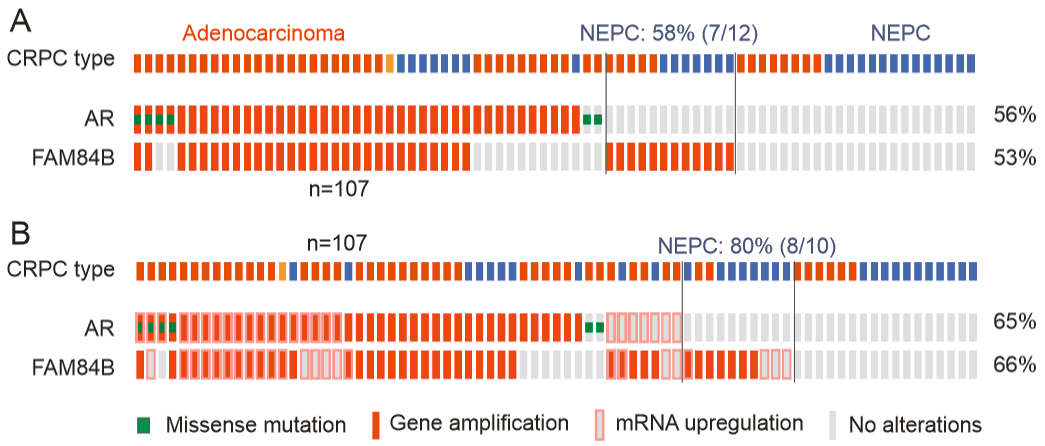

Figure 4.8. Genomic alterations of the AR and FAM84B genes. Data was downloaded from the Beltran dataset within the cBioPortal database [40, 41]. The dataset covers 107 CRPCs derived from 77 patients [52]. The indicated genomic alterations without **(A)** and with the respective mRNA upregulations **(B)** in 77 CRPC patients are shown. The percentages of alterations were based on the patient population (n=77). CRPC tumor types are also indicated. Red bars: adenocarcinoma; Blue bars: neuroendocrine prostate cancer (NEPC); Orange bars: adenocarcinoma mixed with NEPC. Symbols for genomic mutations and mRNA upregulation for the AR and FAM84B genes are indicated.

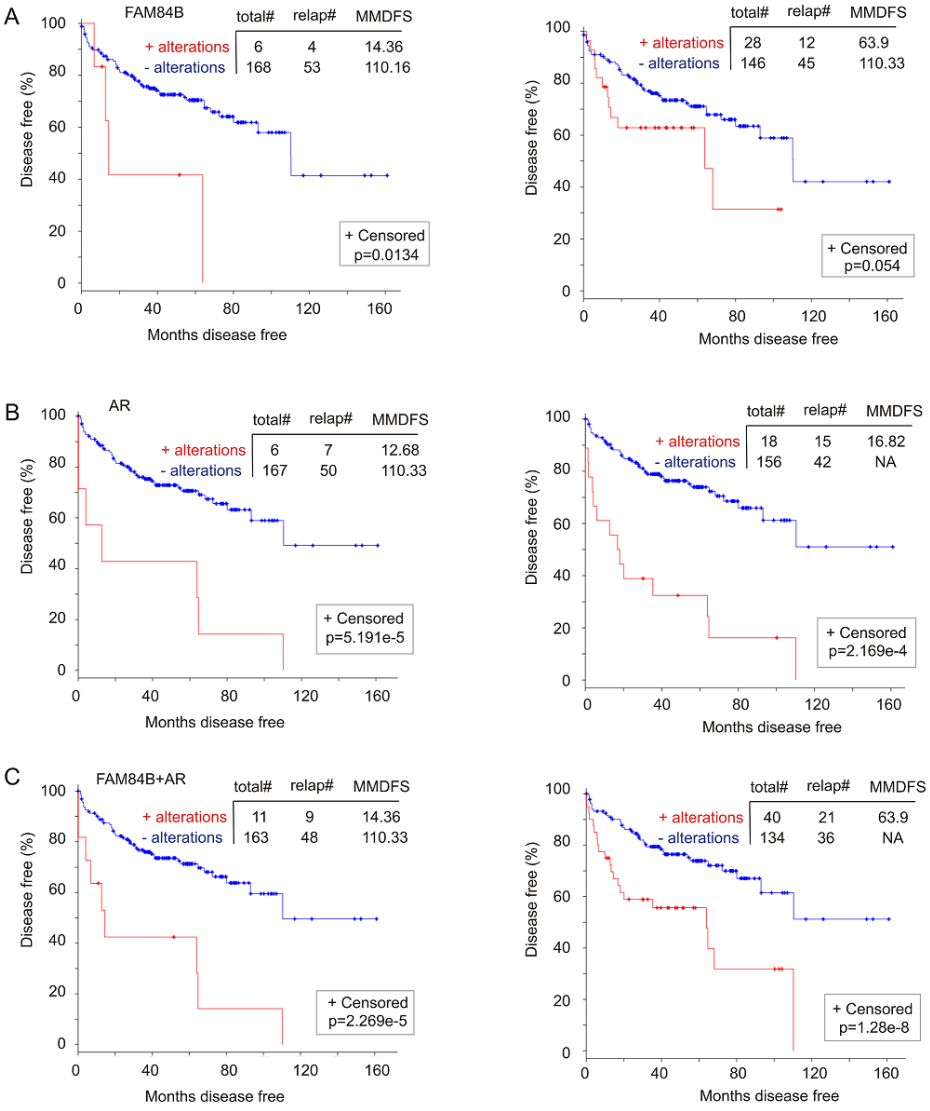

Figure 4.9. Genomic alterations in the FAM84B gene associate with a reduction in disease free survival (DFS). A dataset of primary PCs [45] (within the cBioPortal database [40, 41]) was used to assess the impact of FAM84B (**A**), AR (**B**), and FAM84B+AR (**C**) genomic changes on DFS without (left panels) and with the respective mRNA upregulation (right panels). The detailed alterations are documented in Supplementary Figure 4.9. Statistical analysis was performed using Logrank Test. Total#: total number of cases; relap#: number of relapsed cases; MMDFS: median months disease free survival; NA: not available. Censored individuals are indicated; the number of censored individuals is the total individuals minus relapsed patients.

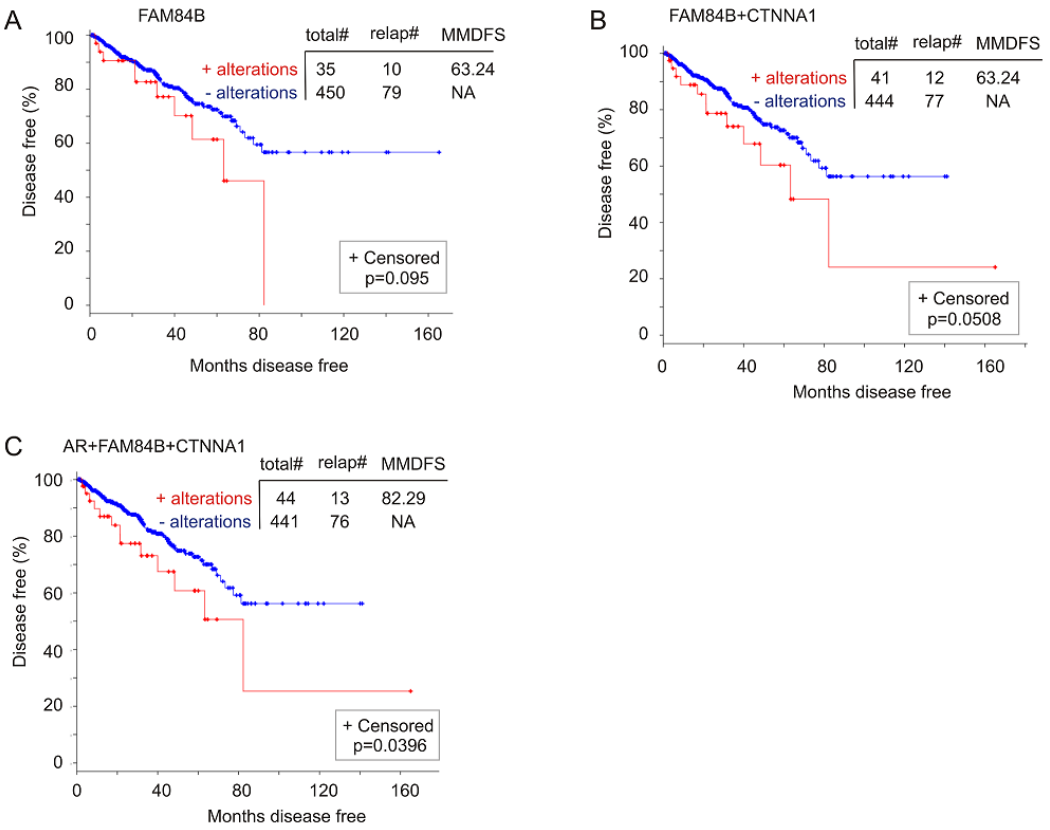

Figure 4.10. Genomic alterations in the FAM84B network genes associate with a reduction in DFS. The TCGA dataset within the cBioPortal database [40, 41] contains 492 primary prostate tumors with copy number variation determined. The detailed genomic alterations in the FAM84B, CTNNA1, and AR genes are presented in Supplementary Figure 4.10A. The effects of these changes with respect to the FAM84B (**A**), FAM84B+CTNNA1 (**B**) or FAM84B+CTNNA1+AR (**C**) are calculated. Statistical analysis was performed using Logrank Test. Total#: total number of cases; relap#: number of relapsed cases; MMDFS: median months disease free survival; NA: not available. Censored individuals are indicated; the number of censored individuals is the total individuals minus relapsed patients.

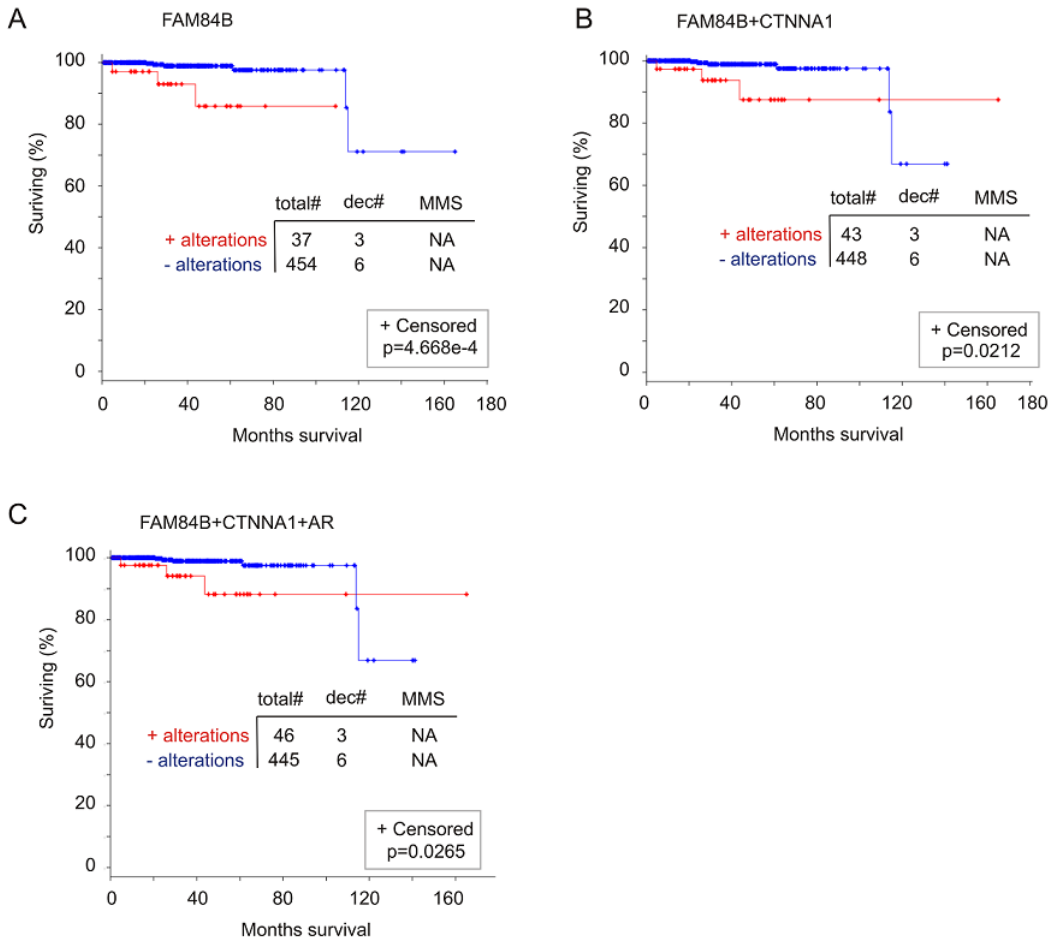

Figure 4.11. Genomic alterations in the FAM84B gene associate with a reduction in overall survival (OS). The TCGA dataset within the cBioPortal database [40, 41] contains 492 primary prostate tumors with copy number variation determined. The detailed genomic alterations in the FAM84B, CTNNA1, and AR genes are presented in Supplementary Figure 4.10A. The effects of genomic alterations involving the FAM84B (**A**), FAM84B+CTNNA1 (**B**) or FAM84B+CTNNA1+AR (**C**) are calculated. Statistical analysis was performed using Logrank Test. Total#: total number of cases; dec#: number of deceased cases; MMS: median months survival; NA: not available. Censored individuals are indicated; the number of censored individuals is the total individuals minus relapsed patients.

SUPPLEMENTARY TABLES

Supplementary Table 4.1. Patient information and FAM84B IHC score

Patient	Age[a]	Gleason Score	Average Score[b]
1	56	3+3	97.55 ± 15.03
2	70	3+3	64.17 ± 27.47
3	60	3+4	80.54 ± 10.14
4	76	4+3	28.76 ± 6.28
5	79	4+4	52.63 ± 11.52
6	60	4+4	41.33 ± 13.89
7	56	4+4	30.84 ± 6.95
8	58	4+4	34.37 ± 11.77
9	64	4+5	40.81 ± 15.75
10	82	4+5	45.59 ± 10.39
11	66	4+5	12.06 ± 10.83
12	64	4+5	107.24 ± 18.83
13	54	4+5	19.10 ± 14.31
14	82	4+5	88.90 ± 14.25
15	64	4+5	24.66 ± 10.23
16	89	5+4	11.57 ± 7.13
17	68	5+5	94.08 ± 14.55
18	74	5+5	65.38 ± 9.42
19	91	5+5	61.37 ± 25.27
20	98	5+5	75.04 ± 13.86
21	75	5+5	72.74 ± 48.46
22	86	5+5	81.97 ± 33.09

a:age at diagnosis; b: average score of stain intensity ± SD

SUPPLEMENTARY FIGURES

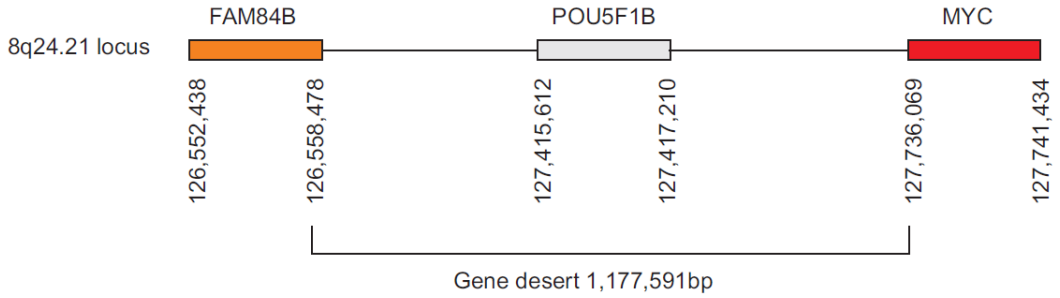

Supplementary Figure 4.1. **A schematic representation of the 8q24.21 locus containing the gene desert.** The gene location information was obtained from the NCBI Resources (http://www.ncbi.nlm.nih.gov/gene).

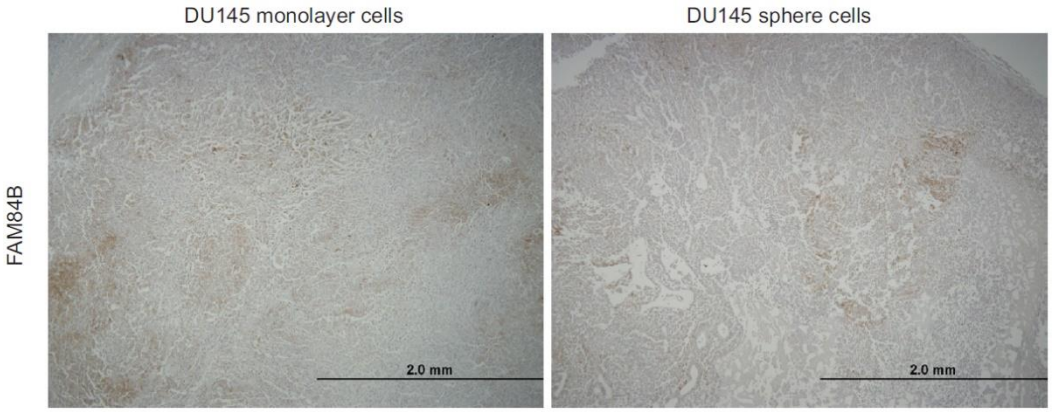

Supplementary Figure 4.2. FAM84B protein expression in prostate cancer xenograft tumors. Overall immunohistochemistry staining for FAM84B in DU145 cell-derived s.c. xenograft tumors.

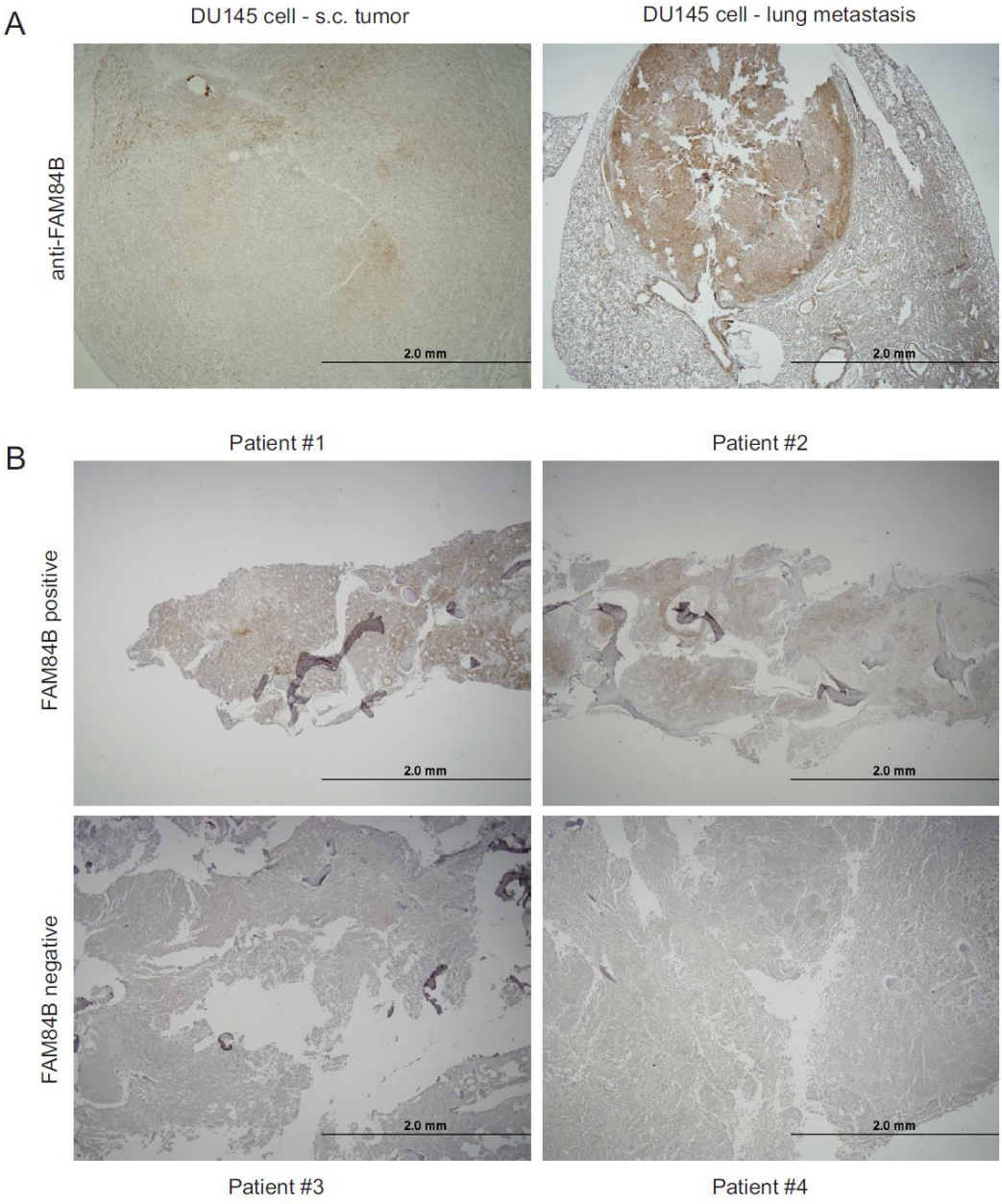

Supplementary Figure 4.3. FAM84B protein expression in metastatic prostate cancer tissues. Overall immunohistochemistry staining for FAM84B in DU145 cell-derived s.c. xenograft tumor and lung metastases (**A**) and in four human bone metastases (**B**).

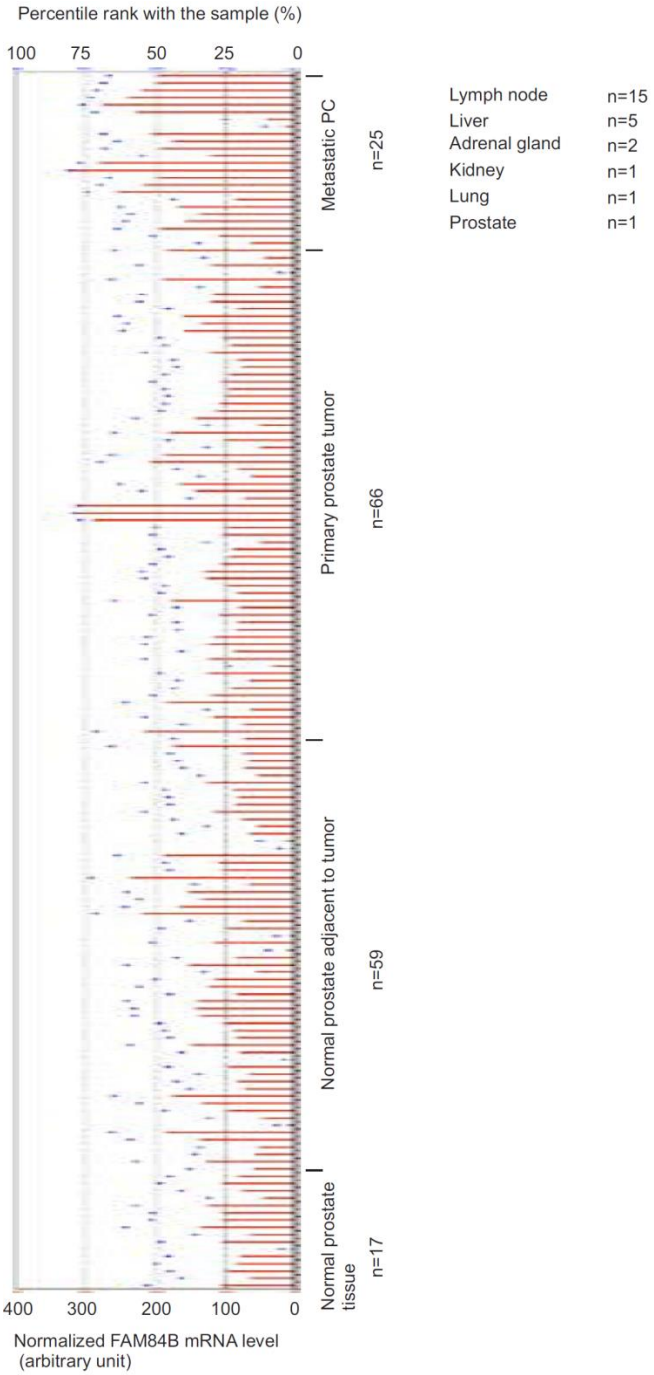

Supplementary Figure 4.4. FAM84B mRNA levels in normal prostate, primary PCs, and metastatic PCs. The illustration was downloaded from the GDS2546 dataset (Gene Expression Omnibus). The composition of the 25 metastases is also included.

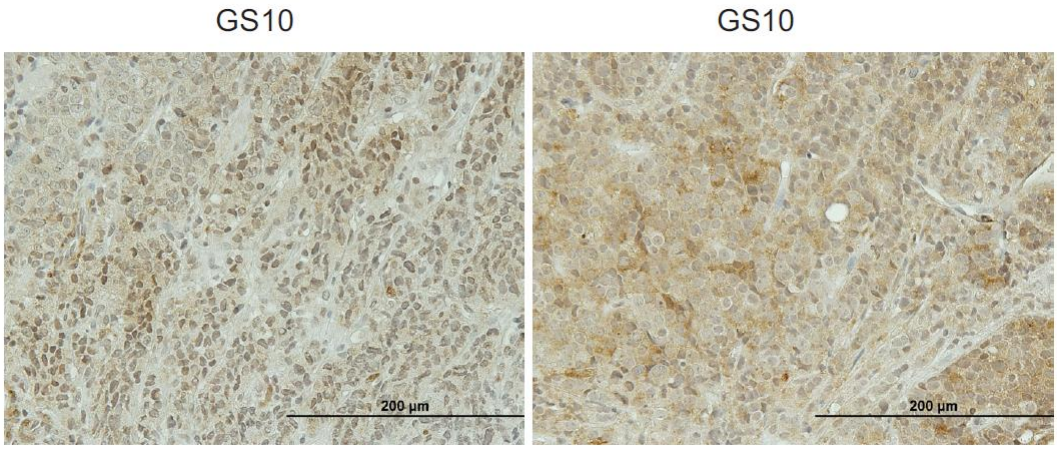

Supplementary Figure 4.5. FAM84B protein expression in primary prostate cancer tumors. FAM84B staining in two Gleason score 10 prostate tumors.

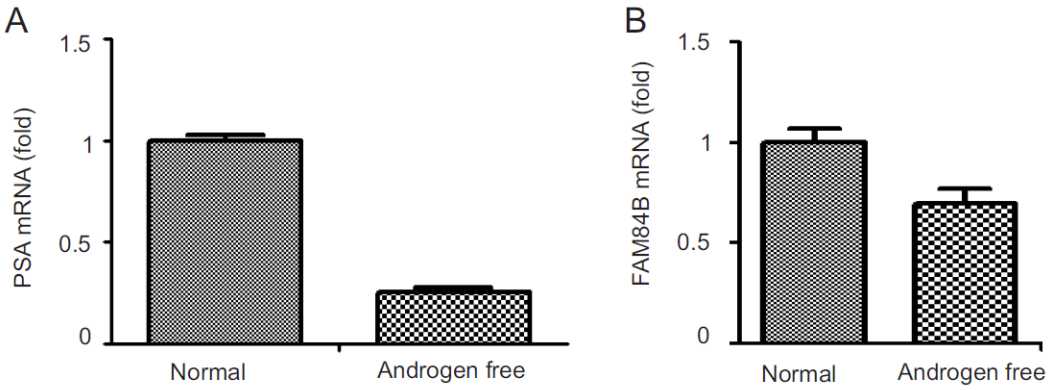

Supplementary Figure 4.6. Examination of FAM84B expression under androgen free conditions. LNCaP cells were cultured in normal or androgen free conditions for 24 hours, followed by real-time PCR examination for PSA (**A**) and FAM84B mRNA (**B**). PCR reactions were carried out in triplicate; experiments were repeated once.

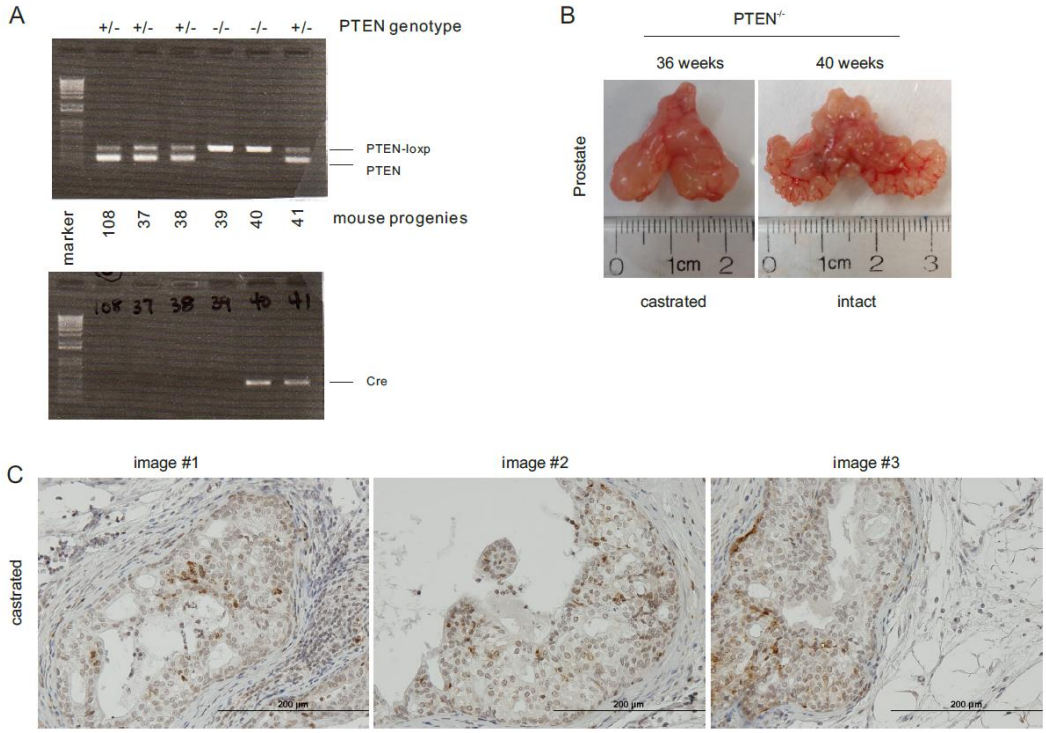

Supplementary Figure 4.7. Generation of castration resistant prostate cancer (CRPC) in prostate specific PTEN$^{-/-}$ knockout mice. (**A**) Prostate specific PTEN$^{-/-}$ mice were produced by crossing PTEN$^{loxp/loxp}$ mice with PB-Cre4 (prostate specific expression of Cre) mice. Genotyping of six mouse progeny for the PTEN locus (top panel) and the Cre transgene locus (bottom panel) using tail genomic DNA. Pten$^{loxp/loxp}$ (Forward): 5'- CAAGCACTCTGCGAACTGAG -3', Pten$^{loxp/loxp}$ (Reverse): 5'- AAGTTTTTGAAGGCAAGATGC -3', PBCre4 (Forward): 5'- CTGAAGAAT GGGACAGGCATTG -3', PB-Cre4 (Reverse): 5'- CATCACTCGTTGCATCGACC -3'. (**B**) PTEN$^{-/-}$ mice were castrated at 23 weeks old for 13 weeks. Typical images of age-matched partial urogenital systems (bladder, prostatic lobes, seminal vesicles) from an intact and a castrated mouse are shown. (**C**) Different images from castrated mice.

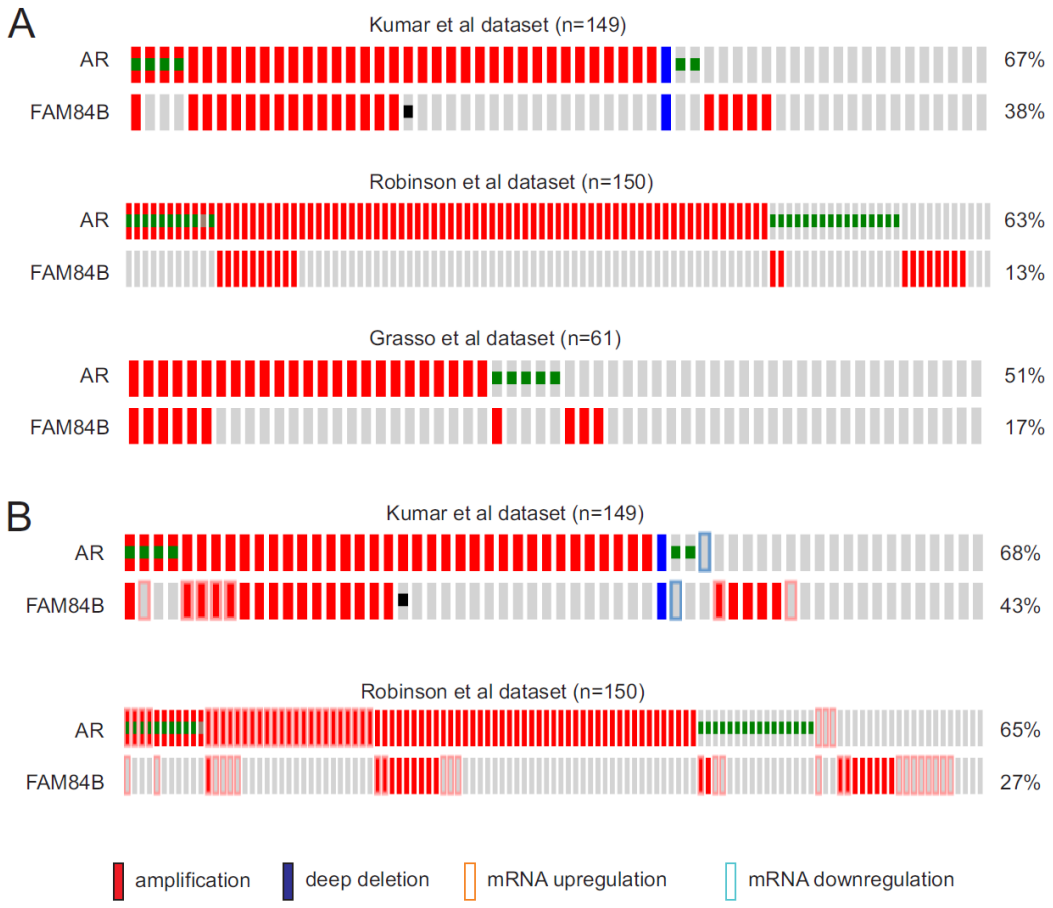

Supplementary Figure 4.8. Genomic alterations in the AR gene and FAM84B gene. Genomic changes alone (**A**) and with mRNA expression alterations (**B**) in the AR and FAM84B genes in the indicated datasets from the cBioPortal database.

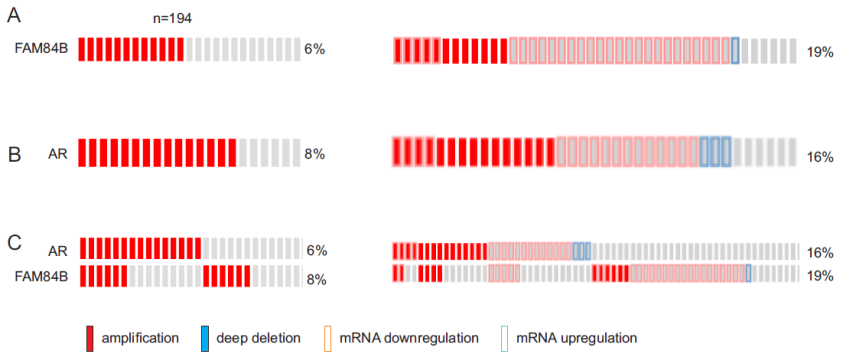

Supplementary Figure 4.9. Genomic alterations and mRNA expression changes in the AR and FAM84B genes. Data was downloaded from the "MSKCC, Cancer Cell 2010" dataset within the cBioPortal database.

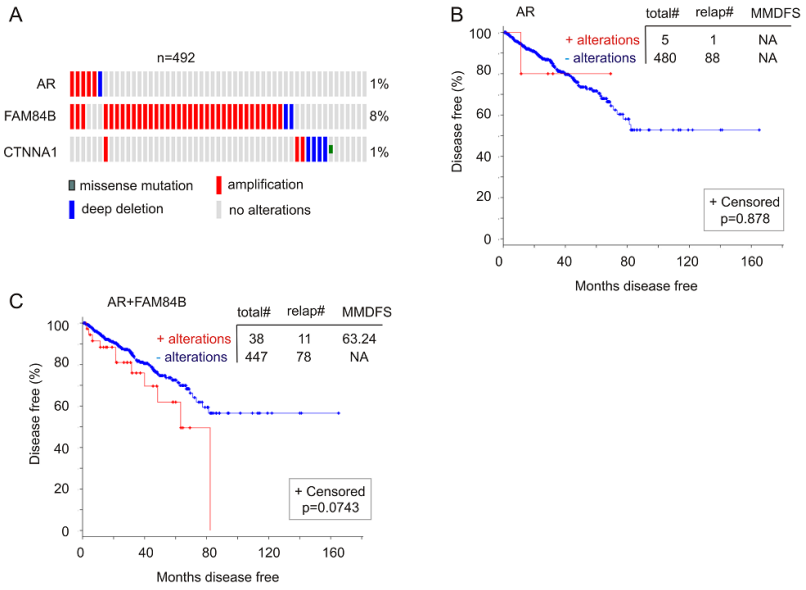

Supplementary Figure 4.10. The relationship of genomic changes in the AR, FAM84B, and CTNNA1 genes with disease free survival (DFS). Data for a 492 patient cohort with gene copy number variations determined was downloaded from the TCGA dataset within the cBioPortal database. (**A**) Only the proportion of patients with the indicated genomic alterations is shown. Number of patients and the rates of genomic changes for the indicated genes are included. Symbols for individual color bars are provided. “no alterations”: no change at either genomic level or mRNA expression. (**B, C**) The association of AR or AR+FAM84B with DFS is shown. Statistical analysis was performed using Logrank Test.

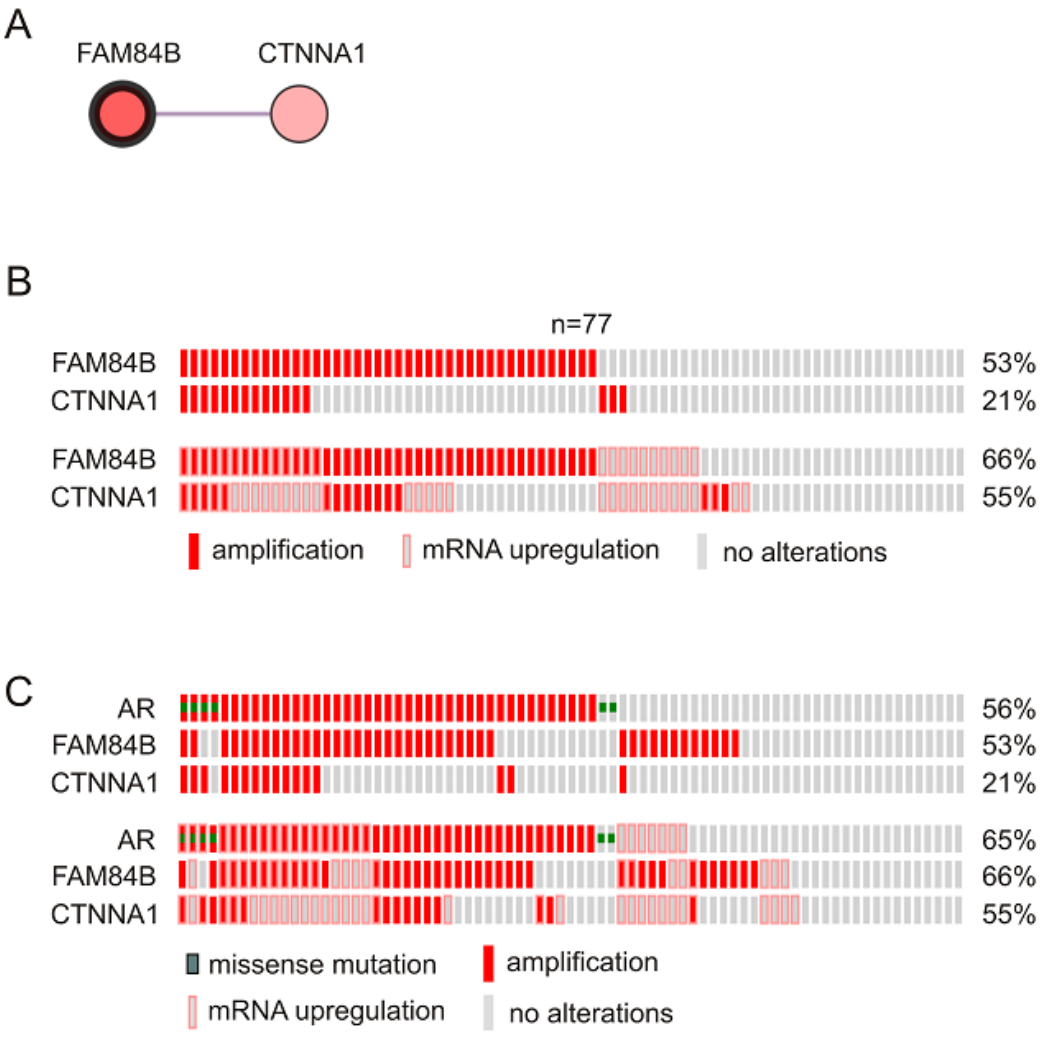

Supplementary Figure 4.11. The FAM84B gene network. (**A**) The network was generated using FAM84B as the seed node; the linker node was identified using the pathway data and interaction data from HPRD, Reactome, NCI-Nature Pathway Interaction Database, and the MSKCC Cancer Cell Map. The pathway was constructed by the system provided by cBioPortal http://www.cbioportal.org/). (**B, C**) Gene amplifications with and without mRNA upregulation in the FAM84B network alone (**B**) and with AR (**C**) are shown. Data was downloaded from the "Trento/Cornell/Broad 2016" dataset within the cBioPortal database. Symbols for individual color bars are provided. “no alterations”: no change at either genomic level or mRNA expression.

CHAPTER FIVE

CONTRIBUTION OF ABCC2 TO DOCETAXEL CHEMORESISTANCE IN CASTRATION RESISTANT PROSTATE CANCER

Relationship to Ph.D. research

Resistance to cytotoxic agents is an important mechanism for cell survival, especially in stem-like populations, and this function can be mediated by ATP-dependent drug transporters. The ATP-binding cassette (ABC) superfamily of transporters are integral to normal detoxification of the body but have been widely implicated in a number of cancers, promoting chemoresistance to various anti-cancer agents. We have identified an upregulation of ABCC2 in our DU145 PCSLCs, which has shown substrate affinity for docetaxel, a common therapeutic for advanced PCs which can potentially develop docetaxel resistance. Here we explore whether ABCC2 confers docetaxel chemoresistance and if this can be associated with PCSCs.

Preface

Through characterization of our DU145 PCSLCs in comparison to DU145 parental cells we have demonstrated that this population is more resistant to docetaxel treatment both *in vitro* and *in vivo*. In our Affymetrix microarray analysis, we discovered a 9.1 fold increase of ABCC2 mRNA levels in our DU145 PCSLCs, which was confirmed by Western blotting and immunocytochemistry. A correlation of ABCC2 with higher Gleason Score was established using a small cohort of patient PC tissues. Knockdown of ABCC2 in DU145 PCSLCs as well as in A549s demonstrated little effect on survival following docetaxel treatment, *in vitro*. However, generation of subcutaneous PCSLC shABCC2-derived xenografts and systemic treatment with docetaxel exhibited possible resensitization. Attempts to overexpress ABCC2 in DU145 parental cells were unsuccessful but will be addressed in future experiments. The work discussed in this chapter is incomplete but will be included in a future publication.

Contribution of ABCC2 to Docetaxel Chemoresistance in Castration Resistant Prostate Cancer

INTRODUCTION

For patients with metastatic castration resistant prostate cancer (mCRPC), the primary method of treatment is the chemotherapeutic drug docetaxel either alone or in combination with other anti-cancer agents such as prednisone and estramustine, with varying success (Qi et al. 2011; Fukuta et al. 2015; Kuramoto et al. 2013; Tannock et al. 2004; Petrylak et al. 2004). During clinical trials, individuals experienced reduction in PSA levels and increases in overall survival, but unfortunately treatment only improved life expectancy by a marginal few months (Hadaschik & Gleave 2007). Docetaxel is administered on a per square meter of body surface ratio, as a 30 minute or 1 hour intravenous infusion throughout varying weekly regiments (Tannock et al. 2004). Tissue uptake occurs throughout the body but primarily in the liver and kidneys, and tumour site retention has been shown to be much longer than in normal tissues. Docetaxel is predominantly metabolized by the cytochrome P450 member CYP3A4 (Kruijtzer 2002) and eliminated through the hepatobiliary route, with over 80% excreted in feces (Belvisi 2004).

Belonging to the taxane family of drugs along with paclitaxel and cabazitaxel, docetaxel binds to microtubules within a cell and stabilizes their structure, preventing depolymerisation. This disruption in cytoskeletal dynamics

leads to suppression of AR nuclear translocation which prevents downstream signalling, and cell cycle arrest during the mitotic phase leading to eventual apoptosis (Ganju et al. 2014). Studies have shown that chemotherapeutic treatment with taxanes also inactivates the anti-apoptotic factor Bcl-2 commonly upregulated in cancers, allowing for cell death. Prostate cancer cell lines that do not express Bcl-2 are unaffected by taxanes (Mahon et al. 2011; Haldar et al. 1996).

Impact on the patient's body must also be taken into consideration, especially since PC patients are predominantly elderly men. In fact, some medical oncologists are reluctant to administer docetaxel-based treatment to the very elderly, concerned about possible cytotoxicity intolerance which could be life threatening (Italiano et al. 2009). As treatment with docetaxel effects all rapidly dividing cells and not just cancerous ones, side effects of docetaxel treatment can include neutropenia, alopecia, nausea, vomiting, diarrhea, and peripheral edema (Tannock et al. 2004). Therefore there is much room for improvement in docetaxel chemotherapy not only to minimize adverse effects on the patient but also to combat the development of chemoresistance. Once this occurs many patients succumb to the advanced stages of PC.

Only about half of all patients respond to docetaxel chemotherapy (Mahon et al. 2011), and although the mechanisms which lead to docetaxel resistance remain unclear there are many theories currently in existence. A large variety of

factors may play a role in chemoresistance, such as epigenetic alterations, poor absorption of the drug, tumour size, and decreased blood flow due to tumour vasculature (Gottesman et al. 2002; Jain 2001). In terms of cellular pathways that may explain docetaxel resistance in CRPC, possibilities include altered apoptosis mechanisms, changes in tubulin isotype, and mutations in signalling pathways which regulate growth (Mahon et al. 2011). But of particular interest to us is the family of ATP-binding cassette (ABC) transporters also known as multidrug resistance proteins (Crea et al. 2011).

The ABC superfamily consists of 49 different transporters that can be divided into 7 separate sub-families based on their domain organization and sequence homology (Hlavac et al. 2013; Dean et al. 2001). They are often found lining cells of the biliary tract, liver, intestine, and the blood-brain barrier, and play a natural part in detoxification (Bradshaw & Arceci 1998). By binding to compounds and releasing them back out of the cell through an ATP-dependent mechanism, these pumps can reduce intracellular drug accumulation and render cytotoxic agents ineffective (Hyde et al. 1990). Within this family, many members have been identified as contributing to the chemoresistance of cancers like breast, lung, prostate, and pancreas. Three of the most commonly studied members include P-glycoprotein (P-gp/ABCB1), ATP-Binding Cassette sub-family C member 1 (ABCC1), and Breast Cancer Resistance Protein (BCRP/ABCG2). These transporters have been shown to enable the efflux of

numerous anti-cancer agents following treatment, allowing for chemoresistance and cancer cell survival (Sparreboom et al. 2003; Hinoshita et al. 2000).

Another member, ABCC2, is most abundantly found in the bile canicular membrane of the liver, but is also located in other areas of the body such as the small intestine, kidney, and brain (Gottesman et al. 2002; Huisman et al. 2005). It consists of 17 transmembrane domains with one ATP-binding site in its interior and another on the carboxyl terminus. For transport to occur, two separate ATP hydrolysis events are required for one molecule of substrate to be exported outside of the cell (Gottesman et al. 2002). Given its substrate specificity and main localization within the tubules of the liver, intestine and kidney, it is apparent that ABCC2 plays a large role in systemic detoxification (Chan et al. 2004). It has been found to localize to the apical side of polarized cells, which is also consistent with its bodily function. Absence of ABCC2 from the canicular membrane as a result of genetic mutation leads to Dubin-Johnson syndrome, characterized by a defect in the ability to transport anionic conjugates from hepatocytes into the bile (Cui et al. 1999; Kartenbeck et al. 1996). Due to its sequence homology with related family members, investigations into ABCC2 have demonstrated its ability to confer resistance to doxorubicin, cisplatin, paclitaxel, vincristine, and etoposide in nasopharyngeal, hepatocellular, and ovarian cancer cell lines. By utilizing anti-sense and RNAi constructs designed against the ABCC2 transcript, researchers have reversed chemoresistance and

illustrated a decrease in mRNA and protein levels as well as an increase in cellular retention of the various agents (Huesker et al. 2002; Xie et al. 2008; Materna et al. 2006). Among many family members, ABCC2 gene expression was revealed to be upregulated in PC versus normal prostate tissues (Karatas et al. 2016). Interestingly, ABCC2 was found to efflux docetaxel as well as other taxanes in an ABCC2 overexpression MDCKII cell line (Huisman et al. 2005). Taken together, it is possible that ABCC2 contributes to CRPCs ability to resist docetaxel chemotherapy.

We report here the upregulation of ABCC2 expression in prostate cancer stem-like cells (PCSLCs) derived from the mCRPC cell line DU145. Utilized as a suitable *in vitro* model for advanced CRPC progression, our PCSLCs exhibited increased resistance to docetaxel treatment *in vitro* and *in vivo*, and we have attempted to elucidate ABCC2s contribution to this chemoresistance. Observations made here may be extended to patient CRPC cases to help circumvent docetaxel chemoresistance and improve chemotherapy strategies in clinical settings.

RESULTS

ABCC2 expression is increased in DU145 PCSLCs

We have previously isolated and characterized a sub-population of prostate cancer stem-like cells (PCSLCs) from the DU145 PC cell line with sphere-propagating capabilities, stem-like properties, and increased tumourigenicity (Rybak et al. 2011). Affymetrix microarray analysis comparing our DU145 PCSLCs versus parental DU145s revealed a 9.1 fold increase of mRNA levels in the stem-like population. Both Western blotting and immunocytochemistry were performed to confirm protein expression. As expected of an ABC transporter, distinct staining was visualized along the outer membrane of cells (Figure 5.1).

ABCC2 associates with primary prostate cancer progression

To help determine whether ABCC2 associates with the progression of primary prostate cancer, tissues can be divided into low Gleason Score (6-7) and high Gleason Score (8-10) cases. Here we examined a small patient cohort of 13 low Gleason and 12 high Gleason prostate cancer tissues for ABCC2 expression (Table 5.1). The ABCC2 protein was more clearly detected in high Gleason cancers, and based on our analysis and final HScores the association with advanced cases is significant (Figure 5.2).

DU145 PCSLCs are more resistant to docetaxel than parental DU145s (non-PCSLCs)

We have previously demonstrated increased resistance to docetaxel in our DU145 PCSLCs compared to parental DU145s (Yan & Tang 2014), grown in serum-containing conditions where stemness is retained for up to 4 passages (Rybak et al. 2011). When dosing between 0-15nM for 6 hours, a significant difference between the two lines could be observed at a final docetaxel concentration of 10nM and 15nM (Yan & Tang 2014). Based on this data, a final concentration of 10nM docetaxel was used for the remaining *in vitro* experiments. To examine this chemoresistance further, subcutaneous xenograft tumours were generated for both lines in NOD/SCID mice and treated with docetaxel (see Materials and Methods). While weekly treatment was effective at reducing tumour growth of DU145 monolayer-derived xenografts (Figure 5.3A), DU145 PCSLC-derived xenografts continued to increase in volume (Figure 5.3B). It is also important to differentiate the proliferative rates of these tumours. When examining docetaxel treated monolayer and PCSLC-derived xenografts side by side as fold change in tumour volumes (Figure 5.3C), it becomes evident that our PCSLCs are also more resistant to docetaxel *in vivo*. Although monolayer-derived xenografts were able to reach 2-fold their initial size with treatment, PCSLC-derived xenografts reached 5-fold their initial volume. Taken together with our *in*

vitro results, DU145 PCSLCs display increased resistance to docetaxel-mediated cytotoxity.

Although there are hundreds of differentially expressed genes between the two DU145 populations, ABCC2 is amongst the top candidates with the greatest change in expression and provides a logical explanation for resistance to docetaxel administration. The presence or absence of ABCC2 in the xenograft tumours was confirmed via IHC staining (Figure 5.4A). In DU145 monolayer-derived xenografts, only 1 out of 9 tissues stained positive for ABCC2. This finding may be a false artifact from staining, but also suggests possible upregulation acquired for chemoresistance. It may also indicate a cluster of stem-like cells induced in such environmental conditions. As for the DU145 PCSLC-derived xenografts, there was a consistent trend where all 9 of the tumours stained positive for ABCC2 (both DMSO and docetaxel treated groups)(Figure 5.4B). This indicates expression may not be induced by docetaxel administration, but rather is initially highly expressed. As such, expression of ABCC2 may prime cancer cells for chemoresistance. Interestingly, positive cells could be visualized in distinct clusters throughout the tissue, supporting the notion that our DU145 PCSLCs represent a stem cell population. When grown *in vivo*, they may establish stem cell niches, while producing $ABCC2^-$ differentiated progenitors which constitute the bulk of the tumour.

Knockdown of ABCC2 does not sensitize DU145 PCSLCs to Docetaxel *in vitro*

To evaluate whether ABCC2 contributes to docetaxel chemoresistance in our DU145 PCSLCs, we generated a knockdown line using a shABCC2 lentiviral vector (along with a shCTRL line) (Figure 5.5A). To ensure stemness was not affected following successful infection, sphere formation capacities were determined for the DU145 shCTRL and shABCC2 PCSLCs (Figure 5.5B).

Individualized PCSLCs were treated with 10nM docetaxel for 2, 4, or 6 hour time points in SFM conditions, and left to form spheres in fresh media. However, despite increased docetaxel resistance in our DU145 PCSLCs (*in vitro* and *in vivo*) and ABCC2s association with advanced cases of primary prostate cancer, we could not demonstrate re-sensitization to docetaxel treatment upon ABCC2 knockdown (Figure 5.5C). On the contrary, shABCC2 PCSLCs displayed slightly higher sphere numbers following treatment, although these differences were not significant at any time point. Based on these findings, it is possible that ABCC2 is not responsible for chemoresistance to docetaxel in our DU145 PCSLCs.

We have previously shown that DU145 PCSLCs can be proliferated as adherent cells in 10% FBS media conditions and maintain the same level of stemness until passage four (Rybak et al. 2011). To examine DU145 shABCC2 PCSLCs in this format of cell organization, cells were treated in 10% serum

conditions. In comparison to the shCTRL line, there was again no difference between the percentages of surviving cells (Figure 5.5D). These findings further support that ABCC2 may not confer chemoresistance to docetaxel in PC. We also attempted this experiment in A549 cells, an adherent lung carcinoma line obtained from a 58 year old Caucasian male in 1972 (Lieber et al. 1976). Previous pilot studies indicated an increased resistance to docetaxel treatment in A549s compared to DU145 monolayers, and this characteristic is supported by a study examining docetaxel resistance in lung carcinoma cell lines (Feng et al. 2012). A549s also exhibit high protein expression of ABCC2, so we determined whether knockdown would sensitize these cells to docetaxel cytotoxicity. If true, then the ability to confer chemoresistance could be extended to our DU145 PCSLCs and PC. Knockdown of ABCC2 was conducted the same way (Supplementary Figure 5.1A), and cells were dosed for 2, 4, or 6 hours with 10nM docetaxel. However, again we saw almost no difference in cell survival between the A549 shCTRL and shABCC2 cell lines (Supplementary Figure 5.1B). From these results it could be concluded that ABCC2 does not play an important role in docetaxel chemoresistance in DU145s or A549s, *in vitro*.

Knockdown of ABCC2 may not sensitize DU145 PCSLCs to Docetaxel *in vivo*

As mentioned above, DU145 PCSLC-derived xenografts exhibited an increased resistance to docetaxel treatment in comparison to DU145 monolayer tumours (Figure 5.3). This was not surprising as CSCs are widely regarded as possessing chemoresistant attributes. Although the *in vitro* data suggests that ABCC2 is not responsible for docetaxel-related chemoresistance, it was necessary to examine DU145 shCTRL and shABCC2 PCSLCs *in vivo*.

Following the same experimental design as before (Figure 5.3), we generated subcutaneous xenograft tumours using the two PCSLC lines. We observed that weekly docetaxel treatments did delay tumour growth for both groups in comparison to the DMSO vehicle control, but xenograft volumes continued to increase each week (Figures 5.6A and 5.6B). Assessing the shCTRL and shABCC2 figures side by side, it is tempting to conclude that knockdown of ABCC2 does in fact sensitize the xenografts to docetaxel treatment as tumour volumes did not increase as drastically in the shABCC2 group. However, when analyzing the weekly proliferation rates as either tumour volume or fold change in tumour volume (Figures 5.6C and 5.6D), none of the differences are statistically significant. Fold change in tumour size is valid in examining proliferation as all tumours were first treated at the same volume (~200mm^3). Although difficult to control, the large p-values are likely due to individual variations in tumour growth. Looking more closely at the differences in fold change of tumours treated

with either docetaxel or DMSO control after 3 weeks (Figure 5.6E), these observations are statistically significant providing evidence of docetaxel's cytotoxicity in PCSLCs and/or their progenitors. However, knockdown of ABCC2 does not appear to sensitize tumours to treatment, as seen at weeks 3 or 5 (Figures 5.6E and 5.6F). Taken together, this work *in vivo* agrees with the *in vitro* findings that ABCC2 is not important for docetaxel resistance in PCSLCs. However this conclusion should be taken with caution as the animal data at first glance appears to contradict this finding, if not for the inter-individual variations in tumour growth. Further experiments will be required before this work can be submitted for publication.

DISCUSSION

ABCC2 expression and its mechanistic function have not been well reported for PC in the literature, in part to the development of a newer class of taxanes with greater efficacy in delaying tumour growth. Cabazitaxel possesses similar tubulin-binding characteristics to docetaxel (Bono et al. 2010) but was synthetically designed to reduce its substrate affinity to ABC transporters, reducing the need to examine drug-efflux mechanisms. It is also able to penetrate the blood-brain barrier much more than the classical taxanes, demonstrated greater intratumoural accumulation, and specifically alters separate molecular pathways (Mita et al. 2009; De Leeuw et al. 2015; de Morrée et al. 2016), making

it a good candidate for multiple cancer types. *In vitro* studies demonstrated anti-cancer effects against models of paclitaxel and docetaxel resistance, and clinical trials revealed greater overall survival for patients with CRPC (some with acquired docetaxel resistance) (Mita et al. 2009; Bono et al. 2010).

Despite this, cabazitaxel is typically used as a second line of defense following failure of docetaxel treatment, making research into drug-efflux mechanisms still valid to determine the cause of docetaxel resistance. The ABC family of transporters is known to contribute to the development of chemoresistance in many cancers. Three of these members, ABCB1, ABCC1, and ABCG2, have been well established as major determinants of drug resistance. Studies have demonstrated the expression of ABCB1 in the gastrointestinal tract which may eliminate docetaxel before reaching systemic circulation, and expression within PC cells themselves allows for docetaxel chemoresistance and survival (Ganju et al. 2014; Kato et al. 2015; Abdulla & Kapoor 2011; Van Zuylen et al. 2000).

Here we provide limited evidence of ABCC2s contribution to docetaxel resistance in PC. We have identified increased expression in our DU145 PCSLCs over the parental population specifically along the cell membrane, which correlates well with a CSCs ability to evade cytotoxic effects. Although docetaxel has been shown to be a substrate for ABCB1, our microarray analysis did not identify this family member as being significantly upregulated in our PCSLCs. In

a small patient cohort of tissues we were able to demonstrate a connection between ABCC2 protein expression and advanced primary PC cases. To our knowledge, there has yet to be any evidence to establish ABCC2s contribution to chemoresistance in PC despite its presence in prostate carcinomas. As high grade cancers possess a greater propensity to metastasize, our observations suggest a possible correlation with ABCC2 and metastasis. Aggressive cancers may upregulate ABCC2 expression to evade chemotherapeutic treatment and continue their progression. Although not attempted here, it would be intriguing to determine whether ABCC2 expression is also upregulated in response to docetaxel treatment by examining docetaxel resistant PC tissues. Notably though, examination in recurrent vs non-recurrent PC tissues revealed no difference in gene expression (Karatas et al. 2016).

Both our *in vitro* and *in vivo* data indicate that the DU145 PCSLC population is able to resist docetaxel treatment much better than the parental DU145s. This is to be expected of a CSC population, but the precise mechanism must be elucidated so enhanced therapeutic methods can be developed. Attempts at ABCC2 overexpression in the DU145 parental cells failed. The ABCC2 cDNA was successfully sub-cloned from the provided vector (pCR-XL-TOPO, Open Biosystems) into pcDNA3.0-Nflag so that the final translated product could be flagged at the N-terminus. This would have facilitated future cell sorting if needed and detection of ectopic expression. Subsequent sub-cloning of this sequence into

the retroviral vector pBABE-puro was also successful. For infection, 293T cells were used for retroviral packaging where increased expression of ABCC2 was confirmed via Western blotting. However, overexpression could not be detected following infection and selection of DU145 monolayer cells (Supplementary Figure 5.2). Survival of these cells after antibiotic selection suggests that the large Nflag-ABCC2 sequence (~5kb) could not be integrated into the retroviral vector.

Knockdown of ABCC2 in DU145 PCSLCs (and also A549s) did not reveal any changes in sensitivity to docetaxel *in vitro*. In fact, shABCC2 PCSLCs actually exhibited slightly increased (although not significant) sphere formation following treatment. It is possible that the absence of ABCC2 stimulated the activation of other chemoresistance mechanisms. In treating the DU145 shABCC2 PCSLC-derived subcutaneous xenografts, at first glance there does appear to be delays in tumour growth during treatment, indicative of re-sensitization. However, because of individual animal variations in xenograft growth rates, these results were not statistically significant when compared to shCTRL xenografts. One method to overcome this variability would be the elimination of endogenous circulating murine testosterone by surgical castration, and subcutaneous implant of a time-release (slow absorption) hormone pellet. This strategy, similar to one taken with breast cancer xenografts (Harrell et al. 2006; Sartorius et al. 2003; Yang et al. 2013), would allow for a more uniform supply of androgen available for tumour growth. This methodology has been used

in studying patient derived transurethral resections of prostates (TURP) from CRPC patients in NOD/SCID mice. Co-implantation of a testosterone pellet stimulated xenograft growth, implying the tissues were androgen responsive despite being castration-resistant (Lawrence et al. 2015). This approach may also work for DU145s, which are a castration resistant cell line (Zhang et al. 1996). Future attempts may also need to involve a larger cohort in order to achieve statistically significant findings.

The possibility of additional docetaxel resistance mechanisms in our PCSLCs cannot be ruled out. This includes alterations in apoptosis pathways, tubulin isotypes, and signalling pathways involved with growth and proliferation. One further option is the presence of other ABC transporter family members such as ABCB1 which are also able to bind docetaxel. Although we did not detect any significantly upregulated members in our initial microarray analysis which would account for the increased resistance in our PCSLCs, it is feasible that there could be pre-existing transporters allowing for innate resistance in the DU145 PC line. This is suggested by our *in vivo* results which demonstrated that DU145 monolayer-derived xenografts continued to grow during docetaxel treatment, albeit slowly. Unfortunately, expression of additional ABC members in the parental line has not yet been thoroughly examined. An intriguing study by van Waterschoot and colleagues investigated the *in vivo* functionality of ABCC2 in a model organism. Using $ABCC2^{-/-}$ mice, the authors were able to demonstrate that

upon either oral or intravenous administration, the bioavailability of docetaxel was no different than in wild-type mice. These findings correspond well with our own xenograft study using DU145 shABCC2 PCSLCs. Further experimentation by additionally knocking out ABCB1 and CYP3A (involved in docetaxel metabolism (Baker et al. 2006)) together with ABCC2 revealed a significant systemic increase in docetaxel exposure compared to double knockout mice ($Cyp3a^{-/-}$/$Abcb1^{-/-}$) (Van Waterschoot et al. 2010). These observations suggest that rather than being an independent factor for chemoresistance, ABCC2 operates in concert with other proteins involved in docetaxel metabolism creating an additive effect. Studies also show that ABCC2 activity can be upregulated by chemical stimulation of agents co-administered during chemotherapy rather than only by increased gene expression (Huisman et al. 2005). Based on these findings it appears the determination of ABCC2s contribution to docetaxel resistance requires a more complex and widespread experimental approach in order to elucidate any chemoresistant attributes in PC xenografts. It may very well be that factors such as ABC transporters, drug metabolism, and intratumour accumulation all operate collectively to facilitate docetaxel chemoresistance in CRPC.

MATERIALS AND METHODS

Cell culture and generation of DU145 spheres (PCSLCs)

DU145 and A549 cells were purchased from American Type Culture Collection (ATCC), and cultured in MEM (DU145) and RPMI-1640 (A549) media supplemented with 10% FBS and 1% Penicillin-Streptomycin (Thermo Fisher Scientific). DU145 spheres were generated and cultured according to our published conditions (Rybak et al. 2011). Briefly, DU145 monolayer cells (non-PCSLCs) were individualized and seeded at a density of 5,000 cells/ml in serum-free media (3:1 DMEM/F12 mixture) (Thermo Fisher Scientific) containing 0.4% bovine serum albumin (BSA) (Bioshop Canada Inc.) supplemented with 0.2x concentration of B27 minus Vitamin A (Thermo Fisher Scientific) and 10ng/ml EGF (Sigma Aldrich), in T75 flasks. Typical spheres were formed in 10 to 12 days.

Sphere formation capacity

Individualized DU145 PCSLCs were seeded in 96-well plates (1 cell/well) in SFM conditions. Seeding was visually confirmed under the microscope. Cells were given 10-12 days to grow, and the number of intact spheres formed was counted. Replicates were carried out in duplicate.

Knockdown of ABCC2 in DU145 PCSLCs and A549s

Lentiviral particles were packaged in 293T cells using shCTRL or shABCC2 lentiviral plasmids (Santa Cruz). Briefly, gag-pol, rev, and envelope expressing vectors (Stratagene) were co-transfected with the short hairpin plasmids. Virus containing media was harvested 48 hours later, concentrated by centrifugation at 20000rpm for 2 hours, and used to infect A549s or individualized DU145 PCSLCs.

Dosing of cells *in vitro*

For treatment of DU145 PCSLCs in SFM media conditions, individualized cells were seeded at a density of 5000 cells/ml. Following immediate treatment with docetaxel or DMSO vehicle control for the stated time points, cells were washed and allowed to grow for 11 days in fresh SFM. The number of spheres formed was determined under the microscope.

For treatment of adhered DU145 PCSLCs (remonolayer), individualized cells were seeded at 30000 cells/well in 6-well plates, and given 48 hours to fully attach. Cells were then treated with docetaxel or DMSO vehicle control for the stated time points, washed, and allowed to grow for 4 days in fresh 10% FBS media. Cells were fixed with a 2% formaldehyde solution and stained with crystal

violet before quantifying. A549 treatment was similarly carried out, but cells were only given 24 hours to fully adhere.

Collection of primary prostate cancer tissues

Prostate biopsies and radical prostatectomy tissues were obtained at St. Joseph's Healthcare Hamilton in Hamilton, Ontario, Canada under approval from the local Research Ethics Board (REB# 11-3472) and with patient consent. Additional tissues were obtained from the Ontario Tumour Bank, which is funded by the Ontario Institute for Cancer Research.

Preparation of DU145 PCSLCs for Immunocytochemistry

DU145 spheres were washed and fixed with 10% neutral buffered formalin for two hours at room temperature. After washing, spheres were then set in 1% agar and paraffin embedded. Sections were stained as per the IHC method below.

Immunohistochemistry (IHC)

IHC was performed on 25 paraffin embedded and serially cut prostate cancer tissues, and on human xenograft tissues. Slides were deparaffinized in xylene and cleared in an ethanol series. Antigen retrieval was performed in a food steamer for 20 minutes using sodium citrate buffer (pH = 6.0). Tissues were blocked for 1 hour in PBS containing 1% BSA and 10% normal goat serum (Vector Laboratories). ABCC2 antibody (1:400, Enzo Life Sciences) was incubated overnight at 4°C. Secondary antibody biotinylated goat anti-mouse IgG and Vector ABC reagent (Vector Laboratories) were incubated according to the manufacturer's instructions. TSA^{TM} Biotin System (Perkin Elmer) was used as per manufacturer's instructions for signal amplification. Secondary antibody only was used as negative control. Washes were performed with PBS. Chromogenic reaction was carried out with diaminobenzidine (Vector Laboratories), and slides were counterstained with haemotoxylin (Sigma Aldrich). Image analysis was performed using ImageScope software (Leica Microsystems Inc.). Staining intensity values derived from ImageScope were converted to an HScore using the formula [HScore = (% Positive) x (intensity) + 1]. The HScore was normalized through background subtraction and averaged amongst multiple images per tissue sample.

Western blot analysis

Cells were lysed in a buffer containing 20mM Tris (pH 7.4), 150mM NaCl, 1mM EDTA, 1mM EGTA, 1% Triton X-100, 25mM sodium pyrophosphate, 1mM NaF, 1mM β-glycerophosphate, 0.1mM sodium orthovanadate, 1mM PMSF, 2μg/ml leupeptin and 10μg/ml aprotinin. 50 or 100μg of whole cell lysate was separated on SDS-PAGE gel, and transferred onto Hybond ECL nitrocellulose membranes (Amersham), followed by blocking with 5% skim milk at room temperature for one hour. Primary antibodies were incubated overnight at 4^{o}C with agitation, and secondary antibodies incubated for one hour at room temperature. Signals were then developed (ECL Western Blotting Kit, Amersham; Immobilon ECL Reagent, Millipore). Primary antibodies: anti-ABCC2 1:50 (Santa Cruz) and anti-Actin 1:1000 (Santa Cruz).

Xenograft tumour formation and docetaxel treatment

DU145 monolayer (non-PCSLCs) and sphere (PCSLCs) cells were resuspended in 0.1 ml MEM/Matrigel mixture (BD) (1:1 volume), followed by subcutaneous implantation into the flanks of 8 week-old male NOD/SCID mice (The Jackson Laboratory). 10^6 DU145 monolayer cells and 10^4 DU145 PCSLCs were implanted, based on our previous report that DU145 PCSLCs display a 100-fold higher capacity to form xenografts (Rybak et al. 2011). Tumours were

assessed through observation and palpation, and tumour growth was measured weekly using calipers. Tumour volume was determined using the formula $V = L \times W^2 \times 0.52$. Once tumours reached a volume of at least $100mm^3$, mice were treated with either DMSO control (Sigma) or Docetaxel (Santa Cruz) at 10mg/kg once a week for three weeks by intraperitoneal injection. After a week of recovery, treatment cycle was repeated until tumours reached a volume $\geq 1000\ mm^3$, at which point animals were sacrificed. All animal work was carried out according to experimental protocols approved by the McMaster University Animal Research Ethics Board.

TABLES

Table 5.1. Patient information and average IHC scores

Patient #	Age	Gleason Score	Average Score
1	52	3+3	-0.73 ± 0.40
2	48	3+3	36.73
3	53	3+3	35.22
4	76	3+3	28.16
5	57	3+3	27.49
6	63	3+4	11.63 ± 10.40
7	62	3+4	8.79 ± 8.33
8	67	3+4	62.60 ± 10.84
9	52	3+4	32.23 ± 4.43
10	-	3+4	24.82 ± 10.97
11	78	3+4	49.56 ± 21.55
12	70	3+4	11.80
13	-	4+3	71.14 ± 10.15
14	60	4+4	110.21 ± 35.07
15	68	4+4	19.55 ± 22.96
16	56	4+4	67.88 ± 6.41
17	58	4+4	83.96 ± 8.36
18	77	4+5	121.26 ± 2.99
19	54	4+5	90.2 ± 27.64
20	81	4+5	98.75 ± 10.55
21	55	4+5	95.12 ± 31.39
22	68	5+5	34.18 ± 19.02
23	75	5+5	84.69 ± 10.14
24	91	5+5	40.36 ± 9.46
25	86	5+5	11.39 ± 8.15

FIGURES

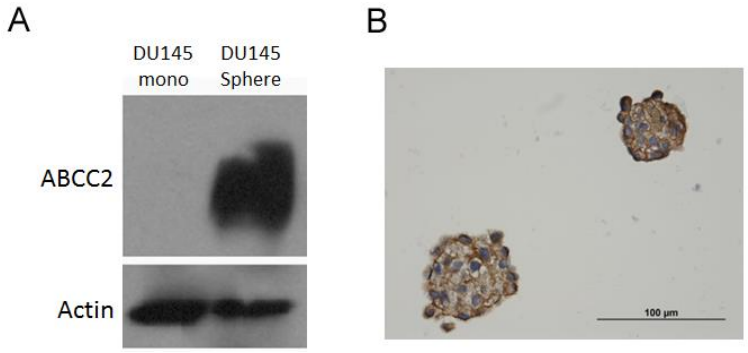

Figure 5.1. ABCC2 expression is higher in DU145 spheres (PCSLCs). **(A)** Confirmation of ABCC2 expression by Western blot in DU145 monolayer and sphere cells. **(B)** ICC staining for ABCC2 in DU145 spheres demonstrates cell membrane-specific protein expression. Scale bar represents 100µm.

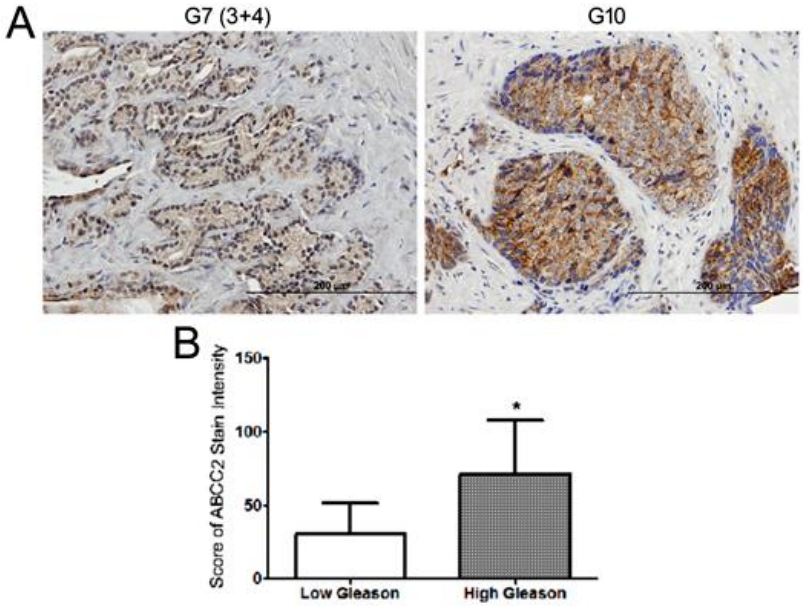

Figure 5.2. ABCC2 expression associates with primary prostate cancer progression. **(A)** IHC was performed on 13 low Gleason score (GS 6-7) and 12 high Gleason score (GS 8-10) primary prostate cancer tissues. Representative images of low and high grade staining are shown here. Scale bars represent 200µm. **(B)** ABCC2 protein expression is significantly increased in high grade primary prostate cancers. See Table 5.1 for the full list of patient information. $p < 0.05$ by Student's t-test.

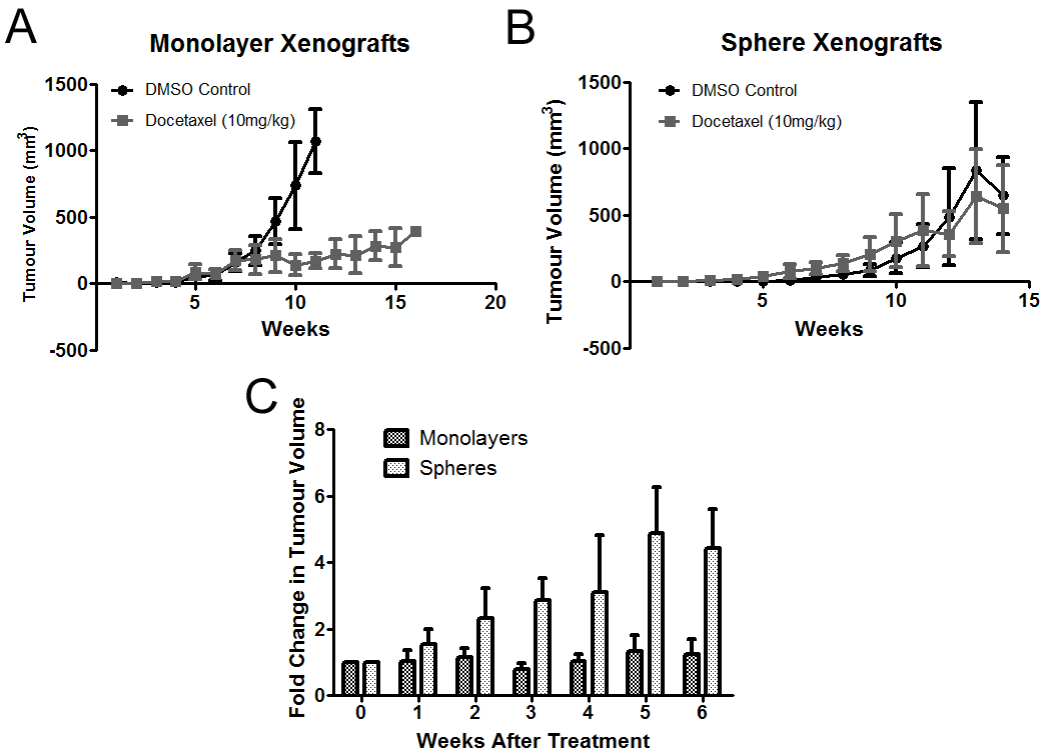

Figure 5.3. Generation of DU145 monolayer and sphere (PCSLC) subcutaneous xenografts, and treatment with Docetaxel. **(A)** Tumour volumes for DU145 monolayer-derived xenografts treated with docetaxel at 10mg/kg, or DMSO vehicle control. 4-5 mice per group. $p < 0.05$ by Two-way ANOVA. **(B)** Tumour volumes for DU145 sphere-derived xenografts treated with docetaxel at 10mg/kg, or DMSO vehicle control. 3-5 mice per group. $p > 0.05$ by Two-way ANOVA. **(C)** Tumour volumes of docetaxel treated DU145 monolayer and PCSLC-derived xenografts presented as fold change from initial week of treatment. $p < 0.05$ by Two-way ANOVA.

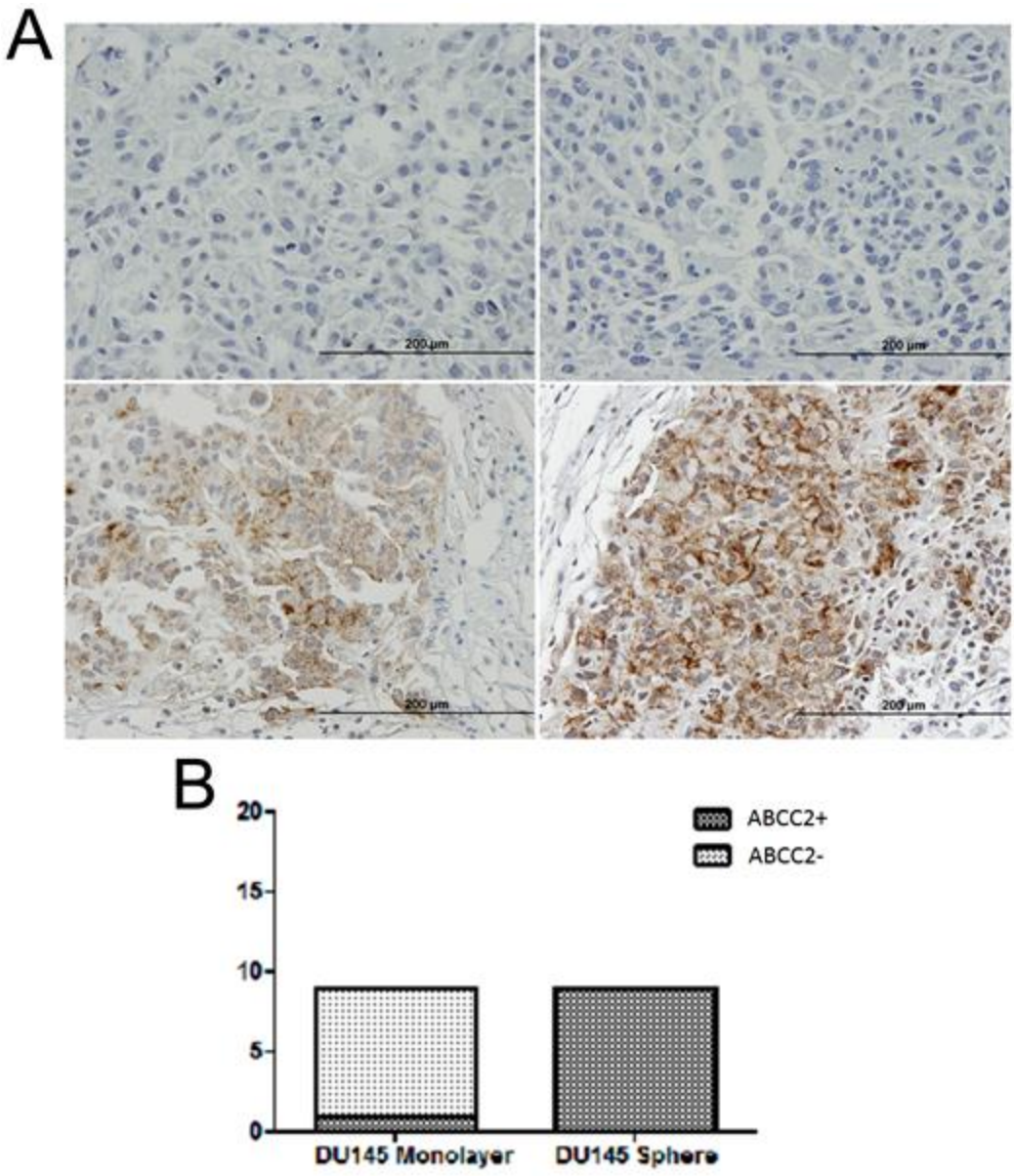

Figure 5.4. ABCC2 expression in DU145 monolayer and sphere-derived xenografts. (A) Representative IHC staining for ABCC2 in DU145 monolayer-derived (top) and DU145 sphere-derived (bottom) xenografts. Scale bars represent 200µm. **(B)** Total number of $ABCC2^{+}$ tumours in 9 xenograft tissues per cell line. $p = 0.0001$ by Chi-squared test.

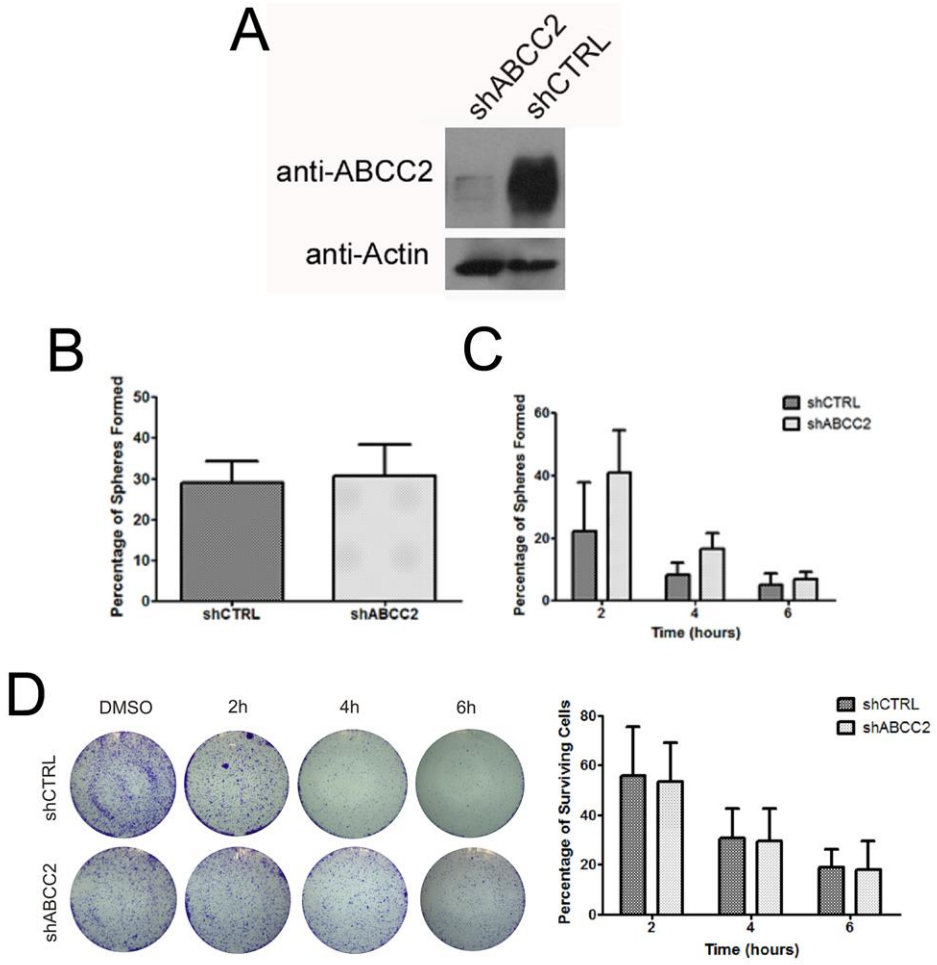

Figure 5.5. Generation of DU145 shCTRL and shABCC2 spheres (PCSLCs), and treatment with 10nM Docetaxel. (A) Knockdown of ABCC2 was carried out using lentiviral plasmids. Confirmation was performed by Western blotting, and Actin was used as loading control. **(B)** Sphere formation capacity was determined for each cell line. Percentage of spheres formed is in comparison to the total number of cells seeded. $p > 0.05$ by Student's t-test. **(C)** 10nM docetaxel dosing was performed at 2, 4, and 6 hour time points along with a 6 hour vehicle control. Percentage of spheres formed was determined in comparison to the DMSO control. Cells were dosed individually immediately after passaging in SFM. Spheres were counted after 11 days. $p > 0.05$ by Student's t-test for all time points. **(D)** DU145 shCTRL and shABCC2 spheres were seeded in 10% FBS media conditions. 10nM docetaxel dosing was performed at 2, 4, and 6 hour time points along with a 6 hour vehicle control. Percentage of surviving remonolayer spheres was determined by quantifying the amount of crystal violet stain in comparison to the DMSO control. $p > 0.05$ by Student's t-test for all time points.

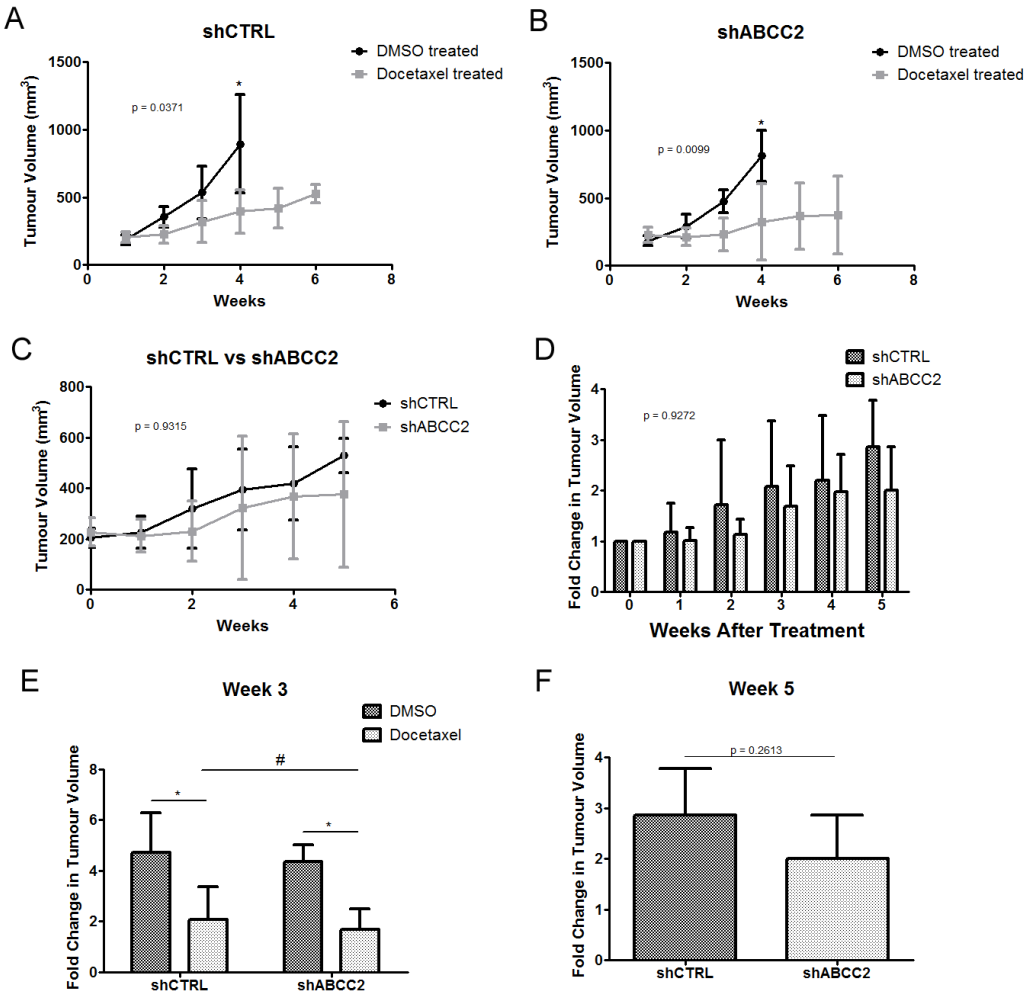

Figure 5.6. Generation of DU145 shCTRL and shABCC2 sphere (PCSLC) subcutaneous xenograft tumours, and treatment with Docetaxel. Weekly measurements on the x-axis start from when the first injection was given, at a tumour volume of 100-200mm^3. **(A**) Weekly tumour volumes of the DU145 shCTRL sphere-derived xenografts treated with either docetaxel (10mg/kg) or vehicle control. The interaction is significant by Two-way ANOVA, p = 0.0371. With a docetaxel-treated outlier included, p = 0.0137. *p < 0.05. **(B)** Weekly tumour volumes of the DU145 shABCC2 sphere-derived xenografts treated with either docetaxel (10mg/kg) or vehicle control. The interaction is significant by Two-way ANOVA, p = 0.0099. With a DMSO-treated outlier included, p = 0.0910. *p < 0.05. (**C**) Comparison of the shCTRL and shABCC2-derived docetaxel treated tumours. The interaction is not significant by Two-way

ANOVA, p = 0.9315. **(D)** Fold change in tumour volumes of all xenografts compared to tumour size before docetaxel treatment (Week 0). The interaction is not significant by Two-way ANOVA, p = 0.9272. **(E)** Tumour volumes of shCTRL and shABCC2 xenografts after 3 weeks of treatment with either DMSO or docetaxel. *p < 0.05 by Student's t-test. #p > 0.05 by Student's t-test. **(F)** Tumour volumes of shCTRL and shABCC2 xenografts after 5 weeks of docetaxel treatment. p > 0.05 by Student's t-test.

SUPPLEMENTARY FIGURES

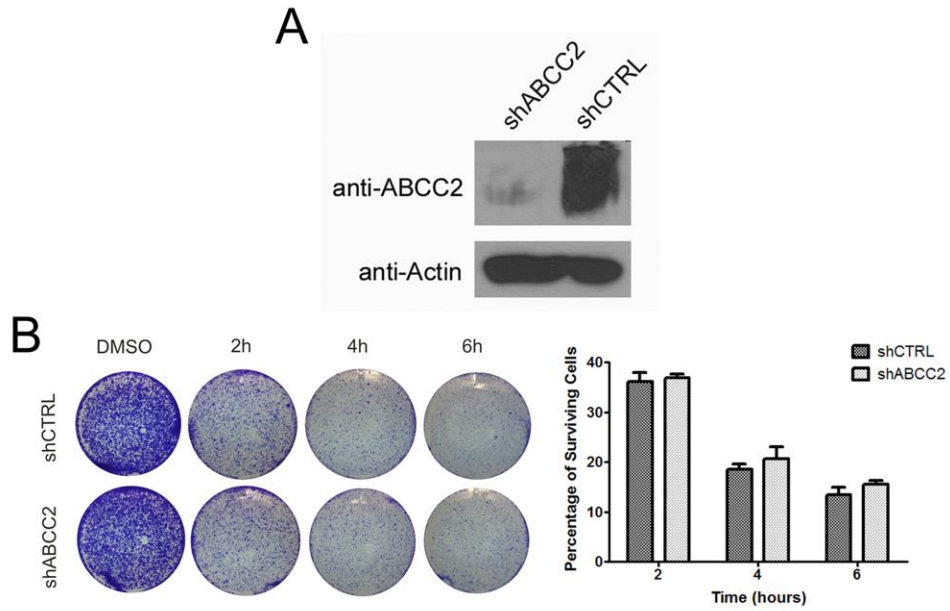

Supplementary Figure 5.1. Generation of A549 shCTRL and shABCC2 cells, and treatment with 10nM Docetaxel. **(A)** Knockdown of ABCC2 was carried out using lentiviral plasmids. Confirmation was performed by Western blotting, and Actin was used as a loading control. **(B)** 10nM docetaxel dosing was done at 2, 4, and 6 hour time points along with a 6 hour vehicle control. Percentage of surviving cells was determined by quantifying the amount of crystal violet stain in comparison to the DMSO control. $p > 0.05$ by Student's t-test for all time points.

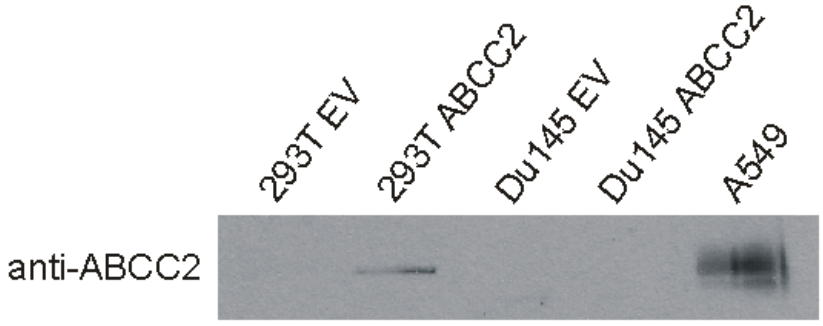

Supplementary Figure 5.2. **Overexpression of ABCC2 in DU145 monolayers**. Attempts were made to sub-clone an Nflag-tagged ABCC2 cDNA sequence into the pBABE-puro retroviral vector. 293T cells were used for retroviral packaging. A549 cell lysate acts as the positive control.

CHAPTER SIX

DISCUSSION AND CLINICAL RELEVANCE

DISCUSSION

6.1 - Prostate Cancer Stem Cells are a Source of Metastatic Prostate Cancer

With growing acceptance of the hierarchical (or CSC) model as an explanation for the heterogeneity of PC tissues, an expanding amount of research supports the notion of a small population of stem-like cells as being a major source of tumour initiation and regeneration (Reya et al. 2001; O'Brien et al. 2009; Dick 2009). Under this model it should be possible to separate tumour initiating from non-tumour initiating cell populations based on either their cell marker profiles or unique characteristics. Altered biological mechanisms may induce expression of distinct cell surface markers, while stem-like traits such as self-renewal, differentiation potential, proliferative capacity, and anti-apoptotic processes could be used for isolation and identification of CSCs (Jordan et al. 2006). Since the discovery of single-cell derived mouse myelomas composed of heterogeneous cell types almost 50 years ago (Park et al. 1971), many tumour initiating populations have been isolated. The first to be studied were of acute myeloid leukemia (Bonnet & Dick 1997), and now numerous possible CSC populations have been discovered in solid tumours including brain, breast, colon, pancreas, prostate, lung, liver, ovarian, and colorectal (Choi et al. 2014; Galli et al. 2004; Hermann et al. 2007; Curtis et al. 2010; Liao et al. 2014; M. F. Shi et al. 2010; Yeung et al. 2010; Brien et al. 2007; Li et al. 2007; Ricci-Vitiani et al. 2007; Singh et al. 2003; Al-Hajj et al. 2003). While similar to normal stem cells in

most aspects, the key features of CSCs is their high plasticity, ability to evade cytotoxic therapies, and regeneration of the bulk tumour, resulting in cancer relapse and metastasis. Ideally, therapeutic treatments should target this small population of stem-like cells rather than the bulk tumour to completely eradicate disease.

Persistent AR signalling despite ADT can be detrimental as it leads to CRPC, the cause of most PC-related deaths. There are several mechanisms which contribute to the elevation of AR activation and transcription of AR-responsive genes. Studies have shown that CRPC tissues display intratumoural retention of androgens, and higher expression of genes which code for androgen synthesizing enzymes, allowing for stimulation of AR (Gregory et al. 2001; Mohler et al. 2004; Stanbrough et al. 2006; Montgomery et al. 2008; Holzbeierlein et al. 2004). Stabilization of AR in recurrent disease may also permit transcriptional activation of targets in response to low circulating levels of androgen following ADT. Additionally, hypersensitivity can also be mediated by AR gene amplification or mutations in the ligand binding domain which can promote binding and activation by progesterone or first-generation AR antagonists (flutamide, bicalutamide, nilutamide) (Hobisch et al. 1995; Visakorpi et al. 1995; Newmark et al. 1992; Taplin et al. 1995; Chen et al. 2004). As observed in multiple studies using PC cell lines, phosphorylation by tyrosine kinases also upregulates AR activity. Two kinases Ack1 and Src have been shown to phosphorylate at Tyr-267, and are

induced upstream by HER2 (a tyrosine kinase in the same family as EGFR). Inhibition of this pathway at several points can inhibit AR recruitment and transcription of AR-responsive genes, resulting in slower cell proliferation and decreased tumour growth. AR activity can also be stimulated by phosphorylation at Tyr-534 by EGF and IL-6 (Yeh et al. 1999; Mahajan et al. 2007; Mellinghoff et al. 2004; Liu et al. 2010; Xu et al. 2009). Additionally, the AKT pathway important in cell survival and proliferation has been implicated in phosphorylating AR at Ser-213 and Ser-791. In a PC cell line this interaction activated a PSA reporter and promoted cell survival, which was found to again be stimulated upstream by HER2 (Wen et al. 2000). Most interestingly are the numerous AR splice variants which are constitutively active due to the lack of their ligand binding domain at the C-terminal end. Increased nuclear expression of these mutants have been demonstrated in androgen-independent PC cell lines, CRPC tissues, and PC metastasis (Dehm et al. 2008; Hu et al. 2009; Li et al. 2012; Zhang et al. 2011; Hörnberg et al. 2011; Watson et al. 2010; Sun et al. 2010). Together the above mechanisms allow for continued activation of AR-responsive genes involved in cell survival and growth, promoting the development of more advanced disease despite treatment with ADT.

Overexpression of AR in PC cell lines leads to the induction of EMT and stem cell signatures (Kong et al. 2015). Research has shown that the gain of a mesenchymal phenotype can be associated with stem-like characteristics, slower

proliferation, therapeutic resistance, and plasticity for adaptation to secondary sites following metastasis (Smith & Bhowmick 2016). Treatment of PC with ADT may actually bring on the acquisition of an EMT phenotype, which has been associated with the recurrence of CRPC and eventual metastasis. In support of this, studies have observed EMT characteristics in normal mouse prostate and PC cell-derived xenografts under androgen-depletion conditions, as well as in castration-resistant patient tumours and circulating tumour cells (Kong et al. 2011; Chen et al. 2013; Armstrong et al. 2011; Sun et al. 2012). Furthermore, the four transcription factors SOX2, OCT4, c-MYC, and KLF4 (the latter two can be substituted with Nanog and Lin28 (Okita et al. 2008)) able to convert somatic cells into iPSCs are expressed in poorly differentiated tumours (Ben-Porath et al. 2008) and in PCSC populations isolated from androgen-independent PC cell lines. These PCSCs expressed classical stem cell markers, demonstrated self-renewal, and were more invasive and tumourigenic (Klarmann et al. 2009; Kong et al. 2010; Rybak et al. 2011). The process of EMT and cell migration occurs in multiple steps, starting with the induction of several EMT-driving transcription factors such as ZEB1/2, Twist, Snail, and Slug which have also been correlated with poor patient prognosis (Blanco et al. 2002; Savagner et al. 1997; Wellner et al. 2009; Yang et al. 2004). These factors are direct repressors of E-cadherin, an important mediator of cell-cell adhesion and a marker of epithelial cells (Hay & Zuk 1995; Van Roy & Berx 2008). During EMT the expression of E-cadherin is

reduced and upregulation of mesenchymal markers such as vimentin and N-cadherin occurs, which aid in cellular migration and stress-resistance (Satelli & Li 2011; Zeisberg & Neilson 2009). Ectopic expression of E-cadherin is enough to inhibit tumour cell invasion and migration, while knockdown induces tumour proliferation and metastasis (Vleminckx et al. 1991; Derksen et al. 2006; Onder et al. 2008). Expanding on this, the activation of EMT involves hundreds of genes including signal transduction pathways known to be involved in cancer and CSC chemoresistance (refer to Introduction, Section 1.5). The PI3K/AKT/mTOR pathways result in activation of Snail-1 which represses E-cadherin expression. The pathways are also involved in stimulation of matrix metalloproteinases which alter the extracellular matrix, and interaction with integrins and the Rho family of GTPases which control cytoskeleton rearrangement (Grotegut et al. 2006; Berrier et al. 2000; Grille et al. 2003; Xia et al. 2008; Zamir & Geiger 2001). The Wnt/β-Catenin pathway, stimulated by EGF, disrupts E-cadherin mediated cell-cell interactions and decreases E-cadherin expression via Snail-1 (Lu et al. 2003; Klymkowsky 2005; Nusse 2004). β-Catenin expression levels were also increased in PC cells overexpressing HIF-1α, establishing a correlation between this pathway and hypoxia which can lead to more aggressive disease (Jiang et al. 2007). Notch signalling and hypoxic conditions (via HIF-1α) also promote EMT by activating Snail-1 transcription and stabilizing its structure (Sahlgren et al.

2008). It appears that in cancer, these pathways involved in stimulating chemoresistant properties coincide with EMT inducing mechanisms.

Accumulating evidence points towards EMT as being a critical step in the generation and maintenance of CSCs, which can then go on to metastasize. The metastatic process is quite similar to tissue repair mechanisms where stem cells leave their resting place (such as haematopoietic stem cells from bone marrow), enter circulation, and proliferate at secondary sites, which would require a highly plastic cell type (Kondo et al. 2003). Furthermore, analysis of PC bone metastases demonstrated increased expression of EMT markers such as vimentin and Notch-1. Staining patterns of these proteins exhibited distinct invading fronts and intratumour cell clusters, supporting the concept of EMT and its reverse process mesenchymal to epithelial transition (MET) respectively. The latter is a critical step in the establishment of metastases at secondary sites where cells regain an epithelial phenotype to allow for attachment and proliferation (Sethi et al. 2010). Cells that have undergone EMT are able to grow as spheres in suspension and possess an increased capacity for xenograft tumour formation, two identifying traits of CSCs (Tiwari et al. 2012). Induction of EMT in non-tumourigenic cells by ectopic expression of EMT transcription factors results in the acquisition of mesenchymal traits, expression of stem cell markers, and ability to grow as spheres in culture. Additionally, stem-like cell populations isolated from tumours express EMT markers (Mani et al. 2008; Morel et al. 2008). Transition to a

mesenchymal phenotype also correlates with increased expression of drug transporters and signalling pathways (discussed above) allowing for greater chemoresistance and evasion of cytotoxic agents (Tiwari et al. 2012). Taken together, the notion that a differentiated cell can acquire stem-like traits and develop aggressive characteristics through EMT is an appealing explanation for the occurrence of PCSCs and severity of mCRPCs.

The work presented in this thesis has largely been based on our own population of PCSLCs isolated from the DU145 mCRPC cell line. Our initial characterization studies determined that the pluripotency transcription factors SOX2, OCT4, and Nanog are all expressed in this subpopulation (Rybak et al. 2011), suggesting the possibility of EMT traits in PCSCs. Adding to this, we found that stimulation of growth with EGF promoted self-renewal and increased expression of SOX2 (Rybak & Tang 2013), which may be mediated by the Wnt/β-Catenin pathway as discussed above. By examining unique genes only expressed in our PCSLCs, we may be able to elucidate proteins and/or mechanisms critical for CRPC development and metastasis based on the CSC and EMT models. Additionally, it might be possible to identify antigens of interest only in PCSCs for targeted immunotherapy.

6.2 - Potential Mechanisms of PKM2 in Prostate Cancer Stem Cells and Castration Resistant Prostate Cancer

In this thesis we demonstrated that the final enzyme of glycolysis, PKM2, associates with more advanced stages of PC as observed in tissues with high Gleason Score and in DU145 PCSLC-derived xenografts (Chapter 2). We also revealed a dissimilar pattern of post-translational modifications in our PCSLCs which may indicate alternative functions, protein interactions, or mechanisms of action. As PCSCs are well accepted to be a cause of cancer relapse and metastasis, investigation of these differences may provide new insights into CSC biology.

There are actually four isoforms of pyruvate kinase (PK); PKL, PKR, PKM1, and PKM2. Expressed in almost all cells except the muscle, brain, and liver, PKM2 has been found to be the most predominant form in tumour cells. It is also the only isoform that can exist as a tetramer to direct energy production through the mitochondria (OXPHOS), or as a dimer to stimulate aerobic glycolysis (Wong et al. 2013). As our methods of detection did not differentiate between dimeric or tetrameric PKM2, it would be interesting to determine its form in our DU145 PCSLCs and whether this is altered in subcutaneous xenografts which proliferate more quickly. Notably, studies have shown that the tetrameric form acts as a pyruvate kinase while the dimeric form acts as a protein kinase. Furthermore, PKM2 has been observed in the nucleus and demonstrated to

regulate expression of many genes. HIF-1α, which is stimulated under hypoxic conditions, induces expression of dimeric PKM2 and translocation to the nucleus. Acting as a protein kinase, PKM2 can then phosphorylate STAT3 which aside from its gene targets also increases HIF-1α expression, creating a feedback loop to amplify the rate of aerobic glycolysis. EGFR activation can also cause PKM2 to bind to β-Catenin and stimulate cyclin D1 and c-MYC, major contributors to tumour cell proliferation and tumourigenesis. These events have been observed in numerous cancers and are associated with poor prognosis (Demaria & Poli 2012; Yang et al. 2011; Gao et al. 2012; Yang et al. 2012). Interestingly, chemoresistance to Gefitinib, an inhibitor of the EGFR pathway, in colorectal cancer is mediated by PKM2 stimulation of STAT3 (Li et al. 2015). This suggests that PKM2 may be involved in additional chemoresistant pathways.

Although we (Chapter 2) and others have established increased PKM2 expression as associating with more advanced disease, it is clear that aside from its metabolic mechanism there is an oncogenic function as well. To this point, specific nuclear localization of PKM2 was found to be associated with higher Gleason Score (Giannoni et al. 2015). With its correlation to more advanced disease, a relationship with EMT is also possible. Induction of EMT in gastrointestinal cancer cells led to increased expression of PKM2 and higher incidence of nuclear translocation. Greater expression in metastasis tissues was also observed (Konno et al. 2015). In colorectal cancer, elevated levels of secreted

PKM2 can be detected in plasma and feces making it a possible biomarker for diagnosis. Treatment of cells with PKM2 induced migration and upregulation of EMT markers, which was found to be mediated by the PI3K/AKT/mTOR and Wnt/β-Catenin pathways (Yang et al. 2015). In addition, PKM2 was found to bind OCT4 in embryonic carcinoma lysates. Overexpression of PKM2 enhanced the transcriptional activation of OCT4 responsive genes involved in pluripotency and maintenance of a mesenchymal phenotype (Lee et al. 2008). On the other hand, combinational treatment of lung cancer cells *in vitro* and *in vivo* with PKM2 shRNA increased intracellular accumulation of docetaxel and cisplatin or sensitized cells to ionizing radiation, which led to cell death (H. shan Shi et al. 2010; Guo et al. 2011; Meng et al. 2015). Taken together these studies provide support that PKM2 is not only involved in glucose metabolism but also cell proliferation, EMT, chemoresistance, and radioresistance. This suggests a critical role within PCSC-derived development of CRPC and metastasis. Therapeutic targeting of dimeric PKM2 to prevent transcription of target genes may aid in delaying the progression of PC. Investigations into the mechanism of nuclear translocation will also prove useful for treatment approaches. For example, phosphorylation of PKM2 at Thr-454 is one such post-translational modification. Experiments using a T454A mutant caused higher mitochondrial respiration (OXPHOS), reversal of chemoresistance, and reduced tumourigenicity in A549 lung cancer cells (Yu et al. 2016; Yu et al. 2013). It would be worthwhile to

investigate the function of each unique post-translational modification observed in our DU145 PCSLCs to determine their contribution to disease progression. Discovery of any protein interactions with PKM2 will also help broaden our knowledge of its role in PC development.

Furthermore, the progression of PC is clearly associated with changes in cancer cell biology, which includes alterations in proliferative capacity and resistance to cell stress brought on by various therapies. Conceptually, adaptive responses to treatments such as ADT inevitably involve changes in cellular metabolism, a process in which PKM2 plays a major role. Along these lines it would not be surprising to observe a critical function of the PKM gene (which codes for both PKM1 and PKM2 (Wong et al. 2015; Wong et al. 2013)) in PCSC-associated plasticity in response to androgen deprivation, essential for PC development. Future experiments can investigate whether survival adaptation to ADT is mediated by PKM2 and enhanced cellular metabolism. Knockout of PKM2 in PC cell lines and growth in androgen depleted conditions, both *in vitro* and *in vivo,* will indicate whether PKM2 is necessary for CRPC development. Should this be the case, PKM2 inhibitors may be tested for their efficacy alongside ADT strategies in preventing progression towards CRPC.

6.3 - MUC1 is a Critical Factor in the Progression of Metastatic Castration Resistant Prostate Cancer

Chapter 3 reports the upregulation of MUC1 in our DU145 PCSLCs *in vitro* and *in vivo*, and elevation in both DU145 parental and PCSLC-derived xenograft tumours in response to docetaxel treatment. Computational analysis using numerous genomic expression datasets revealed amplification of mRNA and gene copy number (GCN) in CRPC and metastasis cases. This analysis also revealed a possible utility for MUC1 and its 25 gene network in predicting CRPC more efficiently than AR and its gene network. Currently, persistence of AR signalling is the best predictor of PC progression.

MUC1 is the most well studied mucin glycoprotein for its role in cancer. Translated as a pre-peptide, an autocleavage event produces a heterodimer consisting of a large extracellular N-terminal fragment (MUC1-N) and a smaller C-terminal fragment (MUC1-C) which spans extracellular, transmembrane, and cytoplasmic regions (Macao et al. 2006; Levitin et al. 2005; Ligtenberg et al. 1992). Both components play their own part in the progression of cancer, making MUC1 a powerful influencer of tumourigenesis.

MUC1-N contains the conserved variable number of tandem repeats which are the sites of glycosylation, with different patterns demonstrated in a number of cancers. In most normal secretory epithelial cells this high glycosylation serves as a physical barrier to protect the organ from abrasion,

microorganisms, and toxic chemicals (Singh & Hollingsworth 2006). In transformed cells however, loss of polarity causes MUC1 to be overexpressed all over the cell surface (Kufe et al. 1984). This increased expression of MUC1-N has been associated with the interference of cell-cell interactions, which may contribute to EMT and disease progression (Pillai et al. 2015). The N-terminal subunit can also be shed off from the cell by cleavage at the SEA domain, often in response to environmental signals (Brayman et al. 2004). High serum levels of MUC1 are associated with progressive disease, and can be used as a biomarker of cancer progression (Moreno et al. 2007). There are also mRNA splice variants that generate a secreted form which lacks the transmembrane and cytoplasmic domains, emphasizing a biological role of the N-terminal subunit alone (Brayman et al. 2004). One study revealed secreted MUC1 as having the capacity to suppress T-cell proliferation and function, implying tumour cells can mediate immune suppression via MUC1-N (Chan et al. 1999). To be heavily glycosylated, MUC1 is translocated and recycled several times between the cell membrane and trans-golgi. Secreted isoforms can be differentiated from membrane-bound forms on this basis, as they are only glycosylated once. In cancer, MUC1 can also be more extensively glycosylated (Hilkens & Buijs 1988; Engelmann et al. 2005; Storr et al. 2008). These factors provide the basis for the variety of immunotherapeutic approaches using antibodies and vaccines against unique MUC1 glycosylation patterns in cancer and CSCs (Vassilaros et al. 2013;

Pichinuk et al. 2012; Sanchez et al. 2013; Danielczyk et al. 2006; Dreicer et al. 2009; Curry et al. 2013; Major et al. 2012). High levels of extracellular MUC1-N also increase chemoresistance to cytotoxic agents. By using a glycosylation inhibitor to reduce the amount of cell surface mucins, cytotoxicity by treatment with 5-fluorouracil was significantly increased in pancreatic cancer cells (Kalra & Campbell 2007). As a whole, these studies provide evidence that the amplification of extracellular MUC1-N enables the evasion of chemotherapeutics and progression of disease in PC.

The C-terminal subunit of MUC1 is divided into 3 distinct regions, each with their own functions. The extracellular domain can be glycosylated like MUC1-N and indirectly interacts with EGFR and other tyrosine kinase receptors (Li et al. 2001; Schroeder et al. 2001). The transmembrane region's function is to relay environmental stimulation to the intracellular domain. The cytoplasmic portion of MUC1 arguably has the largest impact on cancer development. This region contains 7 tyrosine phosphorylation sites which permit binding of other proteins to promote proliferation, invasion, and chemoresistance (Pillai et al. 2015). MUC1-C has been shown to activate the PI3K/AKT pathway leading to tumour cell proliferation and anti-apoptosis mechanisms in response to cytotoxic agents and oxidative stress (Yin et al. 2004; Woo et al. 2012; Ren et al. 2004; Yin et al. 2003; Raina et al. 2004). Additionally, research has shown that MUC1-C directly binds to PKM2 and increases both glucose uptake and lactate production

indicative of aerobic glycolysis (Kosugi et al. 2011). These findings link Chapters 2 and 3 of this thesis together and provide some explanation for their co-expression in our DU145 PCSLC population. Phosphorylation of MUC1 by EGFR causes the cytoplasmic domain to bind the tyrosine kinase Src, which when activated can phosphorylate AR and upregulate its activity. This connects elevated MUC1 expression with AR signalling in PC cells. MUC1 also binds β-catenin (Li et al. 2001), creating a correlation with all of its downstream signalling pathways involved in EMT and cancer progression. These processes are mediated by MUC1-Cs CQC domain which allows for dimerization and translocation to the nucleus for activation of target genes. In renal and pancreatic cancer cells, overexpression of MUC1 was found to trigger the process of EMT by binding β-catenin and activating transcription of Snail and Slug, two major EMT transcription factors. Blocking MUC1-C translocation to the nucleus prevented transcription of these genes associated with EMT and metastasis (Gnemmi et al. 2014; Roy et al. 2011). MUC1-C has also been shown to induce upregulation of ZEB1, another EMT transcription factor, in lung and breast cancer cells. Inhibition of nuclear translocation again reduced proliferation, invasion, and self-renewal capacity (Kharbanda et al. 2014; Rajabi et al. 2014). Lastly, in PC cells MUC1-C was found to both directly bind AR and activate a miRNA mechanism, suppressing AR function. This process allowed for the induction of EMT, which led to increased invasion, growth in androgen-depleted

medium, and resistance to bicalutamide (an antiandrogen). On the other hand, AR was found to bind to the MUC1 promoter, suppressing its function. Reintroduction of AR into androgen-independent PC cell lines reduced MUC1 expression, indicating an inverse relationship between the two (Rajabi et al. 2011; Rajabi et al. 2012). This also implies that the widespread effects of MUC1-C do not occur until after androgen-independence has been established. Together these studies provide strong evidence of MUC1s involvement with EMT and therefore CSCs.

As a whole, the MUC1 protein has a major impact on the progression and severity of cancer. The N-terminal subunit is involved in physical barrier protection and chemoresistance, while the C-terminal subunit participates in cell proliferation, EMT signalling pathways, regulation of AR activity, and even cell metabolism. The observation that MUC1 expression is increased in our DU145 PCSLCs, CRPC cases, and PC metastases fits perfectly with these characteristics that work in concert to promote cell survival and disease progression. Future work will need to determine whether the findings discussed above are relevant in PC before similar therapeutic approaches can be attempted. Applications including the GO-203 inhibitor which blocks MUC1-C dimerization (Raina et al. 2015), and combinational therapy involving ADT, docetaxel, and MUC1-based immunotherapy are currently appealing options. Based on the known functions of

MUC1, these methodologies may very well target PCSCs and halt disease progression.

6.4 - FAM84Bs Mechanism of Action in the Development of Castration Resistant Prostate Cancer

Chapter 4 explores a candidate identified in our PCSLCs and its association with advanced PC. The FAM84B gene resides at the chromosomal locus 8q24, and together with c-MYC flanks a 1.2Mb gene desert characterized by little transcriptional activity. However it has been discovered that this region is frequently modified in many cancers and imparts tumourigenic effects by physically interacting with other chromosomal loci (Du et al. 2015; Ghoussaini et al. 2008; Haiman et al. 2007). Mechanistically, knockdown of FAM84B in esophageal cancer cells was demonstrated to reduce proliferation, migration, and invasion *in vitro* (Cheng et al. 2016), suggesting a possible role in cancer metastasis.

In our study we revealed FAM84B protein expression in PC bone metastases tissues and upregulation in our DU145 PCSLCs. Computational analysis using gene expression datasets demonstrated increases in mRNA levels and GCN in primary PC vs normal, and mCRPC vs primary PC, which is in agreement with the functionality of FAM84B observed in esophageal cancer cells. We were able to provide additional evidence of its importance in PC disease

progression by observing increased expression in DU145 xenograft lung metastasis, particularly in the edge regions, and in two different animal models of CRPC. Upregulation of FAM84B also correlated with reduced overall survival in patient datasets.

As there is very little information in the literature about FAM84B, its contribution to PC progression remains speculative. One study demonstrated high FAM84B expression in esophageal cancer but lower levels of circulating mRNA transcript following chemoradiation, suggesting its potential as a possible biomarker for pathological response (Hsu et al. 2015). Another group demonstrated the elevation of FAM84B in 66% of esophageal cancers, versus c-MYC in 9% of esophageal cancerous nests, suggesting FAM84B as the primary target of 8q24 locus amplification (Huang et al. 2006). Elevation of protein expression has also been associated with breast cancer cells (Adam et al. 2003). FAM84B upregulation in our PCSLCs and association with CRPC also suggests possible relations with EMT. In esophageal cancer increased FAM84B expression coincided with the Notch signalling pathway important in tumour progression, metastasis, CSC self-renewal, and EMT as discussed above (Discussion, Section 6.1) (Cheng et al. 2016). The FAM84B gene itself is also in close proximity with c-MYC, one of the four classical pluripotency factors and well known to be associated with PC tumourigenesis. Although the enhancer and other regulatory elements within the 8q24 gene desert are known to physically interact with c-

MYC, there have been no studies demonstrating that any come in contact with FAM84B (Du et al. 2015; Ghoussaini et al. 2008). However the significant gap in knowledge of this region means the possibility of co-expression cannot be ruled out.

Future work will need to investigate the exact function of FAM84B in PC cells and whether these mechanisms associate with disease progression. One prospective research avenue is to determine whether FAM84B possesses any nuclear activity, a notion supported by its widespread effects in esophageal cancer cells. Additionally, through our IHC analysis of high Gleason primary PC tissues and in the prostate-specific $PTEN^{-/-}$ animal model, we noticed a greater amount of nuclear staining. As a potential explanation for this observation, one group discovered the fission yeast analog, Nse2, as being involved in DNA repair. Two members of the structural maintenance of chromosomes (SMC) superfamily, SMC5 and SMC6, form a heterodimer and are important for repair of double stranded breaks. Nse1 and Nse2 both complex with this heterodimer and together these proteins engage in homologous recombination repair. Mutation of Nse1 and Nse2 produced DNA damage-sensitive cells. Furthermore, these two proteins are conserved from yeast to humans, which taken together provides a possible function for FAM84B in aggressive cancers (Pebernard et al. 2004; McDonald et al. 2003). Examination of nuclear fractions via Western blotting as well as chromatin immunoprecipitation may help to determine whether FAM84B

localizes to the nucleus. Further experiments will then need to determine whether the same mechanism of DNA damage-resistance occurs in humans. Protein interaction studies should also be performed to investigate whether FAM84B binds with any SMC family members or components of signalling pathways important in tumourigenesis or EMT.

6.5 - ABCC2 May be an Indicator of Advanced Prostate Cancer and Chemoresistance

The CSC model attributes the aggressiveness and therapeutic resistance of mCRPC to the small population of cells with self-renewal, anti-apoptotic, and chemoresistant properties. Although the bulk of the tumour may be eliminated through various treatments, it is these cells that are hypothesized to survive and recapitulate the tumour tissue, going on to metastasize. The process of EMT appears to be a critical step during the later stages of PC development, and among a multitude of mechanisms inferring chemoresistance there are numerous studies in breast cancer demonstrating upregulation of ABC drug transporters as a result of its activation. Induction of EMT by introducing Twist or Snail-1 into non-tumourigenic immortalized mammary cells increased expression of CSC surface markers, self-renewal capacity, and sphere formation. In breast cancer cell lines overexpression of Twist allowed for Hoechst dye exclusion indicative of high ABCC1 expression. Silencing of Twist abrogated these effects. Similar findings

were observed in colorectal cancer cells, where overexpression of Twist led to greater migration, invasion, and sphere formation concomitant with upregulation of ABCB1 expression (Deng et al. 2016). Adding to this, treatment of breast cancer cells with cytotoxic agents increased expression of ABC transporters and EMT markers, which could be reversed by knockdown of Twist and ZEB1. These findings suggest that chemotherapy with anti-mitotics such as doxorubicin or docetaxel may actually contribute to the development of chemoresistance. EMT transcription factors such as Snail-1, Twist, and Slug have also been shown to bind to and activate ABC transporter promoters, adding to the list of mechanisms involved in therapeutic resistance that this process influences in advanced cancers (Mani et al. 2008; Vesuna et al. 2009; Saxena et al. 2011).

In Chapter 5 of this thesis we report the possible contribution of ABCC2 to PC progression and chemoresistance. Increased expression of ABCC2 in our DU145 PCSLCs is in agreement with the literature demonstrating stimulation of chemoresistant mechanisms during CSC development. We were also able to establish a correlation between ABCC2 expression and PC progression, where tissues of higher Gleason Score were found to have higher protein levels. This again is in agreement with the concept of PCSCs and their contribution to therapeutic resistance and metastasis in advanced stages of PC. Unfortunately, attempts to investigate whether ABCC2 plays a part in docetaxel resistance *in vitro* were not successful when using our DU145 PCSLCs or A549 lung cancer

cells. Experiments *in vivo* provided promising results, where DU145 shABCC2 PCSLC-derived xenografts appeared to exhibit resensitization to docetaxel treatment. However, these observations were not statistically significant due to individual animal variations.

The notion that ABCC2 may take part in docetaxel chemoresistance is in agreement with the function of CSCs and the ABC transporter family. However, studies have suggested that rather than being an independent factor, ABCC2 works collectively with other docetaxel-related mechanisms (Van Waterschoot et al. 2010). Future work will need to address factors such as systemic docetaxel metabolism, intratumour accumulation, and the possibility of additional ABC transporters at play. Additionally, establishment of ABCC2 overexpression in the DU145 parental line and use of labeled docetaxel (radiolabeled, GFP tag, etc.) will strengthen the *in vitro* experiments performed. Based on our current findings, ABCC2 could be used as a biomarker in PC tissues for acquisition of EMT and chemoresistant attributes.

6.6 - Clinical Relevance

Prostate cancer affects many men world-wide and there is no single cause of the disease. Many risk factors such as age, ethnicity, genetic predisposition, food consumption, and environmental exposure can all play a part in its development. Early detection and treatment of prostate cancer has meant that

many individuals never progress to advanced stages. However, for those that do, relapse and further development of the disease despite various aggressive treatment strategies inevitably leads to poor quality of life, painful symptoms, and fatality. Typically, locally confined prostate tumours do not pose much risk to the individual's health. It is those that progress to castration-resistant and metastatic status that are difficult to treat and frequently result in death. For this reason it is important to understand the mechanisms in which prostate cancer progresses to these stages, and whether targeted therapies can be designed to slow or prevent the disease.

This thesis presents experimental data collected on four different candidate genes all identified in a prostate cancer stem-like cell population; PKM2 (Chapter 2), MUC1 (Chapter 3), FAM84B (Chapter 4), and ABCC2 (Chapter 5). The cancer stem cell model provides an appropriate explanation for the perpetuation of prostate cancer despite an arsenal of therapeutic strategies employed. Rather than eradicating the bulk of the tumour consisting of differentiated progeny, treatments should be designed to target this small population of cells with self-renewal, anti-apoptotic, and chemoresistant properties to prevent tumour recapitulation and relapse. The cancer stem cell model goes hand in hand with the process of epithelial to mesenchymal transition, which is an appealing justification for a tumour cell's ability to develop chemoresistance, and migrate to and invade secondary sites of the body.

Coincidentally, the four candidate proteins discussed in this thesis have been demonstrated by others to be involved in increased cellular proliferation, the process of epithelial to mesenchymal transition, and/or chemoresistance to cytotoxic chemicals. The observation that they were all identified in our DU145 prostate cancer stem-like cells fully supports the cancer stem cell model in the development of metastatic castration resistant prostate cancer. Fortunately, therapeutic approaches for some of these candidates have been studied and tested. However, because the development of advanced prostate cancer is multifactorial, it is likely that combinational treatment to specifically target many aspects of prostate cancer stem cells will be required to successfully combat the progression of prostate cancer.

REFERENCES

Abate-Shen, C., 2000. Molecular genetics of prostate cancer. *Genes & Development*, 14(19), pp.2410–2434.

Abdulla, A. & Kapoor, A., 2011. Emerging novel therapies in the treatment of castrate-resistant prostate cancer. *Journal of the Canadian Urological Association*, 5(2), pp.120–133.

Abidi, A., 2013. Cabazitaxel: A novel taxane for metastatic castration-resistant prostate cancer-current implications and future prospects. *Journal of pharmacology & pharmacotherapeutics*, 4(4), pp.230–237.

Adam, P.J. et al., 2003. Comprehensive proteomic analysis of breast cancer cell membranes reveals unique proteins with potential roles in clinical cancer. *Journal of Biological Chemistry*, 278(8), pp.6482–6489.

Al-Hajj, M. et al., 2003. Prospective identification of tumorigenic breast cancer cells. *Proceedings of the National Academy of Sciences of the United States of America*, 100(7), pp.3983–8.

Armstrong, A.J. et al., 2011. Circulating tumor cells from patients with advanced prostate and breast cancer display both epithelial and mesenchymal markers. *Molecular Cancer research*, 9(8), pp.997–1007.

Attar, R.M., Takimoto, C.H. & Gottardis, M.M., 2009. Castration-resistant prostate cancer: Locking up the molecular escape routes. *Clinical Cancer Research*, 15(10), pp.3251–3255.

Bae, K.M. et al., 2010. Expression of Pluripotent Stem Cell Reprogramming Factors by Prostate Tumor Initiating Cells. *Journal of Urology*, 183(5), pp.2045–2053.

Bagi, C.M., 2003. Skeletal implications of prostate cancer. *Journal of Musculoskeletal Neuronal Interactions*, 3(2), pp.112–117.

Baker, S.D., Sparreboom, A. & Verweij, J., 2006. Clinical pharmacokinetics of docetaxel. *Clinical Pharmacokinetics*, 45(3), pp.235–252.

Belvisi, M.G., 2004. Preclinical pharmacology of ciclesonide. *European Respiratory Review*, 13(90), pp.66–68.

Ben-Porath, I. et al., 2008. An embryonic stem cell-like gene expression signature in poorly differentiated aggressive human tumors. *Nature Genetics*, 40(5), pp.499–507.

Berrier, A.L. et al., 2000. Activated R-ras, Rac1, PI 3-kinase and PKCepsilon can each restore cell spreading inhibited by isolated integrin beta1 cytoplasmic domains. *Journal of Cell Biology*, 151(7), pp.1549–1560.

Berthold, D.R. et al., 2008. Treatment of hormone-refractory prostate cancer with

docetaxel or mitoxantrone: relationships between prostate-specific antigen, pain, and quality of life response and survival in the TAX-327 study. *Clinical Cancer Research*, 14(9), pp.2763–2767.

Bisson, I. & Prowse, D.M., 2009. WNT signaling regulates self-renewal and differentiation of prostate cancer cells with stem cell characteristics. *Cell Research*, 19(6), pp.683–97.

Bitting, R.L. & Armstrong, A.J., 2013. Targeting the PI3K/Akt/mTOR pathway in castration-resistant prostate cancer. *Endocrine-Related Cancer*, 20(3), pp.83–99.

Blanco, M.J. et al., 2002. Correlation of Snail expression with histological grade and lymph node status in breast carcinomas. *Oncogene*, 21, pp.3241–3246.

Bonnet, D. & Dick, J.E., 1997. Human acute myeloid leukemia is organized as a hierarchy that originates from a primitive hematopoietic cell. *Nature Medicine*, 3(7), pp.730–737.

Bono, J.S. De et al., 2010. Prednisone plus cabazitaxel or mitoxantrone for metastatic castration-resistant prostate cancer progressing after docetaxel treatment : a randomised open-label trial. *The Lancet*, 376(9747), pp.1147–1154.

Borst, P. et al., 2000. A Family of Drug Transporters : the Multidrug Resistance-Associated Proteins. *Journal of the National Cancer Institute*, 92(16), pp.1295–1302.

Bourdeau-Heller, J. & Oberley, T.D., 2007. Prostate carcinoma cells selected by long-term exposure to reduced oxygen tension show remarkable biochemical plasticity via modulation of superoxide, HIF-1alpha levels, and energy metabolism. *Journal of Cellular Physiology*, 212(3), pp.744–752.

Bradshaw, D.M. & Arceci, R.J., 1998. Clinical relevance of transmembrane drug efflux as a mechanism of multidrug resistance. *Journal of Clinical Oncology*, 16(11), pp.3674–3690.

Brayman, M., Thathiah, A. & Carson, D.D., 2004. MUC1: a multifunctional cell surface component of reproductive tissue epithelia. *Reproductive Biology and Endocrinology*, 2, p.4.

Brien, C.A.O. et al., 2007. A human colon cancer cell capable of initiating tumour growth in immunodeficient mice. *Nature*, 445(7123), pp.106–110.

Burdova, A. et al., 2014. TMPRSS2-erg gene fusion in prostate cancer. *Biomedical Papers*, 158(4), pp.502–510.

Carmeliet, P. et al., 1998. Role of HIF-1alpha in hypoxia-mediated apoptosis, cell

proliferation and tumour angiogenesis. *Nature*, 394(6692), pp.485–490.

Chaffer, C.L. et al., 2011. Normal and neoplastic nonstem cells can spontaneously convert to a stem-like state. *Proceedings of the National Academy of Sciences of the United States of America*, 108(19), pp.7950–7955.

Chan, A.K. et al., 1999. Soluble MUC1 secreted by human epithelial cancer cells mediates immune suppression by blocking T-cell activation. *International Journal of Cancer*, 82(5), pp.721–6.

Chan, L.M.S., Lowes, S. & Hirst, B.H., 2004. The ABCs of drug transport in intestine and liver: Efflux proteins limiting drug absorption and bioavailability. *European Journal of Pharmaceutical Sciences*, 21(1), pp.25–51.

Chaneton, B. & Gottlieb, E., 2012. Rocking cell metabolism: Revised functions of the key glycolytic regulator PKM2 in cancer. *Trends in Biochemical Sciences*, 37(8), pp.309–316.

Chang, A.J. et al., 2014. High-risk prostate cancer - classification and therapy. *Nature Reviews Clinical Oncology*, 11(6), pp.308–323. Available at: http://www.nature.com/doifinder/10.1038/nrclinonc.2014.68.

Chang, H.-H. et al., 2011. Hedgehog overexpression leads to the formation of prostate cancer stem cells with metastatic property irrespective of androgen receptor expression in the mouse model. *Journal of Biomedical Science*, 18(1), p.6.

Chau, W.K. et al., 2012. c-Kit mediates chemoresistance and tumor-initiating capacity of ovarian cancer cells through activation of Wnt/β-catenin–ATP-binding cassette G2 signaling. *Oncogene*, (May), pp.1–15.

Chen, C.D. et al., 2004. Molecular determinants of resistance to antiandrogen therapy. *Nature Medicine*, 10(1), pp.33–39.

Chen, C.L. et al., 2013. Single-cell analysis of circulating tumor cells identifies cumulative expression patterns of EMT-related genes in metastatic prostate cancer. *Prostate*, 73(8), pp.813–826.

Chen, Y. et al., 2012. Isolation and identification of cancer stem-like cells from side population of human prostate cancer cells. *Journal of Huazhong University of Science and Technology [Medical Sciences]*, 32(5), pp.697–703.

Cheng, C. et al., 2016. Genomic analyses reveal FAM84B and the NOTCH pathway are associated with the progression of esophageal squamous cell carcinoma. *GigaScience*, 5(1), p.1.

Chiba, T. et al., 2006. Side population purified from hepatocellular carcinoma cells harbors cancer stem cell-like properties. *Hepatology*, 44(1), pp.240–251.

Choi, S.A. et al., 2014. Identification of brain tumour initiating cells using the stem cell marker aldehyde dehydrogenase. *European Journal of Cancer*, 50(1), pp.137–149.

Clarke, M.F. & Fuller, M., 2006. Stem Cells and Cancer: Two Faces of Eve. *Cell*, 124(6), pp.1111–1115.

Collins, A., Habib, F. & Maitland, N., 2001. Identification and isolation of human prostate epithelial stem cells based on α2β1-integrin expression. *Journal of Cell Science*, 114(21), pp.3865–3872.

Collins, A.T. et al., 2005. Prospective identification of tumorigenic prostate cancer stem cells. *Cancer Research*, 65(23), pp.10946–51.

Collins, R. et al., 2006. A systematic review of the effectiveness of docetaxel and mitoxantrone for the treatment of metastatic hormone-refractory prostate cancer. *British Journal of Cancer*, 95(4), pp.457–62.

Crea, F. et al., 2011. BMI1 silencing enhances docetaxel activity and impairs antioxidant response in prostate cancer. *International Journal of Cancer*, 128(8), pp.1946–1954.

Di Cristofano, A. & Pandolfi, P.P., 2000. The Multiple Roles of PTEN in Tumor Suppression. *Cell*, 100(4), pp.387–390.

Cui, Y. et al., 1999. Drug resistance and ATP-dependent conjugate transport mediated by the apical multidrug resistance protein, MRP2, permanently expressed in human and canine cells. *Molecular Pharmacology*, 55(5), pp.929–937.

Curry, J.M. et al., 2013. The use of a novel MUC1 antibody to identify cancer stem cells and circulating MUC1 in mice and patients with pancreatic cancer. *Journal of Surgical Oncology*, 107(7), pp.713–722.

Curtis, S.J. et al., 2010. Primary tumor genotype is an important determinant in identification of lung cancer propagating cells. *Cell Stem Cell*, 7(1), pp.127–133.

Dalerba, P., Cho, R.W. & Clarke, M.F., 2007. Cancer stem cells: models and concepts. *Annual Review of Medicine*, 58, pp.267–84.

Danielczyk, A. et al., 2006. PankoMab: A potent new generation anti-tumour MUC1 antibody. *Cancer Immunology, Immunotherapy*, 55(11), pp.1337–1347.

Dean, M., Fojo, T. & Bates, S., 2005. Tumour stem cells and drug resistance. *Nature reviews. Cancer*, 5(4), pp.275–284.

Dean, M., Rzhetsky, A. & Allikmets, R., 2001. The Human ATP-Binding Cassette (ABC) Transporter Superfamily. *Genome Research*, 11(7), pp.1156–1166.

Dehm, S.M. et al., 2008. Splicing of a novel androgen receptor exon generates a constitutively active androgen receptor that mediates prostate cancer therapy resistance. *Cancer Research*, 68(13), pp.5469–5477.

Demaria, M. & Poli, V., 2012. PKM2, STAT3 and HIF-1α: The Warburg's vicious circle. *Jak-Stat*, 1(3), pp.194–6.

Deng, J.-J. et al., 2016. Twist mediates an aggressive phenotype in human colorectal cancer cells. *International Journal of Oncology*, 48(3), pp.1117–1124.

Derksen, P.W.B. et al., 2006. Somatic inactivation of E-cadherin and p53 in mice leads to metastatic lobular mammary carcinoma through induction of anoikis resistance and angiogenesis. *Cancer Cell*, 10(5), pp.437–449.

Diamond, T.H. et al., 2004. Osteoporosis in Men with Prostate Carcinoma Receiving Androgen-Deprivation Therapy: Recommendations for Diagnosis and Therapies. *Cancer*, 100(5), pp.892–899.

Dick, J.E., 2009. Looking ahead in cancer stem cell research. *Nature Biotechnology*, 17(1), pp.44–46.

Domingo-Domenech, J. et al., 2012. Suppression of Acquired Docetaxel Resistance in Prostate Cancer through Depletion of Notch- and Hedgehog-Dependent Tumor-Initiating Cells. *Cancer Cell*, 22(3), pp.373–388.

Dominy, J.E., Vazquez, F. & Puigserver, P., 2012. Glycine Decarboxylase Cleaves a "Malignant" Metabolic Path to Promote Tumor Initiation. *Cancer Cell*, 21(2), pp.143–145.

Dontu, G. et al., 2003. In vitro propagation and transcriptional profiling of human mammary stem / progenitor cells. *Genes & Development*, 17(10), pp.1253–1270.

Dreicer, R. et al., 2009. MVA-MUC1-IL2 vaccine immunotherapy (TG4010) improves PSA doubling time in patients with prostate cancer with biochemical failure. *Investigational New Drugs*, 27(4), pp.379–386.

Du, M. et al., 2015. Prostate cancer risk locus at 8q24 as a regulatory hub by physical interactions with multiple genomic loci across the genome. *Human Molecular Genetics*, 24(1), pp.154–166.

Dubrovska, A. et al., 2008. The role of PTEN / Akt / PI3K signaling in the maintenance and viability of prostate cancer stem-like cell populations. *Proceedings of the National Academy of Sciences of the United States of America*, 106(1), pp.268–73.

Van Duin, M. et al., 2005. High-resolution array comparative genomic hybridization of chromosome arm 8q: Evaluation of genetic progression markers for prostate cancer. *Genes Chromosomes and Cancer*, 44(4), pp.438–449.

Dunning, N.L. et al., 2011. Immunotherapy of prostate cancer: Should we be targeting stem cells and EMT? *Cancer Immunology, Immunotherapy*, 60(8), pp.1181–1193.

Eisenberger, M.A. et al., 1998. Bilateral orchiectomy with or without flutamide for metastatic prostate cancer. *The New England Journal of Medicine*, 339, pp.1036–1042.

Engelmann, K. et al., 2005. Transmembrane and secreted MUC1 probes show trafficking-dependent changes in O-glycan core profiles. *Glycobiology*, 15(11), pp.1111–1124.

Eramo, a et al., 2008. Identification and expansion of the tumorigenic lung cancer stem cell population. *Cell Death and Differentiation*, 15(3), pp.504–514.

Farkona, S., Diamandis, E.P. & Blasutig, I.M., 2016. Cancer immunotherapy: the beginning of the end of cancer? *BMC Medicine*, 14(1), p.73.

Feng, B. et al., 2012. MicroRNA-200b reverses chemoresistance of docetaxel-resistant human lung adenocarcinoma cells by targeting E2F3. *Cancer*, 118(13), pp.3365–3376.

Flahaut, M. et al., 2009. The Wnt receptor FZD1 mediates chemoresistance in neuroblastoma through activation of the Wnt/beta-catenin pathway. *Oncogene*, 28(23), pp.2245–2256.

Fukuta, F. et al., 2015. Efficacy and safety of docetaxel and prednisolone for castration-resistant prostate cancer: A multi-institutional retrospective study in Japan. *Japanese Journal of Clinical Oncology*, 45(7), pp.682–687.

Galli, R. et al., 2004. Isolation and Characterization of Tumorigenic , Stem-like Neural Precursors from Human Glioblastoma Isolation and Characterization of Tumorigenic , Stem-like Neural Precursors from Human Glioblastoma. *Cancer Research*, 64, pp.7011–7021.

Gandaglia, G. et al., 2014. Distribution of metastatic sites in patients with prostate cancer: A population-based analysis. *Prostate*, 74(2), pp.210–216.

Ganju, A. et al., 2014. Nanoways to overcome docetaxel resistance in prostate cancer. *Drug Resistance Updates*, 17(0), pp.13–23.

Gao, X. et al., 2012. Pyruvate Kinase M2 Regulates Gene Transcription by Acting as a Protein Kinase. *Molecular Cell*, 45(5), pp.598–609.

Gerritsen, W.R., 2012. The evolving role of immunotherapy in prostate cancer. *Annals of Oncology*, 23(SUPPL.8), pp.232–240.

Ghafar, M.A. et al., 2003. Acute hypoxia increases the aggressive characteristics and survival properties of prostate cancer cells. *Prostate*, 54(1), pp.58–67.

Ghoussaini, M. et al., 2008. Multiple loci with different cancer specificities within the 8q24 gene desert. *Journal of the National Cancer Institute*, 100(13), pp.962–966.

Giannelli, G. et al., 2016. Role of epithelial to mesenchymal transition in hepatocellular carcinoma. *Journal of Hepatology*.

Giannoni, E. et al., 2015. Targeting stromal-induced pyruvate kinase M2 nuclear translocation impairs oxphos and prostate cancer metastatic spread. *Oncotarget*, 6(27), pp.24061–74.

Gnemmi, V. et al., 2014. MUC1 drives epithelial-mesenchymal transition in renal carcinoma through Wnt/β-catenin pathway and interaction with SNAIL promoter. *Cancer Letters*, 346(2), pp.225–236.

Gonzalgo, M.L. & Isaacs, W.B., 2003. Molecular Pathways to Prostate Cancer. *The Journal of Urology*, 170(6), pp.2444–2452.

Goodell, M.A. et al., 1996. Isolation and functional properties of murine hematopoietic stem cells that are replicating in vivo. *The Journal of Experimental Medicine*, 183, pp.1797–1806.

Gottesman, M.M., Fojo, T. & Bates, S.E., 2002. Multidrug resistance in cancer: role of ATP-dependent transporters. *Nature reviews: Cancer*, 2(1), pp.48–58.

Graham, L. & Schweizer, M.T., 2016. Targeting persistent androgen receptor signaling in castration-resistant prostate cancer. *Medical Oncology*, 33(5), pp.1–17.

Grasso, C.S. et al., 2012. The mutational landscape of lethal castration-resistant prostate cancer. *Nature*, 487(7406), pp.239–43. Available at: http://www.pubmedcentral.nih.gov/articlerender.fcgi?artid=3396711&tool=pmcentrez&rendertype=abstract.

Gregory, C.W. et al., 2001. Androgen Receptor Stabilization in Recurrent Prostate Cancer Is Associated with Hypersensitivity to Low Androgen Androgen Receptor Stabilization in Recurrent Prostate Cancer Is Associated with

Hypersensitivity to Low Androgen 1. *Cancer Research*, 61, pp.2892–2898.

Vander Griend, D.J. et al., 2008. The role of CD133 in normal human prostate stem cells and malignant cancer-initiating cells. *Cancer Research*, 68(23), pp.9703–11.

Grille, S.J. et al., 2003. The Protein Kinase Akt Induces Epithelial Mesenchymal Transition and Promotes Enhanced Motility and Invasiveness of Squamous Cell Carcinoma Lines The Protein Kinase Akt Induces Epithelial Mesenchymal Transition and Promotes Enhanced Motility and Invasiven. *Cancer Research*, 63, pp.2172–2178.

Grotegut, S. et al., 2006. Hepatocyte growth factor induces cell scattering through MAPK/Egr-1-mediated upregulation of Snail. *The EMBO journal*, 25(15), pp.3534–3545.

Group, P.C.T.C., 2000. Maximum androgen blockade in advanced prostate cancer: an overview of the randomised trials. *Lancet*, 355(9214), pp.1491–1498.

Gu, G. et al., 2007. Prostate cancer cells with stem cell characteristics reconstitute the original human tumor in vivo. *Cancer Research*, 67(10), pp.4807–15.

Gulley, J.L. et al., 2016. Perspectives on sipuleucel-T: Its role in the prostate cancer treatment paradigm. *OncoImmunology*, 5(4), p.e1107698.

Guo, W. et al., 2011. Efficacy of RNAi targeting of pyruvate kinase M2 combined with cisplatin in a lung cancer model. *Journal of Cancer Research and Clinical Oncology*, 137(1), pp.65–72.

Gupta, P.B., Chaffer, C.L. & Weinberg, R. a, 2009. Cancer stem cells: mirage or reality? *Nature Medicine*, 15(9), pp.1010–1012.

Hadaschik, B. a & Gleave, M.E., 2007. Therapeutic options for hormone-refractory prostate cancer in 2007. *Urologic Oncology*, 25(5), pp.413–9.

Haiman, C. a et al., 2007. Multiple regions within 8q24 independently affect risk for prostate cancer. *Nature Genetics*, 39(5), pp.638–644.

Haldar, S., Chintapalli, J. & Croce, C.M., 1996. Taxol Induces bcl-2 Phosphorylation and Death of Prostate Cancer Cells Taxol Induces bcl-2 Phosphorylation and Death of Prostate Cancer Cells1. *Cancer Research*, 56, pp.1253–1255.

Han, C.S., Patel, R. & Kim, I.Y., 2015. Pharmacokinetics, pharmacodynamics and clinical efficacy of abiraterone acetate for treating metastatic castration-resistant prostate cancer. *Expert Opinion on Drug Metabolism & Toxicology*, 11(6), pp.967–75.

Harrell, J.C. et al., 2006. Estrogen receptor positive breast cancer metastasis: Altered hormonal sensitivity and tumor aggressiveness in lymphatic vessels and lymph nodes. *Cancer Research*, 66(18), pp.9308–9315.

Hay, D. & Zuk, A., 1995. Transformations Between Epithelium and Mesenchyme: Normal, Pathological, and Experimentally Induced. *American Journal of Kidney Diseases*, 26(4), pp.678–690.

Heiden, M.G. Vander et al., 2009. Understanding the Warburg Effect : Cell Proliferation. *Science*, 324(May), pp.1029–1034.

Heidenreich, A. et al., 2014. EAU guidelines on prostate cancer. Part 1: Screening, diagnosis, and local treatment with curative intent - Update 2013. *European Urology*, 65(1), pp.124–137.

Hendriksen, P.J.M. et al., 2006. Evolution of the androgen receptor pathway during progression of prostate cancer. *Cancer Research*, 66(10), pp.5012–5020.

Hermann, P.C. et al., 2007. Distinct Populations of Cancer Stem Cells Determine Tumor Growth and Metastatic Activity in Human Pancreatic Cancer. *Cell Stem Cell*, 1(3), pp.313–323.

Higgins, L.H. et al., 2009. Hypoxia and the metabolic phenotype of prostate cancer cells. *Biochimica et Biophysica Acta - Bioenergetics*, 1787(12), pp.1433–1443.

Hilkens, J. & Buijs, F., 1988. Biosynthesis of MAM-6, an epithelial sialomucin. Evidence for involvement of a rare proteolytic cleavage step in the endoplasmic reticulum. *Journal of Biological Chemistry*, 263(9), pp.4215–4222.

Hinoshita, E., Uchiumi, T. & Taguchi, K., 2000. Increased expression of an ATP-binding cassette superfamily transporter, multidrug resistance protein 2, in human colorectal carcinomas. *Clinical Cancer Research*, 6, pp.2401–2407.

Hirschhaeuser, F. et al., 2010. Multicellular tumor spheroids: An underestimated tool is catching up again. *Journal of Biotechnology*, 148(1), pp.3–15.

Hirschmann-Jax, C. et al., 2004. A distinct “side population” of cells with high drug efflux capacity in human tumor cells. *Proceedings of the National Academy of Sciences of the United States of America*, 101(39), pp.14228–33.

Hlavac, V. et al., 2013. The expression profile of ATP-binding cassette transporter genes in breast carcinoma. *Pharmacogenomics*, 14(5), pp.515–529.

Hobisch, A. et al., 1995. Distant metastases from prostatic carcinoma express

androgen receptor protein. *Cancer Research*, 55(14), pp.3068–3072.

Holzbeierlein, J. et al., 2004. Gene expression analysis of human prostate carcinoma during hormonal therapy identifies androgen-responsive genes and mechanisms of therapy resistance. *The Americal Journal of Pathology*, 164(1), pp.217–27.

Hörnberg, E. et al., 2011. Expression of androgen receptor splice variants in prostate cancer bone metastases is associated with castration-resistance and short survival. *PLoS ONE*, 6(4).

Hsieh, I.S. et al., 2013. MicroRNA-320 suppresses the stem cell-like characteristics of prostate cancer cells by downregulating the Wnt/beta-catenin signaling pathway. *Carcinogenesis*, 34(3), pp.530–538.

Hsu, F.-M. et al., 2015. Circulating mRNA Profiling in Esophageal Squamous Cell Carcinoma Identifies FAM84B As A Biomarker In Predicting Pathological Response to Neoadjuvant Chemoradiation. *Scientific reports*, 5(April), p.10291.

Hsu, P.P. & Sabatini, D.M., 2008. Cancer cell metabolism: Warburg and beyond. *Cell*, 134(5), pp.703–707.

Hu, R. et al., 2009. Ligand-independent androgen receptor variants derived from splicing of cryptic exons signify hormone-refractory prostate cancer. *Cancer Research*, 69(1), pp.16–22.

Huang, X.P. et al., 2006. Negative implication of C-MYC as an amplification target in esophageal cancer. *Cancer Genetics and Cytogenetics*, 165(1), pp.20–24.

Huesker, M. et al., 2002. Reversal of drug resistance of hepatocellular carcinoma cells by adenoviral delivery of anti-MDR1 ribozymes. *Hepatology*, 36(4 I), pp.874–884.

Huisman, M.T. et al., 2005. MRP2 (ABCC2) transports taxanes and confers paclitaxel resistance and both processes are stimulated by probenecid. *International Journal of Cancer*, 116(5), pp.824–829.

Humphrey, P.A., 2004. Gleason grading and prognostic factors in carcinoma of the prostate. *Modern Pathology*, 17(3), pp.292–306.

Hyde, S.C. et al., 1990. Structural model of ATP-binding proteins associated with cystic fibrosis, multidrug resistance and bacterial transport. *Nature*, 346(6282), pp.362–365.

Italiano, A. et al., 2009. Docetaxel-Based Chemotherapy in Elderly Patients (Age 75 and Older) with Castration-Resistant Prostate Cancer. *European Urology*,

55(6), pp.1368–1376.

Jain, R.K., 2001. Normalizing tumor vasculature with anti-angiogenic therapy: a new paradigm for combination therapy. *Nature Medicine*, 7(1078-8956 SB - IM), pp.987–989.

Jiang, Y.-G. et al., 2007. Role of Wnt/beta-catenin signaling pathway in epithelial-mesenchymal transition of human prostate cancer induced by hypoxia-inducible factor-1alpha. *International Journal of Urology*, 14(11), pp.1034–9.

Jiao, J. et al., 2012. Identification of CD166 as a surface marker for enriching prostate stem/progenitor and cancer initiating cells. *PLoS ONE*, 7(8), pp.1–14.

Jordan, C.T., Guzman, M.L. & Noble, M., 2006. Cancer Stem Cells. *New England Journal of Medicine*, 355(12), pp.1253–1261.

Jordan, M.A. & Wilson, L., 2004. Microtubules as a target for anticancer drugs. *Nature reviews: Cancer*, 4(4), pp.253–265.

Jung, S.J. et al., 2013. Clinical Significance of Wnt/beta-Catenin Signalling and Androgen Receptor Expression in Prostate Cancer. *The World Journal of Men's Health*, 31(1), pp.36–46.

Kahn, B., Collazo, J. & Kyprianou, N., 2014. Androgen receptor as a driver of therapeutic resistance in advanced prostate cancer. *International Journal of Biological Sciences*, 10(6), pp.588–595.

Kalluri, R. & Weinberg, R. a, 2009. Review series The basics of epithelial-mesenchymal transition. *Journal of Clinical Investigation*, 119(6), pp.1420–1428.

Kalra, A. V & Campbell, R.B., 2007. Mucin impedes cytotoxic effect of 5-FU against growth of human pancreatic cancer cells: overcoming cellular barriers for therapeutic gain. *British Journal of Cancer*, 97(7), pp.910–918.

Karatas, O.F. et al., 2016. The role of ATP-binding cassette transporter genes in the progression of prostate cancer. *The Prostate*, 76(5), pp.434–444.

Kartenbeck, J. et al., 1996. Absence of the canalicular isoform of the MRP gene-encoded conjugate export pump from the hepatocytes in Dubin-Johnson syndrome. *Hepatology*, 23(5), pp.1061–6.

Kasper, S., 2008. Exploring the origins of the normal prostate and prostate cancer stem cell. *Stem Cell Reviews*, 4(3), pp.193–201.

Kastler, S. et al., 2010. POU5F1P1, a putative cancer susceptibility gene, is overexpressed in prostatic carcinoma. *Prostate*, 70(6), pp.666–674.

Kato, T. et al., 2015. Serum exosomal P-glycoprotein is a potential marker to diagnose docetaxel resistance and select a taxoid for patients with prostate cancer. *Urologic Oncology*, 33(9), pp.385.e15–385.e20.

Kharbanda, A. et al., 2014. MUC1-C confers EMT and KRAS independence in mutant KRAS lung cancer cells. *Oncotarget*, 5(19), pp.8893–8905.

Klarmann, G.J. et al., 2009. Invasive prostate cancer cells are tumor initiating cells that have a stem cell-like genomic signature. *Clinical and Experimental Metastasis*, 26(5), pp.433–446.

Kluth, M. et al., 2015. Prevalence of chromosomal rearrangements involving non-ETS genes in prostate cancer. *International Journal of Oncology*, 46(4), pp.1637–1642.

Klymkowsky, M.W., 2005. Beta-Catenin and Its Regulatory Network. *Human Pathology*, 36(3), pp.225–227.

Komuro, H. et al., 2007. Identification of side population cells (stem-like cell population) in pediatric solid tumor cell lines. *Journal of Pediatric Surgery*, 42(12), pp.2040–2045.

Kondo, M. et al., 2003. Biology of hematopoietic stem cells and progenitors: implications for clinical application. *Annual Review of Immunology*, 21(1), pp.759–806.

Kondo, T., Setoguchi, T. & Taga, T., 2004. Persistence of a small subpopulation of cancer stem-like cells in the C6 glioma cell line. *Proceedings of the National Academy of Sciences*, 101(3), pp.1–6.

Kong, D. et al., 2015. Androgen receptor splice variants contribute to prostate cancer aggressiveness through induction of EMT and expression of stem cell marker genes. *Prostate*, 75(2), pp.161–174.

Kong, D. et al., 2011. Cancer stem cells and Epithelial-to-Mesenchymal Transition (EMT)-Phenotypic Cells: Are they Cousins or Twins? *Cancers*, 3(1), pp.716–729.

Kong, D. et al., 2010. Epithelial to mesenchymal transition is mechanistically linked with stem cell signatures in prostate cancer cells. *PLoS ONE*, 5(8).

Konno, M. et al., 2015. Novel mechanism for invasion and metastasis involving metabolic enzymes in intractable cancer cells. *Rinsho Ketsueki*, 56(8), pp.1059–1063.

Kosugi, M. et al., 2011. MUC1-C oncoprotein regulates glycolysis and pyruvate kinase m2 activity in cancer cells. *PLoS ONE*, 6(11), pp.1–14.

Kruijtzer, C.M.F., 2002. Improvement of Oral Drug Treatment by Temporary

Inhibition of Drug Transporters and/or Cytochrome P450 in the Gastrointestinal Tract and Liver: An Overview. *The Oncologist*, 7(6), pp.516–530.

Kufe, D. et al., 1984. Differential reactivity of a novel monoclonal antibody (DF3) with human malignant versus benign breast tumors. *Hybridoma*, 3(3), pp.223–32.

Kumar, V.L. & Majumder, P.K., 1995. Prostate Gland: Structure, Functions and Regulation. *International Urology and Nephrology*, 27(3), pp.231–243.

Kuramoto, T. et al., 2013. Docetaxel in combination with estramustine and prednisolone for castration-resistant prostate cancer. *International Journal of Clinical Oncology*, 18(5), pp.890–897.

Kyprianou, N. & Isaacs, J.T., 1988. Identification of a cellular receptor for transforming growth factor-beta in rat ventral prostate and its negative regulation by androgens. *Endocrinology*, 123(4), pp.2124–2131.

Lam, J.S. & Reiter, R.E., 2006. Stem cells in prostate and prostate cancer development. (RETRACTED). *Urologic Oncology*, 24(2), pp.131–40.

Lawrence, M.G. et al., 2015. Establishment of primary patient-derived xenografts of palliative TURP specimens to study castrate-resistant prostate cancer. *Prostate*, 75(13), pp.1475–1483.

Lee, J. et al., 2008. Pyruvate kinase isozyme type M2 (PKM2) interacts and cooperates with Oct-4 in regulating transcription. *International Journal of Biochemistry and Cell Biology*, 40(5), pp.1043–1054.

Lee, J.T., Steelman, L.S. & Mccubrey, J.A., 2004. Phosphatidylinositol 3 ′ -Kinase Activation Leads to Multidrug Resistance Protein-1 Expression and Subsequent Chemoresistance in Advanced Prostate Cancer Cells Phosphatidylinositol 3 -Kinase Activation Leads to Multidrug Resistance Protein-1 Expression. *Cancer Research*, 64(22), pp.8397–8404.

De Leeuw, R. et al., 2015. Novel actions of next-generation taxanes benefit advanced stages of prostate cancer. *Clinical Cancer Research*, 21(4), pp.795–807.

Levitin, F. et al., 2005. The MUC1 SEA module is a self-cleaving domain. *Journal of Biological Chemistry*, 280(39), pp.33374–33386.

Li, C. et al., 2007. Identification of pancreatic cancer stem cells. *Cancer Research*, 67(3), pp.1030–1037.

Li, Q. et al., 2015. Nuclear PKM2 contributes to gefitinib resistance via upregulation of STAT3 activation in colorectal cancer. *Scientific Reports*,

5(October), p.16082.

Li, Y. et al., 2012. AR intragenic deletions linked to androgen receptor splice variant expression and activity in models of prostate cancer progression. *Oncogene*, 31(45), pp.4759–4767.

Li, Y. et al., 2001. The Epidermal Growth Factor Receptor Regulates Interaction of the Human DF3/MUC1 Carcinoma Antigen with c-Src and ??-Catenin. *Journal of Biological Chemistry*, 276(38), pp.35239–35242.

Li, Z. & Rich, J.N., 2010. Hypoxia and hypoxia inducible factors in cancer stem cell maintenance. In *Diverse Effects of Hypoxia on Tumor Progression*. pp. 21–30.

Liao, J. et al., 2014. Ovarian cancer spheroid cells with stem cell-like properties contribute to tumor generation, metastasis and chemotherapy resistance through hypoxia-resistant metabolism. *PLoS ONE*, 9(1), pp.1–13.

Lieber, M. et al., 1976. A continuous tumor-cell line from a human lung carcinoma with properties of type II alveolar epithelial cells. *International Journal of Cancer*, 17(1), pp.62–70.

Ligtenberg, M.J.L. et al., 1992. Cell-associated episialin is a complex containing two proteins derived from a common precursor. *Journal of Biological Chemistry*, 267(9), pp.6171–6177.

Linn, D.E. et al., 2010. A Role for OCT4 in Tumor Initiation of Drug-Resistant Prostate Cancer Cells. *Genes & Cancer*, 1(9), pp.908–916.

Liu, W. et al., 2008. Homozygous deletions and recurrent amplifications implicate new genes involved in prostate cancer. *Neoplasia*, 10(8), pp.897–907.

Liu, Y. et al., 2010. Dasatinib inhibits site-specific tyrosine phosphorylation of androgen receptor by Ack1 and Src kinases. *Oncogene*, 29(22), pp.3208–16.

Lu, Z. et al., 2003. Downregulation of caveolin-1 function by EGF leads to the loss of E-cadherin, increased transcriptional activity of ??-catenin, and enhanced tumor cell invasion. *Cancer Cell*, 4(6), pp.499–515.

Luo, W. & Semenza, G.L., 2012. Emerging roles of PKM2 in cell metabolism and cancer progression. *Trends in endocrinology and metabolism*, 23(11), pp.560–6.

Macao, B. et al., 2006. Autoproteolysis coupled to protein folding in the SEA domain of the membrane-bound MUC1 mucin. *Nature: Structural & Molecular Biology*, 13(1), pp.71–76.

Mahajan, N.P. et al., 2007. Activated Cdc42-associated kinase Ack1 promotes prostate cancer progression via androgen receptor tyrosine phosphorylation.

Proceedings of the National Academy of Sciences of the United States of America, 104(20), pp.8438–8443.

Mahon, K.L. et al., 2011. Pathways of chemotherapy resistance in castration-resistant prostate cancer. *Endocrine-Related Cancer*, 18(4), pp.103–123.

Major, P. et al., 2012. A phase I / II clinical trial of a MUC1 - glycopeptide dendritic cell vaccine in castrate resistant non - metastatic prostate cancer patients. *Cancer Research*, 72, p.A16.

Mani, S.A. et al., 2008. The Epithelial-Mesenchymal Transition Generates Cells with Properties of Stem Cells. *Cell*, 133(4), pp.704–715.

Materna, V. et al., 2006. RNA interference-triggered reversal of ABCC2-dependent cisplatin resistance in human cancer cells. *Biochemical and Biophysical Research Communications*, 348(1), pp.153–157.

McCubrey, J.A. et al., 2010. Targeting signal transduction pathways to eliminate chemotherapeutic drug resistance and cancer stem cells. *Advances in Enzyme Regulation*, 50(1), pp.285–307.

McDonald, W.H. et al., 2003. Novel Essential DNA Repair Proteins Nse1 and Nse2 Are Subunits of the Fission Yeast Smc5-Smc6 Complex. *Journal of Biological Chemistry*, 278(46), pp.45460–45467.

McNeal, J.E., 1988. Normal histology of the prostate. *The American Journal of Surgical Pathology*, 12, pp.619 – 33.

McNeel, D.G., 2007. Prostate cancer immunotherapy. *Current Opinion in Urology*, 17, p.181.

Mellinghoff, I.K. et al., 2004. HER2/neu kinase-dependent modulation of androgen receptor function through effects on DNA binding and stability. *Cancer Cell*, 6(5), pp.517–527.

Meng, M.-B. et al., 2015. Targeting pyruvate kinase M2 contributes to radiosensitivity of non-small cell lung cancer cells in vitro and in vivo. *Cancer Letters*, 356(2), pp.985–993.

Mertz, K.D. et al., 2007. Molecular characterization of TMPRSS2-ERG gene fusion in the NCI-H660 prostate cancer cell line: a new perspective for an old model. *Neoplasia*, 9(3), pp.200–6.

Meyer, K.B. et al., 2011. A functional variant at a prostate cancer predisposition locus at 8q24 is associated with PVT1 expression. *PLoS Genetics*, 7(7).

Mickey, D.D. et al., 2007. Heterotransplantation of a human prostatic adenocarcinoma cell line in nude mice. *Cancer Research*, 37(11), pp.49–58.

Miki, J., 2010. Investigations of prostate epithelial stem cells and prostate cancer stem cells. *International Journal of Urology*, 17(2), pp.139–147.

Mita, A.C. et al., 2009. Phase I and pharmacokinetic study of XRP6258 (RPR 116258A), a novel taxane, administered as a 1-hour infusion every 3 weeks in patients with advanced solid tumors. *Clinical Cancer Research*, 15(2), pp.723–730.

Moad, M. et al., 2013. A novel model of urinary tract differentiation, tissue regeneration, and disease: Reprogramming human prostate and bladder cells into induced pluripotent stem cells. *European Urology*, 64(5), pp.753–761.

Mohler, J.L. et al., 2004. The androgen axis in recurrent prostate cancer. *Clinical Cancer Research*, 10(716), pp.440–448.

Montgomery, R.B. et al., 2008. Maintenance of intratumoral androgens in metastatic prostate cancer: A mechanism for castration-resistant tumor growth. *Cancer Research*, 68(11), pp.4447–4454.

Morel, a P. et al., 2008. Generation of breast cancer stem cells through epithelial-mesenchymal transition. *PLoS One*, 3(8), p.e2888.

Moreno, M. et al., 2007. High level of MUC1 in serum of ovarian and breast cancer patients inhibits huHMFG-1 dependent cell-mediated cytotoxicity (ADCC). *Cancer Letters*, 257(1), pp.47–55.

de Morrée, E. et al., 2016. Understanding taxanes in prostate cancer; importance of intratumoral drug accumulation. *The Prostate*, 76(10), pp.927–936.

Mulholland, D.J. et al., 2011. Cell autonomous role of PTEN in regulating castration-resistant prostate cancer growth. *Cancer Cell*, 19(6), pp.792–804.

Nelson, P.S. et al., 2002. The program of androgen-responsive genes in neoplastic prostate epithelium. *Proceedings of the National Academy of Sciences of the United States of America*, 99(18), pp.11890–5.

Newmark, J.R. et al., 1992. Androgen Receptor Gene Mutations in Human Prostate Cancer. *Proceedings of the National Academy of Sciences*, 89(14), pp.6319–6323.

Ni, J. et al., 2014. Cancer stem cells in prostate cancer chemoresistance. *Current Cancer Drug Targets*, 14(3), pp.225–240.

Noda, T. et al., 2009. Activation of Wnt/ß-catenin signalling pathway induces chemoresistance to interferon-alpha/5-fluorouracil combination therapy for hepatocellular carcinoma. *British Journal of Cancer*, 100(10), pp.1647–1658.

Nusse, W.J.N. and R., 2004. Convergence of Wnt, b -Catenin, and Cadherin

Pathways. *Science*, 303(March), pp.1483–1488.

O'Brien, C.A., Kreso, A. & Dick, J.E., 2009. Cancer Stem Cells in Solid Tumors: An Overview. *Seminars in Radiation Oncology*, 19(2), pp.71–77.

Okada, H. et al., 1997. Early role of Fsp1 in epithelial-mesenchymal transformation. *American Journal of Physiology*, 273(4 Pt 2), pp.F563–574.

Okita, K. et al., 2008. Generation of mouse induced pluripotent stem cells without viral vectors. *Science*, 322(5903), pp.949–953.

Al Olama, A.A. et al., 2009. Multiple loci on 8q24 associated with prostate cancer susceptibility. *Nature Genetics*, 41(10), pp.1058–1060.

Onder, T.T. et al., 2008. Loss of E-cadherin promotes metastasis via multiple downstream transcriptional pathways. *Cancer Research*, 68(10), pp.3645–3654.

Paller, C.J. & Antonarakis, E.S., 2011. Cabazitaxel: A novel second-line treatment for metastatic castration-resistant prostate cancer. *Drug Design, Development and Therapy*, 5, pp.117–124.

Park, C.H., Bergsagel, D.E. & McCulloch, E.A., 1971. Mouse Myeloma Tumor Stem Cells: A Primary Cell Culture Assay. *Journal of the National Cancer Institute*, 46(2), pp.411–422.

Park, I.-H. et al., 2008. Reprogramming of human somatic cells to pluripotency with defined factors. *Nature*, 451(7175), pp.141–6.

Patrawala, L. et al., 2007. Hierarchical organization of prostate cancer cells in xenograft tumors: the CD44+alpha2beta1+ cell population is enriched in tumor-initiating cells. *Cancer Research*, 67(14), pp.6796–805.

Patrawala, L. et al., 2006. Highly purified CD44+ prostate cancer cells from xenograft human tumors are enriched in tumorigenic and metastatic progenitor cells. *Oncogene*, 25(12), pp.1696–1708.

de Paula Peres, L. et al., 2015. Peptide vaccines in breast cancer: The immunological basis for clinical response. *Biotechnology Advances*, 33(8), pp.1868–1877.

Pebernard, S. et al., 2004. Nse1, Nse2, and a Novel Subunit of the Smc5–Smc6 Complex, Nse3, Play a Crucial Role in Meiosis. *Molecular Biology of the Cell*, 15, pp.4866–4876.

Pellacani, D. et al., 2011. Regulation of the stem cell marker CD133 is independent of promoter hypermethylation in human epithelial differentiation and cancer. *Molecular Cancer*, 10(1), p.94.

Petrylak, D.P. et al., 2004. Docetaxel and estramustine compared with mitoxantrone and prednisone for advanced refractory prostate cancer. *The New England Journal of Medicine*, 351(15), pp.1513–20.

Pichinuk, E. et al., 2012. Antibody targeting of cell-bound MUC1 SEA domain kills tumor cells. *Cancer Research*, 72(13), pp.3324–3336.

Pillai, K. et al., 2015. MUC1 as a potential target in anticancer therapies. *American Journal of Clinical Oncology*, 38(1), pp.108–18.

Pomerantz, M.M. et al., 2009. The 8q24 cancer risk variant rs6983267 shows long-range interaction with MYC in colorectal cancer. *Nature Genetics*, 41(8), pp.882–4.

Porporato, P.E. et al., 2011. Anticancer targets in the glycolytic metabolism of tumors: A comprehensive review. *Frontiers in Pharmacology*, AUG(August), pp.1–18.

Pourmand, G. et al., 2007. Role of PTEN gene in progression of prostate cancer. *Urology Journal*, 4(2), pp.95–100.

Preston, D.M. et al., 2002. Androgen deprivation in men with prostate cancer is associated with an increased rate of bone loss. *Prostate Cancer and Prostatic Diseases*, 5(4), pp.304–10.

Qi, W.-X., Shen, Z. & Yao, Y., 2011. Docetaxel-based therapy with or without estramustine as first-line chemotherapy for castration-resistant prostate cancer: a meta-analysis of four randomized controlled trials. *Journal of Cancer Research and Clinical Oncology*, 137(12), pp.1785–1790.

Raina, D. et al., 2015. Characterization of the MUC1-C cytoplasmic domain as a cancer target. *PLoS ONE*, 10(8), pp.1–17.

Raina, D., Kharbanda, S. & Kufe, D., 2004. The MUC1 oncoprotein activates the anti-apoptotic phosphoinositide 3-kinase/Akt and Bcl-xL pathways in rat 3Y1 fibroblasts. *Journal of Biological Chemistry*, 279(20), pp.20607–20612.

Rajabi, H. et al., 2011. Androgen receptor regulates expression of the MUC1-C oncoprotein in human prostate cancer cells. *The Prostate*, 71(12), pp.1299–308. Available at: http://www.ncbi.nlm.nih.gov/pubmed/21308711.

Rajabi, H. et al., 2014. MUC1-C oncoprotein activates the ZEB1/miR-200c regulatory loop and epithelial-mesenchymal transition. *Oncogene*, 33(13), pp.1680–9.

Rajabi, H. et al., 2012. MUC1-C oncoprotein confers androgen-independent growth of human prostate cancer cells. *Prostate*, 72(15), pp.1659–1668.

Regenbrecht, C.R.A., Lehrach, H. & Adjaye, J., 2008. Stemming cancer:

Functional genomics of cancer stem cells in solid tumors. *Stem Cell Reviews*, 4(4), pp.319–328.

Reid, a H.M. et al., 2010. Molecular characterisation of ERG, ETV1 and PTEN gene loci identifies patients at low and high risk of death from prostate cancer. *British Journal of Cancer*, 102(4), pp.678–684.

Ren, J. et al., 2004. Human MUC1 carcinoma-associated protein confers resistance to genotoxic anticancer agents. *Cancer Cell*, 5(2), pp.163–175.

Reya, T. et al., 2001. Stem cells, cancer, and cancer stem cells. *Nature*, 414(November), pp.105–111.

Reynolds, B.A. & Weiss, S., 1992. Generation of neurons and astrocytes from isolated cells of the adult mammalian central nervous system. *Science*, 255(5052), pp.1707–1710.

Ricci-Vitiani, L. et al., 2007. Identification and expansion of human colon-cancer-initiating cells. *Nature*, 445(7123), pp.111–115.

Richardson, G.D. et al., 2004. CD133, a novel marker for human prostatic epithelial stem cells. *Journal of Cell Science*, 117(16), pp.3539–3545.

Van Roy, F. & Berx, G., 2008. The cell-cell adhesion molecule E-cadherin. *Cellular and Molecular Life Sciences*, 65(23), pp.3756–3788.

Roy, L.D. et al., 2011. MUC1 enhances invasiveness of pancreatic cancer cells by inducing epithelial to mesenchymal transition. *Oncogene*, 30(12), pp.1449–1459.

Rybak, A.P. et al., 2011. Characterization of sphere-propagating cells with stem-like properties from DU145 prostate cancer cells. *Biochimica et Biophysica Acta*, 1813(5), pp.683–94.

Rybak, A.P. & Tang, D., 2013. SOX2 plays a critical role in EGFR-mediated self-renewal of human prostate cancer stem-like cells. *Cellular Signalling*, 25(12), pp.2734–42.

Sahlgren, C. et al., 2008. Notch signaling mediates hypoxia-induced tumor cell migration and invasion. *Proceedings of the National Academy of Sciences of the United States of America*, 105(17), pp.6392–7.

Sanchez, C. et al., 2013. Combining T-cell immunotherapy and anti-androgen therapy for prostate cancer. *Prostate Cancer and Prostatic Diseases*, 16(2), pp.123–31, S1.

Sartorius, C.A., Shen, T. & Horwitz, K.B., 2003. Progesterone receptors A and B differentially affect the growth of estrogen-dependent human breast tumor xenografts. *Breast Cancer Research and Treatment*, 79(3), pp.287–299.

Satelli, A. & Li, S., 2011. Vimentin in cancer and its potential as a molecular target for cancer therapy. *Cellular and Molecular Life Sciences*, 68(18), pp.3033–3046.

Savagner, P., Yamada, K.M. & Thiery, J.P., 1997. The Zinc-Finger Protein Slug Causes DesmosomeDissociation, an Initial and Necessary Step for Growth Factor–induced Epithelial–Mesenchymal Transition. *The Journal of Cell Biology*, 137(6), pp.1403–1419.

Saxena, M. et al., 2011. Transcription factors that mediate epithelial-mesenchymal transition lead to multidrug resistance by upregulating ABC transporters. *Cell Death & Disease*, 2(7), p.e179.

Schalken, J. & Fitzpatrick, J.M., 2016. Enzalutamide: Targeting the androgen signalling pathway in metastatic castration-resistant prostate cancer. *BJU International*, 117(2), pp.215–225.

Schalken, J.A. & Van Leenders, G., 2003. Cellular and molecular biology of the prostate: Stem cell biology. *Urology*, 62(5 SUPPL. 1), pp.11–20.

Scher, H.I. et al., 2008. Design and end points of clinical trials for patients with progressive prostate cancer and castrate levels of testosterone: Recommendations of the Prostate Cancer Clinical Trials Working Group. *Journal of Clinical Oncology*, 26(7), pp.1148–1159.

Schroeder, J.A. et al., 2001. Transgenic MUC1 Interacts with Epidermal Growth Factor Receptor and Correlates with Mitogen-activated Protein Kinase Activation in the Mouse Mammary Gland*. *Journal of Biological Chemistry*, 276(16), pp.13057–13064.

Schweizer, M.T. & Antonarakis, E.S., 2012. Abiraterone and other novel androgen-directed strategies for the treatment of prostate cancer: a new era of hormonal therapies is born. *Therapeutic Advances in Urology*, 4(4), pp.167–78.

Semenza, G.L., 2000. Hypoxia, clonal selection, and the role of HIF-1 in tumor progression. *Critical Reviews in Biochemistry and Molecular Biology*, 35(2), pp.71–103.

Semenza, G.L., 2007. Hypoxia-inducible factor 1 (HIF-1) pathway. *Science's STKE : Signal Transduction Knowledge Environment*, 2007(407), p.cm8.

Sethi, S. et al., 2010. Molecular signature of epithelial-mesenchymal transition (EMT) in human prostate cancer bone metastasis. *American Journal of Translational Research*, 3(1), pp.90–99.

Shahinian, V.B. et al., 2005. Risk of Fracture after Androgen Deprivation for

Prostate Cancer. *The New England Journal of Medicine*, 352, pp.154–164.

Shaw, G. & Prowse, D.M., 2008. Inhibition of androgen-independent prostate cancer cell growth is enhanced by combination therapy targeting Hedgehog and ErbB signalling. *Cancer Cell International*, 8, p.3.

Shi, H. shan et al., 2010. Silencing of pkm2 increases the efficacy of docetaxel in human lung cancer xenografts in mice. *Cancer Science*, 101(6), pp.1447–1453.

Shi, M.F. et al., 2010. Identification of cancer stem cell-like cells from human epithelial ovarian carcinoma cell line. *Cellular and Molecular Life Sciences*, 67(22), pp.3915–3925.

Shmelkov, S. V. et al., 2005. AC133/CD133/Prominin-1. *The International Journal of Biochemistry & Cell Biology*, 37(4), pp.715–719.

Singh, P.K. & Hollingsworth, M.A., 2006. Cell surface-associated mucins in signal transduction. *Trends in Cell Biology*, 16(9), pp.467–476.

Singh, S. et al., 2012. Chemoresistance in prostate cancer cells is regulated by miRNAs and Hedgehog pathway. *PLoS ONE*, 7(6).

Singh, S.K. et al., 2003. Identification of a Cancer Stem Cell in Human Brain Tumors Identification of a Cancer Stem Cell in Human Brain Tumors. *Cancer Research*, 63, pp.5821–5828.

Smith, B. & Bhowmick, N., 2016. Role of EMT in Metastasis and Therapy Resistance. *Journal of Clinical Medicine*, 5(2), p.17.

Smith, D.C. et al., 2003. Phase II trial of paclitaxel, estramustine, etoposide, and carboplatin in the treatment of patients with hormone-refractory prostate carcinoma. *Cancer*, 98(2), pp.269–276.

Solit, D.B. et al., 2003. Clinical Experience with Intravenous Estramustine Phosphate, Paclitaxel, and Carboplatin in Patients with Castrate, Metastatic Prostate Adenocarcinoma. *Cancer*, 98(9), pp.1842–1848.

Soloway, M., Hardeman, S. & Hickey, D., 1988. Stratification of patients with metastatic prostate cancer based on extent of disease on initial bone scan. *Cancer*, 61, pp.195–202.

Sparreboom, A. et al., 2003. Pharmacogenomics of ABC transporters and its role in cancer chemotherapy. *Drug Resistance Updates*, 6(2), pp.71–84.

Stanbrough, M. et al., 2006. Increased expression of genes converting adrenal androgens to testosterone in androgen-independent prostate cancer. *Cancer Research*, 66(5), pp.2815–2825.

Storr, S.J. et al., 2008. The O-linked glycosylation of secretory/shed MUC1 from an advanced breast cancer patient's serum. *Glycobiology*, 18(6), pp.456–462.

Sun, S. et al., 2010. Castration resistance in human prostate cancer is conferred by a frequently occurring androgen receptor splice variant. *The Journal of Clinical Investigation*, 120(8), pp.2715–2730.

Sun, Y. et al., 2012. Androgen deprivation causes epithelial-mesenchymal transition in the prostate: Implications for androgen- deprivation therapy. *Cancer Research*, 72(2), pp.527–536.

Szotek, P.P. et al., 2006. Ovarian cancer side population defines cells with stem cell-like characteristics and Mullerian Inhibiting Substance responsiveness. *Proceedings of the National Academy of Sciences of the United States of America*, 103(30), pp.11154–9.

Takahashi, K. & Yamanaka, S., 2006. Induction of Pluripotent Stem Cells from Mouse Embryonic and Adult Fibroblast Cultures by Defined Factors. *Cell*, 126(4), pp.663–676.

Tan, M.E. et al., 2014. Androgen receptor: structure, role in prostate cancer and drug discovery. *Acta Pharmacologica Sinica*, 36(1), pp.1–21.

Tannock, I.F. et al., 2004. Docetaxel plus Prednisone or Mitoxantrone plus Prednisone for Advanced Prostate Cancer. *The New England Journal of Medicine*, 351(15), pp.1502–1512.

Taplin, M.-E. et al., 1995. Mutation of the androgen-receptor gene in metastatic androgen-independent prostate cancer. *The New England Journal of Medicine*, 332(21), pp.1393–1398.

Taylor, B.S. et al., 2010. Integrative Genomic Profiling of Human Prostate Cancer. *Cancer Cell*, 18(1), pp.11–22.

Tiwari, N. et al., 2012. EMT as the ultimate survival mechanism of cancer cells. *Seminars in Cancer Biology*, 22(3), pp.194–207.

Tomlins, S. a et al., 2005. Recurrent Fusion of TMPRSS2 and. *Science*, 310(October), pp.644–648.

Tomlins, S.A. et al., 2008. Role of the TMPRSS2-ERG gene fusion in prostate cancer. *Neoplasia*, 10(2), pp.177–88.

Tran, C. et al., 2009. Development of a second-generation antiandrogen for treatment of advanced prostate cancer. *Science*, 324(5928), pp.787–790.

Trivedi, C. et al., 2000. Weekly 1-hour infusion of paclitaxel: Clinical feasibility and efficacy in patients with hormone-refractory prostate carcinoma. *Cancer*, 89(2), pp.431–436.

Truica, C.I., Byers, S. & Gelmann, E.P., 2000. Advances in Brief B-Catenin Affects Androgen Receptor Transcriptional Activity and. *Cancer*, 60, pp.4709–4713.

Tsujimura, A. et al., 2002. Proximal location of mouse prostate epithelial stem cells: a model of prostatic homeostasis. *The Journal of Cell Biology*, 157(7), pp.1257–1265.

Vassilaros, S. et al., 2013. Up to 15-year clinical follow-up of a pilot Phase III immunotherapy study in stage II breast cancer patients using oxidized mannan-MUC1. *Immunotherapy*, 5(11), pp.1177–82.

Vaupel, P., Kelleher, D.K. & Höckel, M., 2001. Oxygen status of malignant tumors: pathogenesis of hypoxia and significance for tumor therapy. *Seminars in Oncology*, 28, pp.29–35.

Vesuna, F. et al., 2009. Twist modulates breast cancer stem cells by transcriptional regulation of CD24 expression. *Neoplasia*, 11(12), pp.1318–28.

Vincent, A. & Van Seuningen, I., 2012. On the epigenetic origin of cancer stem cells. *Biochimica et Biophysica Acta - Reviews on Cancer*, 1826(1), pp.83–88.

Visakorpi, T. et al., 1995. In vivo amplification of the androgen receptor gene and progression of human prostate cancer. *Nature Genetics*, 9(4), pp.401–406.

Vleminckx, K. et al., 1991. Genetic manipulation of E-cadherin expression by epithelial tumor cells reveals an invasion suppressor role. *Cell*, 66(1), pp.107–119.

Wang, S. et al., 2003. Prostate-specific deletion of the murine Pten tumor suppressor gene leads to metastatic prostate cancer. *Cancer Cell*, 4, pp.209–221.

Wang, Z. et al., 2011. Down-regulation of Notch-1 is associated with Akt and FoxM1 in inducing cell growth inhibition and apoptosis in prostate cancer cells. *Journal of Cellular Biochemistry*, 112(1), pp.78–88.

Wani, M.C. et al., 1971. Plant antitumor agents. VI. The isolation and structure of taxol, a novel antileukemic and antitumor agent from Taxus brevifolia. *Journal of the American Chemical Society*, 93(9), pp.2325–2327.

Warburg, O., 1956. On The Origins of Cancer Cells. *Science*, 123, pp.309–314.

Warburg, O., Wind, F. & Negelein, E., 1927. The metabolism of tumors in the body. *The journal of General Physiology*, 8(6), pp.519–530.

Van Waterschoot, R.A.B. et al., 2010. Individual and combined roles of CYP3A,

P-glycoprotein (MDR1/ABCB1) and MRP2 (ABCC2) in the pharmacokinetics of docetaxel. *International Journal of Cancer*, 127(12), pp.2959–2964.

Watson, P.A. et al., 2010. Constitutively active androgen receptor splice variants expressed in castration-resistant prostate cancer require full-length androgen receptor. *Proceedings of the National Academy of Sciences of the United States of America*, 107(39), pp.16759–65.

Watson, P.A., Arora, V.K. & Sawyers, C.L., 2015. Emerging mechanisms of resistance to androgen receptor inhibitors in prostate cancer. *Nature Reviews: Cancer*, 15(12), pp.701–711. Available at: https://gateway.itc.u-tokyo.ac.jp/nrc/journal/v15/n12/abs/,DanaInfo=www.nature.com+nrc4016.html.

Wei, C. et al., 2007. Cancer stem-like cells in human prostate carcinoma cells DU145: the seeds of the cell line? *Cancer Biology & Therapy*, 6(5), pp.763–768.

Wellner, U. et al., 2009. The EMT-activator ZEB1 promotes tumorigenicity by repressing stemness-inhibiting microRNAs. *Nature Cell Biology*, 11(12), pp.1487–1495.

Wen, Y., Hu, M.C. & Makino, K., 2000. HER-2 / neu Promotes Androgen-independent Survival and Growth of Prostate Cancer Cells through the Akt Pathway Cancer Cells through the Akt Pathway 1. *Cancer Research*, 60, pp.6841–6845.

West, T.A., Kiely, B.E. & Stockler, M.R., 2014. Estimating scenarios for survival time in men starting systemic therapies for castration-resistant prostate cancer: A systematic review of randomised trials. *European Journal of Cancer*, 50(11), pp.1916–1924.

Wong, N. et al., 2015. PKM2 contributes to cancer metabolism. *Cancer letters*, 356, pp.184–191.

Wong, N., De Melo, J. & Tang, D., 2013. PKM2, a Central Point of Regulation in Cancer Metabolism. *International Journal of Cell Biology*, 2013(Figure 1), p.242513.

Woo, J.K. et al., 2012. Mucin 1 enhances the tumor angiogenic response by activation of the AKT signaling pathway. *Oncogene*, 31(17), pp.2187–98.

Xia, N. et al., 2008. Directional control of cell motility through focal adhesion positioning and spatial control of Rac activation. *Federation of American Societies for Experimental Biology*, 22(6), pp.1649–1659.

Xie, S.M. et al., 2008. Lentivirus-mediated RNAi silencing targeting ABCC2 increasing the sensitivity of a human nasopharyngeal carcinoma cell line against cisplatin. *Journal of Translational Medicine*, 6, p.55.

Xu, J., Wu, R.-C. & O'Malley, B.W., 2009. Normal and cancer-related functions of the p160 steroid receptor co-activator (SRC) family. *Nature Reviews: Cancer*, 9(9), pp.615–30.

Yan, J. & Tang, D., 2014. Prostate cancer stem-like cells proliferate slowly and resist etoposide-induced cytotoxicity via enhancing DNA damage response. *Experimental Cell Research*, 328(1), pp.132–142.

Yang, J. et al., 2004. Twist , a Master Regulator of Morphogenesis , Plays an Essential Role in Tumor Metastasis Ben Gurion University of the Negev. *Cell*, 117, pp.927–939.

Yang, P. et al., 2015. Secreted pyruvate kinase M2 facilitates cell migration via PI3K/Akt and Wnt/β-catenin pathway in colon cancer cells. *Biochemical and Biophysical Research Communications*, 459(2), pp.327–332.

Yang, W. et al., 2011. Nuclear PKM2 regulates β-catenin transactivation upon EGFR activation. *Nature*, 478(7375), pp.118–122.

Yang, W. et al., 2012. PKM2 phosphorylates histone H3 and promotes gene transcription and tumorigenesis. *Cell*, 150(4), pp.685–696.

Yang, X. et al., 2013. Estradiol increases ER-negative breast cancer metastasis in an experimental model. *Clinical and Experimental Metastasis*, 30(6), pp.711–721.

Yasumizu, Y. et al., 2014. Dual PI3K/mTOR inhibitor NVP-BEZ235 sensitizes docetaxel in castration resistant prostate cancer. *Journal of Urology*, 191(1), pp.227–234.

Ye, Q.F. et al., 2012. siRNA-mediated silencing of notch-1 enhances docetaxel induced mitotic arrest and apoptosis in prostate cancer cells. *Asian Pacific Journal of Cancer Prevention*, 13(6), pp.2485–2489.

Yeh, S. et al., 1999. From HER2/Neu signal cascade to androgen receptor and its coactivators: a novel pathway by induction of androgen target genes through MAP kinase in prostate cancer cells. *Proceedings of the National Academy of Sciences of the United States of America*, 96(10), pp.5458–63.

Yeung, T.M. et al., 2010. Cancer stem cells from colorectal cancer-derived cell lines. *Proceedings of the National Academy of Sciences of the United States of America*, 107(8), pp.3722–7.

Yilmaz, O.H. et al., 2006. Pten dependence distinguishes haematopoietic stem

cells from leukaemia-initiating cells. *Nature*, 441(7092), pp.475–82.

Yin, L. et al., 2003. Human MUC1 carcinoma antigen regulates intracellular oxidant levels and the apoptotic response to oxidative stress. *The Journal of Biological Chemistry*, 278(37), pp.35458–35464.

Yin, L., Huang, L. & Kufe, D., 2004. MUC1 Oncoprotein Activates the FOXO3α Transcription Factor in a Survival Response to Oxidative Stress. *The Journal of Biological Chemistry*, 279(44), pp.45721–45727.

Yu, X. et al., 2011. Wnt/β-catenin activation promotes prostate tumor progression in a mouse model. *Oncogene*, 30(16), pp.1868–79.

Yu, Z. et al., 2016. PKM2 Thr454 phosphorylation increases its nuclear translocation and promotes xenograft tumor growth in A549 human lung cancer cells. *Biochemical and Biophysical Research Communications*, 473, pp.953–958.

Yu, Z. et al., 2013. Proviral insertion in murine lymphomas 2 (PIM2) oncogene phosphorylates pyruvate kinase M2 (PKM2) and promotes glycolysis in cancer cells. *The Journal of Biological Chemistry*, 288(49), pp.35406–35416.

Zamir, E. & Geiger, B., 2001. Molecular complexity and dynamics of cell-matrix adhesions. *Journal of Cell Science*, 114(Pt 20), pp.3583–3590.

Zeisberg, M. & Neilson, E.G., 2009. Biomarkers for epithelial-mesenchymal transitions. *Journal of Clinical Investigation*, 119(6), pp.1429–1437.

Zhang, G. et al., 2013. Unraveling the mystery of cancer metabolism in the genesis of tumor-initiating cells and development of cancer. *Biochimica et Biophysica Acta - Reviews on Cancer*, 1836(1), pp.49–59.

Zhang, H. et al., 1996. Induction of apoptosis in prostatic tumor cell line DU145 by staurosporine, a potent inhibitor of protein kinases. *Prostate*, 29(2), pp.69–76.

Zhang, L. et al., 2012. Tumorspheres derived from prostate cancer cells possess chemoresistant and cancer stem cell properties. *Journal of Cancer Research and Clinical Oncology*, 138(4), pp.675–686.

Zhang, S. et al., 2008. Identification and characterization of ovarian cancer-initiating cells from primary human tumors. *Cancer Research*, 68(11), pp.4311–20.

Zhang, X. et al., 2011. Androgen receptor variants occur frequently in castration resistant prostate cancer metastases. *PLoS ONE*, 6(11).

Zhu, H. et al., 2013. Elevated Jagged-1 and Notch-1 expression in high grade and

metastatic prostate cancers. *American Journal of Translational Research*, 5(3), pp.368–378.

Van Zuylen, L. et al., 2000. Role of intestinal P-glycoprotein in the plasma and fecal disposition of docetaxel in humans. *Clinical Cancer Research*, 6(7), pp.2598–2603.

APPENDIX

PERMISSION TO REPRINT MANUSCRIPTS

Cancer Investigation (Taylor and Francis Group)

AM: Accepted Manuscript

The version of a journal article that has been through peer review and accepted for publication in a journal, but not the version created by the publisher. This is the Version of Record.

'Gold' Open Access

The final published article is made permanently OA. An article publishing charge (APC) may apply on Taylor & Francis journals. Authors may need to sign a Creative Commons Attribution (CC BY) Licence to comply with some research funders' mandates.

'Green' Open Access

Deposit of the AM (after peer review but prior to publisher formatting) in a repository, with non-commercial reuse rights. Embargo periods run from the date of publication of the final article (Version of Record).

Show 25 entries Search: Cancer Investigation

Title	ISSN (Print)	ISSN (Online)	Open Select (Optional Gold OA Available)	AM embargo for personal / departmental website archiving (Green OA)	AM embargo for social scientific network / repository archiving (Green OA)	Gold OA content licence	Gold OA alternative licence	Gold OA APC (VAT may be applicable)
Cancer Investigation	0735-7907	1532-4192	Yes	0	12	CC BY-NC-ND	CC BY	£1,788 / 2,150 / $2,950

Oncotarget (Impact Journals)

Copyright and License Policies

Open-Access License
No Permission Required

Oncotarget applies the **Creative Commons Attribution License** (CCAL) to all works we publish (read the **human-readable summary** or the **full license legal code**). Under the CCAL, authors retain ownership of the copyright for their article, but authors allow anyone to download, reuse, reprint, modify, distribute, and/or copy articles in *Oncotarget* journal, so long as the original authors and source are cited.